New Long End-Associative Polymers for Mist Control in
I. Aqueous Solutions and
II. Hydrocarbon Solvents

Thesis by

Hojin Kim

In Partial Fulfillment of the Requirements for
the Degree of Doctor of Philosophy

Caltech

CALIFORNIA INSTITUTE OF TECHNOLOGY
Pasadena, California

2023
(Defended August 10, 2022)

ACKNOWLEDGEMENTS

To begin, I would like to thank my advisor, Professor Julie Kornfield for the support and advice I received during the last 6 years. I thank Professor Kornfield for allowing creativity in research and giving me opportunities to be involved in many different projects. I would also like to thank the members of my thesis committee: Professor John Brady, Professor Zhen-Gang Wang, and Professor Max Robb.

I started my research career as an undergraduate researcher in Professor Rafael Verduzco's lab at Rice University. I thank Professor Verduzco and my first research mentor Dr. Aditya Agrawal for their mentorship.

I was involved in multiple projects, which included both external and internal collaborations. I would like to first thank Dr. Chris Nelson and the rest of the UPI team at Dow Chemical Company for supporting my research on water-soluble end associative polymers. I thank my collaborators at ARL, Dr. Jacob Temme and Dr. Mike Kweon. I also thank fellow Caltech students Rob and Red who worked on these projects with me.

I thank my collaborators in the DOE project: Professor Judit Puskas, Professor Carin Helfer, and Dr. Kristof Molnar, for sharing their polymers with me and teaching me about polymer chemistry. I thank Professor Gregory McKenna and Dr. Dongjie Chen for their rheological experiments.

I thank Dr. Jeremy Wei for teaching me (and other members of the group) about polymer chemistry, training us on instruments, and providing necessary materials and synthetic protocols that allowed our group to continue the collaboration project with ARL.

I am also very grateful for the interactions I had with the members of the Kornfield lab. I thank Jeremy and his wife Wei-Ling for their kindness and support in my early years of graduate school. I thank the senior members of the groups, Karthik, Tiziana, Dan, and Rachel for always providing support. I also want to thank Paresh and Priya for giving me helpful feedback on my research, presentations, and my thesis chapters, and Paresh especially for sharing his scientific knowledge and always helping and encouraging other group members. I also appreciate the people who shared the synthesis area with me: Orland, Andy, and Hyesoo. I thank Jinmo for co-TAing ChE103 with me. I thank undergraduate student Derek Poletti who worked with me during the summer of 2021 on synthesizing polymers together. I also thank our group's administrative staff members: Abigail McCann and Christine Jary. Lastly, I would like to thank my parents and my sister for their support and love. I could not have finished my Ph.D without my family's unconditional support and encouragement.

ABSTRACT

Ultralong linear polymers are well known to be useful in a variety of applications such as mist control[1,2], drag reduction[3,4], and agricultural spray drift control[5]. However, the application of ultralong linear polymers is limited by shear degradation of the ultralong polymer chains that occurs under strong flow conditions. To overcome the issue of shear degradation, our group previously designed long end-associative polymers that can self-assemble into megasupramolecules ($M_w > 2000$ kg/mol) in low polarity solvents like jet fuel. The previously developed long end associative polymers had polycyclooctadiene backbones (1,4 polybutadiene) with carboxylic acid or tertiary amine end groups that associated via hydrogen bonding. They were shear degradation resistant and used as mist-control agents that provided fire-protection to jet fuel at concentrations as low as 0.3wt%.

Building upon the previous work, this thesis describes efforts toward expanding the applicability of long end-associative polymers. We first describe the design and synthesis of water-soluble long end-associative polymers for agricultural spray mist-control. We synthesized telechelic polyacrylamides using reversible addition fragmentation chain transfer (RAFT) polymerization. We explored two types of associations that can form stable supramolecules in water: host-guest interactions between adamantane and beta-cyclodextrin (Chapter 1), and metal-ligand association between terpyridine and transition metal ions (Chapter 2). Careful optimization of polymerization conditions allowed the synthesis of ultra-high molecular weight telechelic polyacrylamides with narrow polydispersity. We found that the terpyridine functionalized polyacrylamides with M_w 820 kg/mol could assemble into megasupramolecules ($M_w > 2000$ kg/mol) upon addition of Fe^{2+} or Ni^{2+}.

In Chapters 3 and 4, we return to long end-associative polymers in hydrocarbon solvents. In Chapter 3, we tackle the issue of poor solubility of the previous generation of associative PCODs in a highly nonpolar solvent, PAO. In Chapter 4, we develop a new generation of end groups for improved solubility and ease of synthesis.

Finally in Chapter 5, we discuss polyDODT (poly(3,6-dioxa-1,8-octanedithiol)), a polydisulfide that tends to form a mixture of linear and cyclic species. We present new methods to detect the presence of linear species in the mixture, as well as an alternative synthesis route for synthesis of polyDODT.

TABLE OF CONTENTS

LIST OF SCHEMATICS AND SCHEMES

Chapter 1

Chapter 2

Chapter 3

Chapter 4

Chapter 5

LIST OF FIGURES

LIST OF TABLES

Chapter 1

Water-soluble long linear supramolecular polymers based on host-guest interaction between beta-cyclodextrin and adamantane functionalized polyacrylamides

1.1 Introduction

1.1.1 Background

Development of long end-associative polymers in hydrocarbon solvents

Ultralong linear polymers (weight-average molecular weight M_w > 1M g/mol) are well known to be useful in a variety of applications such as mist control[1,2], drag reduction[3,4], and agricultural spray drift control[5]. However, the application of ultralong linear polymers is limited by the shear degradation of the ultralong polymer chains that occurs during routine handling of fluids such as pumping and passing the solution through various pipe fittings and orifices. Once the polymers are degraded into shorter chains, they quickly lose their efficacy and become ineffective[3,6,7]. To overcome the issue of shear degradation of ultralong linear polymers, our group previously reported the synthesis of long end-associative polymers that can self-assemble into megasupramolecules (M_w > 2000 kg/mol) in low polarity solvents like jet fuel.[4] Dr. Ameri David developed a model that predicted the distribution of individual end-functional polymers among cyclic and linear supramolecules (ring-chain equilibrium).[4,8] The theoretical model predicted that ultrahigh molecular weight supramolecules could be formed at low total polymer concentration if the backbones are long (M_w > 400 kg/mol for polycyclooctadiene) with appropriate end association strength of 16-18 kT. Dr. Jeremy (Ming-Hsin) Wei synthesized polycyclooctadiene (PCOD) backbones with M_w > 670 kg/mol and end groups that can associate via charge-assisted hydrogen bonds with total association strength of 16-18 kT.[4,9] The synthesized long end-associative polymers indeed showed the formation of ultralong linear supramolecules with an effective molecular weight of M_w ~2200 kg/mol, at concentrations as low as 0.3 wt%. The polymers survived repeated pumping through a fuel pump and showed long-lasting anti-misting ability in jet-A-fuel. Our group's previous work established a reliable protocol for the synthesis of high molecular weight telechelic PCOD with high end group fidelity. Before our group's work, the previously reported molecular weight of the longest telechelic PCOD in literature was M_n=196 kg/mol[10], and our group was able to synthesize longer telechelic PCOD only after careful purification of the monomer *cis,cis*-1,5-cyclooctadiene and optimization of polymerization conditions.

After establishing a method for long telechelic polymers optimized for hydrocarbons and fuels, we continued to work on expanding the applicability of the megasupramolecules to be useful in wider range of solvents and applications. The previous version of the megasupramolecules was specifically designed to work as an anti-misting agent in jet fuel, which is a mixture of both aliphatic and aromatic hydrocarbons. We expanded the use of the previously developed megasupramolecules to extremely non-polar lubricants like polyalphaolefin (Chapter 3) and designed a new end group for improved solubility and ease of synthesis (Chapter 4).

Need for megasupramolecules in water

In addition to continuing to work with megasupramolecules in hydrocarbon solvents, we sought to design water-soluble long end-associative polymers for potential use in aqueous solutions. Developing water-soluble long end-associative will be beneficial to both industrial and agricultural applications where drag reduction and mist-control of aqueous solutions are necessary.

One specific example is in agricultural sprays, where the control over droplet size is necessary for two main reasons. Fine droplets with average diameter 50-200 μm can drift away in the wind and lead to eventual overuse of agrochemicals and contamination of the nearby soil and water sources.[5,11] Large droplets tend to rebound or shatter and fall off of targeted plant leaves, often leaving less than 50% of the initial spray retained on the leaves.[12] While ultrahigh molecular weight polymers like polyacrylamide (PAM) and poly(ethylene oxide) (PEO) are commonly used to minimize the spray drift, these ultralong polymers suffer from mechanical chain degradation, making it difficult to control the size of the droplets. Therefore, we tried to design water-soluble long end-associative polymers to resist shear degradation when used as water-soluble polymeric additives for agricultural spray applications.

Chosen polymer backbone: Polyacrylamide (PAM)

As discussed in our group's previous work on long end-associative polymers in hydrocarbons, the length of the individual chains plays a crucial role in the final ratio of ultralong linear supramolecules and cyclic species in solution. Therefore, we wanted to work with a polymer backbone that can be easily synthesized with molecular weight control over a large range. We chose to work with polyacrylamide as our polymer backbone since it is already widely used for agricultural applications[5] and there are several established polymerization techniques for the synthesis of PAM. While controlled free radical polymerization methods like reversible addition-fragmentation chain-transfer (RAFT)[13], atom transfer radical polymerization (ATRP)[14], and nitroxide mediated polymerization

(NMP)[15] can be used to make polyacrylamide, we chose RAFT polymerization since it does not require a metal catalyst like ATRP, and telechelic polymers can be synthesized using an appropriately functionalized RAFT chain transfer agent.

Supramolecular chemistry in water

There has been ongoing research in supramolecular chemistry in the last two decades, and several review articles highlight the recent progresses.[16–20] However, conducting supramolecular chemistry in water is not easy. Polar interactions such as hydrogen bonding and donor-acceptor interactions are relatively weak due to competition from the solvent. Moreover, many water-soluble molecules are difficult to work with using standard organic synthesis methods due to the limited solubility of the molecules in common organic solvents. While searching for a new associative end group for the long telechelic polymers, we considered association strength, ability to form pairwise association, ease of synthesis, and scalability. Based on these considerations, we decided to focus on host-guest chemistry (Chapter 1) and metal-ligand association (Chapter 2). We considered a variety of host-guest pair systems that were known to form stable complexes in water, and a brief review of different host-guest pairs is described below.

Biotin-(strept)avidin

Biotin-(strept)avidin association is one of the most specific and stable non-covalent interactions (avidin K_a 1.3×10^{15} M^{-1}, streptavidin K_a 4×10^{17} M^{-1}).[21] However, both avidin and streptavidin contain four biotin binding sites, so the biotin-(strept)avidin pair was not suitable for forming 1:1 end association for formation of ultralong linear supramolecules.

Cucurbituril host

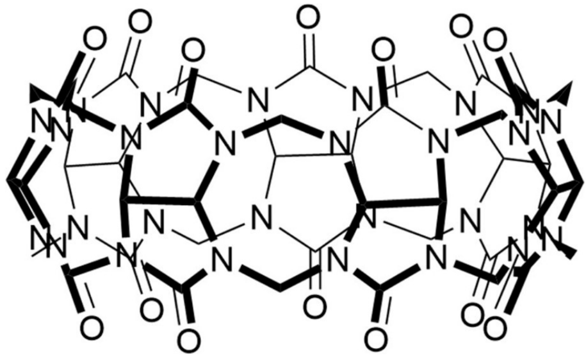

Scheme 1.1 Structure of Cucurbit[7]uril

Cucurbiturils are a family of macrocycles made by a condensation reaction between glycoluril (tetrahydroimidazo[4,5-d]imidazole-2,5(1H,3H)-dione) and formaldehyde. The number of glycoluril units can be 5-14, with 5,6,7,8 and 10 being more common.[22] Cucurbiturils are known as suitable hosts for a variety of neutral and ionic species.[23] The hydrophobic guest molecules interact with the hydrophobic cavity of cucurbiturils, while cationic guests utilize ion-dipole forces.[24] Among the different cucurbit[n]urils, cucurbit[6]uril (CB6) and cucurbit[7]uril (CB7) are known as excellent hosts for a variety of guest molecules. For example, CB7 can form stable 1:1 inclusion complexes with adamantanes, diamantanes, bicyclooctanes, ferrocene, and cobaltocene (K_a=10^3-10^{17} M).[22] Cucurbit[8]uril (CB8) has a large inner cavity and typically forms 2:1 inclusion complexes with bi or tricyclic species like naphthyl alanine or acridine orange.[25] While CB6 or CB7 would be ideal host molecules for achieving stable pairwise inclusion complexes in water, chemically modifying CB6 or CB7 to incorporate these molecules into the polymer ends is a difficult task. There are no reliable commercial sources for pure cucurbit[n]urils, and the synthesis of cucurbit[n]urils requires reacting glycoluril with formaldehyde in strong acids (H_2SO_4 or HCl), and heating to 75-110°C, and the reaction condition determines the ratio of the final products (CB5-8).[26] Isolation of pure CB[n] from the isomers requires chromatographic separations. Furthermore, the solubility of the CB homologues in common solvents is low (CB[7] solubility in water is only 2-3 x 10^{-2} M), requiring acidic aqueous solutions or aqueous solutions containing alkali metal ions.[26] In addition to CB[n]'s poor solubility in common organic solvents, introducing a single reactive functional group on the surface of CB is an even more challenging task.[26]

Beta cyclodextrin host

Cyclodextrins (CD) are cyclic oligomers of glucopyranose units linked by α-(1-4)-glycosidic bonds. Depending on the number of glucopyranose units, they are classified as α-CD (6), β-CD (7), or γ-CD (8). Like CBs, CDs have a toroid structure with interior hydrophobic cavities and exterior hydrophilic rims, and a tendency to form solid inclusion complexes with a wide variety of solid, liquid and gaseous compounds.[27] CDs are widely used in various applications like drug-delivery[27], chromatography[28], cosmetics and fragrances[29], and catalysis[30]. The association between β-CD and adamantane derivatives is one of the most widely studied host-guest pairs for the formation of supramolecular structures due to the wide availability of the molecules and a good size match.[31–33]

Beta cyclodextrin and adamantane derivatives have a high association equilibrium constant in water with $K_a = 10^4 - 10^5$ at 25°C.[34,35] Unmodified β-CD has limited solubility in pure water (18.5 g/L) because the hydroxyl groups are optimally arranged on the rims to form strong intramolecular hydrogen bonding interactions that result in inadequate hydration by water molecules.[36] However, aqueous solubility can be increased significantly once the β-CD molecules are functionalized.[37] For example, even replacing one hydroxyl group on the primary hydroxyl rim with a mercapto group can increase aqueous solubility from 18.5 g/L to 220 g/L.

Therefore, we decided to work with β-CD as our host molecule in our efforts toward synthesizing long end-associative polymers because it satisfied the criteria we looked for. For the guest molecule, we decided to work with adamantane, also due to low cost, ease of availability, and good size match with the inner hydrophobic cavity of β-CD.[35]

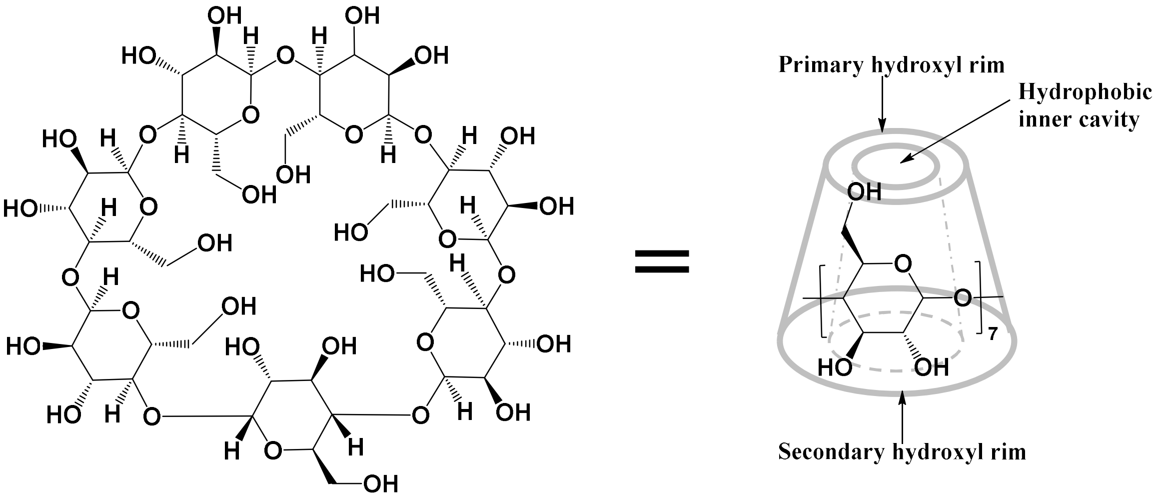

Scheme 1.2 Structure of β-CD

1.1.2 Scope of the present work

In prior literature, most of the work related to introducing β-CD and adamantane groups into polymers was mainly for the formation of hydrogels for biomedical applications.[38–42] The polymers were typically short (Mw < 50kg/mol), and used at high concentrations (>>1wt%). Adamantane and β-CD inclusion complexes were achieved between i) adamantane-ended polymers and β-CD functionalized small molecules, ii) polymers functionalized with β-CD along the backbone and adamantane functionalized small molecules.

In this chapter, we describe several synthetic approaches we considered for synthesizing long telechelic polyacrylamides (M_w > 400kg/mol) with adamantane and β-CD groups suitable for the formation of ultralong linear supramolecules in water. We report a successful synthesis of long adamantane-ended polyacrylamide via light-initiated aqueous RAFT polymerization. We also report our efforts to synthesize long β-CD-ended polyacrylamides and the difficulties associated with working with β-CD. We tried three different synthetic approaches for synthesizing β-CD functionalized RAFT agents, but only one approach yielded reliable synthesis of polyacrylamides, albeit with less-than-optimal molecular weight control (PDI 1.5-1.9). Lastly, we measured shear viscosity of the polymer solutions (Ada PAM, β-CD PAM, and Ada: β-CD=1:1 PAM, and polymer solutions with excess β-CD molecules) to measure the extent of the formation of ultralong linear complexed polymers in solution.

1.2 Experimental

1.2.1 Materials and instrumentation

All chemical reagents were obtained from Sigma Aldrich at 98% purity or higher unless otherwise stated. All solvents were obtained from Sigma Aldrich, at ACS reagent grade or higher (> 99.5% purity) and used as received without further purification.

NMR spectroscopy

^{1}H-NMR spectra were obtained using a Varian Inova 500 spectrometer (500 MHz); spectra were recorded in $CDCl_3$, d-DMSO, and D_2O (purchased from Cambridge Isotope Laboratories). Chemical shifts were reported in parts per million (ppm) and were referenced to residual solvent resonances.

Gel permeation chromatography (GPC)

The molecular weights and dispersity index of the polymers were determined on a GPC system with an Agilent pump (G7110B), equipped with an autosampler (G7129A), a Wyatt DAWN 8 multi-angle laser light scattering detector (λ=658.9nm), a Wyatt Optilab refractive index detector (RI) (λ=658nm), and an Agilent PL Aquagel-OH MIXED-H column. Aqueous buffer was prepared containing 0.2M $NaNO_3$, with 200 ppm NaN_3. Filtered aqueous buffer was used as the eluent at the flow rate of 0.3mL/min at 25°C. The data were analyzed using Wyatt Astra 7 using the Zimm fitting formula with *dn/dc* = 0.1590 mL/g to obtain molecular weight (M_w, and M_n) for each polyacrylamide reported.

Rheology

The shear viscosity of the polymer solutions was measured using a strain-controlled rheometer TA ARES-RFS, equipped with a cone-plate geometry (angle 2°, diameter 50 mm) with shear rates ranging from 1 s^{-1} to 1000 s^{-1}. The data points below the shear rate of 2.5 s^{-1} were below the TA ARES-RFS rheometer torque limit (0.196 μNm), so viscosity values were reported for shear rates ranging from 2.5 s^{-1} to 1000 s^{-1}. Three replicates were measured to obtain the error bars (standard error).

Custom built visible light LED reactor for polymer synthesis

A custom photo-reactor was constructed to avoid heating the reaction vessel. A Chanzon 30W LED (λ_{peak}= 440-450nm) powered by a Chanzon 900mA constant current LED driver was attached to an aluminum heatsink (11 x 58.5 x 89 mm) using thermally conductive adhesive (MG Chemicals). A 70 mm computer CPU cooler fan (AMD) was attached to the back side of the aluminum heatsink, and the fan was connected to a 12V 2A DC power supply. An enclosure (28 cm x 18 cm x 13 cm) containing the light and the body of a round bottom flask was lined with aluminum foil. The LED-heat sink-fan was mounted through a wall in the enclosure.

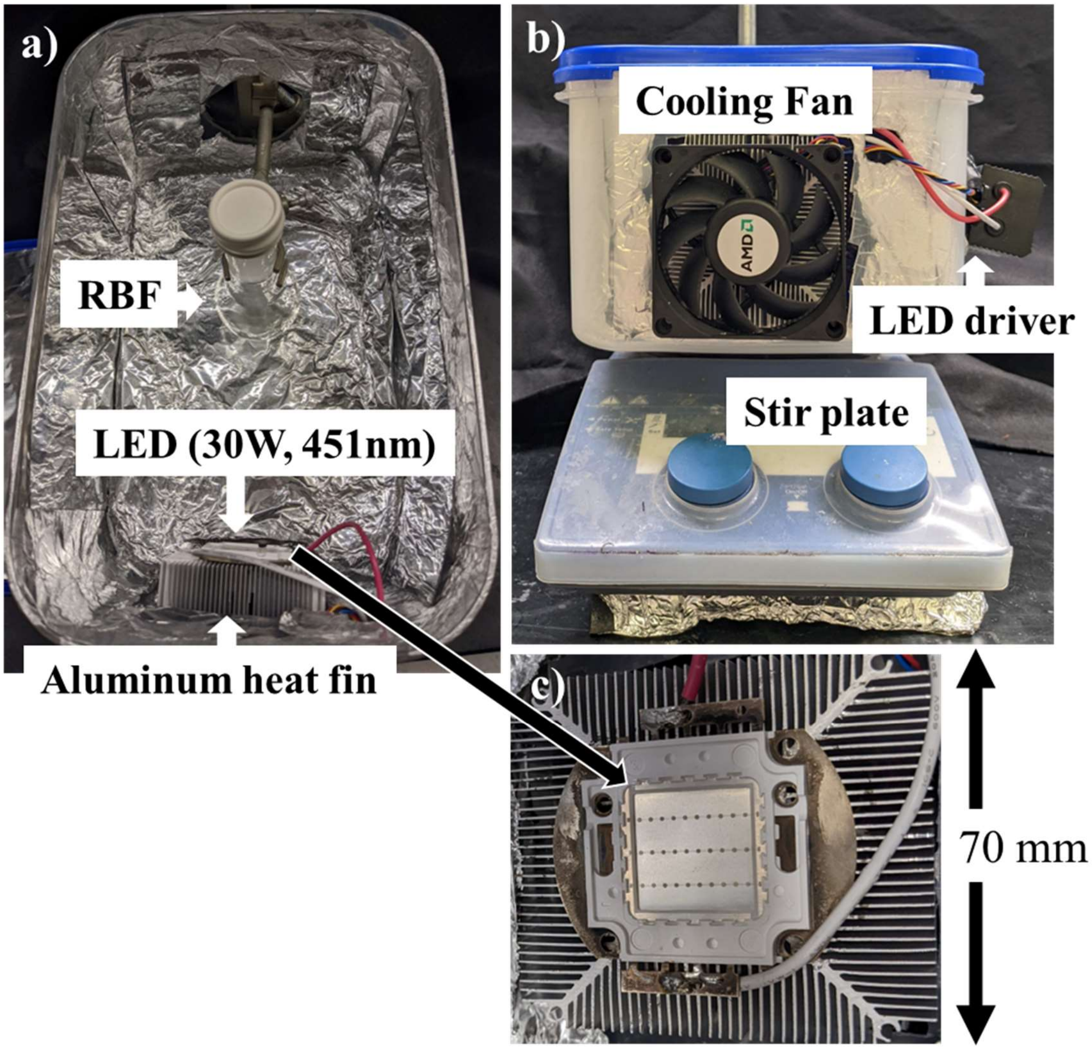

Figure 1.1 Photos of custom photopolymerization reactor with cooled 30 W LED (λ_{peak} = 451 nm), which enables reaction T < 35 °C as needed to prevent degradation of the trithiocarbonate RAFT iniferter. (a) Top view of an aluminum foil-lined enclosure (28 x 18 x 13 cm) that houses the clamp stand, clamp, and round-bottom flask (RBF) and has the LED array-heat sink assembly mounted through one wall. (b) Front view of the enclosure placed on a stir plate during use with the fan that cools the heat fins on the outside, facing the sash of the fume hood. (c) The LED array is mounted on the heat sink using thermally conductive adhesive.

1.2.2 Synthesis of RAFT agents and intermediates

Synthesis of 2-(((2-carboxyethyl)thio(carbonothioyl)thio))-2-methylpropanoic acid (CEMP)

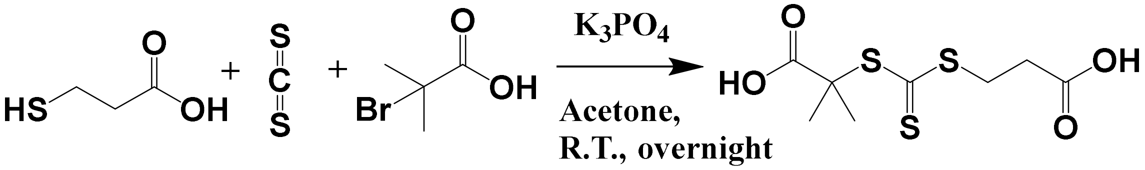

Scheme 1.3 Synthesis of 2-(((2-carboxyethyl)thio(carbonothioyl)thio))-2-methylpropanoic acid (CEMP) Procedure modified from[43]

In a 100mL round bottom flask, 30mL of acetone was added. K_3PO_4 (3 g, 14.1 mmol) was added to make a slurry. 3-mercapto propionic acid (1.5 g, 14.1 mmol) was added and the solution was stirred for 10 minutes. Carbon disulfide (3.23 g, 42.4 mmol) was syringe transferred into the flask. The solution became a yellow slurry. After 10 minutes, 2-bromo-2-methylpropionic acid (2.32 g, 13.9 mmol) was added to the flask, and the solution became a clear yellow liquid after 10 minutes. The mixture was stirred at room temperature overnight. The next day, the mixture was diluted with ethyl acetate (150 mL), washed with 1M HCl_{aq} twice (100 mL each time), and washed with saturated brine (100 mL) once in a 250 mL separatory funnel, and the organic phase was dried with $MgSO_4$ and filtered. Solvent was removed by rotary evaporation, and the yellow crude product was recrystallized in ethyl acetate and collected by filtration. The product was crushed into powder and washed with ethyl acetate. The yellow powder was dried under vacuum. Yield 35%.

^{1}H-NMR (DMSO, 500MHz) 1.60 (s, 6H), 2.65 (t, 2H), 3.45 (t, 3H)

Synthesis of S,S-bis(a, a'-dimethyl-a"-acetic acid) trithiocarbonate (BDMAT)

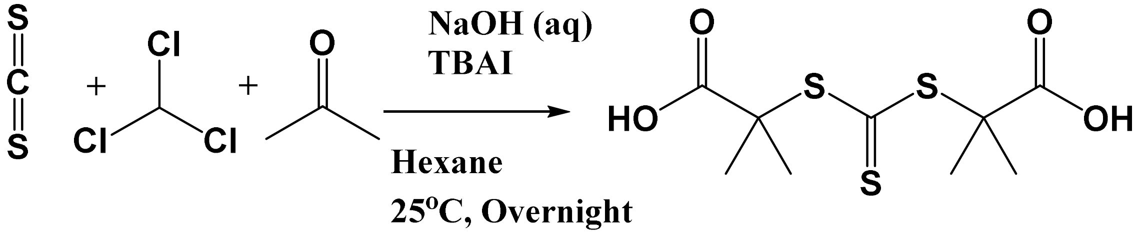

Scheme 1.4. Synthesis of S,S-bis(α, α'-dimethyl-α"-acetic acid) trithiocarbonate (BDMAT). Procedure modified from[44]

Carbon disulfide (4.4 g, 0.058 mol), chloroform (17.24 g, 0.144 mol), acetone (8.4g, 0.144 mol), and tetrabutylammonium iodide (0.43 g, 1.16 mmol) were mixed with 23 mL of n-hexane. The reaction flask was cooled with an ice bath. Aqueous sodium hydroxide solution (50%) was added slowly while keeping the temperature below 25 °C (measured with an IR temperature meter). The reaction mixture was removed from the ice bath after 2 hours and left to stir overnight. DI water (140mL) was added to dissolve the solid formed inside the flask, and 12M $HCl_{(aq)}$ was added slowly and stirred for 30 mins. The mixture was filtered, and the solids were washed thoroughly with DI water. The crude product was recrystallized twice in a mixture of acetone and hexane (4:1, v/v) to give the product as yellow crystals. Yield 11%.

Synthesis of adamantan-1-ylmethyl 2-bromo-2-methylpropanoate

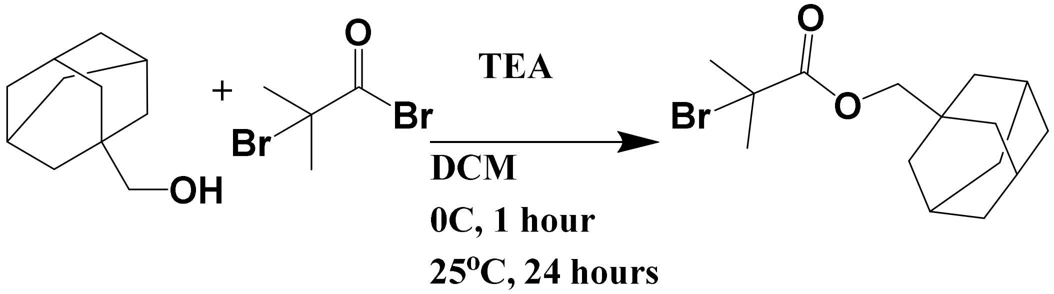

Scheme 1.5 Synthesis of adamantan-1-ylmethyl 2-bromo-2-methylpropanoate. Procedure modified from[45]

In a 100mL round bottom flask, 1-adamantane methanol (3 g, 18 mmol) and TEA (2.88 g, 28.5 mmol) were dissolved in dry DCM. The flask was placed in an ice water bath and stirred for 30 minutes. 2-bromoisobutyryl bromide (6.2 g, 27 mmol) was added dropwise over 1 hour. The reaction mixture was stirred at 0 °C for 1 hour and then stirred at room temperature for 24 hours. After 24 hours, the mixture was diluted with 100mL of DCM, and washed with 3M HCl_{aq} (100 mL), 3M NaOH solution (100 mL), and deionized water (100 mL) in a 250 mL separatory funnel. The organic phase was dried over anhydrous $MgSO_4$. The resulting brown solution was passed through a short plug of silica gel, and the solvent was removed via rotary evaporation. The product was obtained as white crystals. 88% yield.

^{1}H-NMR ($CDCl_3$, 500MHz) 1.56 (s, 6H), 1.63-1.75 (m, 6H), 1.94 (br, 6H), 2.00 (s, 3H), 3.7 (s, 2H)

Synthesis of bis(adamantan-1-ylmethyl) 2,2'-(thiocarbonylbis(sulfanediyl))bis(2-methylpropanoate) (Bis-adamantane BDMAT)

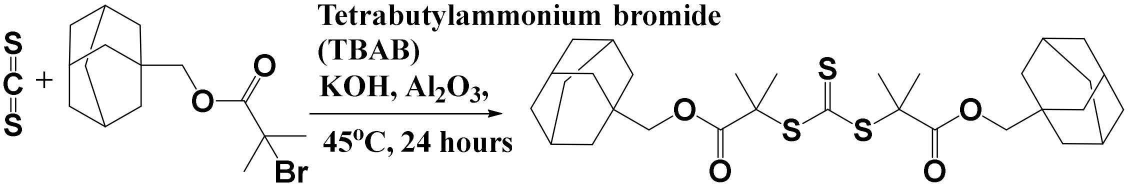

Scheme 1.6 Synthesis of bis(adamantan-1-ylmethyl) 2,2' -(thiocarbonylbis(sulfanediyl))bis(2-methylpropanoate) (Bis-adamantane BDMAT)

Adamantan-1-ylmethyl 2-bromo-2-methylpropanoate (2 g, 6.3 mmol) was dissolved in carbon disulfide (13g, 0.17mol) in a 50mL round bottom flask. Potassium hydroxide (1.06 g, 18.9 mmol) and tetrabutylammonium bromide (0.61 g, 1.89 mmol) were finely crushed into powder using a mortar and pestle. The powder was added to the mixture, and neutral alumina (2g) was added to the flask. The reaction was stirred at 45°C for 24 hours. The solution was dark orange initially and became a lighter orange after one day. The excess carbon disulfide was evaporated under reduced pressure, and the mixture was purified via silica gel flash column chromatography and eluted with ethyl acetate/hexane (1:9, v/v). Column chromatography was monitored by TLC (visualized with $KMnO_4$ stain). The solvent was removed via rotary evaporation; the yellow crude product was recrystallized in acetone twice to give clear yellow crystals as product. Yield 25%.

^{1}H-NMR ($CDCl_3$, 500MHz) 1.56 (s, 12H), 1.63-1.75 (m, 24H), 1.94 (br, 6H), 3.7 (s, 4H)

Synthesis of 2-(2-hydroxyethyl)-3a,4,7,7a-tetrahydro-1H-4,7-epoxyisoindole-1,3(2H)-dione (Furan protected maleimide alcohol)

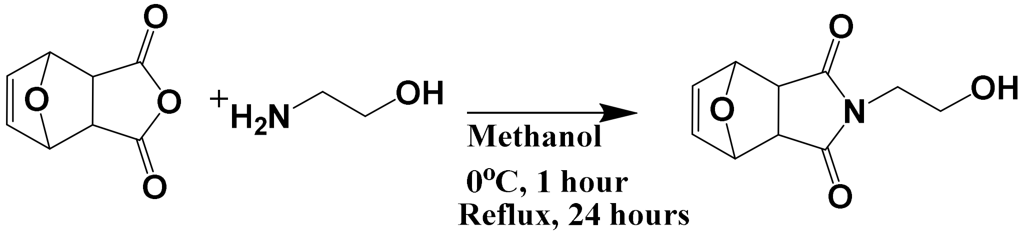

Scheme 1.7 Synthesis of 2-(2-hydroxyethyl)-3a,4,7,7a-tetrahydro-1H-4,7-epoxyisoindole-1,3(2H)-dione (Furan protected maleimide alcohol). Procedure modified from[46]

Exo-3,6-epoxy-1,2,3,6-tetrahydrophthalic anhydride (20 g, 0.12 mol) was suspended in 30 mL of methanol and cooled to 0°C. Ethanolamine (7.43 g, 0.122 mol) was dissolved in methanol (15 mL) and the solution was added to the flask dropwise. Cooling was removed and the reaction was warmed to room temperature and refluxed for 20 hours. After 20 hours, the reaction mixture was cooled to room temperature and stored in a refrigerator overnight to allow crystallization. The precipitate was collected by vacuum filtration and washed with diethyl ether. Yield 59%.

^{1}H-NMR (CDCl$_3$, 500MHz) 2.21 (bs, 1H), 2.92 (s, 2H), 3.79 (m, 2H), 5.31 (s, 2H), 6.55 (s, 2H)

Synthesis of 1-(2-hydroxyethyl)-1H-pyrrole-2,5-dione (maleimide alcohol)

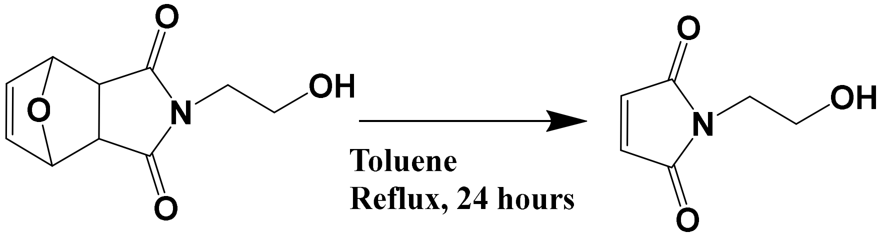

Scheme 1.8 Synthesis of 1-(2-hydroxyethyl)-1H-pyrrole-2,5-dione (maleimide alcohol). Procedure modified from[47]

Furan protected maleimide alcohol was deprotected by refluxing in toluene for 24 hours. Solvent was removed by rotary evaporation. The product was obtained as a white solid. Yield 80%.

^{1}H-NMR ($CDCl_3$, 500MHz) 3.73 (t, 2H), 3.79 (t, 2H), 6.74 (s, 2H)

Synthesis of bis-maleimide BDMAT

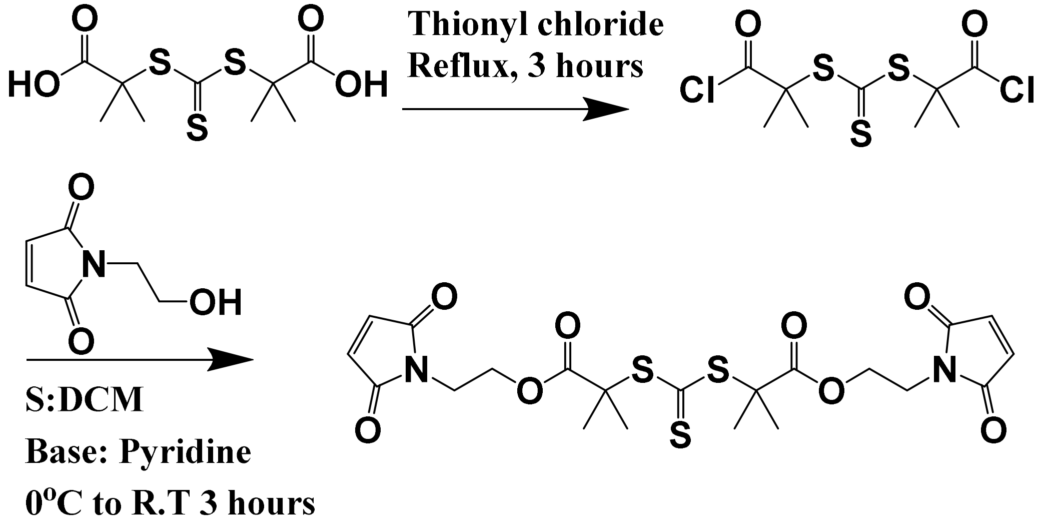

Scheme 1.9 Synthesis of bis-maleimide BDMAT. Procedure modified from[48]

BDMAT (0.5 g, 1.77 mmol) was refluxed in 15mL of thionyl chloride for 3 hours. The excess thionyl chloride was removed by vacuum distillation. The acid chloride form of the BDMAT intermediate was an orange solid. The intermediate product was dissolved in 20 mL of anhydrous DCM and pyridine (0.29 g, 3.72 mmol) was added. The mixture was cooled to 0 °C using an ice bath. Maleimide alcohol (0.52 g, 3.72 mmol) was dissolved in 10 mL of DCM and added to the reaction mixture dropwise under argon atmosphere. After the addition of maleimide alcohol, the mixture was allowed to warm to room temperature, and stirred for 3 hours. After 3 hours, the mixture was diluted with DCM (100 mL) and washed with DI water twice (100 mL each time) and once with saturated brine (100 mL). The organic phase was dried with $MgSO_4$ and filtered. The solvent was removed by rotary evaporation, and the crude product was further purified by recrystallization in ethyl acetate. Yield 60%.

^{1}H-NMR ($CDCl_3$, 500MHz) 1.64 (s, 12H), 3.81 (t, 4H), 4.26 (t, 4H), 6.76 (s, 4H)

Synthesis of bis-β cyclodextrin ended BDMAT (β-CD BDMAT)

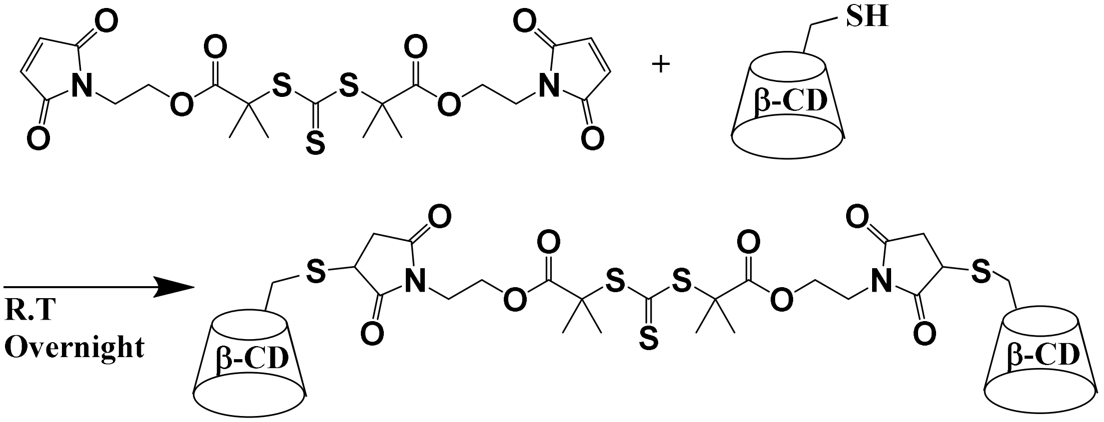

Scheme 1.10 Synthesis of bis-β cyclodextrin ended BDMAT (β-CD BDMAT)

Bis-maleimide BDMAT (0.1 g, 0.2 mmol) was dissolved in 15 mL of DMSO. Mono-(6-mercapto-6-deoxy)-β-cyclodextrin (purchased from BOC Sciences, NY, USA) (0.471 g, 0.41 mmol) was added to the reaction mixture. The mixture was stirred for 24 hours at room temperature. After 24 hours, the crude product was precipitated in acetone, dissolved in 10 mL of water, re-precipitated in acetone, and filtered via vacuum filtration. After washing the crude product with acetone, a yellow powder was obtained. To react the excess thiols remaining in the mixture, the crude product was reacted with maleimide (40 mg, 0.41 mmol) in 5 mL of DMSO for 24 hours and precipitated in acetone. The product was dissolved in 5 mL of DI water, reprecipitated in acetone twice, and dried under vacuum. The product was used for polymerization without further purification.

1.2.3 Polymer synthesis

Synthesis of bis-adamantane macro-RAFT agents (Ada mCTA)

Bis-adamantane BDMAT (50 mg, 86.37 µmol) and acrylamide (571 mg, 8.03 mmol) were dissolved in 1,4-dioxane (4 mL) in a 10mL Schlenk flask sealed with a rubber septum. The mixture was degassed by three freeze pump thaw cycles and the flask was filled with argon at the end. The degassed mixture was placed inside of the LED reactor on top of a stirring plate, and the mixture was set to stir at 200 rpm and irradiated. The irradiation was stopped after 2 hours because polymers started to precipitate out of the 1,4-dioxane. The reaction mixture was added to 200 mL of acetone dropwise and more polymers precipitated. The precipitated polymers were dried under vacuum. The polymers were obtained as a yellow powder, insoluble in water. Yield 16%, and M_n was typically ~1600g/mol.

The yellow powder (M_n=1615g/mol, 50mg, 31μmol) and acrylamide (1g, 14 mmol) were dissolved in DMSO (7mL) in a 25 mL round bottom flask. The mixture was degassed by bubbling argon for 15 minutes, the flask was placed inside the LED reactor on top of a stirring plate (Figure 1.1 b), and the mixture was set to stir at 200 rpm and irradiated for 4 hours. After 4 hours, the mixture was diluted with 10 mL of DI water. The polymers were precipitated in acetone (200 mL). After drying under vacuum, the polymers were obtained as slightly yellow and flaky solids. Yield 75%, typical M_n=24 kg/mol.

Representative procedure for synthesis of Adamantane-ended polyacrylamide (Ada-PAM)

Ada mCTA (M_n=24 kg/mol, 40 mg, 2.5 μmol) and acrylamide (1 g, 14 mmol) were dissolved in 7 mL of molecular biology grade water in a 50 mL round bottom flask. 0.1 N HCl_{aq} (0.1 mL) was added, and the flask was sealed with rubber septum. The mixture was degassed by bubbling argon for 15 minutes, the flask was placed inside of the LED reactor on top of a stirring plate, and the mixture was set to stir at 200 rpm and irradiated for 8 hours. The polymers were dissolved in 25 mL of DI water and precipitated in acetone (250 mL). After drying under vacuum, the polymers were obtained as white solids.

Representative procedure for synthesis of β-CD-ended polyacrylamide (β-CD-PAM)

β-CD BDMAT (16 mg, 5.71 μmol) and acrylamide (1 g, 14 mmol) were dissolved in 7 mL of water in a 50 mL round bottom flask. 0.1 N HCl_{aq} (0.1mL) was added, the mixture was degassed by bubbling argon for 15 minutes, and the flask was placed inside of the LED reactor and irradiated for 8 hours. The polymers were dissolved in 25 mL of DI water and precipitated in acetone (250 mL) to remove excess acrylamide. The polymers were further purified by dialyzing against DI water using Spectra Por 6 dialysis tubing with molecular weight cut-off of 3500 g/mol, following which the polymers were precipitated again in acetone (250 mL) and dried under vacuum. The polymers were obtained as white solids.

1.2.4 Solution preparation

1 wt% polyacrylamide solutions were prepared by dissolving the polymer in Milli-Q water in a 20 mL glass scintillation vial. 0.2 wt% polymer solutions were prepared by diluting the 1wt% solution with Milli-Q water in another 20 mL glass scintillation vial.

Ada: β-CD=1:1 solution was prepared by mixing the ada-PAM solution with β-CD-PAM solution (polymers have closely matching weight average molecular weight M_w) in a 1:1 ratio (w/w). The solutions were mixed at either 1 wt% or 0.2 wt% concentration.

The scintillation vials containing the mixture of polymer solutions were placed on a Wrist-Action Shaker (Burrell Scientific) for 1 hour and used for shear viscosity measurements.

For control polymer solutions containing ada-PAM or the mixture of ada-PAM and β-CD PAM, an excess amount (200 molar excess) of 2-hydroxypropyl-β-cyclodextrin (HP-β-CD) was added with respect to the amount of adamantane groups in solution (the number of adamantane groups was determined by using M_n of the polymer obtained from GPC). After adding HP-β-CD, the solutions were placed on the shaker for 1 hour and then used for shear viscosity measurements.

1.3 Results and discussions

1.3.1 Synthesis of RAFT agents and intermediates

Choosing a central structure for functionalized RAFT agent: CEMP vs. BDMAT

We synthesized two versions of RAFT agents: CEMP and BDMAT. Both RAFT agents were previously used to make polyacrylamides using light-initiated aqueous RAFT polymerization.[13,49] Despite the similar molecular structures of both CEMP and BDMAT, CEMP required a UV light source (λ=365nm) and resulted in a relatively high PDI of 1.4 - 1.6, in comparison to BDMAT, which allowed the synthesis of well controlled polyacrylamides (PDI < 1.1) with an LED visible light source (λ=451nm). Therefore, we chose to work with BDMAT as the central structure for adamantane or β-CD functionalized RAFT agents.

Adamantane functionalized BDMAT

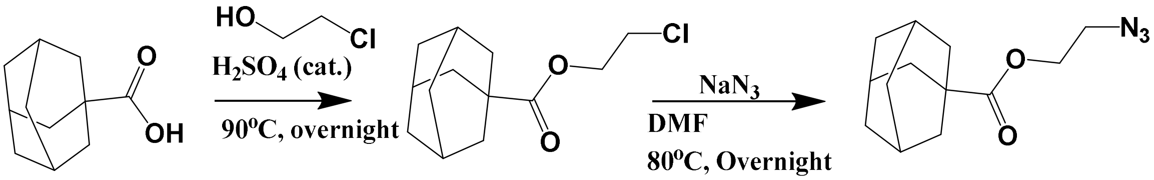

Scheme 1.11 Synthesis of 2-azidoethyl adamantane-1-carboxylate

We initially tried to synthesize adamantane BDMAT by copper-catalyzed azide-alkyne cycloaddition (CuAAC) between azide functionalized adamantane and alkyne functionalized BDMAT. We successfully synthesized azide functionalized adamantane in high yield without a need for chromatographic purification (Scheme 1.11). The main reason for trying

CuAAC reaction was because we were also trying to use alkyne functionalized BDMAT to make β-CD functionalized BDMAT by reacting it with β-CD-N_3. However, as described in the next section, the CuAAC reaction with β-CD molecules was extremely difficult despite numerous efforts to optimize the reaction conditions. Therefore, we looked for more straightforward method to synthesize adamantane functionalized BDMAT that involved fewer reaction steps.

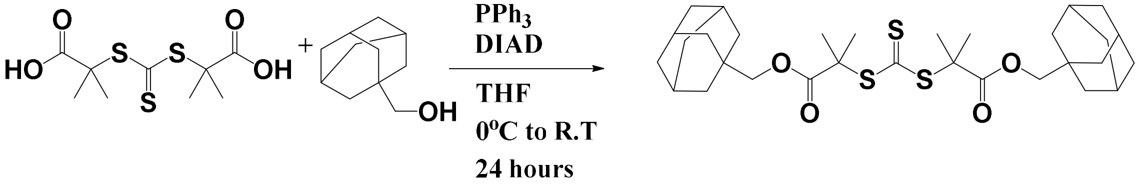

Scheme 1.12 Synthesis of adamantane-ended BDMAT using Mitsunobu reaction

We tried the Mitsunobu reaction between carboxylic acids of the BDMAT and commercially available adamantane alcohol (Schematic 1.12). However, a clean product was not obtained even after two rounds of flash column chromatography. Therefore, we looked for another method for the synthesis of adamantane functionalized BDMAT. We directly reacted CS_3^{2-} ions with adamantan-1-ylmethyl 2-bromo-2-methylpropanoate (Schematic 1.6). The intermediate product was easily obtained by reacting 1-adamantane methanol with 2-bromoisobutyryl bromide, without the need for chromatographic purification. This intermediate product can be used as an initiator for ATRP polymerization to synthesize mono adamantane functionalized polymers[50]. The intermediate product was reacted with CS_3^{2-} and purified by column chromatography followed by recrystallization in acetone, resulting in a pure product (Figure 1.4).

Synthesis of β-CD functionalized BDMAT

β-CD molecules contain multiple hydroxyl groups on both the primary and secondary rims. To obtain β-CD with one reactive group for further functionalization, most methods reported in the literature start with converting β-CD to mono-6-tosyl- β-cyclodextrin (TsO-CD).[51–53] Using TsO-CD, various functional groups like halides, azide, amine, and imidazole groups can be introduced, but the tosylation of β-CD results in randomly substituted products, and separating pure mono-substituted product can be very challenging due to similar physical properties.[51] Previously reported literature methods for purification typically used recrystallization in hot water, but when we tried this procedure, the final product was not completely pure. We obtained analytically pure TsO-CD by three rounds of recrystallization in a methanol/water mixture (1:1, v/v).[54] We then reacted TsO-CD with NaN_3 in water attempting to obtain mono-6-azide-deoxy-6-cyclodextrin (N_3-CD) following the protocol used by Tang and Ng.[55] We tried CuAAC reaction between N_3-CD and alkyne ended RAFT agents. We first followed typical reaction conditions, using $CuSO_4$ and ascorbic acid in DMF at room temperature for 48-72 hours, as previously reported in literature.[56–59] However, the reaction did not yield the desired product. We tried to optimize the reaction conditions by increasing the reaction time, temperature, and amount of copper catalyst, but our efforts were unsuccessful. Following previously reported work[60,61], we also tried using CuBr and N,N,N′,N″,N″-Pentamethyldiethylenetriamine (PMDETA) in degassed DMF at various reaction conditions, but failed to obtain the desired product.

While several studies in the literature claimed successful CuAAC reaction with β-CD derivatives, other researchers reported difficulties associated with performing CuAAC with β-CD derivatives with typical reaction conditions.[62,63] Jurczak and coworkers reported challenges due to copper catalysts being taken up by the hydrophobic cavity of β-CD.[62] The authors suggested generating Cu(I) in situ using sodium ascorbate, and performing the reaction under an inert atmosphere and adding tris[(1-benzyl-1*H*-1,2,3-triazol-4-yl)methyl]amine (TBTA).[62] TBTA is a tertiary amine with three 1,2,3-triazole groups, and it is a bulky ligand, so it should not enter the inner cavity of β-CD. We followed this reaction protocol, but the result was still unsatisfactory. Therefore, we looked for alternative methods to synthesize a β-CD functionalized RAFT agent. We chose maleimide-thiol chemistry due to the commercial availability of thiolated β-CD (β-CD-SH), and the mild reaction conditions required. The reaction between β-CD-SH and maleimide was reported in the previous literature to prepare hydrogels.[64–66]. Upon reacting maleimide functionalized BDMAT with a slight excess (~ 1.1 molar excess) of β-CD-SH, we observed the complete consumption of maleimide groups (Figure 1.5 (a)). The crude product was used without further purification (below).

1.3.2 Polymer synthesis

Polymers were synthesized using visible light initiated aqueous RAFT polymerization using a custom designed visible light LED reactor (Figure 1.1). The modified BDMAT RAFT agents are called iniferters (initiator + chain transfer agent) in the prior literature due to the fact that they act as both initiators and chain transfer agents for RAFT polymerization.[13] Using the iniferter is better than using exogeneous initiators like 4,4′-Azobis(4-cyanopentanoic acid) since we can eliminate any dead chains end capped with initiator molecules. The LED reactor was designed to provide sufficient light irradiation while keeping the reaction temperature below 35°C. The polymerizations were conducted in acidic water to minimize hydrolysis of acrylamides.[67] The effect of temperature and pH of the aqueous medium on RAFT polymerization of acrylamide will be discussed in detail in Chapter 2.

Bis-adamantane BDMAT was not soluble in water and was only marginally soluble in DMSO. To overcome this issue, we first synthesized a short molecular weight polymer in 1,4-dioxane, called a "macro CTA", abbreviated mCTA. The polymers were precipitated as a yellow powder in acetone. The obtained short polymer was still not soluble in water (M_n 1600 g/mol), so we performed another chain extension reactions in DMSO. After chain extension in DMSO, we were able to use the resulting polymer (M_n 24 kg/mol) as a macro chain transfer agent (mCTA) for aqueous RAFT polymerization to make polymers with a desired molecular weight with a narrow polydispersity (Table 1). For Ada-PAM with M_w = 80 kg/mol, we analyzed the molecular weight via both ^{1}H-NMR and GPC, and the number averaged molecular weights agreed well (77 kg/mol vs. 78 kg/mol) (Figure 1.6).

β-CD-BDMAT was soluble in water, so aqueous RAFT polymerization was possible without the need for the synthesis of mCTA. However, the polydispersity of the synthesized polymers was relatively high (>1.5). We suspected residual β-CD-SH as a potential cause of broad polydispersity, so we tried consuming the free thiols remaining in the crude product mixture by reacting them with excess maleimides, following which the product was purified by repeated precipitation in acetone to remove unused maleimides. However, even after this additional step, the polymers still had high PDI, similar to before. Lastly, making relatively short β-CD-PAM (M_w near 30 kg/mol) was difficult due to the excessive foaming of the aqueous reaction mixture when trying to degas by bubbling argon (Figure 1.2).

Table 1.1 Molecular weight characterization (kg/mol) of the telechelic PAMs (GPC)

	M_n	M_w	PDI
Ada 80k	78	80	1.03
Ada 462k	448	462	1.03
Ada 727k	675	727	1.08
Ada 1.08M	932	1077	1.15
Ada 1.56M	1391	1560	1.12
β-CD 471k	248	471	1.90
β-CD 548k	324	548	1.69
β-CD 824k	434	824	1.90
β-CD 1.36M	727	1361	1.87

Figure 1.2. Excessive foaming inside of the flask when degassing an aqueous reaction mixture containing β-CD-BDMAT in high concentrations (>0.5 mg/mL).

1.3.3 Viscosity measurements

With the caveat that β-CD-PAM should be regarded as "putative" β-CD-PAM with unknown fraction of mono-functionalized chains (unintended termination must have occurred as high PDI > 1.6 is observed), we compared the viscosities of ada-PAM, β-CD-PAM, and ada-PAM:β-CD-PAM=1:1 mixture (Figure 1.3). For both molecular weights (470k and 800k), we saw an increase in viscosity upon mixing the ada-PAM and β-CD-PAM solutions especially at low shear rates (< 10 s^{-1}). We wanted to see if the increase in the viscosity was due to the complexation between adamantane and β-CD end groups, so we added a 200- fold excess of a highly water-soluble form of β-CD to these solutions to mask the complexation between the polymer end groups. Specifically, we used hydroxypropyl-β-CD (HP- β-CD) functionalized with 0.5 to 1.3 HP groups per glucose ring because it is readily soluble in water unlike pure β-CD, enabling us to add β-CD molecules without diluting the polymer solutions. We also added HP-β-CD to ada-PAM solutions because ada-PAM can also self-associate via weak hydrophobic interactions between adamantane molecules. Upon addition of HP-β-CD, the specific viscosities ($\eta_{specific} = \eta_{solution}/\eta_{solvent} - 1$) of ada-PAM and ada-PAM: β-CD-PAM=1:1 solutions decreased, suggesting that the higher viscosities of ada-PAM: β-CD-PAM=1:1 solutions especially at low shear rates ($< 10\ s^{-1}$) were due to complexation between adamantane and β-CD. Our group's previous work showed that longer backbones favor the formation of longer supramolecules by suppressing the formation of small cyclic supramolecules.[4,8,9] Between polymers with M_w ~470 kg/mol and M_w~ 800 kg/mol, using higher molecular weight telechelic PAM resulted in a higher increase in viscosity upon mixing ada-PAM with β-CD-PAM, in agreement with the trend observed in our group's previous work. This effect is independent of complexation, as a 200-fold excess of HP-β-CD gives a viscosity that is not significantly lower than that of Ada+β-CD in Figure 1.3b.

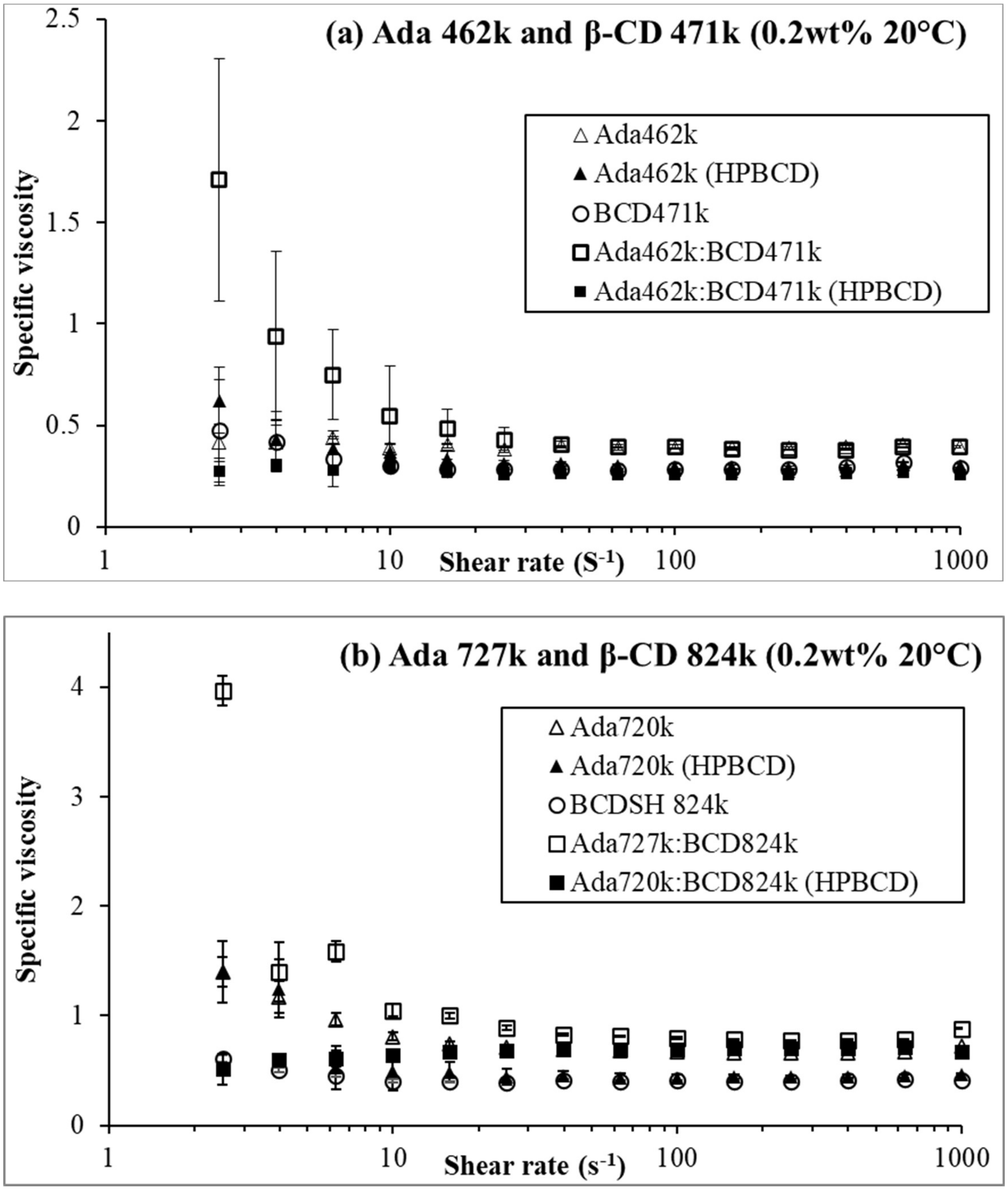

Figure 1.3 Specific viscosity ($\eta_{specific}$) of adamantane or β-cyclodextrin (β-CD) functionalized polyacrylamide at 0.2 wt% polymer concentration in water at 20 °C. $\eta_{specific} = \eta_{solution}/\eta_{solvent} - 1$. HP-β-CD is 2-hydroxypropyl-β-cyclodextrin, a highly water-soluble version of free β-CD. HP-β-CD was added in excess to mask the association between the adamantane PAM and β-CD PAM. (a) Adamantane PAM with $M_w = 462$ kg/mol, and β-cyclodextrin PAM with $M_w = 471$ kg/mol. (b) Adamantane PAM with $M_w = 727$ kg/mol, and β-cyclodextrin PAM with $M_w = 824$ kg/mol.

1.4 Conclusion

In this chapter, we described the synthesis of water-soluble linear supramolecular polymers based on host-guest interactions between β-CD-PAM and ada-PAM. We successfully synthesized adamantane functionalized BDMAT RAFT iniferter and used it to synthesize well-controlled high molecular weight ada-PAM using aqueous light-initiated RAFT. We chose β-CD as our host molecule due to its ease of availability and low price in comparison to other possible host molecules known to form stable inclusion complexes in water. We tried synthesizing β-CD-BDMAT via CuAAC reaction between β-CD-N_3 and alkyne functionalized BDMAT, but our attempts were unsuccessful despite numerous attempts to optimize the reaction conditions. We obtained β-CD-BDMAT via a thiol-maleimide reaction between β-CD-SH and maleimide BDMAT. Using β-CD-BDMAT, we were able to synthesize β-CD-PAM with various molecular weights, but the polymers had relatively high polydispersity of about 1.8.

To our knowledge, the synthesized polymers for this chapter are the first examples of high molecular weight (M_w > 400 kg/mol) telechelic polymers with either adamantane or β-CD end groups. Upon mixing the ada-PAM solution with β-CD-PAM solution, we saw an increase in $\eta_{specific}$ of the polymer solution, suggesting that the formation of supramolecular complexes occurred between the polymer end groups.

While our preliminary data suggests that it could be possible for these polymers to form supramolecular complexes in water, further work would be required for using these polymers in agricultural spray applications. In particular, improving synthesis methods for making both ada-PAM and β-CD-PAM at scale would be necessary but would also be challenging. Due to the hydrophobicity of adamantane, high M_w ada-PAM could only be obtained after 3 step polymerizations involving two chain extensions. β-CD derivatives have low solubility in common organic solvents, so purification of β-CD-BDMAT using common organic chemistry techniques was not possible, and reactions were inefficient (e.g., CuAAC) possibly due to the bulky nature of β-CD. Furthermore, tuning the properties of the complexed polymer solutions would be more difficult in applications. For example, if we need to increase the strength of the end-association between the polymers, we would need to attach more than one β-CD or adamantane to each end of the polymers. A tetra-adamantane RAFT agent would be even more hydrophobic than the bis-adamantane RAFT agent described in this chapter, so aqueous RAFT polymerization with this molecule would be even more challenging. For synthesis of tetra-β-CD RAFT agent, attaching two β-CD groups on one side would also be more difficult due to the bulkiness of the β-CD molecules.

Therefore, it would be more practical to consider using different end groups for water-soluble associative polymers. In the next chapter, we describe the synthesis of terpyridine ended polyacrylamides that can coordinate with transition metal ions to form ultralong linear supramolecular polymers in water.

1.5 Supplementary data

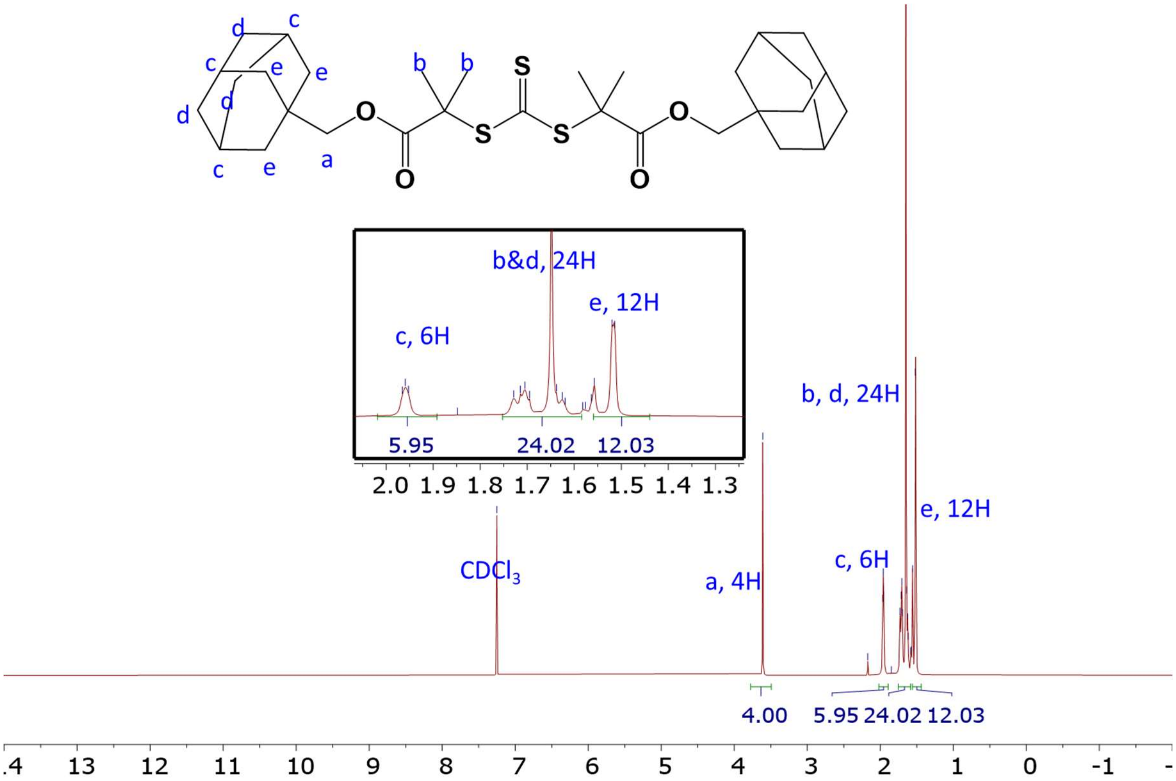

Figure 1.4. ^{1}H-NMR spectra of adamantane functionalized BDMAT RAFT agent in $CDCl_3$.

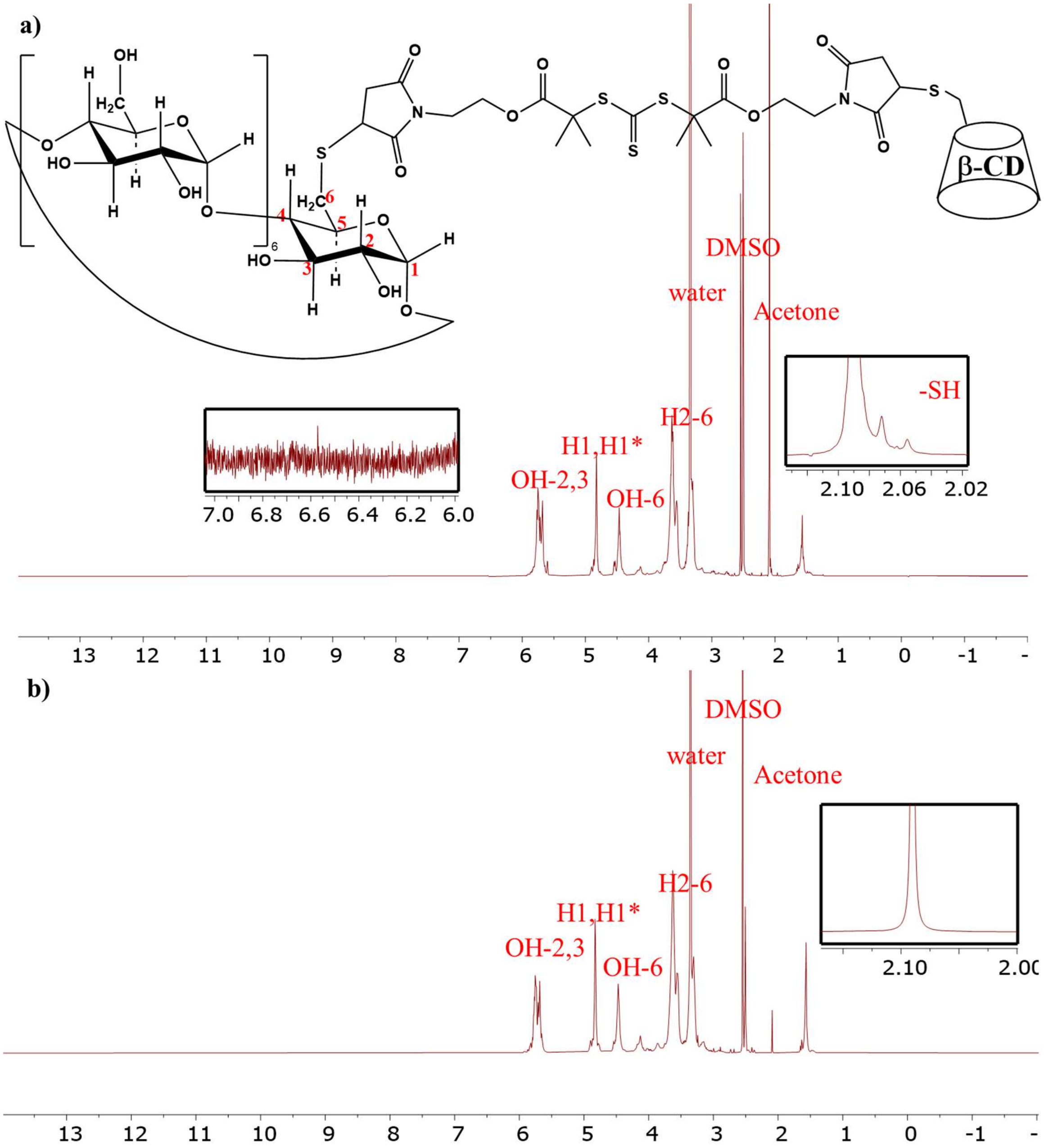

Figure 1.5. ^{1}H-NMR of β-CD functionalized RAFT agent **(a)** ^{1}H-NMR of crude product. Insets show complete disappearance of maleimide peaks (6.76 ppm) and presence of free thiol (2.09 ppm) **(b)** After reaction with excess maleimide to remove free thiols.

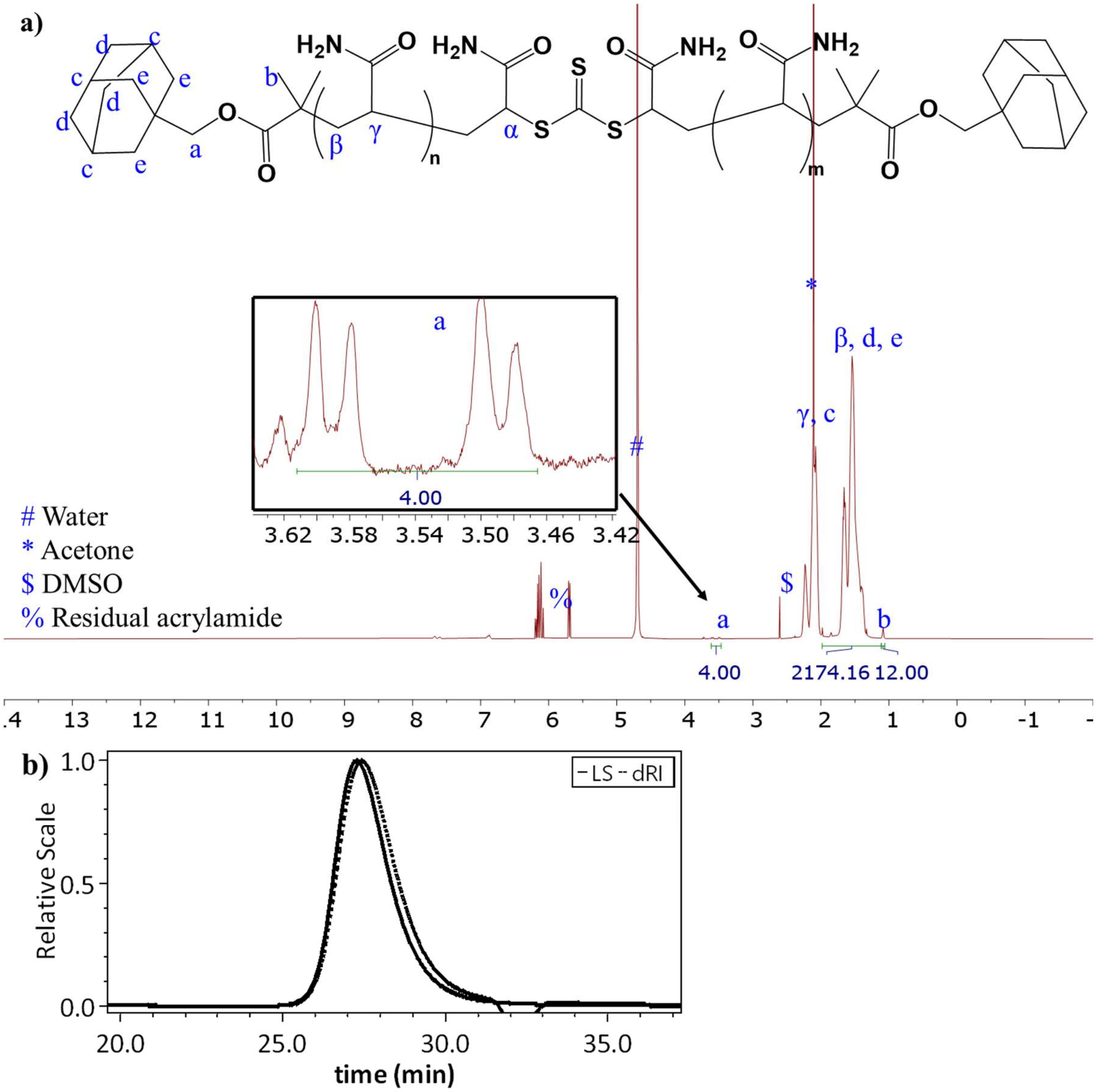

Figure 1.6. Molecular weight characterization of adamantane functionalized polyacrylamide with M_w = 80 kg/mol **(a)** ^{1}H-NMR spectra of adamantane functionalized polyacrylamide in D_2O **(b)** GPC chromatogram of the same polymer (entry 2 of table 1)

$M_{n,NMR}$ for polymer = (H's for β)/2* $M_{\text{repeat unit}}$+ $M_{\text{end groups}}$

From the structure of adamantane, doubled to account for groups at both ends of the chain d+e=24H. From the integration of the peak β+d+e, subtract off the contribution due to d+e to obtain β = 2174.16-24 = 2150.16H. $M_{\text{end groups}}$ = 578.89 g/mol, and $M_{\text{repeat unit}}$ = 71.08 g/mol. $M_{n,NMR}$ for polymer = (2150.16)/2*71.08+578.89 = 77000 g/mol

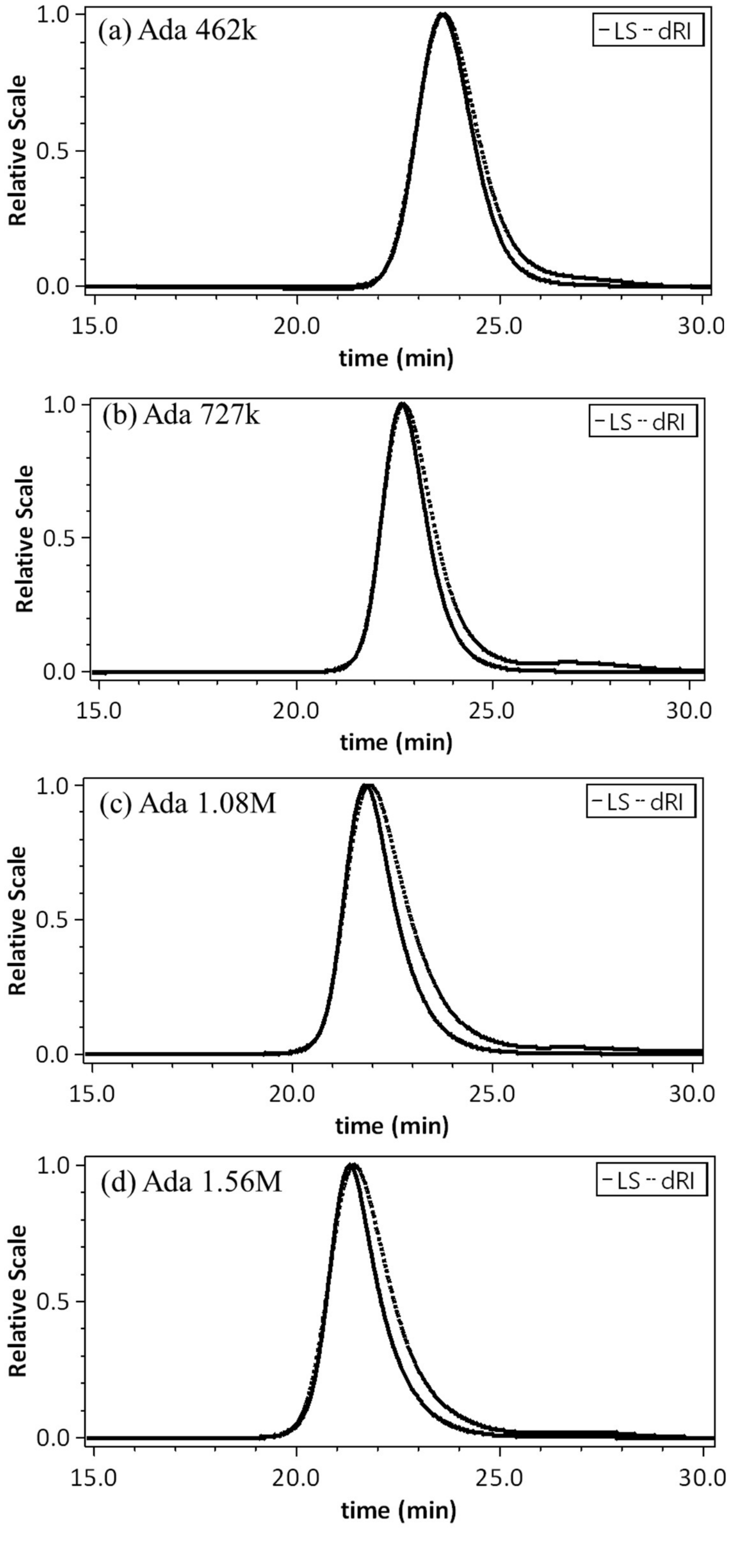

Figure 1.7. GPC chromatograms of adamantane functionalized PAM (a) M_w 462 kg/mol (b) M_w 727 kg/mol (c) M_w 1.08 Mg/mol (d) M_w 1.56 Mg/mol

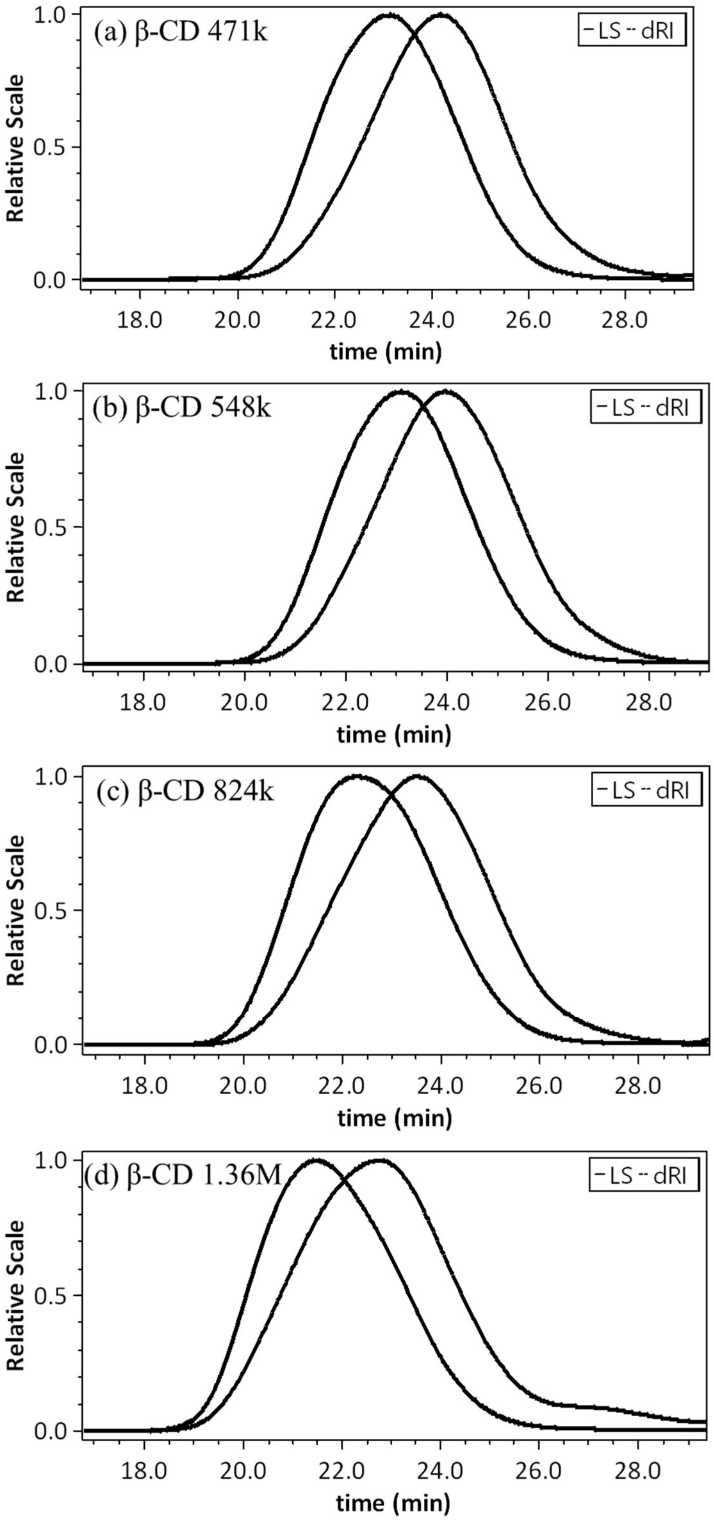

Figure 1.8. GPC chromatograms of β-CD functionalized PAM (a) M_w 471 kg/mol (b) M_w 548 kg/mol (c) M_w 824 Mg/mol (d) M_w 1.36 Mg/mol

References

1. McKinley, G. H. & Sridhar, T. Filament-Stretching Rheometry of Complex Fluids. *Annu. Rev. Fluid Mech.* **34**, 375–415 (2002).
2. Chao, K. K., Child, C. A., Grens, E. A. & Williams, M. C. Antimisting Action of Polymeric Additives in Jet Fuels. *AIChE J.* **30**, 111–120 (1984).
3. Paterson, R. W. & Abernathy, F. H. Turbulent Flow Drag Reduction and Degradation with Dilute Polymer Solutions. *J. Fluid Mech.* **43**, 689–710 (1970).
4. Wei, M.-H. *et al.* Megasupramolecules for Safer, Cleaner Fuel by End Association of Long Telechelic Polymers. *Science (80-.).* **350**, 72–75 (2015).
5. Lewis, R. W., Evans, R. A., Malic, N., Saito, K. & Cameron, N. R. Polymeric Drift Control Adjuvants for Agricultural Spraying. *Macromol. Chem. Phys.* **217**, 2223–2242 (2016).
6. Fisher, D. H. & Rodriguez, F. Degradation of drag-reducing polymers. *J. Appl. Polym. Sci.* **15**, 2975–2985 (1971).
7. Sung, J. H. *et al.* Turbulent Drag Reduction Efficiency and Mechanical Degradation of Poly(Acrylamide). *J. Macromol. Sci. Part B* **43**, 507–518 (2004).
8. Leonard, R. & David, A. Associative Polymers as Antimisting Agents and Other Functional Materials via Thiol-Ene Coupling. (California Institute of Technology, 2008).
9. Wei, M.-H. Synthesis and Potency of Long End-Associative Polymers for Mist Control. (California Institute of Technology, 2014).
10. Ji, S., Hoye, T. R. & Macosko, C. W. Controlled Synthesis of High Molecular Weight Telechelic Polybutadienes by Ring-Opening Metathesis Polymerization. *Macromolecules* **37**, 5485–5489 (2004).
11. Hilz, E. & Vermeer, A. W. P. Spray drift review: The Extent to Which a Formulation Can Contribute to Spray Drift Reduction. *Crop Prot.* **44**, 75–83 (2013).
12. Bergeron, V., Bonn, D., Martin, J. Y. & Vovelle, L. Controlling Droplet Deposition with Polymer Additives. *Nature* **405**, 772–775 (2000).
13. Carmean, R. N., Becker, T. E., Sims, M. B. & Sumerlin, B. S. Ultra-High Molecular Weights via Aqueous Reversible-Deactivation Radical Polymerization. *Chem* **2**, 93–101 (2017).
14. Jones, G. R. *et al.* Rapid Synthesis of Well-Defined Polyacrylamide by Aqueous Cu(0)-Mediated Reversible-Deactivation Radical Polymerization. *Macromolecules* **49**, 483–489 (2016).
15. Rigolini, J., Grassl, B., Billon, L., Reynaud, S. & Donard, O. F. X. Microwave-Assisted Nitroxide-Mediated Radical Polymerization of Acrylamide in Aqueous Solution. *J. Polym. Sci. Part A Polym. Chem.* **47**, 6919–6931 (2009).
16. Kataev, E. A. & Müller, C. Recent Advances in Molecular Recognition in Water: Artificial Receptors and Supramolecular Catalysis. *Tetrahedron* **70**, 137–167 (2014).
17. Oshovsky, G. V., Reinhoudt, D. N. & Verboom, W. Supramolecular Chemistry in Water. *Angew. Chemie Int. Ed.* **46**, 2366–2393 (2007).
18. Teresa Albelda, M., Frías, J. C., García-España, E. & Schneider, H.-J. Supramolecular complexation for environmental control. *Chem. Soc. Rev.* **41**, 3859 (2012).
19. Stefan Kubik. *Supramolecular Chemistry in Water*. Wiley-VCH (2019).

20. Biros, S. M. & Rebek, Jr., J. Structure and Binding Properties of Water-Soluble Cavitands and Capsules. *Chem. Soc. Rev.* **36**, 93–104 (2007).
21. Liu, W., Samanta, S. K., Smith, B. D. & Isaacs, L. Synthetic Mimics of Biotin/(strept)avidin. *Chem. Soc. Rev.* **46**, 2391–2403 (2017).
22. Assaf, K. I. & Nau, W. M. Cucurbiturils: From Synthesis to High-Affinity Binding and Catalysis. *Chem. Soc. Rev.* **44**, 394–418 (2015).
23. Malaspina, T., Fileti, E. & Chaban, V. V. Peculiar Aqueous Solubility Trend in Cucurbiturils Unraveled by Atomistic Simulations. *J. Phys. Chem. B* **120**, 7511–7516 (2016).
24. Barrow, S. J., Kasera, S., Rowland, M. J., del Barrio, J. & Scherman, O. A. Cucurbituril-Based Molecular Recognition. *Chem. Rev.* **115**, 12320–12406 (2015).
25. Gao, Z.-Z. *et al.* Host-Guest Complexation of Cucurbit[8]uril with Two Enantiomers. *Sci. Rep.* **7**, 44717 (2017).
26. Kim, K. *et al.* Functionalized Cucurbiturils and Their Applications. *Chem. Soc. Rev.* **36**, 267–279 (2007).
27. Sharma, N. & Baldi, A. Exploring Versatile Applications of Cyclodextrins: An Overview. *Drug Deliv.* **23**, 729–747 (2016).
28. Motoyama, A., Suzuki, A., Shirota, O. & Namba, R. Direct Determination of Pindolol Enantiomers in Human Serum by Column-Wwitching LC-MS/MS Using a Phenylcarbamate-β-cyclodextrin Chiral Column. *J. Pharm. Biomed. Anal.* **28**, 97–106 (2002).
29. Wimmer, T. Cyclodextrins. in *Ullmann's Encyclopedia of Industrial Chemistry* (Wiley-VCH Verlag GmbH & Co. KGaA, 2003). doi:10.1002/14356007.e08_e02.
30. Bai, C., Tian, B., Zhao, T., Huang, Q. & Wang, Z. Cyclodextrin-Catalyzed Organic Synthesis: Reactions, Mechanisms, and Applications. *Molecules* **22**, 1475 (2017).
31. Enright, G. D., Udachin, K. A. & Ripmeester, J. A. Complex Packing Motifs Templated by a Pseudo-Spherical Guest: The Structure of β-cyclodextrin–adamantaneinclusion Compounds. *CrystEngComm* **12**, 1450–1453 (2010).
32. Mejia-Ariza, R., Graña-Suárez, L., Verboom, W. & Huskens, J. Cyclodextrin-based Supramolecular Nanoparticles for Biomedical Applications. *J. Mater. Chem. B* **5**, 36–52 (2017).
33. Vícha, R. *et al.* Novel Adamantane-bearing Anilines and Properties of Their Supramolecular Complexes with β-cyclodextrin. *Supramol. Chem.* **23**, 663–677 (2011).
34. Carrazana, J., Jover, A., Meijide, F., Soto, V. H. & Vázquez Tato, J. Complexation of Adamantyl Compounds by β-Cyclodextrin and Monoaminoderivatives. *J. Phys. Chem. B* **109**, 9719–9726 (2005).
35. Wang, J.-W. *et al.* Structural Insights into the Host–Guest Complexation between β-Cyclodextrin and Bio-Conjugatable Adamantane Derivatives. *Molecules* **26**, 2412 (2021).
36. Miyazawa, I. *et al.* Physicochemical Properties and Inclusion Complex Formation of δ-cyclodextrin. *Eur. J. Pharm. Sci.* **3**, 153–162 (1995).

37. Haroon Khalid, S., Bashir, M., Asghar, S., Hussain Mallhi, T. & Ullah Khan, I. Effect of Cyclodextrin Derivatization on Solubility and Efficacy of Drugs. in *Colloid Science in Pharmaceutical Nanotechnology* (IntechOpen, 2020). doi:10.5772/intechopen.90364.
38. Sandier, A., Brown, W., Mays, H. & Amiel, C. Interaction between an Adamantane End-Capped Poly(ethylene oxide) and a β-Cyclodextrin Polymer. *Langmuir* **16**, 1634–1642 (2000).
39. Wang, J. *et al.* Supramolecular Polymer Assembly in Aqueous Solution Arising from Cyclodextrin Host–guest Complexation. *Beilstein J. Org. Chem.* **12**, 50–72 (2016).
40. Zhou, Y., Yang, R., Fan, X., Sun, M. & He, X. Self-assembly of telechelic polymers bearing adamantane groups via host-guest inclusion complexes with cyclodextrin polymer. *J. Appl. Polym. Sci.* **138**, 49520 (2021).
41. Lee, H. J., Le, P. T., Kwon, H. J. & Park, K. D. Supramolecular assembly of tetronic–adamantane and poly(β-cyclodextrin) as injectable shear-thinning hydrogels. *J. Mater. Chem. B* **7**, 3374–3382 (2019).
42. Pu, W.-F., Yang, Y., Wei, B. & Yuan, C.-D. Potential of a β-Cyclodextrin/Adamantane Modified Copolymer in Enhancing Oil Recovery through Host–Guest Interactions. *Ind. Eng. Chem. Res.* **55**, 8679–8689 (2016).
43. Wang, R., McCormick, C. L. & Lowe, A. B. Synthesis and Evaluation of New Dicarboxylic Acid Functional Trithiocarbonates: RAFT Synthesis of Telechelic Poly(n -butyl acrylate)s. *Macromolecules* **38**, 9518–9525 (2005).
44. Lai, J. T., Filla, D. & Shea, R. Functional polymers from novel carboxyl-terminated trithiocarbonates as highly efficient RAFT agents. *Macromolecules* **35**, 6754–6756 (2002).
45. Yang, L., Guo, Y. & Lei, Z. Synthesis of a smart Janus-like supramolecular polymer based on the host–guest chemistry and its self-assembly. *J. Mater. Chem. A* **3**, 17098–17105 (2015).
46. Gil Alvaradejo, G., Glassner, M., Hoogenboom, R. & Delaittre, G. Maleimide end-functionalized poly(2-oxazoline)s by the functional initiator route: synthesis and (bio)conjugation. *RSC Adv.* **8**, 9471–9479 (2018).
47. Thompson, M. S., Vadala, T. P., Vadala, M. L., Lin, Y. & Riffle, J. S. Synthesis and applications of heterobifunctional poly(ethylene oxide) oligomers. *Polymer (Guildf).* **49**, 345–373 (2008).
48. Lampley, M. W. & Harth, E. Photocontrolled Growth of Cross-Linked Nanonetworks. *ACS Macro Lett.* **7**, 745–750 (2018).
49. Lewis, R. W., Evans, R. A., Malic, N., Saito, K. & Cameron, N. R. Ultra-fast aqueous polymerisation of acrylamides by high power visible light direct photoactivation RAFT polymerisation. *Polym. Chem.* **9**, 60–68 (2018).
50. Kavitha, A. A. & Singha, N. K. Atom Transfer Radical Polymerization (ATRP) of Methyl Methacrylate using a Functional Initiator Bearing an Amino-Adamantane. *Macromol. Chem. Phys.* **210**, 1536–1543 (2009).
51. Tan, T., Tan, T., Ng, S., Wang, Y. & Xiao, Y. Synthesis of mono-6-tosyl-β-cyclodextrin, a key intermediate for the functional cyclodextrin derivatives. *Protoc. Exch.* (2011) doi:10.1038/protex.2011.214.

52. Tripodo, G., Wischke, C., Neffe, A. T. & Lendlein, A. Efficient synthesis of pure monotosylated beta-cyclodextrin and its dimers. *Carbohydr. Res.* **381**, 59–63 (2013).
53. Kasal, P. & Jindřich, J. Mono-6-Substituted Cyclodextrins—Synthesis and Applications. *Molecules* **26**, 5065 (2021).
54. Bednářová, E., Hybelbauerová, S. & Jindřich, J. Optimized methods for preparation of 6 I -(ω-sulfanyl-alkylene-sulfanyl)-β-cyclodextrin derivatives. *Beilstein J. Org. Chem.* **12**, 349–352 (2016).
55. Tang, W. & Ng, S.-C. Facile synthesis of mono-6-amino-6-deoxy-α-, β-, γ-cyclodextrin hydrochlorides for molecular recognition, chiral separation and drug delivery. *Nat. Protoc.* **3**, 691–697 (2008).
56. Quadrelli, P. & Moiola, M. Cycloaddition reactions for antiviral compounds. in *Modern Applications of Cycloaddition Chemistry* 1–83 (Elsevier, 2019). doi:10.1016/B978-0-12-815273-7.00001-0.
57. Zhang, Y. *et al.* Preparation of novel β-cyclodextrin chiral stationary phase based on click chemistry. *J. Chromatogr. A* **1191**, 188–192 (2008).
58. Guo, Z. *et al.* "Click saccharides": novel separation materials for hydrophilic interaction liquid chromatography. *Chem. Commun.* 2491–2493 (2007) doi:10.1039/B701831B.
59. Zhao, Y. *et al.* Retention properties of novel β-CD bonded stationary phases in reversed-phase HPLC mode. *Talanta* **78**, 916–921 (2009).
60. Mourer, M., Hapiot, F., Tilloy, S., Monflier, E. & Menuel, S. Easily Accessible Mono- and Polytopic -β-Cyclodextrin Hosts by Click Chemistry. *European J. Org. Chem.* **2008**, 5723–5730 (2008).
61. Boyer, C. *et al.* Copper-Mediated Living Radical Polymerization (Atom Transfer Radical Polymerization and Copper(0) Mediated Polymerization): From Fundamentals to Bioapplications. *Chem. Rev.* **116**, 1803–1949 (2016).
62. Chmurski, K., Stepniak, P. & Jurczak, J. Improved Synthesis of C2 and C6 Monoderivatives of α- and β-Cyclodextrin via the Click Chemistry Approach. *Synthesis (Stuttg).* **47**, 1838–1843 (2015).
63. Sak, H., Mawick, M. & Krause, N. Sustainable Gold Catalysis in Water Using Cyclodextrin-tagged NHC-Gold Complexes. *ChemCatChem* **11**, 5821–5829 (2019).
64. Peng, K., Tomatsu, I., Korobko, A. V. & Kros, A. Cyclodextrin–dextran based in situ hydrogel formation: A carrier for hydrophobic drugs. *Soft Matter* **6**, 85–87 (2010).
65. Arslan, M., Gevrek, T. N., Sanyal, A. & Sanyal, R. Cyclodextrin mediated polymer coupling via thiol–maleimide conjugation: Facile access to functionalizable hydrogels. *RSC Adv.* **4**, 57834–57841 (2014).
66. Zhang, M., Wei, X., Xu, X., Jin, Z. & Wang, J. Synthesis and characterization of water-soluble β-cyclodextrin polymers via thiol-maleimide 'click' chemistry. *Eur. Polym. J.* **128**, 109603 (2020).
67. Sumerlin, B. S., Lowe, A. B., Thomas, D. B. & McCormick, C. L. Aqueous Solution Properties of pH-Responsive AB Diblock Acrylamido Copolymers Synthesized via Aqueous RAFT. *Macromolecules* **36**, 5982–5987 (2003).

Chapter 2

Water-soluble long linear supramolecular polymers based on metal-ligand coordination with terpyridine functionalized polyacrylamide

2.1 Introduction

In the previous chapter, we described the synthesis of long telechelic polyacrylamides (PAM) end-functionalized with adamantane or β-cyclodextrin (β-CD) for making supramolecules based on host-guest interactions, and challenges associated with the synthesis. The adamantane functionalized RAFT iniferter was not soluble in water or polar organic solvents like dimethyl sulfoxide (DMSO), so the synthesis of long adamantane functionalized PAM was achieved via three step polymerization reactions as described in Chapter 1. On the other hand, β-CD molecules were only soluble in polar-organic solvents like DMSO and dimethylformamide (DMF), making the purification of β-CD functionalized molecules challenging at scale. Therefore, we looked for different associative groups that could form stable complexes in water while also being soluble in both water and organic solvents for ease of synthesis. In this chapter, we show that metal-ligand association with 2,2′:6′,2″-terpyridine ligand satisfies these criteria. We describe the facile synthesis of terpyridine functionalized polyacrylamides (TPAM) and the formation of ultralong supramolecular polymers (> 2000 kg/mol) based on metal-ligand coordination at low polymer concentration (< 0.2wt%) in water.

2,2';6,2'-terpyridine

2,2′:6′,2″-Terpyridine is one of the most widely used ligands in supramolecular chemistry due to its ability to reversibly complex with a variety of transition metal ions (e.g., Fe^{2+}, Ni^{2+},

Cu^{2+}, Co^{2+}, Ru^{2+}, etc).[1] In the last few decades, terpyridine has been incorporated into polymers for various applications such as catalysis[2,3], self-healing materials[4,5], photovoltaic materials[6], and mist-control agents[7]. Terpyridine is a tridentate ligand that only forms 2:1 complexes (terpyridine:metal), suitable for creating long linear supramolecules, in contrast to bidentate ligands (e.g., ethylenediamine, 2,2'-bipyridine or 1,10-phenanthroline) that form 3:1 complexes. Furthermore, the association strength of the terpyridine-metal complexes can be tuned by simply changing the type of metal ion used (Fe > Ni > Co > Cu > Zn).[7] There are several strategies for attaching terpyridine groups to polymers for both side chains and end groups.[8] Previously reported approaches include free radical polymerizations with terpyridine functionalized initiators and chain transfer agents via nitro oxide-mediated radical polymerization (NMP)[9] and reversible addition-fragmentation chain transfer polymerization (RAFT)[7]. We chose to use RAFT polymerization since bis-terpyridine ended polymers could be prepared from bis-terpyridine functionalized iniferter.

Previously reported water-soluble terpyridine-ended polymers

Schubert and coworkers[10,11] were among the first to report the synthesis of water-soluble end-functionalized polyethylene oxide (PEO) (M_n > 16500 g/mol). The hydroxyl ends of the PEO were reacted with 4'-chloro-2,2':6',2" terpyridine via a nucleophilic substitution reaction. While Schubert and coworkers demonstrated the successful formation of metal coordinated terpy-PEOs that resulted in apparent molecular weight up to 80 kg/mol, the coordination occurred at a relatively high concentration of 25 mg/mL in methanol (~3 wt%), and the molecular weights of the terpyridine functionalized PEOs were too small to be useful in agricultural mist applications. We also tried end functionalizing longer PEOs but working with longer PEOs ($M_n > 100$ kg/mol) was challenging because they were more susceptible to chain degradation. (See Appendix A)

Cameron and coworkers recently reported the synthesis of bis-terpyridine ended polyacrylamides (M_n 455~570 kg/mol, PDI 1.53-2.44) via aqueous RAFT polymerization, and showed the formation of ultrahigh molecular weight linear coordination polymers with M_w around 2000 kg/mol.[7] While Cameron and coworkers demonstrated the possibility of using the linear coordination polymers for agricultural mist control applications, we noticed that theory would suggest that longer terpyridine functionalized PAM might open the way to stronger rheological effects at lower concentrations. Our group's previous work with long end-associative polymers in jet-A fuel showed that using longer chains discourages the formation of small cyclic species, as the entropy cost of ring closure increases with chain length.[12] Therefore, we hypothesized that using a longer terpyridine functionalized PAM would favor the formation of ultralong linear coordination polymers by suppressing the formation of small cyclic supramolecules.

The theory also underscores the importance of high-fidelity α,ω-functionalization. The terpyridine functionalized PAM used in the work of Cameron and coworkers had relatively high PDI (1.5-2.44) for polyacrylamides prepared by aqueous RAFT polymerization (typically < 1.2)[13], so we also saw the need for optimizing the polymerization conditions to synthesize longer terpyridine-functionalized PAM with control over molecular weight with narrow PDI. Here, we build on the work of Cameron and coworkers, the first report of terpyridine-ended PAM as drift-control adjuvants for agricultural spray applications.

Scope of current work

We report the 1) facile synthesis and purification of terpyridine functionalized RAFT iniferter; 2) careful optimization of aqueous RAFT polymerization conditions that enabled the synthesis of terpyridine-ended polyacrylamides with narrow polydispersity (<1.1) and molecular weight control up to (>3000 kg/mol); 3) judicious choice of pH of the aqueous solution both to simplify purification of terpyridine-functionalized RAFT iniferter and to enable one-step polymerization of high molecular weight terpyridine-functionalized polyacrylamides. We also demonstrate the successful formation of ultralong supramolecular coordination polymers (> 2000 kg/mol) at low concentrations (< 0.2 wt%) upon mixing metal ions with aqueous solutions of terpyridine-functionalized PAM. Lastly, we demonstrate that ultralong coordinated TPAMs recover after shearing by passing through a recirculating pump.

2.2 Experimental

2.2.1 Materials and instrumentation

All chemical reagents were obtained from Sigma Aldrich at 98% purity or higher unless otherwise stated. All solvents were obtained from Sigma Aldrich, at ACS reagent grade or higher (> 99.5% purity) and used as received without further purification.

NMR spectroscopy

^{1}H-NMR spectra were obtained using a Varian Inova 500 spectrometer (500 MHz); spectra were recorded in $CDCl_3$, d-DMSO, and D_2O (purchased from Cambridge Isotope Laboratories). Chemical shifts were reported in parts per million (ppm) and were referenced to residual solvent resonances.

Gel permeation chromatography

The molecular weights and dispersity index of the polymers were determined on a GPC system with an Agilent pump (G7110B), equipped with an autosampler (G7129A), a Wyatt DAWN 8 multi-angle laser light scattering detector (λ=658.9nm), a Wyatt Optilab refractive index detector (RI) (λ=658nm), and an Agilent PL Aquagel-OH MIXED-H column. Aqueous buffer was prepared containing 0.2M $NaNO_3$, with 200 ppm NaN_3. Filtered aqueous buffer was used as the eluent at the flow rate of 0.3mL/min at 25°C. The data were analyzed using Wyatt Astra 7 using the Zimm fitting formula with *dn/dc* = 0.1590 mL/g to obtain molecular weight (M_w, and M_n) for each polyacrylamide reported.

Rheology

The shear viscosity of the polymer solutions was measured using a strain-controlled rheometer TA ARES-RFS, equipped with a cone-plate geometry (angle 2°, diameter 50mm) with a shear rate ranging from 1 s^{-1} to 1000 s^{-1}. The specific viscosity ($\eta_{specific} = \eta_{solution}/\eta_{solvent} - 1$) values were averaged over data points taken from the range that did not show shear rate dependence (10 to 300 s^{-1}). (Figure 2.11 in section 2.5 for additional information regarding the shear rate range used) Three replicates were measured to obtain the error bars (standard error).

Custom built visible light LED reactor for polymer synthesis

A custom photo-reactor was constructed to avoid heating the reaction vessel. A Chanzon 30W LED (λ_{peak}= 440-450nm) powered by a Chanzon 900mA constant current LED driver was attached to an aluminum heatsink (11 x 58.5 x 89 mm) using thermally conductive adhesive (MG Chemicals). A 70 mm computer CPU cooler fan (AMD) was attached to the back side of the aluminum heatsink, and the fan was connected to a 12V 2A DC power supply. An enclosure (28 cm x 18 cm x 13 cm) containing the light and the body of a round bottom flask was lined with aluminum foil. The LED-heat sink-fan was mounted through a wall in the enclosure (see Figure 1.1).

2.2.2 Synthesis of RAFT agents and intermediates

Synthesis of S,S-bis(a, a'-dimethyl-a"-acetic acid) trithiocarbonate (BDMAT)

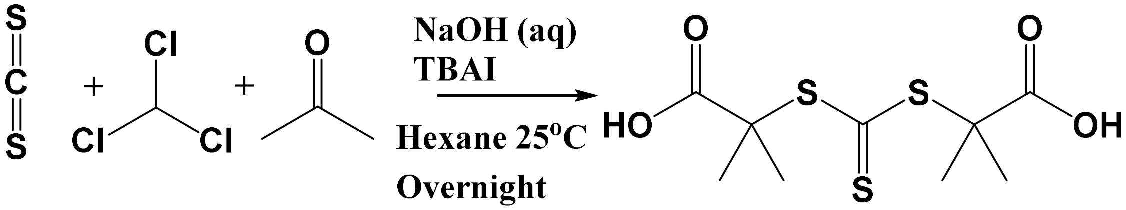

Scheme 2.1 Synthesis of S,S-bis(α, α'-dimethyl-α"-acetic acid) trithiocarbonate (BDMAT) Procedure modified from[14], synthesized as described in Chapter 1.

Synthesis of terpyridine triethylene glycol (terpy-teg-OH)

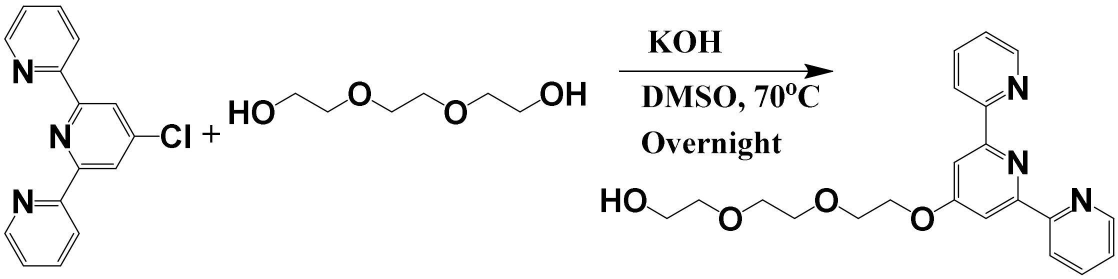

Scheme 2.2 Synthesis of terpyridine triethylene glycol (terpy-teg-OH) Procedure was modified from[15,16,17]

Finely crushed KOH (12.57 g, 0.224 mol) was suspended in 25mL of dry DMSO in a 50mL round bottom flask. Triethylene glycol (33.63 g, 0.224 mol) was added to the flask. The mixture was stirred for 30 minutes at 50°C to dissolve solids and 4'-chloro-2,2':6',2"-terpyridine (3 g, 11.2 mmol) was added incrementally over 20 minutes. The mixture was stirred at 60°C for 24 hours. After 24 hours, the reaction mixture was cooled to room temperature, diluted with DI water (200 mL), and filtered. The filtrate was extracted with DCM (3 x 60 mL), dried over anhydrous $MgSO_4$ and filtered and the solvent was removed by rotary evaporation. The product was obtained as a yellow oil. Yield 95 %.

^{1}H-NMR ($CDCl_3$, 500 MHz) 3.60 (t, 2H), 3.73-3.65 (m, 6H), 3.92 (t, 2H), 4.40 (t, 2H), 7.31 (t, 2H), 7.83 (t, 2H), 8.03 (s, 2H), 8.59 (d, 2H), 8.66(d, 2H).

Synthesis of bis terpyridine functionalized BDMAT

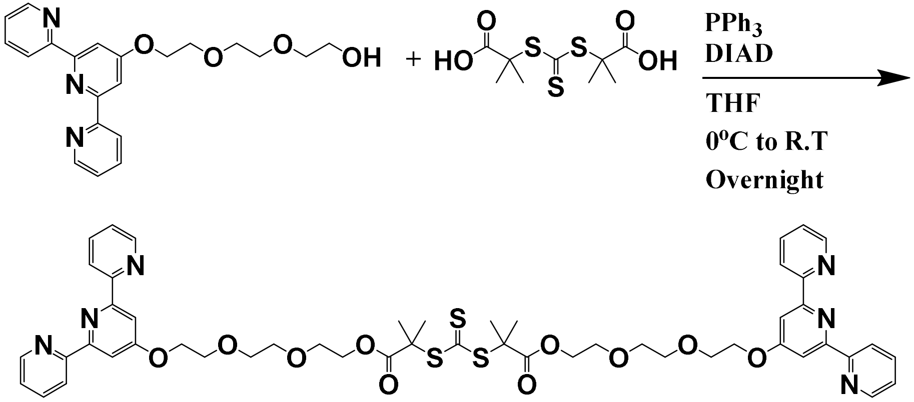

Scheme 2.3 Synthesis of bis terpyridine functionalized BDMAT via Mitsunobu reaction

S,S-bis(α, α'-dimethyl-α''-acetic acid) trithiocarbonate (BDMAT) (0.5 g 1.77 mmol) and triphenylphosphine (1.695 g, 6.46 mmol) were dissolved in anhydrous THF (20 mL) in a 100 mL round bottom flask. After complete dissolution, the flask was placed in an ice bath and diisospropyl azodicarboxylate (DIAD) (1 g, 4.95 mmol) was added slowly dropwise. After the addition of DIAD, the mixture was removed from the ice bath and stirred at room temperature overnight. The mixture was diluted with 1M HCl_{aq} (100 mL) and washed with ethyl acetate (100 mL) twice, discarding the ethyl acetate layer each time. The aqueous layer was neutralized with 50% NaOH solution to neutral pH, and the crude product was extracted in ethyl acetate (150 mL). The organic layer was washed with DI water (100 mL) twice and dried over $MgSO_4$. The solution was filtered, and the solvent was removed under reduced pressure to yield the crude product as a sticky yellow solid. The crude product was further purified by silica gel column chromatography. The column was initially eluted with ethyl acetate to remove the undesired products and then eluted with acetone and dried to obtain the product as a sticky yellow solid. Yield 85 %.

^{1}H-NMR ($CDCl_3$, 500 MHz) 8.66(d, 4H), 8.59 (d, 4H) 8.03 (s, 4H), 7.83 (t, 4H), 7.31 (t, 4H), 4.40 (t, 4H), 4.20 (t, 4H), 4.20 (t, 4H), 3.8-3.65 (m, 12H), 1.56 (s, 12H)

2.2.3 Polymer synthesis, supramolecule formation, and degradation

Representative procedure for bis terpyridine ended polyacrylamide

Acrylamide (4 g, 0.056 mol) was dissolved in molecular biology grade water (27.6 mL) in a 50mL round bottom flask. Bis terpyridine BDMAT (4.5 mg, 4.46 μmol) was dissolved in DMSO (0.5 mL) and 0.1N HCl (0.4 mL) was slowly added to protonate the terpyridine groups. The bis terpyridine trithiocarbonate RAFT iniferter solution was added to acrylamide solution under stirring, and the flask was capped with a Suba-Seal rubber septum and the mixture was degassed by bubbling argon for 45 minutes. The reaction flask was then placed in the LED reactor on a magnetic stir plate. The reaction was started by turning on the LED and the flask was irradiated for 8 hours with stirring. The reaction was quenched by removing the reaction flask from the light source and the LED was turned off. The polymer was removed from the 50mL RBF using a plastic spatula, and transferred to a 250 mL beaker, where it was dissolved in molecular biology grade water (100 mL), precipitated in acetone (700 mL), and dried under vacuum before use.

Solution preparation and coordination polymer formation

1wt% terpyridine polyacrylamide solutions were prepared by dissolving the polymer in molecular biology grade water in a 20 mL glass scintillation vial. For complete dissolution of the polymers in water, the vials were shaken overnight using a wrist-action shaker (Burrell Scientific). The coordination polymers were formed by adding precise amounts of transition metal ion stock solutions. The amount of metal ions to add for formation of linear coordination polymers was determined based on the concentration of terpyridine end groups present in the polymer solution. The concentration of the terpyridine end groups was determined using the Mn of the polymers from GPC analysis and assuming 100% end group fidelity. After addition of the metal solutions, the scintillation vials were placed on a wrist-action shaker (Burrell Scientific) for 1 hour and used immediately for shear viscosity measurements and GPC analysis.

All transition metal ion stock solutions (2mM) were prepared from the chloride salts of each metal ion ($FeCl_2$, $NiCl_2$). $FeCl_2$ solution was prepared with 0.01 M HCl_{aq} instead of water under an argon atmosphere to minimize oxidation of Fe^{2+} to Fe^{3+} and the solution was freshly prepared before each use.[18]

Shear degradation test

Polymer solutions were prepared at 0.1 wt% concentration (1000 ppm) in 500 mL of ultrapure water (Milli-Q) inside of a 1 L glass media bottle with a plastic screw cap. The polymers were dissolved by stirring the solution with a PTFE coated magnetic stir bar (40 mm x 7.9 mm) at 90 rpm for 24 hours. Three bottles of polymer solutions were prepared: two bottles of terpyridine functionalized PAM (M_n 820 kg/mol), 500 mL each, and a bottle of PAM (M_n 2080 kg/mol). To a bottle of terpyridine functionalized PAM solution, Ni^{2+} ions were added from a 20 mM stock solution of $NiCl_2$ (prepared in Milli-Q water) such that $[Ni^{2+}]/[\text{Terpyridine}] = 0.5$, and the solution was stirred at 90 rpm for an additional 24 hours before use. The three solutions were recirculated through a pump (Imagitarium, 5.05 GPM) for 30 minutes (fluid passed through the pump approximately 138 times). Specific viscosity ($\eta_{specific}$) of the polymer solutions and molecular weights of the polymers were measured before and after the shearing using the rheometer and GPC. To minimize cross-contamination between the experiments, the pump was washed thoroughly with DI water, rinsed with ultrapure (molecular biology grade) water, and air dried prior to each use.

2.3 Results and discussion

2.3.1 Synthesis of RAFT agents and intermediates

For the synthesis of bis-terpyridine RAFT agents, we tried to simplify the synthesis route as much as possible. The first intermediate, terpyridine triethylene glycol was synthesized using commercially available 4'-chloro-2,2':6',2"-terpyridine and triethylene glycol. The previously reported methods typically used a 5-10 times molar excess of triethylene glycol[15–17], but 20x molar excess was required to completely limit the formation of bis-terpyridine byproducts (Figure2.1).

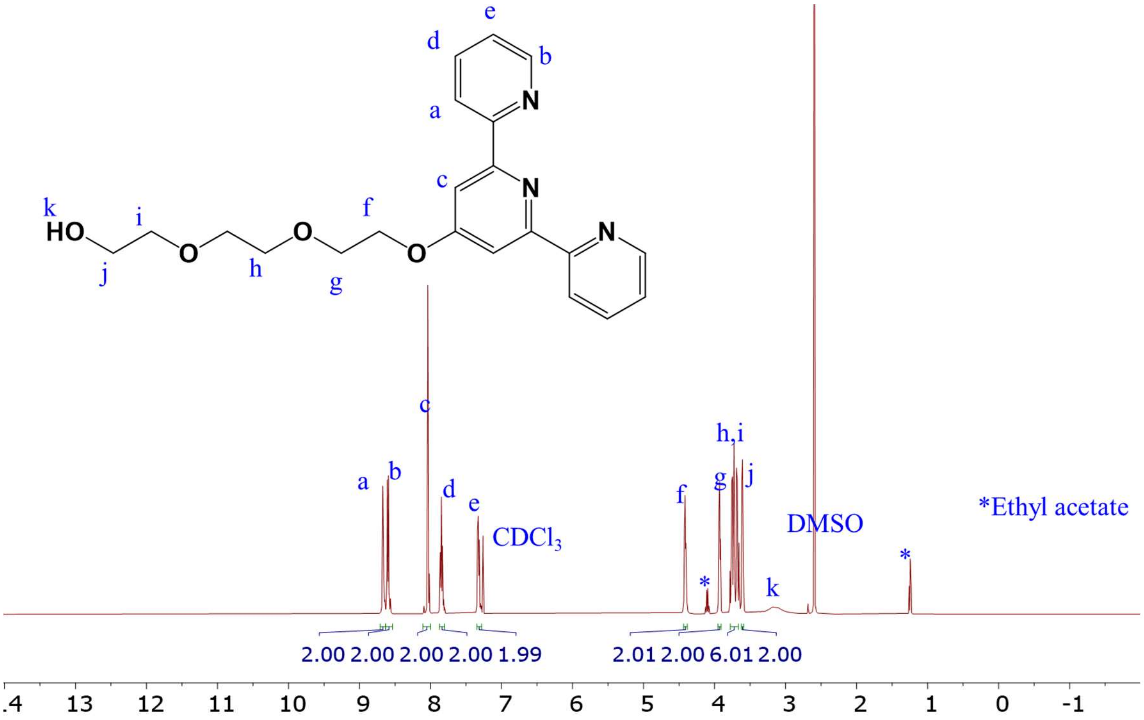

Figure 2.1 ^{1}H-NMR of terpyridine triethylene glycol in CDCl$_3$.

For the synthesis of bis-terpyridine BDMAT, we compared five different synthetic routes (Table 2.1) and the Mitsunobu reaction provided the highest yield.

Table 2.1 List of reactions tried for the synthesis of bis-terpyridine ended RAFT iniferter

References	**Reaction conditions**	**Outcome**
Synthesis of terpyridine ended RAFT iniferter from reactions with trithiocarbonate ions (CS_3^{2-})		
[34]	CS_2 and Cs_2CO_3 in DMSO	Reaction did not occur
[35,36]	CS_2, KOH, TBAB, Al_2O_3	Low yield
[37]	CS_2, DBU	Side reactions*
Synthesis of terpyridine ended RAFT iniferter from BDMAT		
[7]	BDMAT to BDMAT acid chloride using oxalyl chloride followed by the addition of terpyridine triEG	Reaction mixture turned black; crude product showed unknown peaks in ~1.5-2ppm region in ^{1}H-NMR
This work	Mitsunobu reaction between BDMAT and terpyridine triethyleneglycol	85 % yield

*Possible scenario: Hydrolysis of DBU will result in formation of primary amine and cause aminolysis of trithiocarbonate molecules.

The Mitsunobu reaction uses mild reaction conditions with excellent functional group tolerance and broad substrate tolerance, but it also generates triphenylphosphine oxide (TPPO) and hydrazine byproducts that complicate purification.[19] In particular, removing TPPO can be challenging after the Mitsunobu reaction (or any other reaction that uses triphenylphosphine and generates TPPO, such as the Wittig reduction or the Staudinger reaction)[20]. While there are established methods for removing TPPO, the presence of terpyridine groups in the mixture made the purification step even more challenging. For example, the typical methods for removing TPPO from the reaction mixture include precipitation of TPPO in non-polar solvents like hexane and filtering[20], precipitation with zinc chloride in common polar organic solvents[21], and (multiple) column chromatography[7,22]. The crude product was not soluble in non-polar solvents like hexane and diethyl ether, and selective precipitation of TPPO with Zn^{2+} was not possible since terpyridine would also complex with Zn^{2+}. Cameron and coworkers had to perform two rounds of column chromatography to fully remove TPPO from their reaction mixture when they purified their terpyridine functionalized RAFT agent.[7]

However, we discovered that the purification process could be simplified if we could make terpyridine derivatives water-soluble since TPPO and other byproducts of the Mitsunobu reaction are not soluble in water. While neutral terpyridines are not soluble in water, terpyridine molecules can be protonated twice depending on the pH of the solution, and the protonated cationic terpyridines are highly soluble[23] (Scheme 2.4).

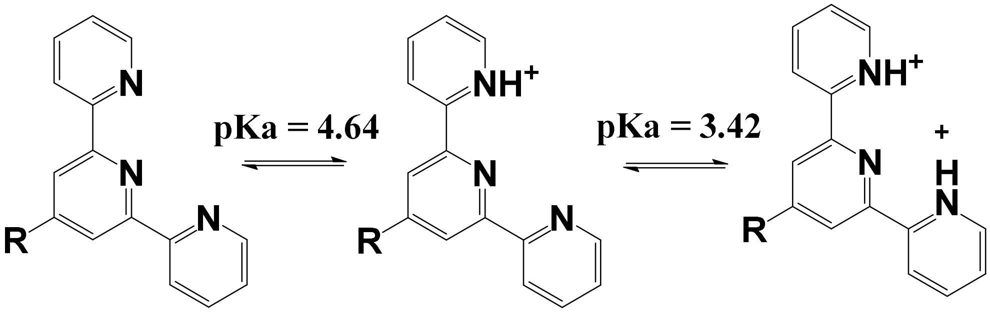

Scheme 2.4 Protonation of terpyridine

After the Mitsunobu reaction in THF, we diluted the reaction mixture with 1M HCl_{aq} and the aqueous mixture was washed with ethyl acetate thrice to remove any water-insoluble impurities (TPPO, DIAD, triphenylphosphine, and diisopropyl hydrazine-1,2-dicarboxylate). After this liquid extraction, we neutralized the aqueous layer with sodium hydroxide to neutral pH. The solution turned cloudy as the terpyridine containing molecules were precipitating out of the aqueous mixture. Terpyridine containing molecules were then extracted in ethyl acetate, and the organic phase was washed with water. After this simple liquid extraction step, Mitsunobu reaction byproducts were completely removed (Figure 2.2 (a)). However, the integral of the NMR peak of the methyl groups adjacent to the trithiocarbonate was too weak relative to the terpyridine peaks. This suggested that some terpyridine in excess of the terpyridine of the iniferter was present. Therefore, the product was further purified via column chromatography. (Figure 2.2 (b)). The desired product was yellow colored, so elution of the product-containing band during column chromatography was monitored by observing the progression of a yellow band through the column. The purified product had ^{1}H-NMR integrals consistent with its structure.

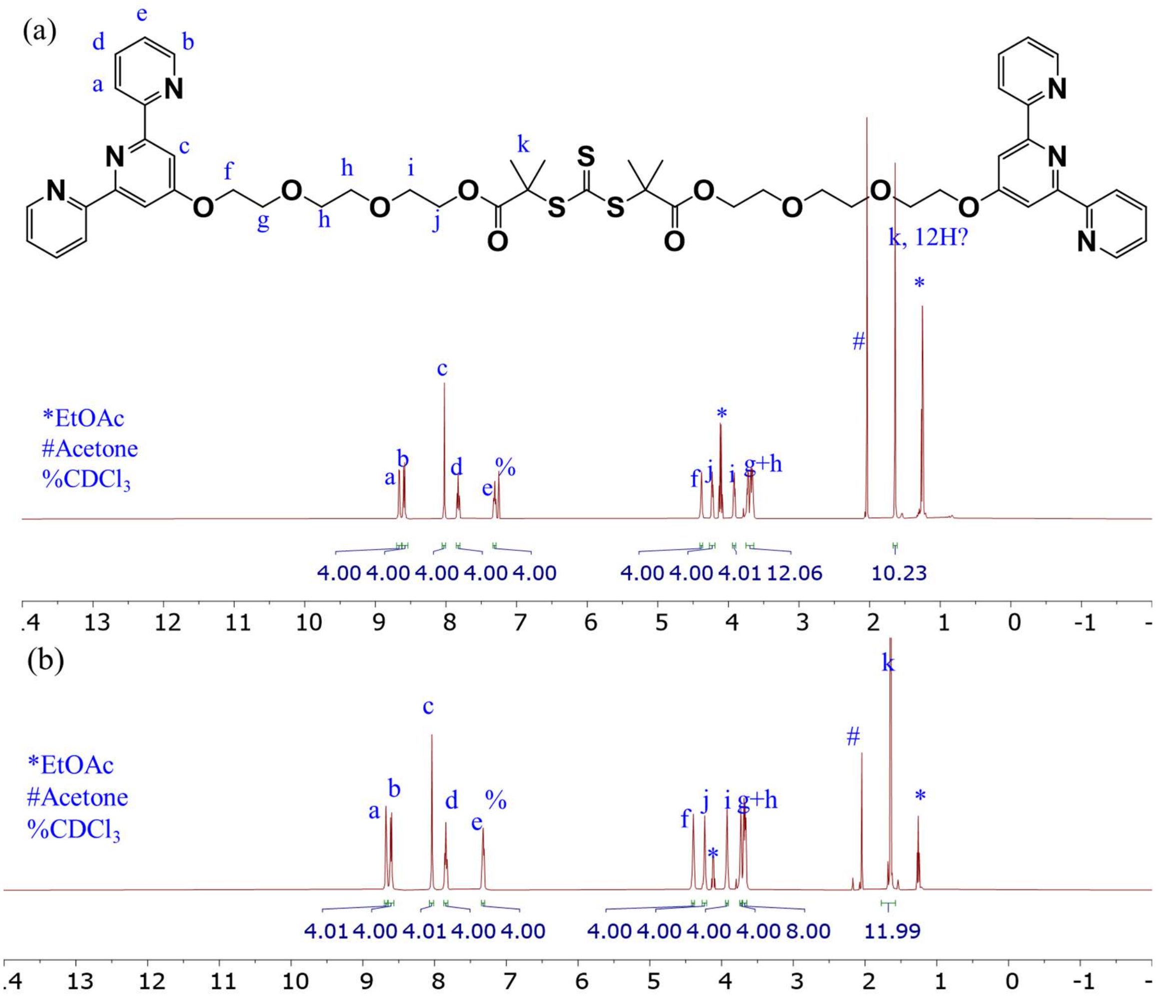

Figure 2.2 (a) ^{1}H-NMR of bis-terpyridine-BDMAT after liquid extraction in CDCl$_3$, showing the absence of Mitsunobu reaction byproducts (typically at 7-8 ppm, broad peak). **(b)** ^{1}H-NMR of bis-terpyridine BDMAT after column chromatography in CDCl$_3$.

2.3.2 Polymer synthesis

In the work of Cameron and coworkers,[7] a two-step method was used for terpyridine functionalized polyacrylamide. The first step involved a short bis-terpyridine PAM in DMSO and purification by dialysis or precipitation to make a macro chain transfer agent (mCTA) that is soluble in water. By chain extending the mCTA in water, high molecular weight terpyridine-functionalized PAM was synthesized.

We were able to make high molecular weight bis-terpyridine PAM without a first step in DMSO by carrying out the polymerization in acidic water by adding HCl (pH ~3), which solubilizes the terpyridine-functionalized RAFT agent in water. In addition to improving the solubility of the RAFT agent, we observed (in accordance with prior literature[24]) that low pH was essential to carry out aqueous RAFT polymerization of acrylamide free of side reactions. In aqueous solutions, acrylamide (any acrylamide derivatives such as *N,N*-dimethylacrylamide) can slowly undergo hydrolysis at elevated pH, generating free amines (Scheme 2.5). Specifically, hydrolysis of acrylamide generates ammonia, which causes aminolysis of trithiocarbonate[24,25] (Scheme 2.6).

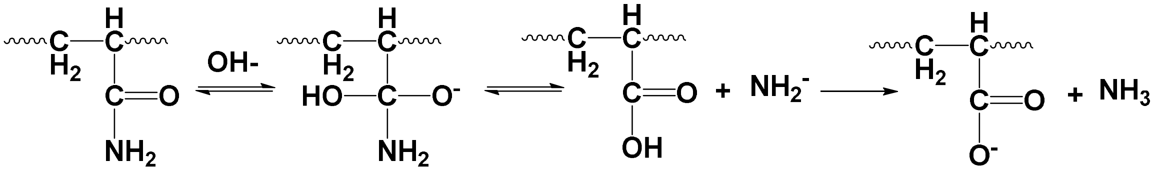

Scheme 2.5 Hydrolysis of acrylamide at pH > 7

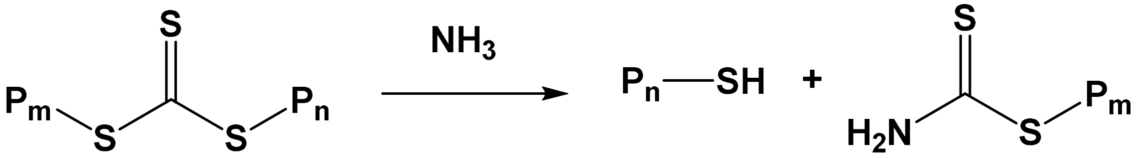

Scheme 2.6 Aminolysis of trithiocarbonate structure of RAFT polymers by ammonia

Even a trace amount of aminolysis can be detrimental to RAFT polymerization. For example, for the synthesis of 800 kg/mol polyacrylamide, the [RAFT agent]/[monomer]$_0$ ratio would be less than 0.0001. Even if 0.01 mol% of the acrylamide in the solution experienced hydrolysis, it could result in the complete decomposition of every RAFT agent in the solution since [NH$_3$] > [RAFT agent]. However, both hydrolysis of acrylamide and aminolysis can be prevented if pH stays below 7 during the aqueous RAFT polymerization. McCormick and coworkers showed that aminolysis of trithiocarbonate could be prevented even in the presence of excess primary amines when pH was below 7.[24] During the polymerization, we are not adding any base to the reaction mixture. Ideally, the pH of pure water should be close to 7. However, doubly distilled water or water from a Milli-Q system often has a pH below 7, close to 5.5-6.5. This is because dissolution of CO$_2$ lowers the pH of the aqueous solution as shown in Schematic 2.7.

$$CO_2 + H_2O \rightleftharpoons H_2CO_3 \rightleftharpoons H^+ + HCO_3^- \rightleftharpoons H^+ + CO_3^{2-}$$

Schematic 2.7 Effect of degassing aqueous solution on pH

When the aqueous solution is degassed to remove dissolved oxygen by bubbling inert gas (N$_2$ or Ar), we also remove dissolved CO$_2$ from the solution. When CO$_2$ is removed, the pH of the solution increases (i.e., the equilibrium will shift toward the left-hand side of the equation in Schematic 2.7). After degassing, the pH of the water was often higher than 7, and sometimes closer to 8. Therefore, when carrying out aqueous RAFT polymerization, it is necessary to acidify the aqueous solution to ensure pH stays below 7.

In addition to adjusting the pH, we designed a custom LED reactor (451 nm, 30 W) to prevent excessive heating of the reaction vessel. It is known that trithiocarbonate RAFT agents can decompose in aqueous solutions at temperatures above 50 °C.[25] When building an LED reactor for photoinitiated polymerization, LED power strongly affects the reaction temperature. Cameron and coworkers (2018) studied the effect of visible light LED (λ = 400-451 nm) power (6 W - 206 W) on aqueous RAFT polymerization.[27] The authors observed that using a higher powered LED results in shorter polymerization time, but the temperature of the reaction flask increased with the LED power (as high as 80 °C). We tested three different LEDs ($\lambda \sim 451$ nm), (5 W, 30 W, and 100 W), with aluminum heat fins and a cooling fan to remove heat from the LED (Figure 1.1). We chose the 30 W LED because we were able to keep the temperature of the reaction flask below 35 °C (measured with an IR temperature meter, after 8 hours of irradiation), while allowing the synthesis of polymers within a reasonable amount of time (8 hours for approximately 80% conversion). We stopped the polymerization before full conversion of monomers to minimize bimolecular radical termination between propagating chains. Optimization of the polymerization conditions allowed us to synthesize narrowly dispersed terpyridine ended PAMs (Table 2.2).

For M_n up to 92 kg/mol, we were able to analyze M_n of the terpyridine functionalized PAM with ^{1}H-NMR, and the obtained $M_{n,NMR}$ agreed reasonably well with $M_{n,GPC}$, suggesting high end group fidelity of the TPAM (Figure 2.3).

Table 2.2 GPC molecular weight characterization of terpyridine PAM

Polymer	Reaction time (hrs)	Conversion	Mn (kg/mol)	Mw (kg/mol)	PDI
TPAM 92k	8	0.94	92.5	93	1.01
TPAM 145k	8	0.89	145	148	1.02
TPAM 215k	8	0.86	215	226	1.05
TPAM 370k	8	0.84	370	375	1.02
TPAM 473k	8	0.81	473	482	1.04
TPAM 666k	8	0.83	666	690	1.04
TPAM 719k	8	0.84	719	750	1.04
TPAM 775k	8	0.79	775	800	1.03
TPAM 820k	8	0.81	820	837	1.03
TPAM 900k	8	0.78	898	928	1.03
TPAM 1036k	8	0.75	1036	1077	1.04
TPAM 1100k	8	0.76	1100	1189	1.08
TPAM 1513k	8	0.75	1513	1573	1.04
TPAM 1726k	8	0.72	1726	1948	1.15
TPAM 2998k	8	0.67	2998	3181	1.06
TPAM 3434k	8	0.56	3434	4869	1.42

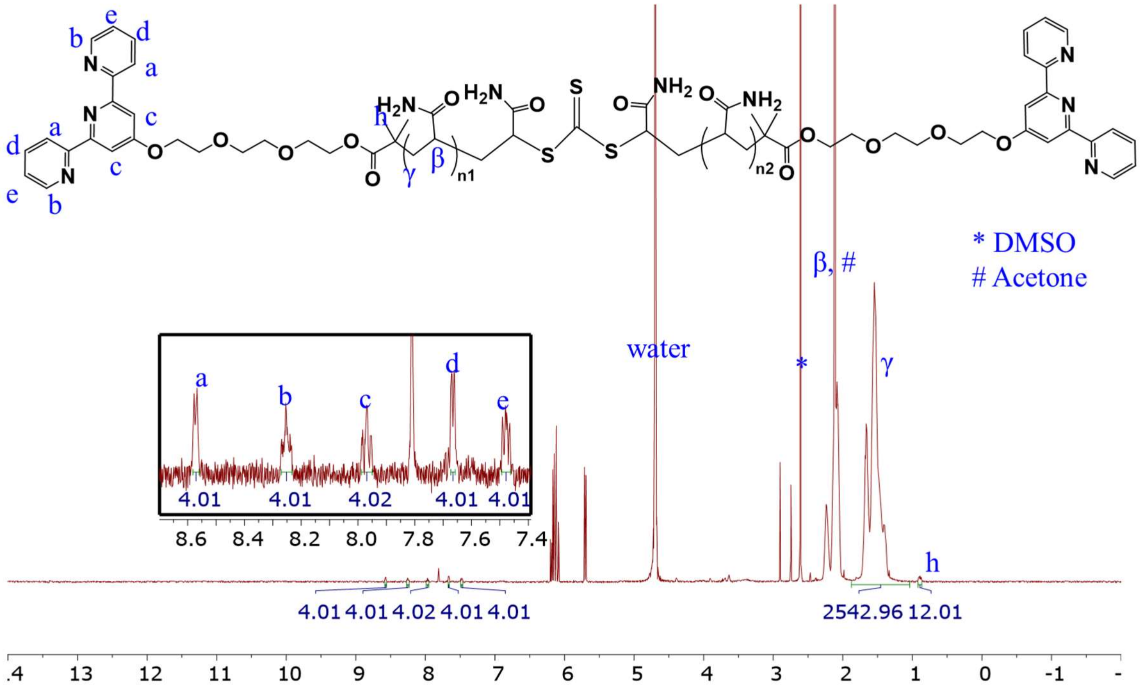

Figure 2.3 ^{1}H-NMR of TPAM 92k. $M_{n,NMR}$ = (# of protons for γ)/(# of protons per repeat unit)*(M_w of repeat unit) + (M_w of end groups) = (2542.96)/(2)*(71.08)+1009 = 91.4 kg/mol.

Observing ultralong supramolecular polymers based on metal-ligand coordination with terpyridine functionalized polyacrylamide (TPAM)

We observed evidence of formation of ultralong supramolecules upon the addition of metal ions to terpyridine PAM solutions. We were able to measure the effective molecular weight of the coordinated TPAMs using GPC, and an increase in the shear viscosity of the polymer solutions using a rheometer. We discuss the effects of some experimental factors that can affect the formation of ultralong supramolecules in solution to guide the design of optimal polymeric additives for spray applications.

Each transition metal ion can complex with two terpyridine molecules, so the optimal ratio should be [Metal^{2+}]/[terpyridine] = 0.5. We prepared coordinated polymer solutions with different [Fe^{2+}]/[terpyridine] ratios and measured the specific viscosity ($\eta_{specific}$) of the resulting coordinated TPAM solutions to see if the highest increase in viscosity occurred when [Metal^{2+}]/[terpyridine]=0.5. (Figure 2.4).

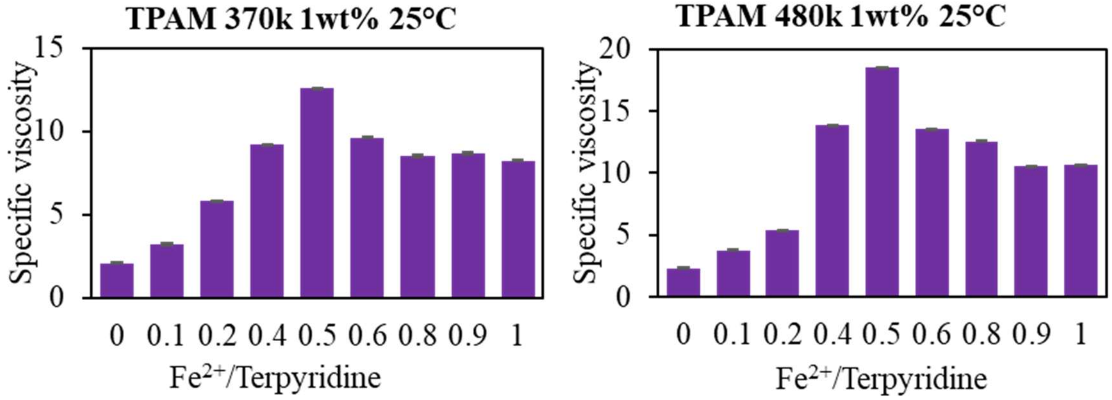

Figure 2.4 Specific viscosity ($\eta_{specific}$) of (Fe^{2+}) coordinated terpyridine PAM solutions at 1wt% at a shear rate of 500 s^{-1}. $\eta_{specific} = \eta_{solution}/\eta_{solvent} - 1$. As expected, the viscosity was highest when [Fe^{2+}]/[terpyridine] = 0.5.

The peaking of viscosity at [Fe^{2+}]/[terpyridine] = 0.5 suggests that the actual molecular weight of the polymer was close to $M_{n,GPC}$, since we calculated [terpyridine] based on $M_{n,GPC}$ of the TPAM. When metal ions are added to TPAM solutions, there would be an equilibrium of linear and cyclic supramolecules with varying lengths, as shown in Schematic 2.8.

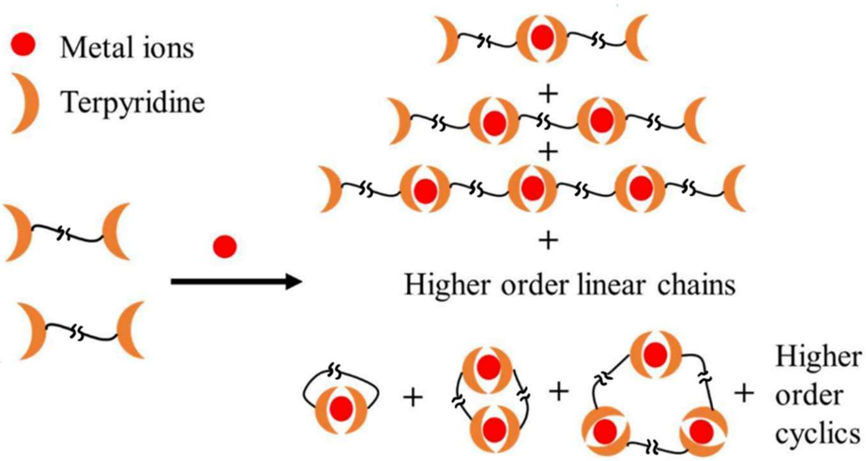

Schematic 2.8 Possible coordination polymers that can be obtained by metal-terpyridine complexation. Note that the schematic is not to scale: the backbones of polymers that provide strong effects are 300 to 800 times the mass of an end group.

For the mist-control (or drag reduction) applications, small cyclic species are not very useful, so maximizing the formation of long linear supramolecules is desired.

What is the optimal length of the backbone for the formation of ultralong linear coordination polymers? To answer this question, we prepared various metal (Fe^{2+} or Ni^{2+}) coordinated TPAM solutions ([M^{2+}]/[terpyridine]=0.5) with different backbone lengths at 1 wt% (10 mg/mL) concentration and characterized the effective molecular weights of the coordinated TPAMs using GPC (Figure 2.5). We hypothesized that the ould result in higher effective molecular weight of the coordinated TPAMs since the entropy cost of closing the ring increases with the increase in the backbone length.[12] We observed an increase in the effective molecular weight as M_n of the backbone increased from 215 kg/mol to 820 kg/mol, even reaching a remarkably high M_w of ~5 Mg/mol. However, the higher molecular weight backbones (1100 kg/mol and 1513 kg/mol) had smaller effective molecular weights of the coordinated TPAMs. This behavior correlates with evidence of shear degradation.

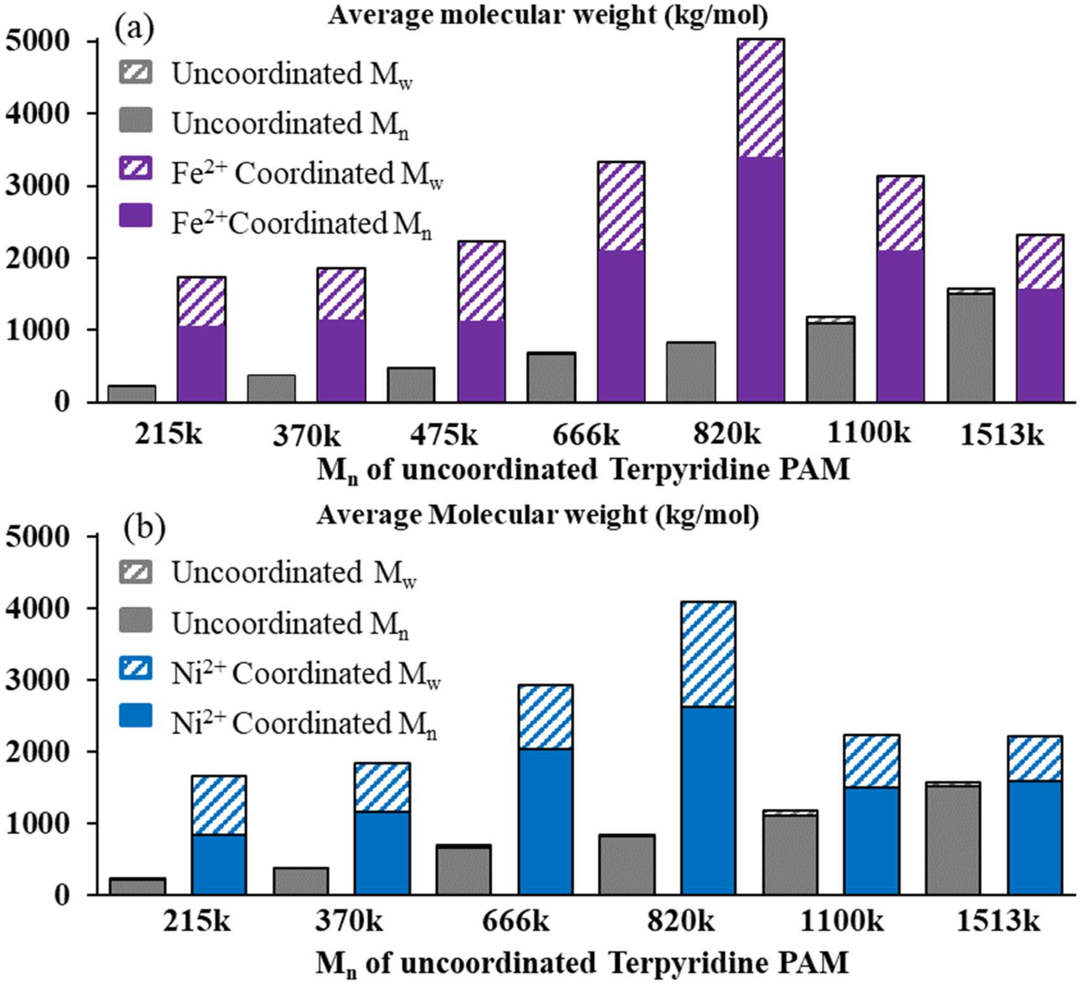

Figure 2.5 (GPC) Molecualr weight of coordinated polymers (a) Fe (II) added at 1:2 molar ratio [Fe^{2+}]:[terpyridine] to 1 wt% TPAM solutions, (b) Ni(II) added at 1:2 molar ratio [Ni^{2+}]:[terpyridine] to 1 wt% TPAM solutions

Ultra-long linear PAM is susceptible to shear degradation. In shear degradation tests where non-associative polyacrylamide with M_n = 2080 kg/mol was sheared using a water circulation pump, we observed that polymer chains with molecular weight > 1600 kg/mol experienced shear degradation (Figure 2.10 (a)). Looking at the distribution of molecular weight for the polymers used in the current study, the TPAMs with M_n > 1100 kg/mol contained significant amount of polymer chains that were susceptible to shear degradation with molecular weight > 1600 kg/mol (> 20%) (Figure 2.6). While handling the polymers, ultralong polymers especially with molecular weight > 1600 kg/mol, can break and generate mono-terpyridine functionalized chains that act as "end cappers" that limit the formation of longer supramolecules (Scheme 2.9).

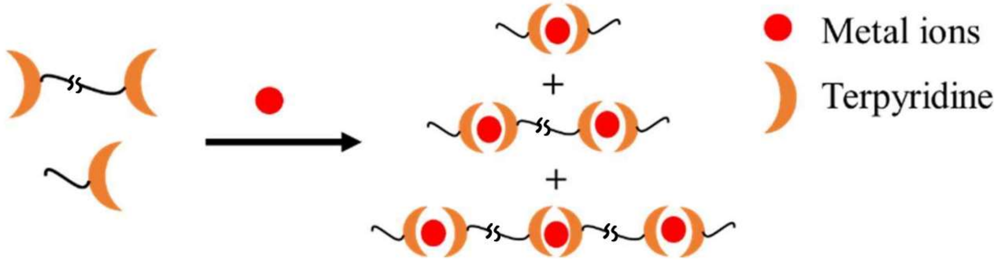

Scheme 2.9 Mono-terpyridine functionalized polymers acting as chain end cappers hypothesized to have formed by hydrodynamic degradation in TPAM 1100k and 1500k. Drawing is not to scale: the intact PAM is more than 1000x the mass of the end groups.

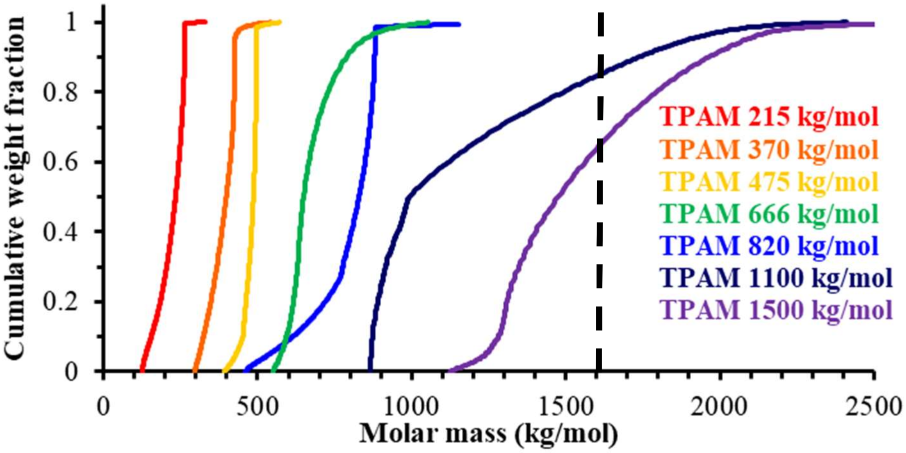

Figure 2.6 Molecular weight distribution of terpyridine PAM samples with M_n = 820 kg/mol, M_n = 1100 kg/mol, and M_n = 1500 kg/mol.

A similar result was obtained when the polymer concentration was lowered to 0.2 wt% and the TPAMs were coordinated with Ni^{2+} (Figure 2.7).

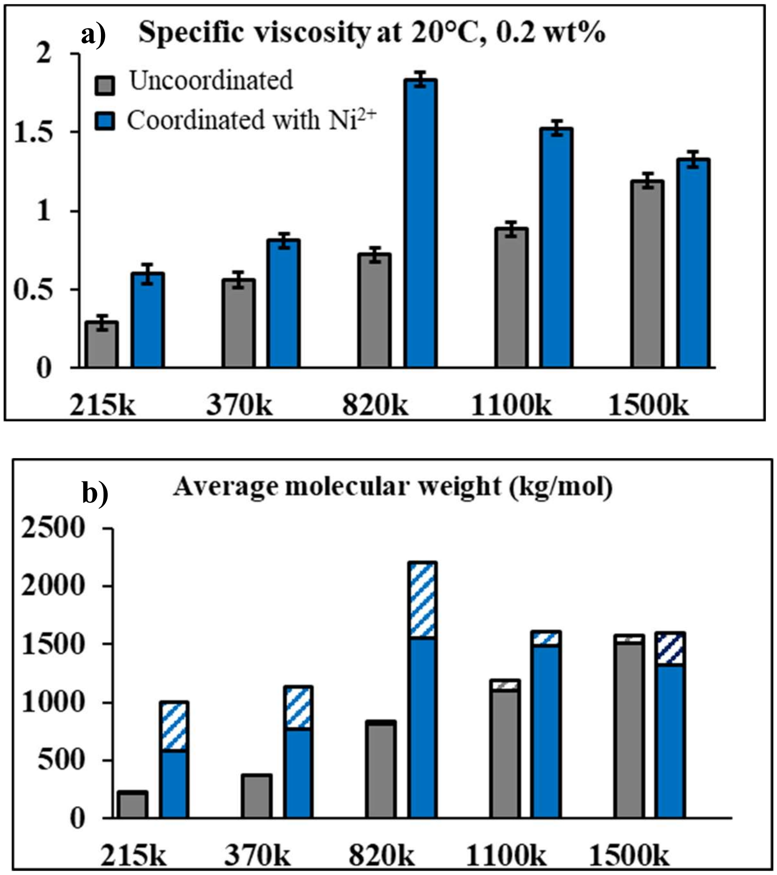

Figure 2.7 Viscosity measurement and GPC molecular weight characterization of Ni^{2+} coordinated TPAM solutions. **(a)** Specific viscosity of coordinated polymer solutions. $[Ni^{2+}]/[terpyridine] = 0.5$, **(b)** GPC molecular weight characterization of coordinate polymers.

While the longest molecular weight of PAM that can survive shear degradation would be different for different applications, we used terpyridine PAM with $M_n = 820$ kg/mol for the experiments in the remainder of this chapter since using this sample provided the highest effective molecular weight of coordinated TPAM.

Effect of polymer concentration on coordination of the terpyridine ended polymers

The concentration of polymers at the time of the metal ion addition also affects the equilibrium between linear/ring supramolecular polymers as the terpyridine end groups can participate in both intramolecular and intermolecular associations. In general, a more dilute polymer concentration will favor intramolecular association, and the formation of more cyclic supramolecules. We prepared terpyridine PAM (M_n = 820 kg/mol) solutions at 0.01 – 1 wt% concentrations and added the appropriate amount of metal ions (Fe (II) or Ni (II)) at [metal^{2+}]/[terpyridine] = 0.5 and measured the effective molecular weights of the coordinated polymers using GPC (Table 2.3). Note that the order of operations is important (See Table 2.4 & Figure 2.16).

Table 2.3 Molecular weights of coordinated terpyridine PAM (GPC)

Uncoordinated terpyridine PAM M_n = 820 kg/mol, [Metal^{2+}]/[terpyridine] = 0.5

Fe^{2+}	**Mw (kg/mol)**	**Mn (kg/mol)**	**PDI**	**Ni^{2+}**	**Mw (kg/mol)**	**Mn (kg/mol)**	**PDI**
1wt%	5036	3407	1.46	**1wt%**	4090	2630	1.56
0.5wt%	3480	2480	1.4	**0.5wt%**	3360	2200	1.53
0.25wt%	3110	2120	1.47	**0.25wt%**	2610	1880	1.39
0.1wt%	1950	1400	1.4	**0.1wt%**	2480	1630	1.53
0.05wt%	1760	1240	1.42	**0.05wt%**	1620	1220	1.32
0.01wt%	822	730	1.13	**0.01wt%**	852	766	1.11
Control	837	815	1.03	**Control**	837	815	1.03

As expected, the higher polymer concentration resulted in a higher effective molecular weight of the coordinated polymers. When the concentration was lowered to 0.01 wt%, the average molecular weight of the coordinated polymer was close to that of the uncoordinated control polymer. However, the GPC chromatograms (light scattering detector signals) of the coordination polymer at 0.01wt% showed a few interesting features. (Figure 2.8). There was a left shoulder, which indicates the formation of coordination polymers with molecular weight > 820 kg/mol. In general, cyclic polymers have smaller hydrodynamic volume than that of linear analogues.[30–33] In the GPC chromatogram, the apex of the peak of the coordinated polymer at 0.01 wt% was at a later time than that of the control polymer, suggesting the formation of monocyclic species in the solution.

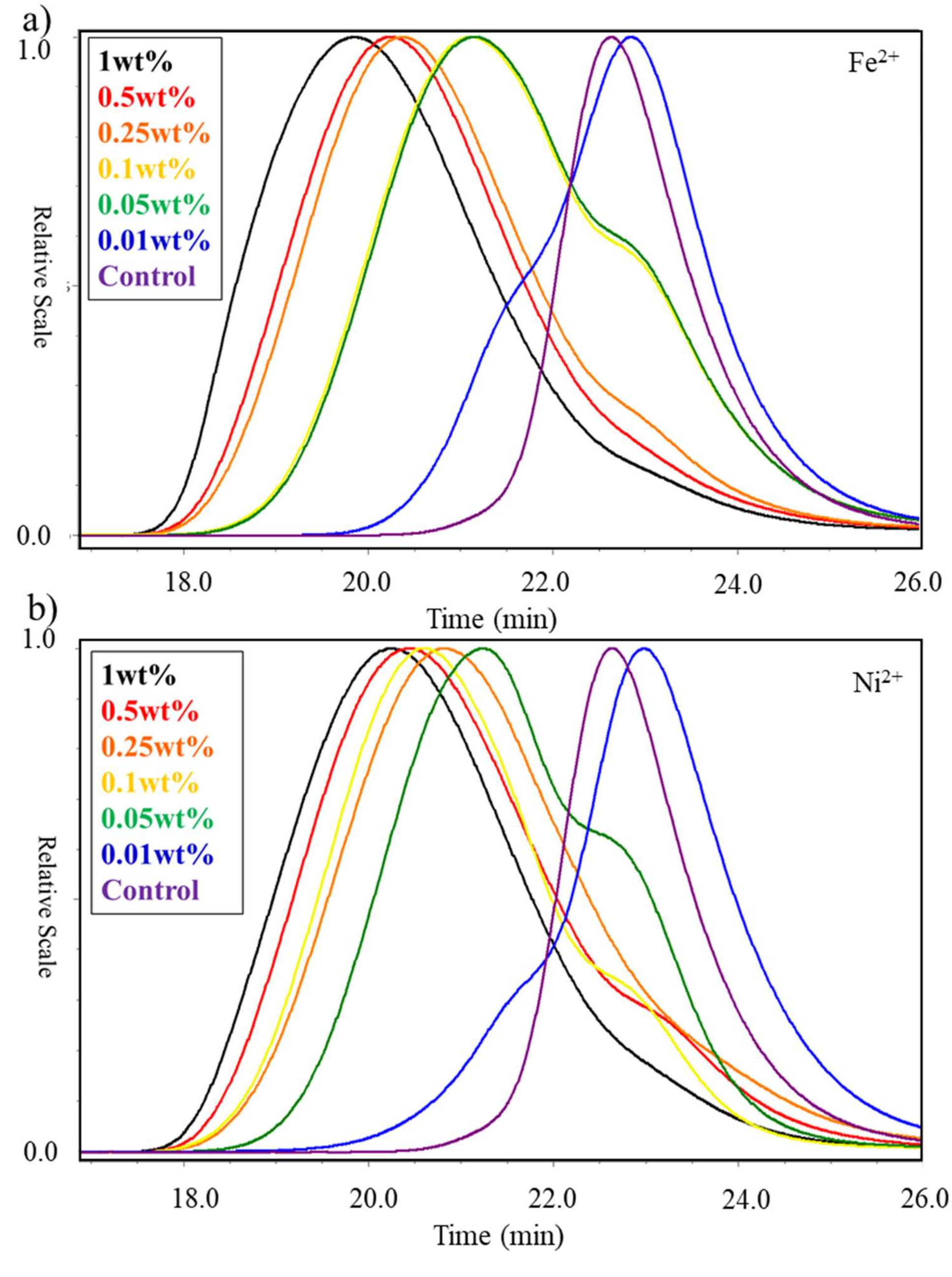

Figure 2.8 GPC chromatogram (light scattering detector signal) of coordinated terpyridine PAM. Uncoordinated terpyridine PAM M_n = 820 kg/mol. [Metal^{2+}]/[terpyridine] = 0.5.

Shear recovery of coordinated polymers

We wanted to demonstrate the coordinated polymer's ability to recover from shear degradation. We prepared three polymer solutions (PAM 2M, TPAM 820k, and TPAM 820k with Ni^{2+}) at 0.1 wt% concentration in ultrapure water (Milli-Q grade). Due to the increased volume of polymer solution necessary for this experiment (500 mL), we stirred the solutions using a magnetic stirrer with a PTFE coated magnetic stir bar at 90 rpm instead of using the wrist action shaker. To prepare Ni^{2+} coordinated solution, Ni^{2+} (from a stock solution of 20 mM $NiCl_2$) was added to TPAM 820k solution (500 mL) to provide $[Ni^{2+}]$:[terpyridine] = 1:2, and the solution was stirred for an additional 24 hours. We measured the viscosity of the polymer solutions using the rheometer and characterized the molecular weights of the polymers in the solution using GPC. After these measurements, each solution was passed through a recirculating pump (5.05 gallons/minute), for 30 minutes, following which we measured the viscosity and characterized the molecular weights of the polymers in the solution again for comparison. (Figure 2.9)

TPAM 820k showed negligible change (~1-3%) before and after shearing in both GPC analysis and specific viscosity ($\eta_{specific}$) measurements. For the TPAM 820k with Ni^{2+}, both the viscosity and the effective molecular weight of the polymers decreased slightly after shearing. However, PAM 2M experienced a significant shear degradation. M_w decreased from 2.2 Mg/mol to 1.4 Mg/mol, and the molecular mass distribution of the polymers before and after shearing showed that the pump was able to break polyacrylamide chains with $M_n > 1600$ kg/mol (Figure 2.10 (a)). Based on this observation, the terpyridine ended polymers were able to recover after shearing, forming the majority of the ultralong coordination polymers again when the shearing stopped.

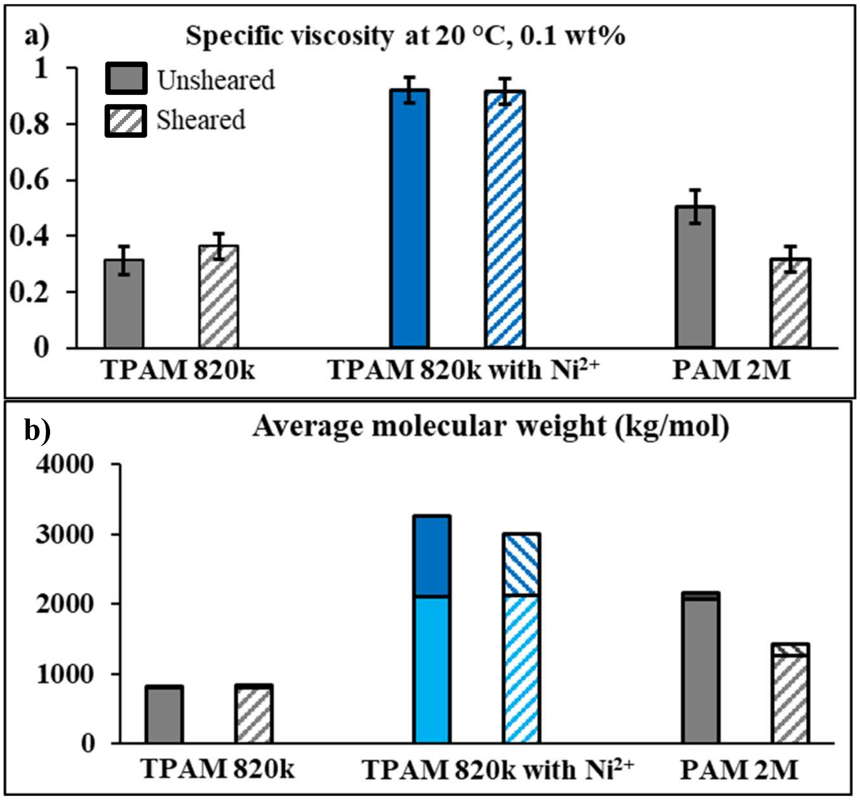

Figure 2.9 Viscosity measurement and GPC molecular weight characterization of polymers before and after passing through pump. **(a)** Specific viscosity of polymer solutions before and after passing through pump, **(b)** GPC molecular weight of the polymer solutions before and after passing through pump.

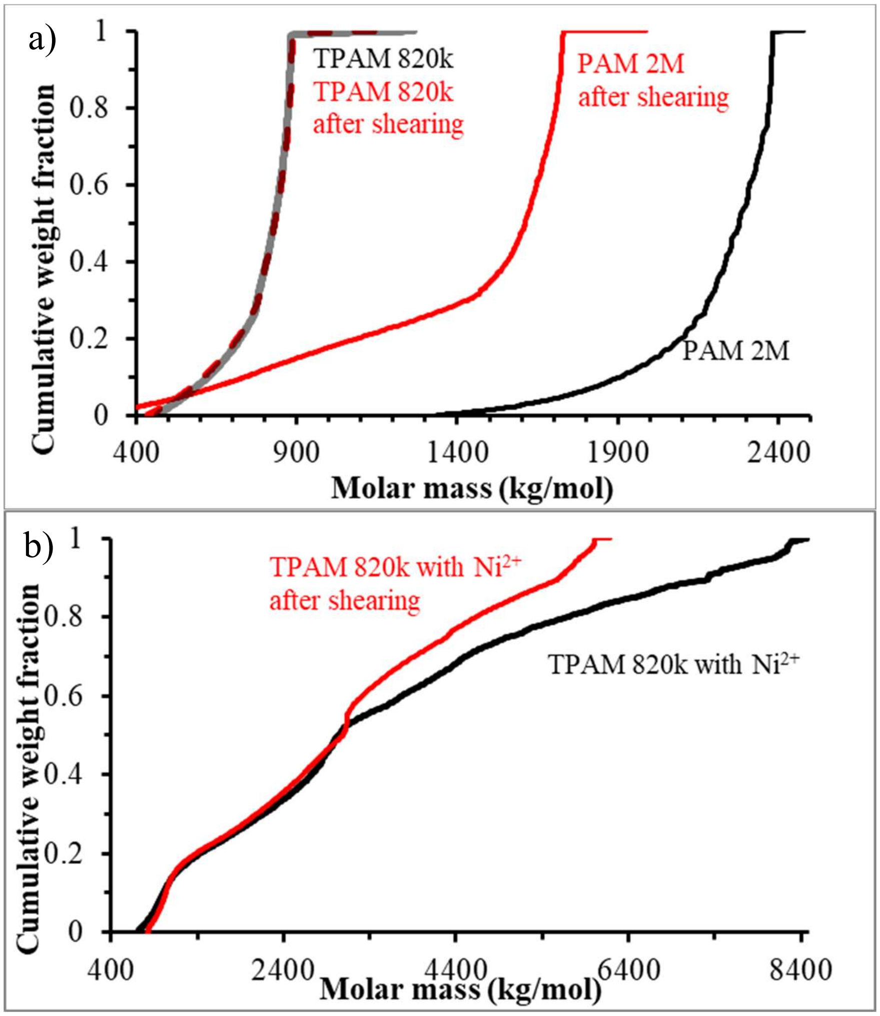

Figure 2.10 Molar mass distribution of polymers before and after passing through the pump **(a)** molar mass distribution of the TPAM 820k and PAM 2M polymers before and after passing through the pump **(b)** molar mass distribution (RI signal) of TPAM 820k (0.1wt%) with Ni^{2+} before and after passing through the pump.

2.4 Conclusion

In this chapter, we described the facile synthesis of terpyridine functionalized RAFT agents, and the synthesis of high molecular weight polyacrylamides with molecular weight control. Tuning the protonation state of terpyridine enabled both more straightforward purification of the RAFT agent and one-step polymerization to reach the desired molecular weight (obviating the need for macro chain transfer agent synthesis and a chain extension reaction). Ultralong supramolecules (> 2000 kg/mol) were formed when metal ions (Fe^{2+} or Ni^{2+}) were added to terpyridine functionalized PAM solutions in water even at low concentrations (> 0.2 wt%). We also compared backbone lengths for TPAM in the range M_n 215 kg/mol – 1500 kg/mol and found that the longest supramolecules were formed when M_n was 820 kg/mol. Longer samples contained ultralong TPAMs (> 1600 kg/mol) that were susceptible to shear degradation, which tended to form undesired mono-terpyridine functionalized polymer products over time.

We also demonstrated shear recovery in coordinated TPAM, where TPAM 820k with Ni^{2+} was able to recover after passage through a pump. The same conditions resulted in irreversible degradation of covalent PAM with M_n 2080 kg/mol.

The methods described in this chapter provide a basis for designing and optimizing associative polymer additives for various aqueous applications such as agricultural sprays and drag reduction in pipe flows. Further work on the characterization of coordinated TPAM solutions using dripping-onto-substrate rheometry and aging of the polymer solutions can be found in Robert Learsch's thesis.

2.5 Supplementary data

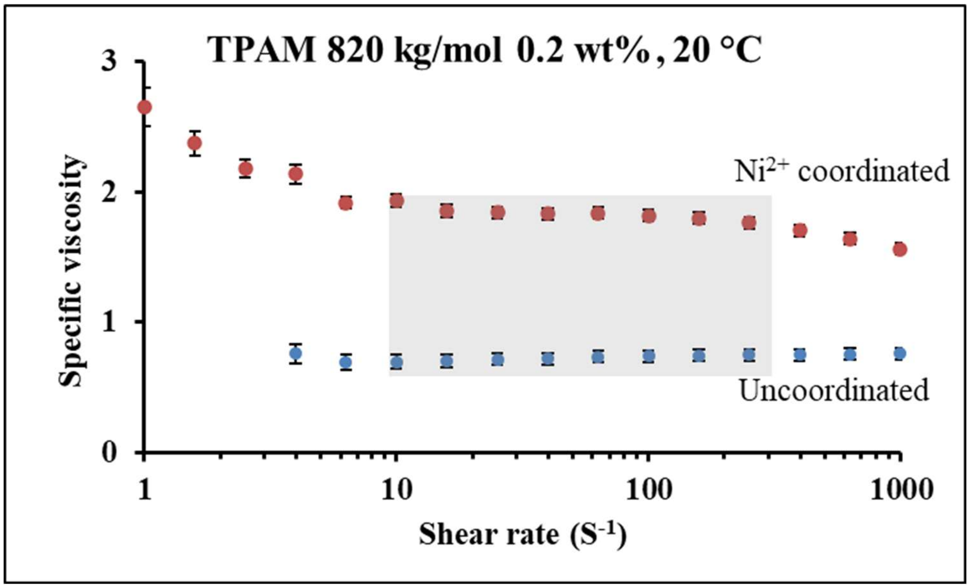

Figure 2.11 Specific viscosity ($\eta_{specific}$) of terpyridine functionalized polyacrylamide at 0.2 wt% polymer concentration in water at 20 °C. $\eta_{specifc} = \eta_{solution}/\eta_{solvent} - 1$ For Ni^{2+} coordinated solution, $[Ni^{2+}]/[Terpyridine]=0.5$. For coordinated solutions, shear thinning behavior was observed for shear rates between 1-10 s^{-1}. For uncoordinated solutions, the first few data points corresponding to shear rate < 4 s^{-1} were measured below the TA ARES-RFS rheometer torque limit (0.196 µNm) so they were not included in the plot. The ($\eta_{specific}$) values were averaged over data points taken from the range that did not show shear rate dependence (10 to 300 s^{-1}, shaded region in the figure).

(a) TPAM 92k

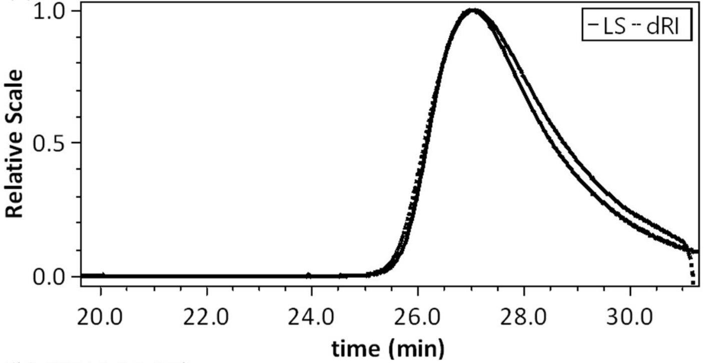

(b) TPAM 145k

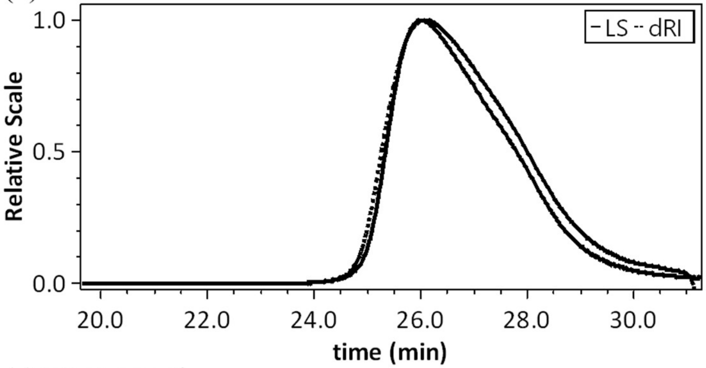

(c) TPAM 215k

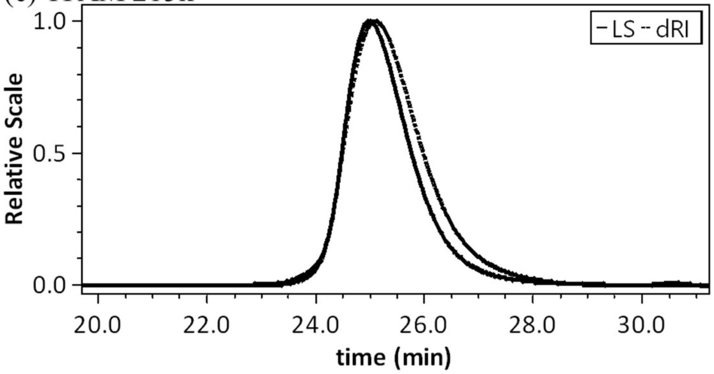

(d) TPAM 370k

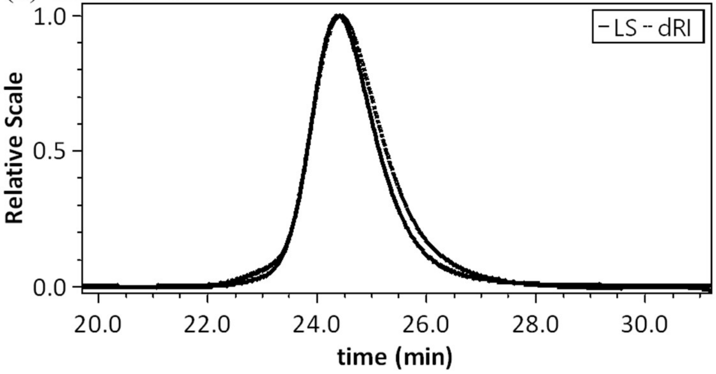

Figure 2.12 GPC chromatogram of terpyridine functionalized PAM (a) M_n 92 kg/mol (b) M_n 145 kg/mol (c) M_n 215 kg/mol (d) M_n 370 kg/mol

(e) TPAM 473k

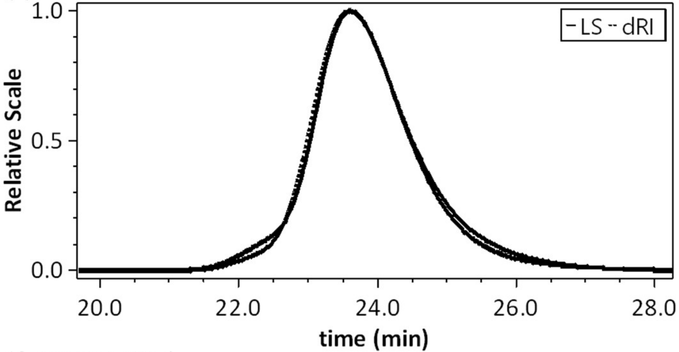

(f) TPAM 666k

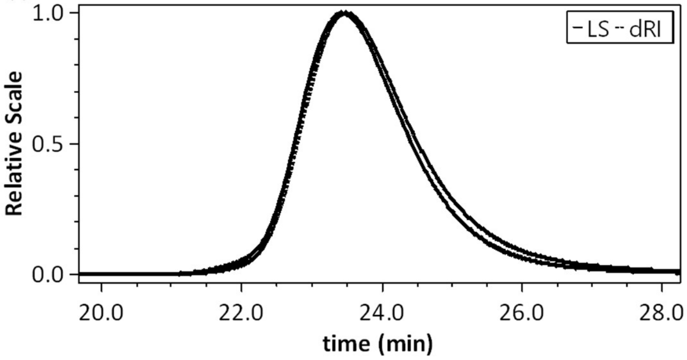

(g) TPAM 719k

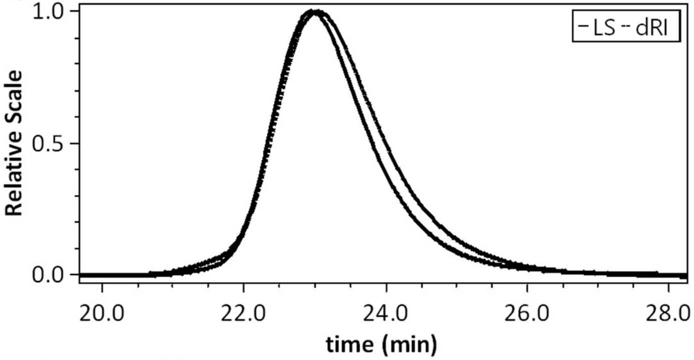

(h) TPAM 775k

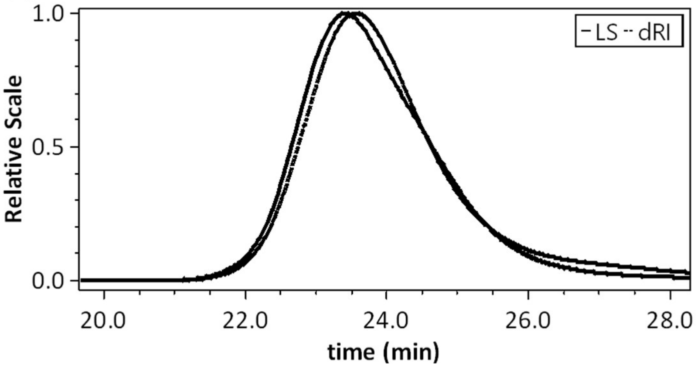

Figure 2.12 continued (e) M_n 473 kg/mol (f) M_n 666 kg/mol (g) M_n 719 kg/mol (h) M_n 775

(i) TPAM 820k

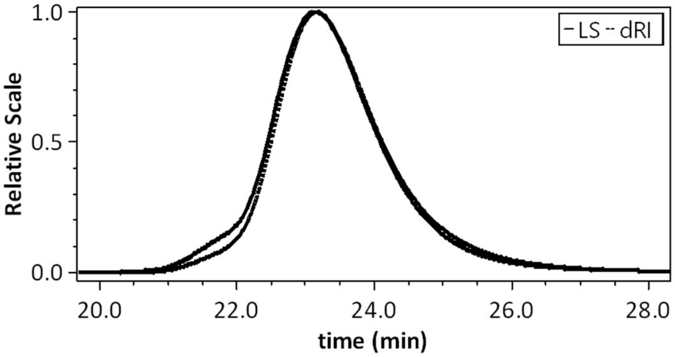

(j) TPAM 900k

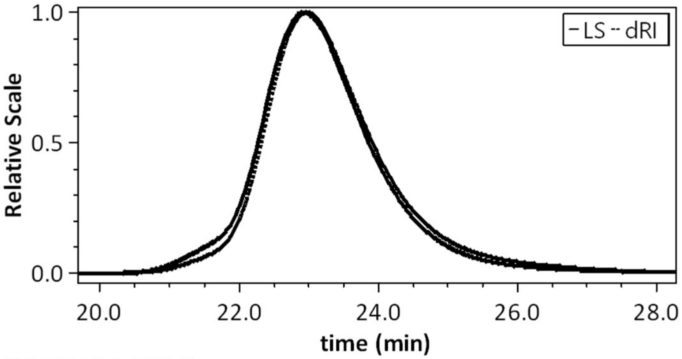

(k) TPAM 1036k

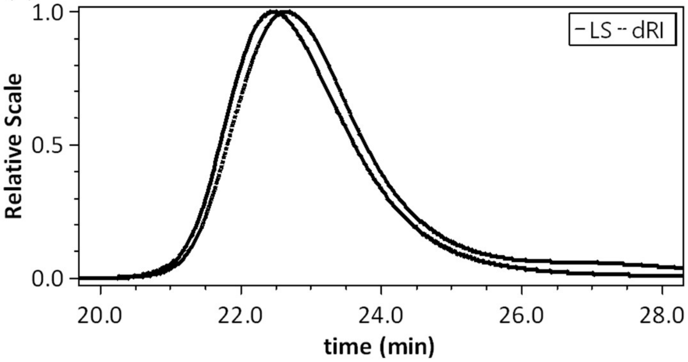

(l) TPAM 1100k

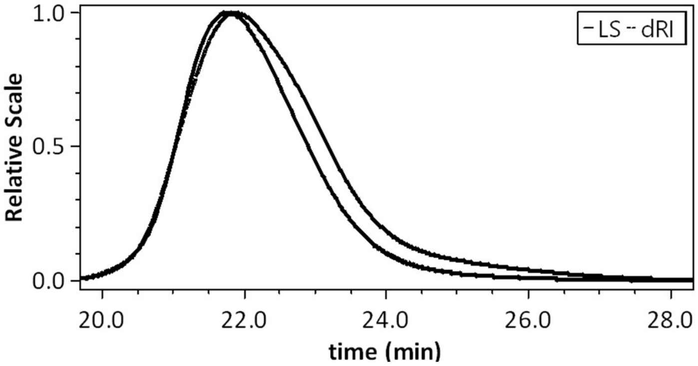

Figure 2.12 continued (i) M_n 820 kg/mol (j) M_n 900 kg/mol (k) M_n 1036 kg/mol (l) M_n 1100 kg/mol

(m) TPAM 1513k

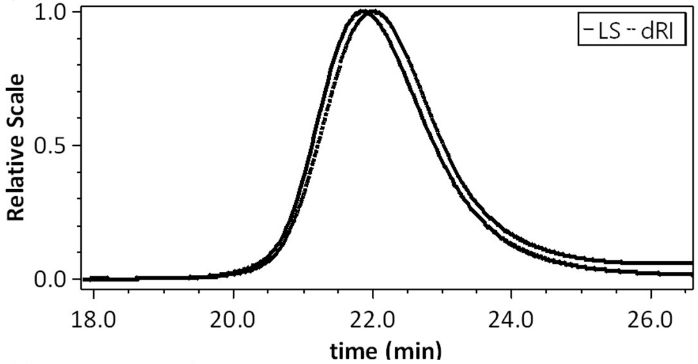

(n) TPAM 1726k

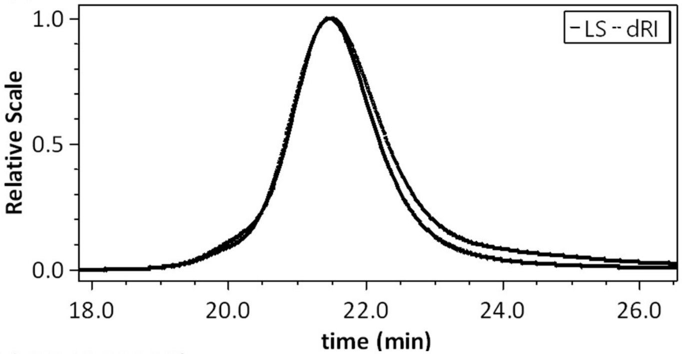

(o) TPAM 2998k

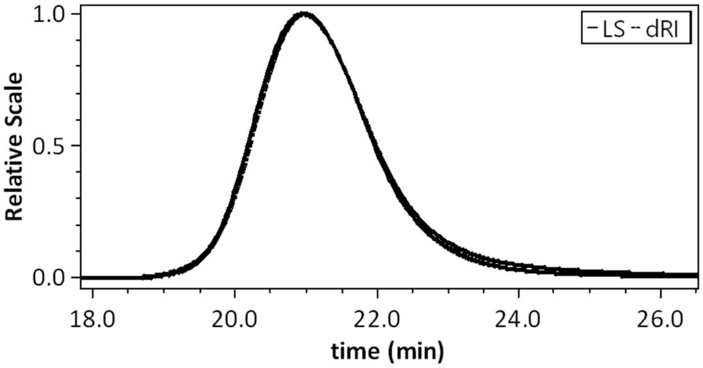

(p) TPAM 3434k

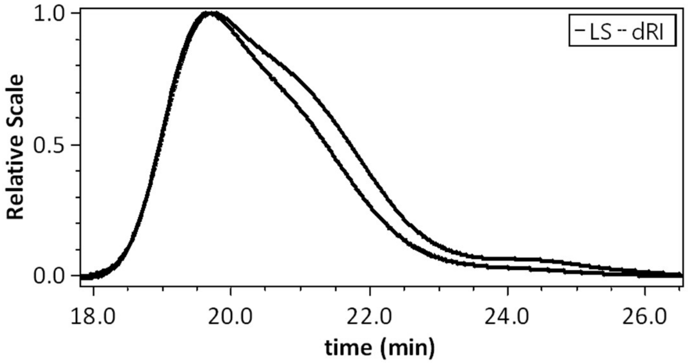

Figure 2.12 continued (m) M_n 1513 kg/mol (n) M_n 1762 kg/mol (o) M_n 2998 kg/mol (p) M_n 3434 kg/mol

(a) TPAM 215k (Fe^{2+})

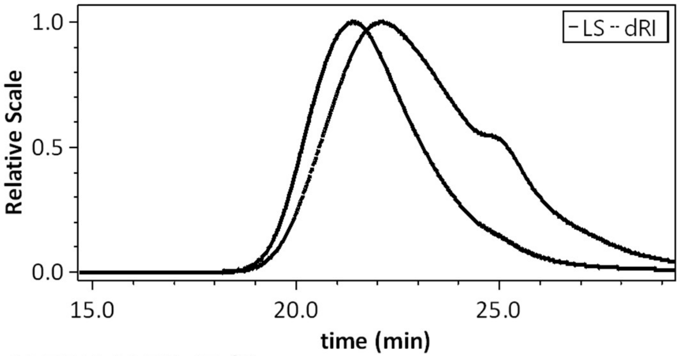

(b) TPAM 370k (Fe^{2+})

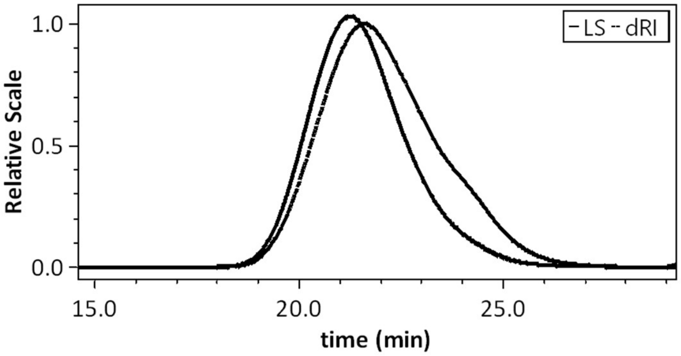

(c) TPAM 475k (Fe^{2+})

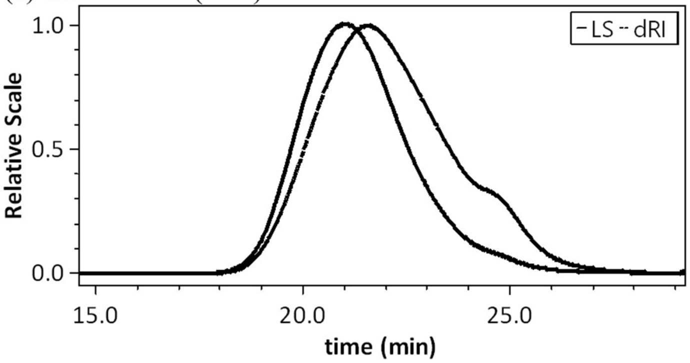

Figure 2.13 GPC chromatogram of Fe^{2+} coordinated terpyridine PAM solution. Fe (II) added at 1:2 molar ratio [Fe^{2+}]:[terpyridine] to 1 wt% TPAM solutions (a) TPAM 215 kg/mol (b) TPAM 370 kg/mol (c) TPAM 475 kg/mol

(d) TPAM 666k (Fe^{2+})

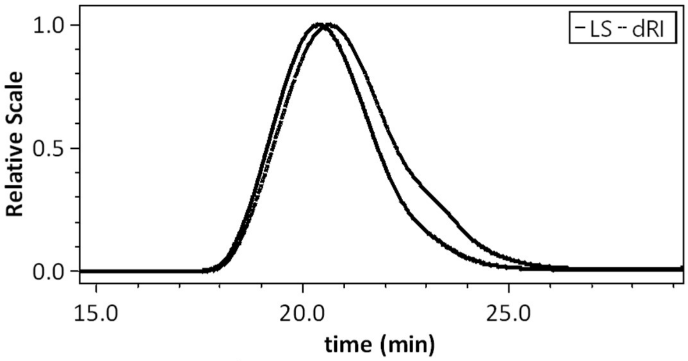

(e) TPAM 820k (Fe^{2+})

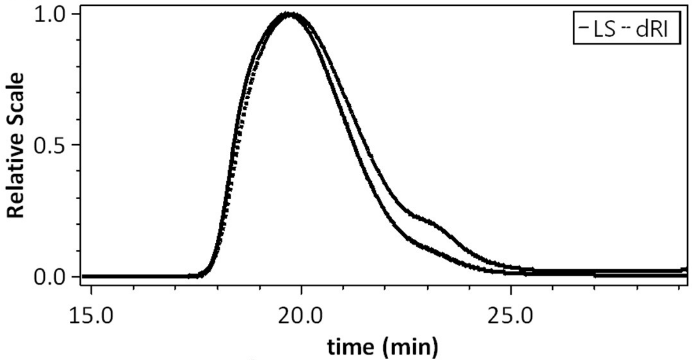

(f) TPAM 1100k (Fe^{2+})

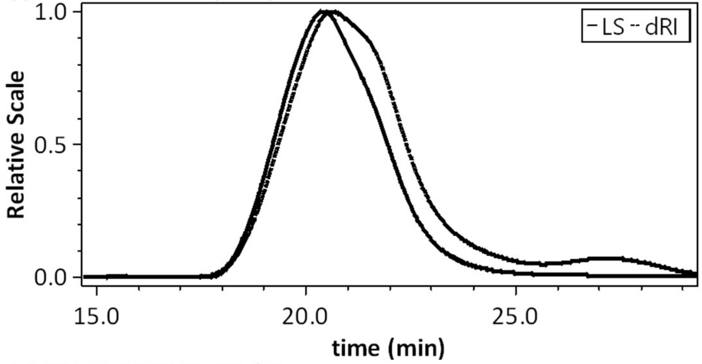

(g) TPAM 1513k (Fe^{2+})

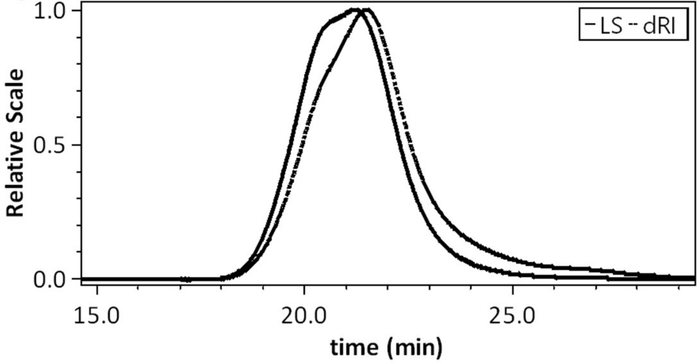

Figure 2.13 continued (d) TPAM 666 kg/mol (e) TPAM 820 kg/mol (f) TPAM 1100 kg/mol (g) TPAM 1513 kg/mol

(a) TPAM 215k (Ni^{2+})

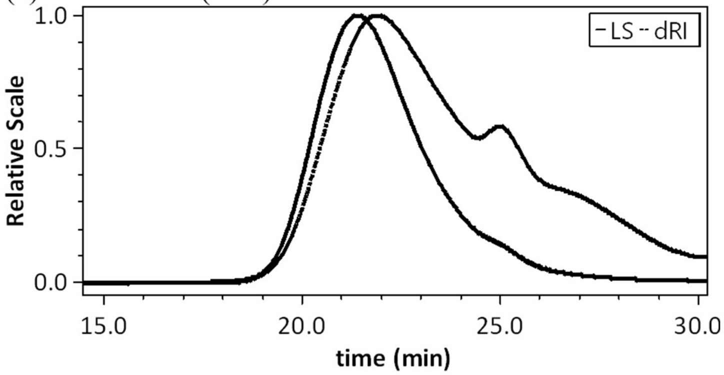

(b) TPAM 370k (Ni^{2+})

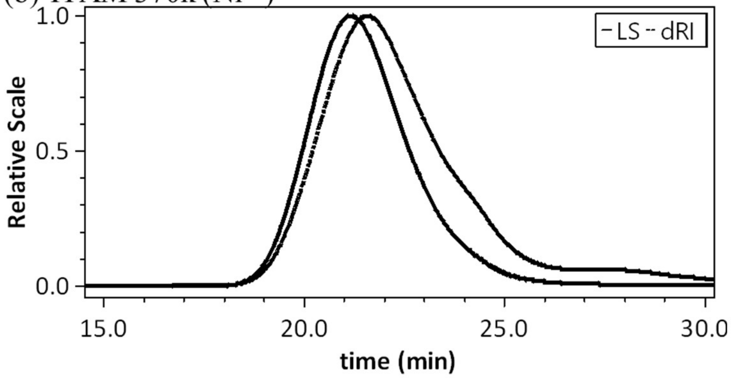

(c) TPAM 666k (Ni^{2+})

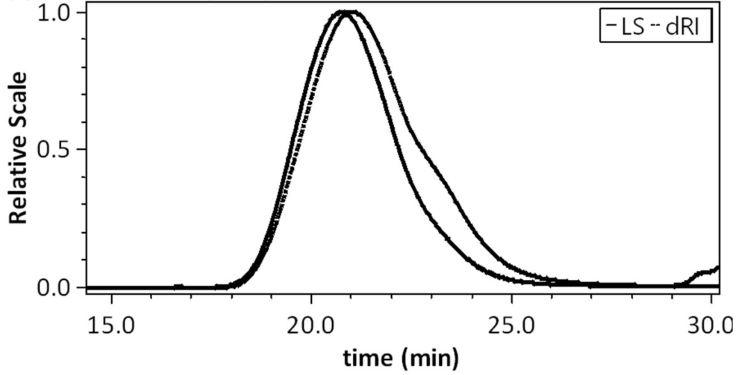

Figure 2.14 GPC chromatogram of Ni^{2+} coordinated terpyridine PAM solution. Ni (II) added at 1:2 molar ratio [Ni^{2+}]:[terpyridine] to 1 wt% TPAM solutions (a) TPAM 215 kg/mol (b) TPAM 370 kg/mol (c) TPAM 666 kg/mol

(d) TPAM 820k (Ni^{2+})

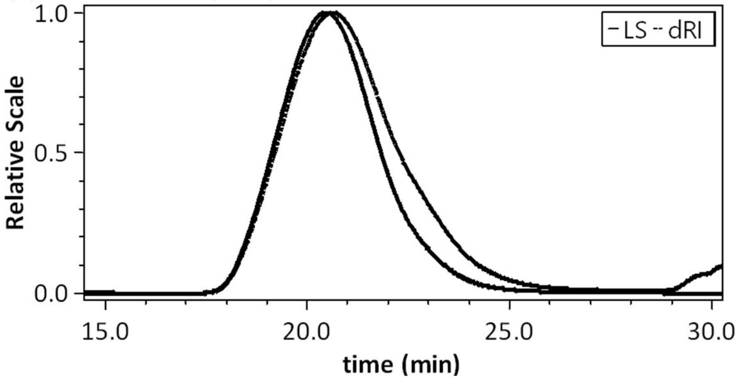

(e) TPAM 1100k (Ni^{2+})

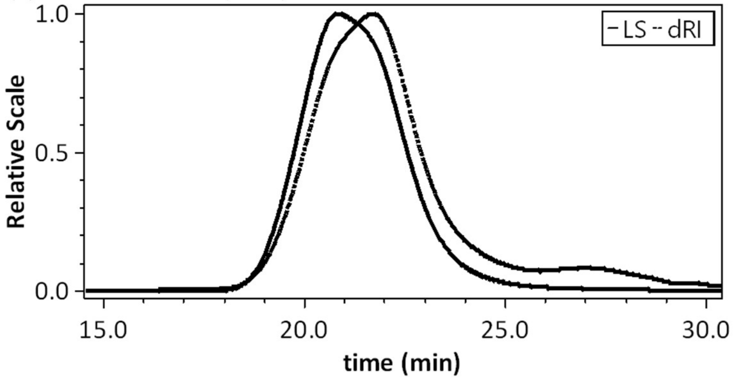

(f) TPAM 1513k (Ni^{2+})

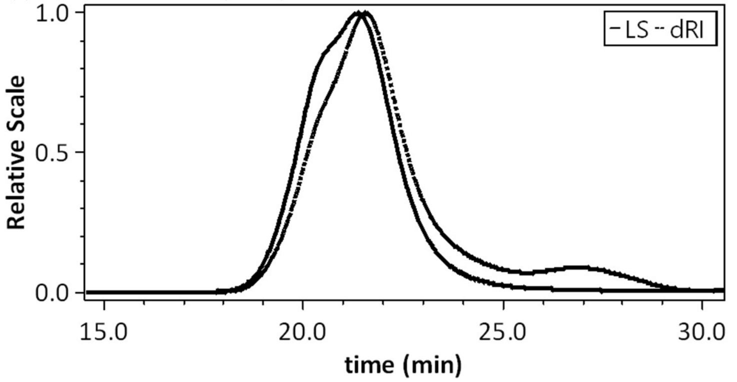

Figure 2.14 continued (d) TPAM 820 kg/mol (e) TPAM 1100 kg/mol (f) TPAM 1513 kg/mol

(a) TPAM 215k (Ni^{2+})

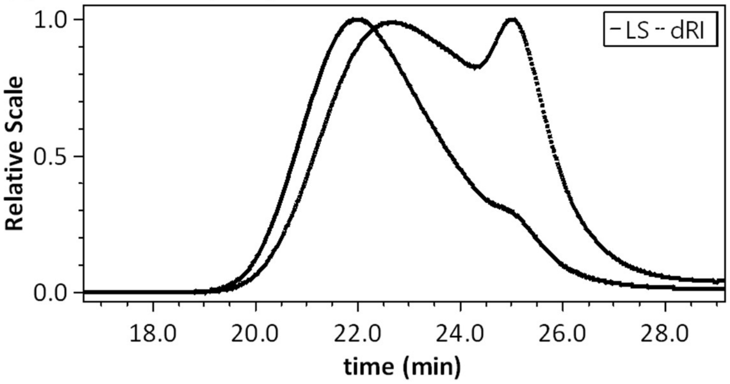

(b) TPAM 370k (Ni^{2+})

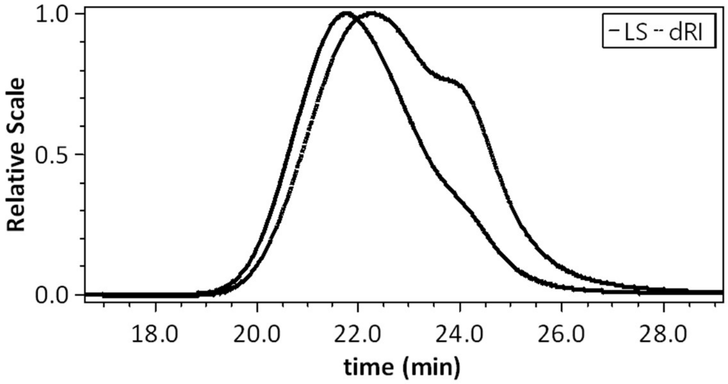

(c) TPAM 820k (Ni^{2+})

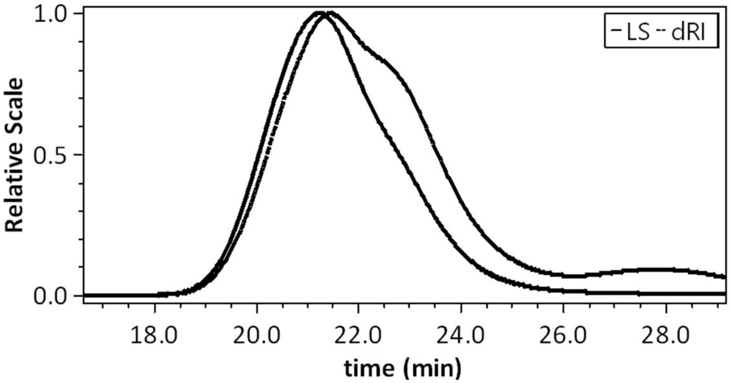

Figure 2.15 GPC chromatogram of Ni^{2+} coordinated terpyridine PAM solution. Ni (II) added at 1:2 molar ratio [Ni^{2+}]:[terpyridine] to 0.2 wt% TPAM solutions (a) TPAM 215 kg/mol (b) TPAM 370 kg/mol (c) TPAM 820 kg/mol

(d) TPAM 1100k (Ni^{2+})

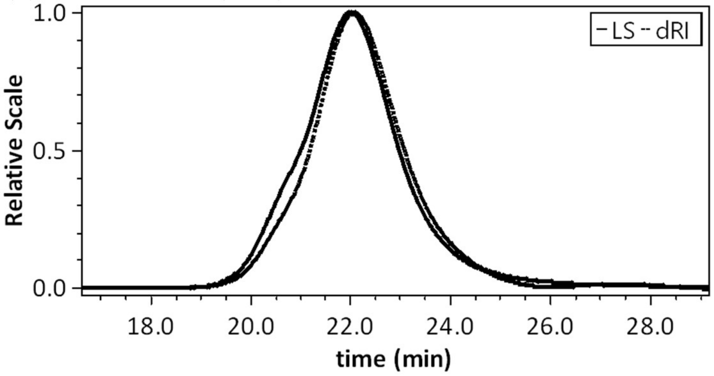

(e) TPAM 1513k (Ni^{2+})

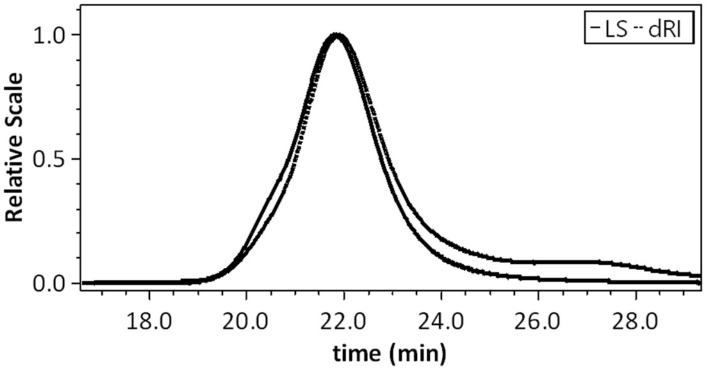

Figure 2.15 continued (d) TPAM 1100 kg/mol (e) TPAM 1513 kg/mol

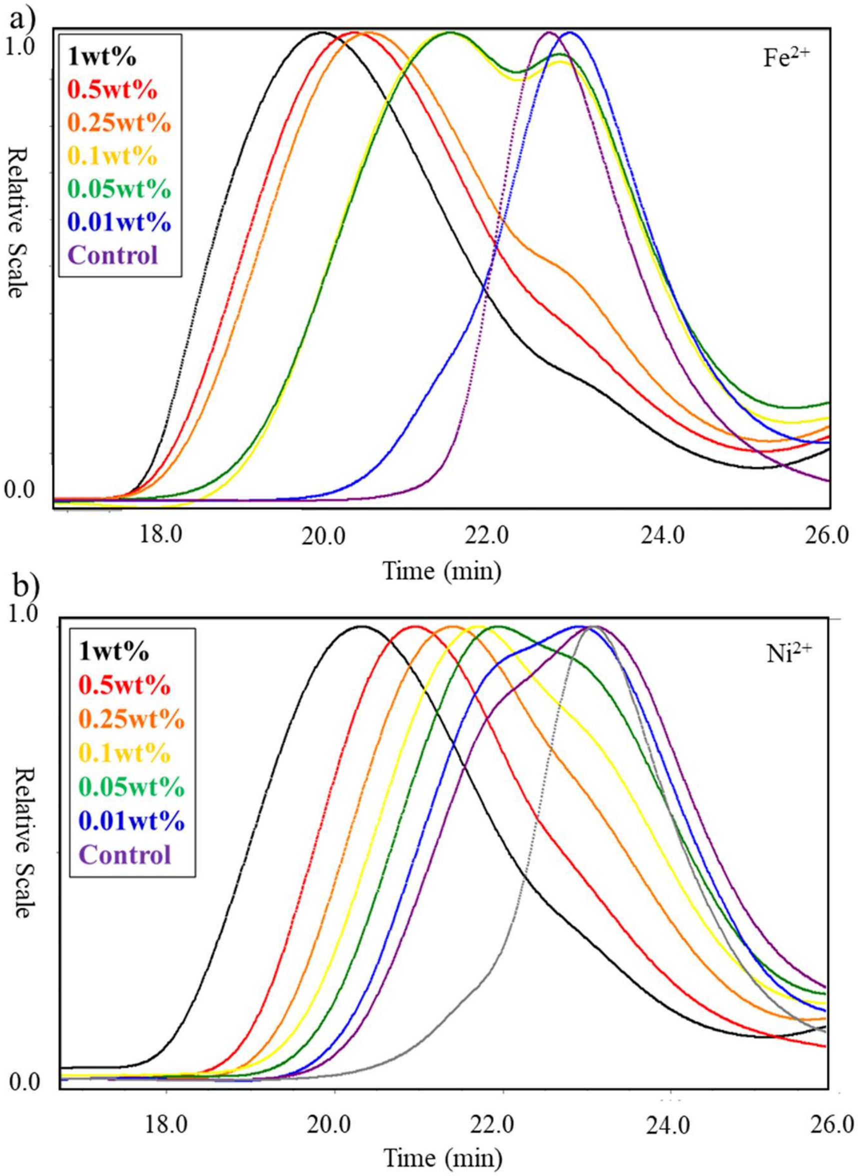

Figure 2.16 GPC chromatogram (RI signal) of coordinated terpyridine PAM. Uncoordinated terpyridine PAM M_n = 820 kg/mol. [Metal^{2+}]/[terpyridine] = 0.5

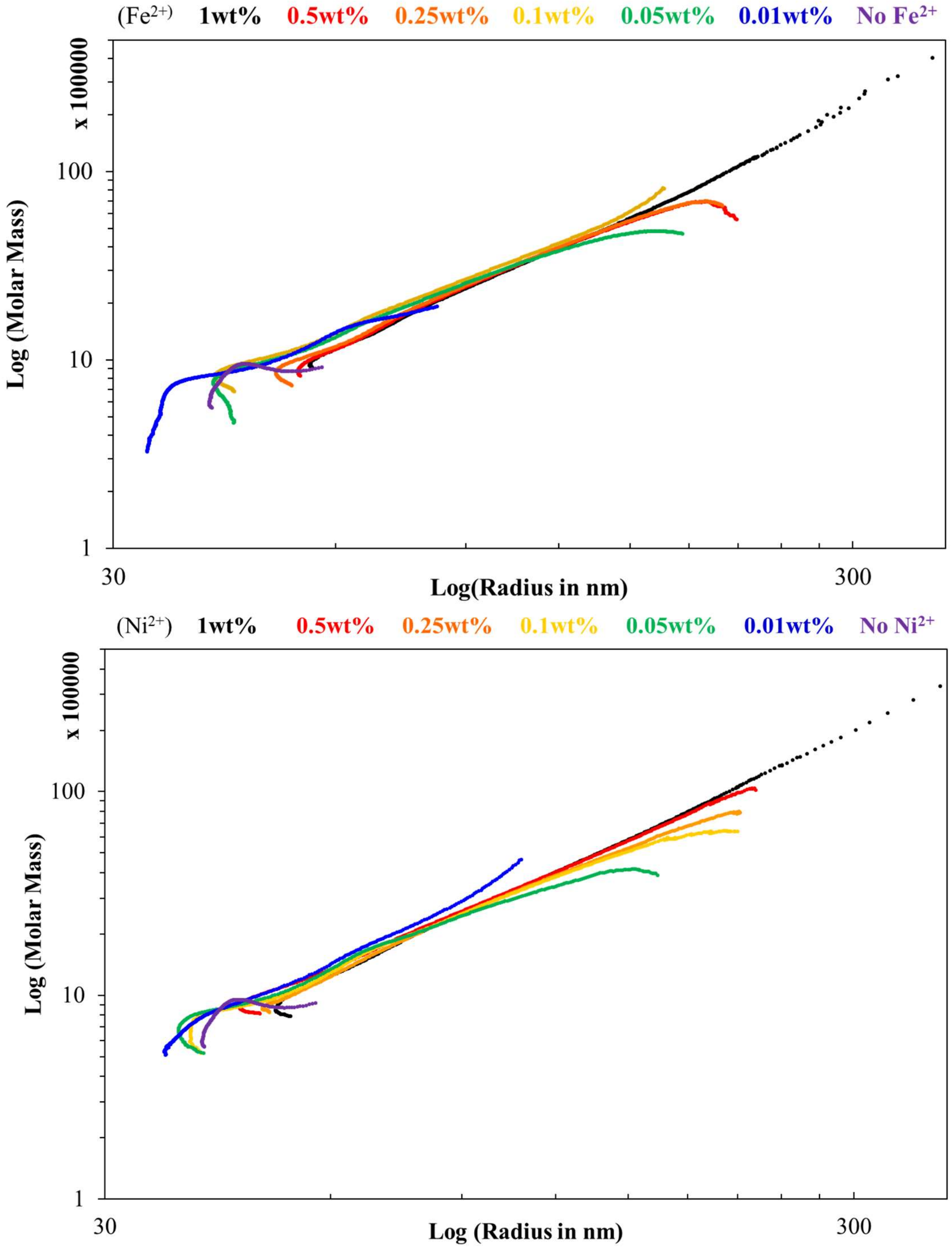

Figure 2.17 Plot of molar mass vs. radius of coordinated terpyridine PAM. Uncoordinated terpyridine PAM M_n = 820 kg/mol. [Metal^{2+}]/[terpyridine] = 0.5. The concentrations indicate initial polymer concentrations in solution at the time of metal ion addition (a) Fe^{2+}, (b) Ni^{2+}

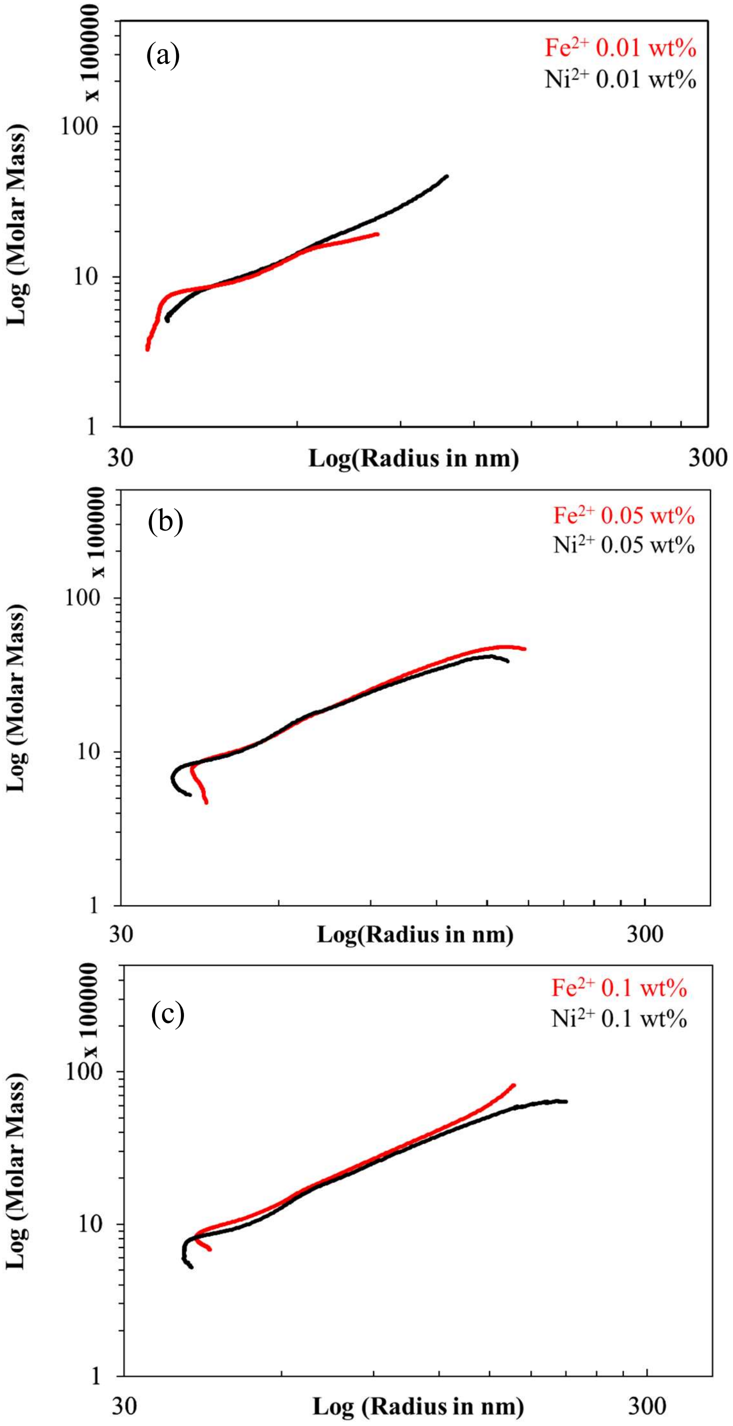

Figure 2.18 Plot of molar mass vs. radius of coordinated terpyridine PAM. Uncoordinated terpyridine PAM M_n = 820 kg/mol. [Metal^{2+}]/[terpyridine] = 0.5. The concentrations indicate initial polymer concentrations in solution at the time of metal ion addition (a) 0.01 wt%, (b) 0.05 wt% (c) 0.1 wt%

Table 2.4 Changes in molecular weight of coordinated polymers after dilution from 1wt% to 0.01wt% [Ni2+]/[Terpyridine]=0.5

	Mw (kg/mol)	**Mn (kg/mol)**	**PDI**
Day 0	3500	2300	1.52
Day 1	2300	1660	1.39
Day 2	1610	1370	1.38
Day 3	1210	1210	1.33
Day 4	1360	1010	1.35
Day 5	1180	875	1.35
Day 6	1060	793	1.33
0.01wt%	852	766	1.12

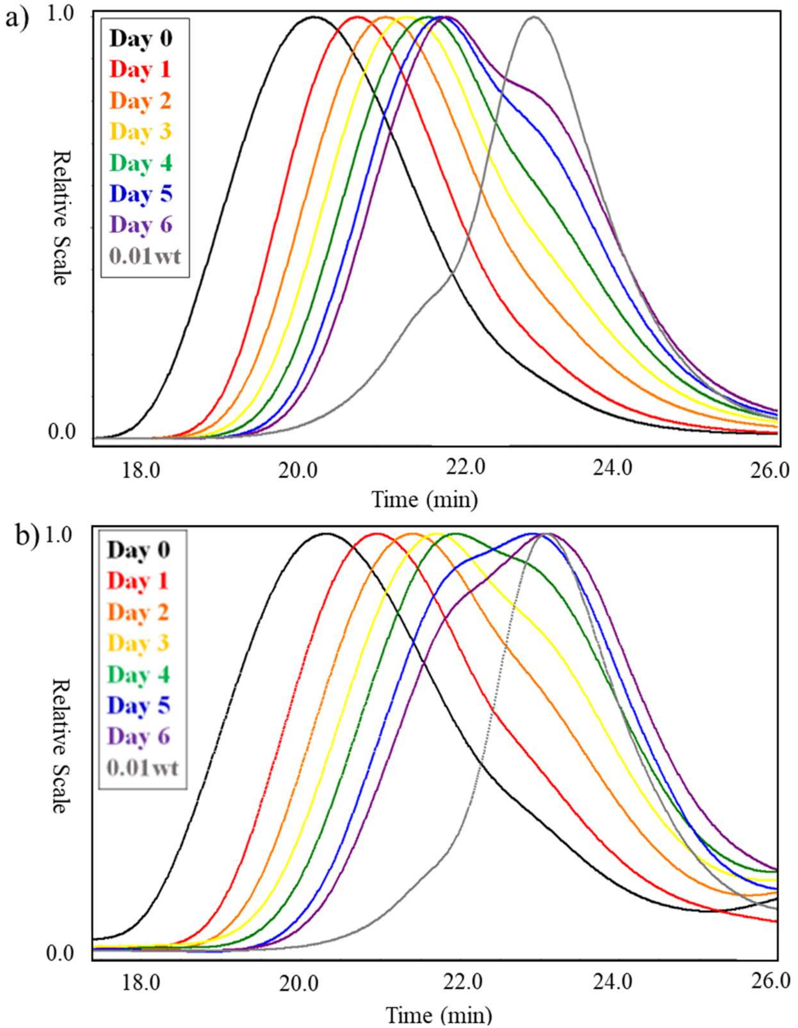

Figure 2.19 GPC chromatogram of Ni^{2+} coordinated terpyridine PAM. Uncoordinated terpyridine PAM M_n = 820 kg/mol. $[Ni^{2+}]/[\text{terpyridine}] = 0.5$. The polymers were coordinated at 1 wt% and diluted to 0.01 wt%. The changes in molecular weight were observed using GPC for 6 days. (a) LS signal (b) RI signal

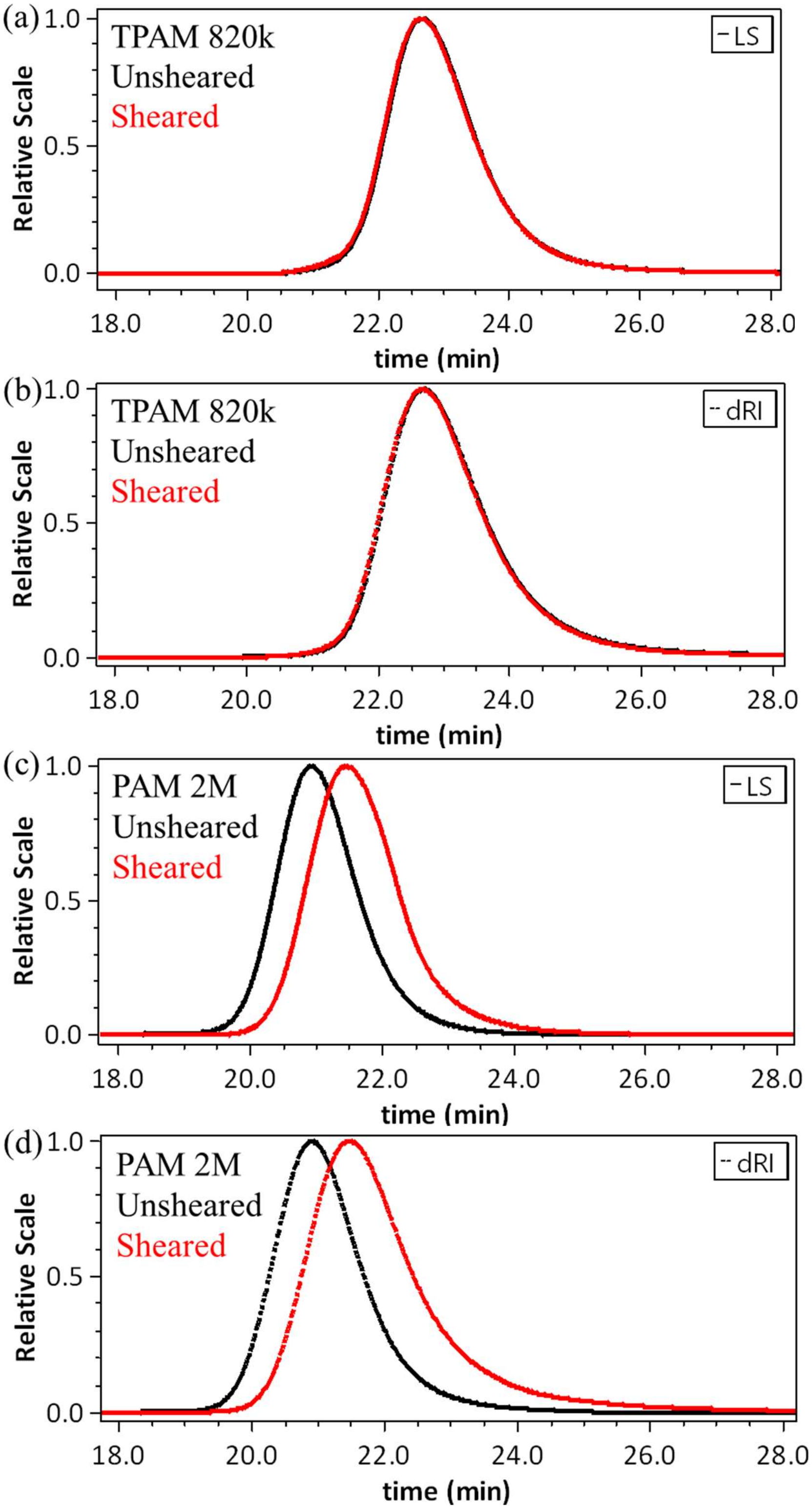

Figure 2.20 GPC chromatogram of polyacrylamide before and after shearing using the recirculation pump. (a) TPAM 820 kg/mol (LS signal) (b) TPAM 820 kg/mol (RI signal) (c) PAM 2 Mg/mol (LS signal) (d) PAM 2 Mg/mol (RI signal)

(e) TPAM 820k (Ni^{2+})

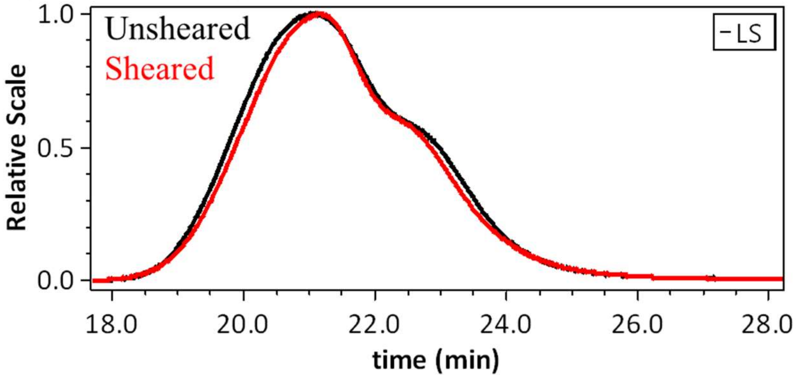

(f) TPAM 820k (Ni^{2+})

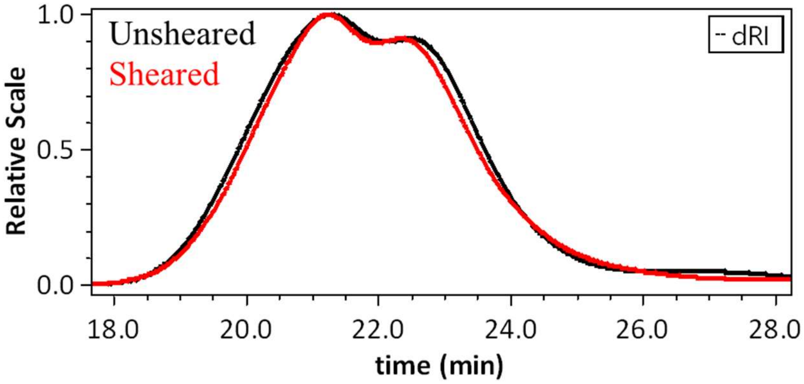

Figure 2.20 continued (e) Ni^{2+} coordinated TPAM 820 kg/mol (LS signal) (f) Ni^{2+} coordinated TPAM 820 kg/mol (RI signal). Ni (II) added at 1:2 molar ratio [Ni^{2+}]:[terpyridine] to 0.1 wt% TPAM solutions

References

(1) Shunmugam, R.; Gabriel, G. J.; Aamer, K. A.; Tew, G. N. Metal-Ligand-Containing Polymers: Terpyridine as the Supramolecular Unit. *Macromol. Rapid Commun.* **2010**, *31* (9–10), 784–793.

(2) Suzuka, T.; Sueyoshi, H.; Ogihara, K. Recyclable Polymer-Supported Terpyridine–Palladium Complex for the Tandem Aminocarbonylation of Aryl Iodides to Primary Amides in Water Using NaN3 as Ammonia Equivalent. *Catalysts* **2017**, *7* (12), 107.

(3) Leung, J. J.; Vigil, J. A.; Warnan, J.; Edwardes Moore, E.; Reisner, E. Rational Design of Polymers for Selective CO 2 Reduction Catalysis. *Angew. Chemie* **2019**, *131* (23), 7779–7783.

(4) Bode, S.; Bose, R. K.; Matthes, S.; Ehrhardt, M.; Seifert, A.; Schacher, F. H.; Paulus, R. M.; Stumpf, S.; Sandmann, B.; Vitz, J.; Winter, A.; Hoeppener, S.; Garcia, S. J.; Spange, S.; van der Zwaag, S.; Hager, M. D.; Schubert, U. S. Self-Healing Metallopolymers Based on Cadmium Bis(Terpyridine) Complex Containing Polymer Networks. *Polym. Chem.* **2013**, *4* (18), 4966.

(5) Jeong, D.-C.; Lee, J.; Ro, Y. H.; Song, C. Repairable Photoactive Polymer Systems via Metal–Terpyridine-Based Self-Assembly. *Polym. Chem.* **2017**, *8* (12), 1923–1931.

(6) Liu, P.; Shi, G.; Chen, X. Terpyridine-Containing π-Conjugated Polymers for Light-Emitting and Photovoltaic Materials. *Front. Chem.* **2020**, *8*.

(7) Lewis, R. W.; Malic, N.; Saito, K.; Evans, R. A.; Cameron, N. R. Ultra-High Molecular Weight Linear Coordination Polymers with Terpyridine Ligands. *Chem. Sci.* **2019**, *10* (24), 6174–6183.

(8) Winter, A.; Schubert, U. S. Synthesis and Characterization of Metallo-Supramolecular Polymers. *Chem. Soc. Rev.* **2016**, *45* (19), 5311–5357.

(9) Mansfeld, U.; Winter, A.; Hager, M. D.; Günther, W.; Altuntaş, E.; Schubert, U. S. A Homotelechelic Bis-Terpyridine Macroligand: One-Step Synthesis and Its Metallo-Supramolecular Self-Assembly. *J. Polym. Sci. Part A Polym. Chem.* **2013**, *51* (9), 2006–2015.

(10) Schmatloch, S.; van den Berg, A. M. J.; Alexeev, A. S.; Hofmeier, H.; Schubert, U. S. Soluble High-Molecular-Mass Poly(Ethylene Oxide)s via Self-Organization. *Macromolecules* **2003**, *36* (26), 9943–9949.

(11) Lohmeijer, B. G. G.; Schubert, U. S. Water-Soluble Building Blocks for Terpyridine-Containing Supramolecular Polymers: Synthesis, Complexation, and PH Stability Studies of Poly(Ethylene Oxide) Moieties. *Macromol. Chem. Phys.* **2003**, *204* (8), 1072–1078.

(12) Wei, M.-H.; Li, B.; David, R. L. A.; Jones, S. C.; Sarohia, V.; Schmitigal, J. A.; Kornfield, J. A. Megasupramolecules for Safer, Cleaner Fuel by End Association of Long Telechelic Polymers. *Science (80-.).* **2015**, *350* (6256), 72–75.

(13) Carmean, R. N.; Becker, T. E.; Sims, M. B.; Sumerlin, B. S. Ultra-High Molecular Weights via Aqueous Reversible-Deactivation Radical Polymerization. *Chem* **2017**, *2* (1), 93–101.

(14) Lai, J. T.; Filla, D.; Shea, R. Functional Polymers from Novel Carboxyl-Terminated Trithiocarbonates as Highly Efficient RAFT Agents. *Macromolecules* **2002**, *35* (18),

6754–6756.

(15) Shaira, A.; Jaganyi, D. Understanding the Role of Flexible 4'-Functionalized Polyethylene Glycoxy Chains on the Behavior of Platinum(II)(4'-(Ethylene Glycoxy)-2,2':6',2''-Terpyridine: A Kinetic and a Mechanistic Study. *J. Coord. Chem.* **2014**.

(16) Abd-El-Aziz, A. S.; Dalgakiran, S.; Vandel, M.; Owen, E. M.; Wagner, B. D. Synthesis and Electrochemical Characterization of Thiophenes with Pendant Fluorescent Terpyridine. *J. Electrochem. Soc.* **2013**.

(17) Schubert, U. S.; Eschbaumer, C.; Hien, O.; Andres, P. R. 4′-Functionalized 2,2′:6′,2″-Terpyridines as Building Blocks for Supramolecular Chemistry and Nanoscience. *Tetrahedron Lett.* **2001**, *42* (28), 4705–4707.

(18) Morgan, B.; Lahav, O. The Effect of PH on the Kinetics of Spontaneous Fe(II) Oxidation by O2 in Aqueous Solution – Basic Principles and a Simple Heuristic Description. *Chemosphere* **2007**, *68* (11), 2080–2084.

(19) Buonomo, J. A.; Aldrich, C. C. Mitsunobu Reactions Catalytic in Phosphine and a Fully Catalytic System. *Angew. Chemie Int. Ed.* **2015**, *54* (44), 13041–13044.

(20) Tamboli, Y.; Kashid, B. B.; Yadav, R. P.; Rafeeq, M.; Yeole, R.; Merwade, A. Y. Triphenylphosphine Oxide Removal from Reactions: The Role of Solvent and Temperature. *ACS Omega* **2021**, *6* (21), 13940–13945.

(21) Batesky, D. C.; Goldfogel, M. J.; Weix, D. J. Removal of Triphenylphosphine Oxide by Precipitation with Zinc Chloride in Polar Solvents. *J. Org. Chem.* **2017**, *82* (19), 9931–9936.

(22) Saadeh, H. A.; Shairah, E. A. A.; Charef, N.; Mubarak, M. S. Synthesis and Adsorption Properties, toward Some Heavy Metal Ions, of a New Polystyrene-Based Terpyridine Polymer. *J. Appl. Polym. Sci.* **2012**, *124* (4), 2717–2724.

(23) Kim, K.-Y.; Nancollas, G. H. Calorimetric Studies of Complex Formation of Transition Metal Ions with 2,2',2"-Terpyridine. *J. Phys. Chem.* **1977**, *81* (10), 948–952.

(24) Thomas, D. B.; Convertine, A. J.; Hester, R. D.; Lowe, A. B.; McCormick, C. L. Hydrolytic Susceptibility of Dithioester Chain Transfer Agents and Implications in Aqueous RAFT Polymerizations. *Macromolecules* **2004**, *37* (5), 1735–1741.

(25) Convertine, A. J.; Lokitz, B. S.; Lowe, A. B.; Scales, C. W.; Myrick, L. J.; McCormick, C. L. Aqueous RAFT Polymerization of Acrylamide AndN,N-Dimethylacrylamide at Room Temperature. *Macromol. Rapid Commun.* **2005**, *26* (10), 791–795.

(26) Sumerlin, B. S.; Lowe, A. B.; Thomas, D. B.; McCormick, C. L. Aqueous Solution Properties of PH-Responsive AB Diblock Acrylamido Copolymers Synthesized via Aqueous RAFT. *Macromolecules* **2003**, *36* (16), 5982–5987.

(27) Lewis, R. W.; Evans, R. A.; Malic, N.; Saito, K.; Cameron, N. R. Ultra-Fast Aqueous Polymerisation of Acrylamides by High Power Visible Light Direct Photoactivation RAFT Polymerisation. *Polym. Chem.* **2018**, *9* (1), 60–68.

(28) Fu, Q.; McKenzie, T. G.; Tan, S.; Nam, E.; Qiao, G. G. Tertiary Amine Catalyzed Photo-Induced Controlled Radical Polymerization of Methacrylates. *Polym. Chem.* **2015**, *6* (30), 5362–5368.

(29) Fu, Q.; Xie, K.; McKenzie, T. G.; Qiao, G. G. Trithiocarbonates as Intrinsic Photoredox Catalysts and RAFT Agents for Oxygen Tolerant Controlled Radical Polymerization. *Polym. Chem.* **2017**, *8* (9), 1519–1526.

(30) Bielawski, C. W.; Benitez, D.; Grubbs, R. H. An "Endless" Route to Cyclic Polymers. *Science (80-.).* **2002**, *297* (5589), 2041–2044.

(31) Kricheldorf, H. R. Cyclic Polymers: Synthetic Strategies and Physical Properties. *J. Polym. Sci. Part A Polym. Chem.* **2010**, *48* (2), 251–284.

(32) Alberty, K. A.; Hogen-Esch, T. E.; Carlotti, S. Synthesis and Characterization of Macrocyclic Vinyl-Aromatic Polymers. *Macromol. Chem. Phys.* **2005**, *206* (10), 1035–1042.

(33) Hadziioannou, G.; Cotts, P. M.; ten Brinke, G.; Han, C. C.; Lutz, P.; Strazielle, C.; Rempp, P.; Kovacs, A. J. Thermodynamic and Hydrodynamic Properties of Dilute Solutions of Cyclic and Linear Polystyrenes. *Macromolecules* **1987**, *20* (3), 493–497.

(34) Chaturvedi, D.; Mishra, N.; Chaturvedi, A. K.; Mishra, V. An Efficient, One-Pot Synthesis of Trithiocarbonates from Alcoholic Tosylates Using the Cs_2CO_3/CS_2 System. *Monatshefte für Chemie - Chem. Mon.* **2008**, *139* (12), 1467–1470.

(35) Reza Kiasat, A.; Kazemi, F.; Savari, A. Basic Al 2 O 3 as an Efficient Heterogeneous Reagent for the Synthesis of Symmerical Dialkyl Trithiocarbonates. *Synth. Commun.* **2008**, *38* (7), 1057–1063.

(36) Kiasat, A. R.; Mehrjardi, M. F. A Novel One-Step Synthesis of Symmetrical Dialkyl Trithiocarbonates in the Presence of Phase-Transfer Catalysis. *J. Chinese Chem. Soc.* **2008**, *55* (3), 639–642.

(37) Otsuka, H.; Sanbai, T.; Matsukuma, D.; Ikenaga, Y. Self-Assembly of Poly(Ethylene Glycol)-Block-Polypyridine Copolymer into Micelles and at Silica Surface: Effect of Molecular Architecture on Silica Dispersion. *Colloid Polym. Sci.* **2014**, *292* (2), 291–300.

Chapter 3

Improving solubility of end-associative polymers for mist control in highly non-polar solvents

3.1 Introduction

Ultra-high molecular weight linear polymers are useful in many applications such as drag reduction and mist-control in hydrocarbon solvents. For example, the addition of a small amount of ultralong polyisobutylene (50 ppm) to crude oil or refined oil can reduce pipeline drag by 50%.[1] In mist control applications, polyisobutylene chains with ultrahigh molecular weight (> 5000 kg/mol) were shown to be effective at reducing the flammability of jet-A-fuel sprays even at a low concentration (50 ppm).[2] In particular, the use of ultralong linear polymers suppresses the formation of fine droplets, which have a high surface area available for vaporization that leads to flame propagation in the presence of an ignition source. The mist suppressing ability of the ultralong polymers increases with the increase in the molecular weight and concentration.[2] However, ultrahigh molecular weight polymer chains that are long enough to be effective mist-control agents are susceptible to shear degradation, rendering their use impractical. To overcome the issue of shear degradation, previous members of the Kornfield group worked on the design and synthesis of end-associative polymers that are made of shear-stable polymer chains ($M_w < 10^6$ g/mol) that have the ability to reversibly assemble into effectively ultralong supramolecules via hydrogen bonding. Our group's previous work focused on the development of mist control agents for jet-A-fuel.[3] The end-associative polymers for mist control in jet-A-fuel were synthesized by using ring-opening metathesis polymerization (ROMP) of cis-cis-1,5 cyclooctadiene (COD) with chain-transfer agents (CTAs) to produce end-associative long telechelic polymers with the molecular structures shown in Schematic 3.1.

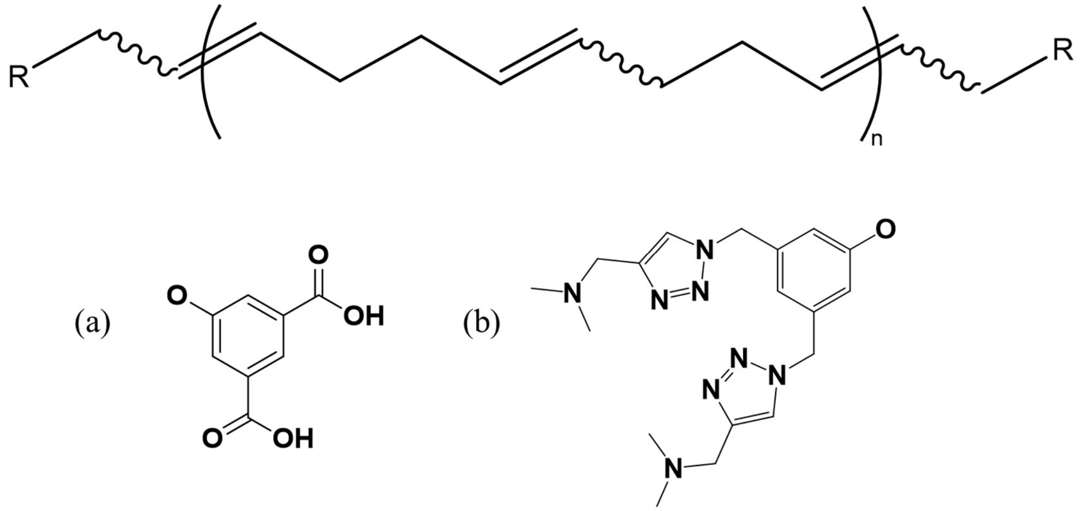

Schematic 3.1 Structure of end-associative polycyclooctadiene (top) Polycyclooctadiene backbone made by ROMP into long telechelic polymers with associative end groups designated by R, where R is one of the end groups shown below. **(a)** α,ω-di(isophthalic acid) (di-acid, DA) group **(b)** and α,ω -di(di(tertiary amine)) (di-base, DB) group[3]

The polymers had either two carboxylic acids or two tertiary amines on each end of the polycyclooctadiene (DA-PCOD or DB-PCOD). A 1:1 mixture of DA-PCOD and DB-PCOD (average molecular weight ~ 670 kg/mol) had the ability to associate end-to-end to form ultralong supramolecules with apparent molecular weights exceeding 2000 kg/mol at a low concentration of 0.3 wt%. Unlike the conventional ultralong polymer polyisobutylene (PIB, 4200 kg/mol), which degraded upon passing through a fuel pump 60 times and became ineffective at mist-control, the DA-PCOD and DB-PCOD mixture survived pumping and retained its efficacy.[3]

After successfully demonstrating shear degradation resistant mist-control in jet-A-fuel, our group continued to work on expanding the applicability of the end-associative polymers in a wide variety of solvents. We hoped to adapt the previously designed long end-associative polymers as mist control agents for lubricants and heat transfer fluids, recognizing the need to reduce the risk of mist fire.[4] In particular, our group's main objective was to reduce the fire vulnerability of polyalphaolefin oil (PAO) in collaboration with the Army Research Laboratory (ARL). DA-PCOD and DB-PCOD polymers were designed to be soluble in jet-A-fuel (a mixture of hydrocarbons and additives), and unfortunately, it was not possible to dissolve them in PAO.

In this chapter, we describe our efforts toward improving the solubility of the long end-associative polymers (DA PCOD and DB PCOD) in PAO to reduce the risk of mist fire.

Polyalphaolefin oil (PAO)

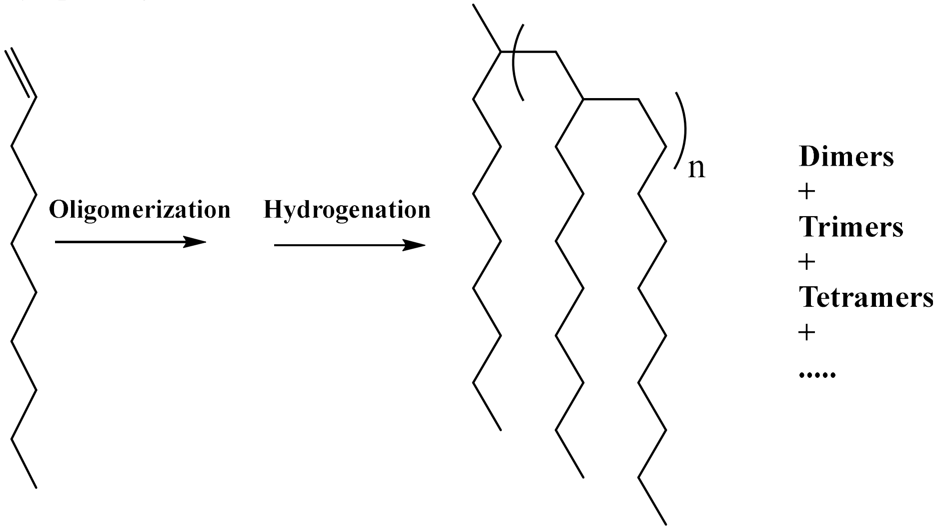

1-decene

Polyalphaolefin (PAO)

Scheme 3.2 Structure of polyalphaolefin oil (PAO)

Polyalphaolefin is the most common major synthetic base oil used in industrial and automotive lubricants, engine oils, hydraulic fluids, and gear oils.[5] It is also widely used as a coolant for avionic systems, a lubricant, and a hydraulic fluid inside of aircrafts due to PAO's stability over a wide temperature range and relatively low toxicity.[6] Although PAO has low volatility, it is used in systems with high pressure (e.g, hydraulic systems) and so contributes significantly to fire risk when a pressurized fluid line gets damaged. When a fluid line is compromised due to accidental impact (e.g., a collision between vehicles), PAO gets ejected as fine mists that can propagate fire from any ignition event nearby.[7] Therefore, the use of mist control agents can reduce the risk of PAO fires.

In this chapter, we focus our efforts on solubilizing the existing long end-associative polymers which were originally designed for solubility in jet-A-fuel. Due to the highly non-polar nature of the PAO solvent, it was not possible to dissolve DA-PCOD or DB-PCOD. However, we observed that the polymer backbone, polycyclooctadiene, was soluble in PAO down to 4 °C, suggesting that the associative end groups were mainly responsible for the insolubility of the polymers in PAO even though the end groups only account for only a small fraction of the entire polymer chain. We first describe the choice of a co-solute molecule that allowed the dissolution of DA-PCOD and DB-PCOD in PAO at room temperature without compromising the hydrogen bonding between the DA and DB groups. The associative PCODs were not soluble at sub-ambient temperatures (< 15 °C) even when the co-solutes were added to the solution. We will conclude this chapter by describing different strategies for modifying the backbone structure to help guide future work towards achieving the solubility of these polymers at sub-ambient temperatures.

3.2 Experimental

3.2.1 Materials and instrumentation

All chemical reagents were obtained from Sigma Aldrich at 98% purity or higher unless otherwise stated. Polyalphaolefin (Brayco micronic 889) was obtained from QC lubricants. All solvents were obtained from Sigma Aldrich, at ACS reagent grade or higher (> 99.5% purity) and used as received without further purification.

NMR spectroscopy

^{1}H-NMR spectra were obtained using a Varian Inova 500 spectrometer (500 MHz); all spectra were recorded in $CDCl_3$ or d-DMSO (purchased from Cambridge Isotope Laboratories). Chemical shifts were reported in parts per million (ppm) and were referenced to residual solvent resonances.

Gel permeation chromatography (GPC)

The molecular weights and dispersity indices of the polymers were determined on a GPC system with a Wyatt DAWN EOS multi-angle laser light scattering detector (λ=690nm), a Waters 410 differential refractometer (RI) (λ=930nm), and four Agilent PLgel columns (pore sizes 103, 104, 105, and 106 Å) connected in series. THF was used as the eluent at a flow rate of 0.9mL/min with a temperature of 35 °C. The data were analyzed using Wyatt Astra (version 5.3.4) using the Zimm fitting formula with $dn/dc = 0.125$ for each polymer reported.

Viscosity measurement

The shear viscosity of the polymer solutions was measured using a strain-controlled rheometer TA ARES-RFS, equipped with a cone-plate geometry (angle 2°, diameter 50mm). Specific viscosity ($\eta_{specific}$) is defined as $\eta_{specific} = (\eta_{solution}/\eta_{solvent} - 1)$. Three replicates were measured to obtain the error bars (standard error).

3.2.2 Chain transfer agent (CTA) synthesis

Dr. Ming-Hsin (Jeremy) Wei provided the protocols for the synthesis of chain transfer agents (and the intermediates) and ROMP of COD.

Synthesis of (E)-1,20-dibromoicos-10-ene

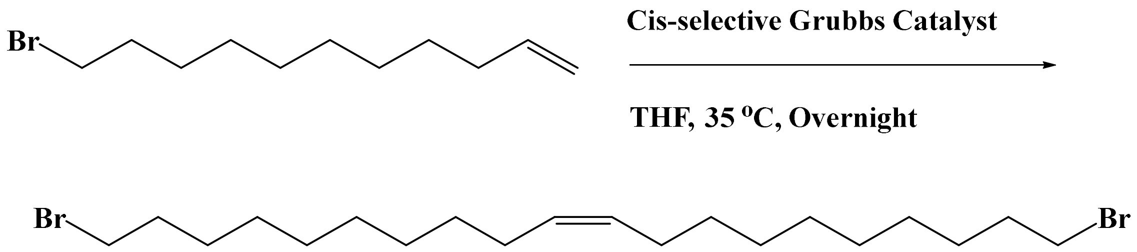

Scheme 3.3 Synthesis of (E)-1,20-dibromoicos-10-ene (Dibromo icosene)

11-Bromo-1-undecene (Sigma Aldrich, 95%) was vacuum distilled twice at 110 °C, and the resulting distillate was colorless. Distilled 11 bromo-1-undecene (10 g, 42.88 mmol) and THF (8 mL) were mixed in a 50 mL Schlenk flask, and the solution was degassed by three freeze-pump-thaw cycles. The degassed solution of cis-selective Grubbs catalyst, (Hoveyda-Grubbs catalyst M2001) (9.5 mg, 0.015 mmol) in THF (1 mL) was syringe transferred to the Schlenk flask. During the reaction, the flask was continuously flushed with a stream of argon gas through a 25-G needle as an inlet and another 25-G needle as the outlet to purge ethene gas that formed as a byproduct of the reaction. The mixture was stirred at 35 °C overnight. The next day, the reaction was stopped by exposing it to air and diluted with hexane (100 mL). The resulting solution was passed through a short plug of silica gel to remove the catalyst, and the solvent was removed using a rotary evaporator. Most of the unreacted 11-bromo-1-undecene was removed by vacuum distillation at 110 °C, and the product was used in the next step without further purification. Yield 65%.

Synthesis of di-ester CTA (DE-CTA)

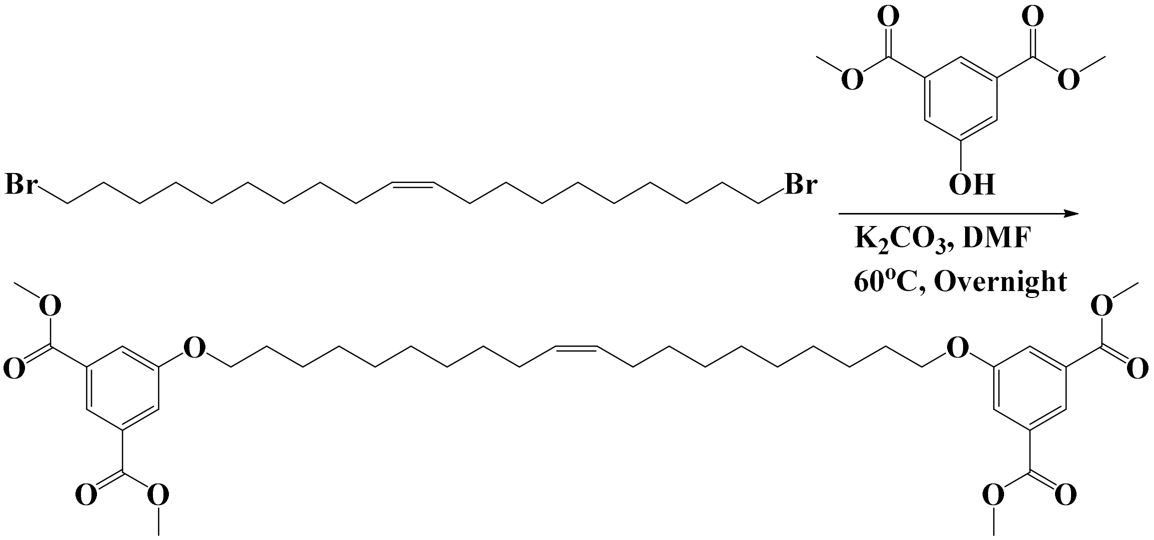

Scheme 3.4 Synthesis of Di-ester CTA intermediate (DE-CTA)

(E)-1,20-dibromoicos-10-ene (5 g, 11.4 mmol), dimethyl 5-hydroxyisophthalate (6.32 g, 29.7 mmol), and K_2CO_3 (6.3 g, 45.6 mmol) were dissolved in DMF (65 mL) in a 250 mL round bottom flask with a magnetic stir bar. The mixture was stirred at 60 °C overnight. The next day, the mixture was diluted with DCM (180 mL) and washed with deionized water twice (100 mL each time). The organic phase was washed with 1M $HCl_{(aq)}$ five times to remove residual DMF. The organic phase was dried with $MgSO_4$ and filtered and the solvent was removed by rotary evaporation. The crude solid product was recrystallized from a mixture of isopropyl alcohol and THF (9:1) three times. Yield 75%.

^{1}H-NMR ($CDCl_3$, 500MHz) 1.25-1.35 (Br, 20H), 1.43 (m, 4H), 1.80 (m, 4H), 2.02 (m, 4H), 3.94 (s, 6H), 4.03 (t, 4H), 5.35 (t, 2H), 7.73 (d, 4H), 8.25 (t, 2H)

Synthesis of di-Acid CTA (DA-CTA)

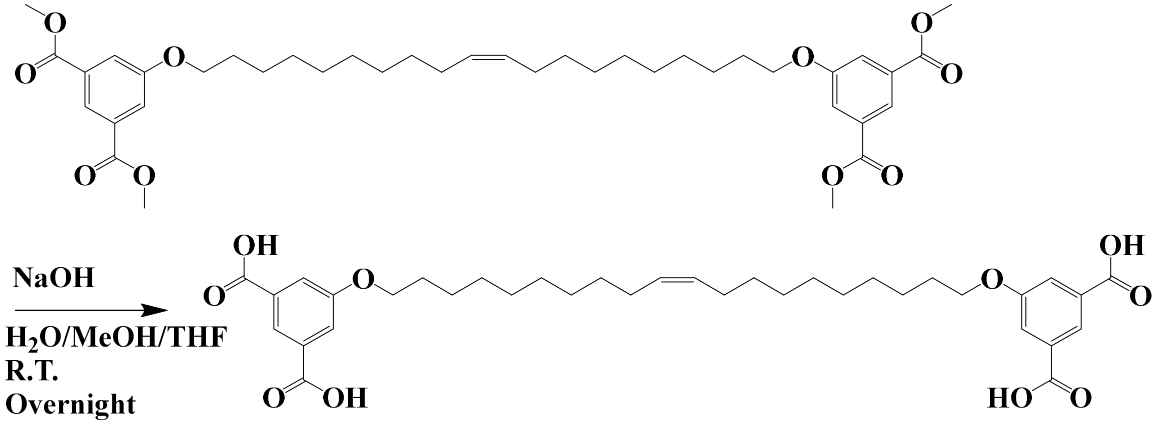

Scheme 3.5 Synthesis of Di-Acid CTA (DA-CTA)

NaOH (1.15 g, 28.7 mmol) was dissolved in deionized water (5 mL) in a 250 mL round bottom flask with a magnetic stir bar, and methanol (10 mL) was added. In a separate container, DE-CTA (1 g, 1.43 mmol) was dissolved in THF (15 mL), and this solution was transferred into the round bottom flask. The mixture was stirred at room temperature overnight. The next day, the mixture was neutralized with 3M $HCl_{(aq)}$, and the product was extracted with ethyl acetate (150 mL) and washed with deionized water (100 mL each time) twice to remove salts. The organic phase was dried with MgSO4 and filtered, and the ethyl acetate was removed via rotary evaporation. Yield 96%.

^{1}H-NMR (d-DMSO, 500MHz) 1.2-1.35 (Br, 20H), 1.40 (m, 4H),1.72 (m, 4H), 1.97 (m, 4H), 4.05 (t, 4H), 5.32 (t, 2H), 7.61 (d, 4H), 8.05 (t, 2H)

Synthesis of dihydroxy CTA

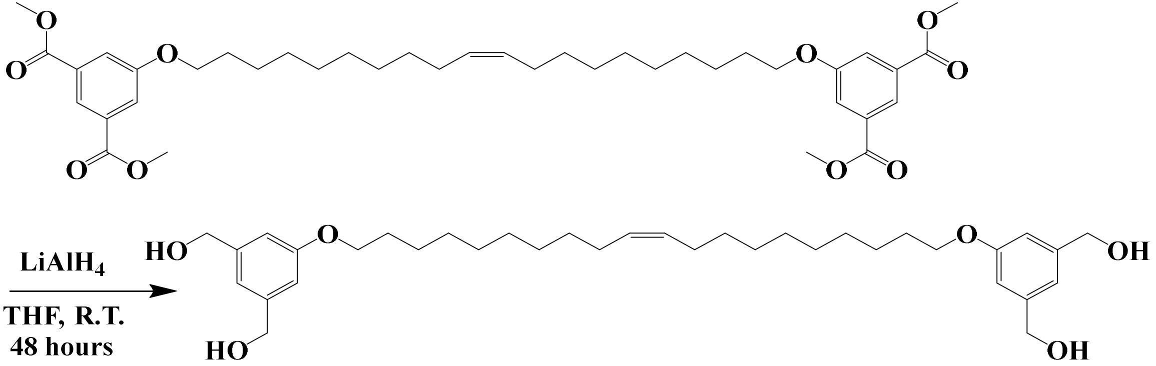

Scheme 3.6 Synthesis of dihydroxy CTA

DE-CTA (2 g, 2.87 mmol) was dissolved in anhydrous THF (30 mL) in a 100 mL round bottom flask, and the solution was cooled in an ice bath. $LiAlH_4$ (545 mg, 14.35 mmol) was suspended slowly in anhydrous THF (10 mL) in a 20 mL glass scintillation vial. The suspension was added dropwise into the DE-CTA solution while stirring with a magnetic stir bar. The solution turned into cake after adding about half of the $LiAlH_4$ suspension, and a stainless-steel spatula was used to break up the cake into small pieces to allow the stir bar to rotate freely. The remaining $LiAlH_4$ was added to the mixture, and the flask was removed from the ice bath, moved to an oil bath, and heated to 40 °C for 48 hours. After 48 hours, the mixture was cooled using an ice bath, and water (2 mL) was added dropwise, followed by dropwise addition of 15% $NaOH_{(aq)}$ solution (2 mL) and more water (3 mL). The mixture was stirred at room temperature for two hours to allow the formation of $Al_2(OH)_3$ salt as white solids. The solution was filtered, dried with $MgSO_4$, and filtered again, and the solvent was removed using a rotary evaporator and solid products were dried further under reduced pressure. Yield 98%.

^{1}H-NMR (d-DMSO, 500MHz) 1.2-1.35 (Br, 20H), 1.40 (m, 4H),1.67 (m, 4H), 1.98 (m, 4H), 3.91 (t, 4H), 4.43 (s, 8H) 5.32 (t, 2H), 6.70 (d, 4H), 6.81 (t, 2H)

Synthesis of dichloro CTA

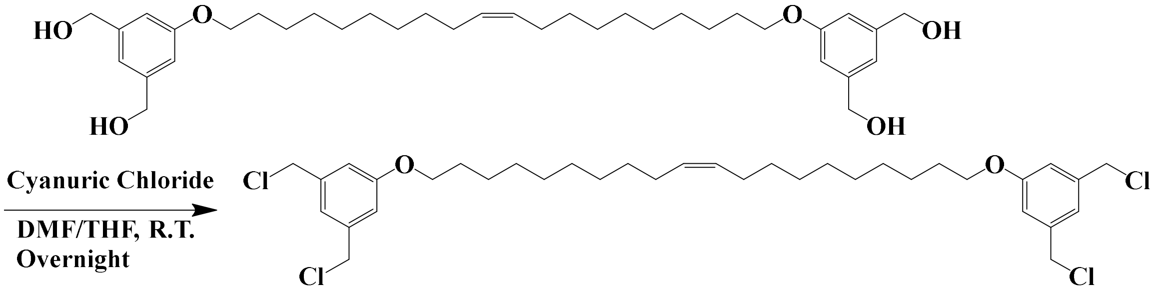

Scheme 3.7 Synthesis of dichloro CTA

Cyanuric chloride (1.89 g, 10.3 mmol) was dissolved in a mixture of anhydrous DMF (2 mL) and anhydrous THF (5 mL) in a 100 mL round bottom flask with a magnetic stir bar. The mixture was stirred for 15 minutes. Dihydroxy CTA (1 g, 1.7 mmol) was dissolved in anhydrous THF (20 mL) in a separate container and the solution was slowly added to the cyanuric chloride mixture. The mixture was stirred at room temperature overnight. The next day, the mixture was diluted with THF (25 mL) and vacuum filtered to remove solids and the filtrate was concentrated by rotary evaporation. The concentrated crude was diluted with ethyl acetate and the organic phase was washed with water (100 mL) and 1M $HCl_{(aq)}$ 5 times (80 mL each time) to remove DMF and some of the unreacted cyanuric acid. The resulting organic phase was dried using $MgSO_4$, filtered, and concentrated by rotary evaporation to obtain an oil-like crude product. This intermediate product was used in the next step without further purification.

Synthesis of di-azido CTA

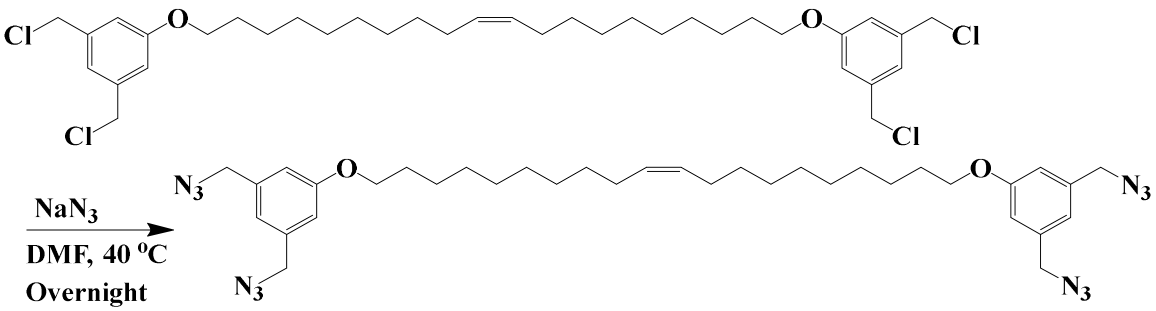

Scheme 3.8 Synthesis of di-azido CTA

Dichloro-CTA (1 g, 1.5 mmol) was dissolved in DMF (10 mL), and sodium azide (592 mg, 9.1 mmol) was added to the mixture. The mixture was stirred at 40 °C overnight. The next day, the mixture was diluted with ethyl acetate. The resulting organic phase was washed with water twice (100 mL each time) and washed with 1M $HCl_{(aq)}$ 5 times (80 mL each time) to remove residual DMF, dried using $MgSO_4$, and concentrated using rotary evaporation. The oil like crude product was purified using (silica gel) flash column chromatography with a mixture of ethyl acetate and hexane as eluent (1:4, v/v). The final product was a clear oil. Yield 87%.

^{1}H-NMR($CDCl_3$, 500MHz) 1.25-1.4 (Br, 20H), 1.45 (m, 4H),1.79 (m, 4H), 2.03 (m, 4H), 3.97 (t, 4H), 4.32 (s, 8H) 5.36 (t, 2H), 6.82 (m, 6H)

Synthesis of di-Base CTA (DB-CTA)

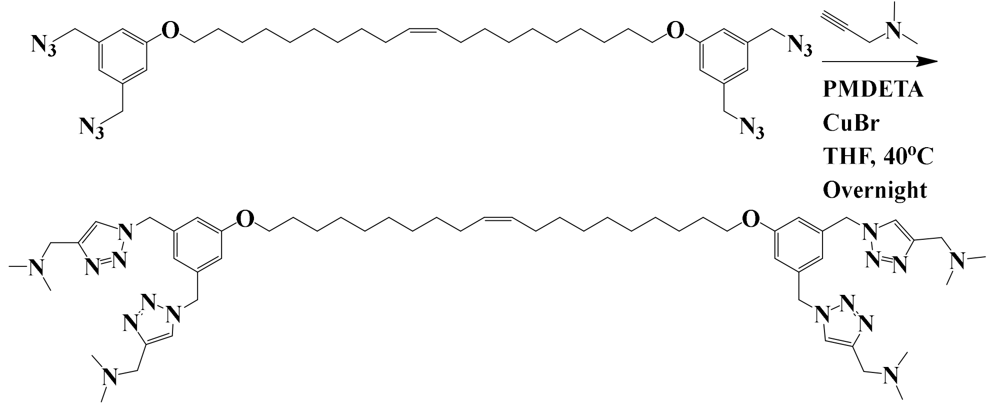

Scheme 3.9 Synthesis of di-base CTA (DB-CTA)

CuBr (1 mg, 7.2 μmol) was added to a 50 mL Schlenk flask, and di-azido CTA (1 g, 1.44 mmol) was dissolved in THF (10 mL) and transferred to the Schlenk flask. The mixture was degassed by three freeze-pump-thaw cycles and the flask was filled with argon. Pentamethyldiethylenetriamine (PMDETA) (2.5 mg, 14.5 μmol) was added to THF (0.5 mL) in a 10 mL Schlenk flask, and the mixture was degassed by three freeze-pump-thaw cycles and the flask was filled with argon. PMDETA solution was syringe transferred to the di-azido CTA mixture and stirred for 20 minutes and the solution turned bright green. 3-dimethylamino-1-propyne (0.57 g, 6.65 mmol) was degassed in a separate container by three freeze-pump-thaw cycles, and syringe transferred to the reaction mixture. The mixture was stirred at 40 °C overnight. The next day, the reaction mixture was diluted with more THF (80 mL) and passed through a short plug of neutral alumina to remove the copper catalyst. The resulting filtrate was bright yellow. The mixture was concentrated using rotary evaporation, and dried at 80 °C under reduced pressure for two days to remove residual solvent, PMDETA and 3-dimethylamino-1-propyne. Yield 94%

^{1}H-NMR ($CDCl_3$, 500MHz) 1.25-1.35 (Br, 20H), 1.42 (m, 4H),1.72 (m, 4H), 2.01 (m, 4H), 2.25 (s, 24H), 3.58 (s, 8H), 3.83 (t, 4H), 5.33 (t, 2H), 5.43 (s, 8H), 6.72 (m, 6H) 7.40 (s, 4H)

3.2.3 Polymer synthesis

Purification of cis,cis-1,5-cyclooctadiene (COD) by Zeolite (Zeolite Socony Mobile-5)

Commercially available COD may contain impurities such as 4-vinylcyclohexene, which can act as unwanted chain transfer agents that terminate a growing chain during the ring opening metathesis of COD.[8] The following protocol was developed by Kornfield and coworkers[9] and the protocol was provided by Dr. Ming-Hsin (Jeremy) Wei.

In a 250 mL Schlenk flask, 2.5 g of magnesium silicate (Magnesol®XL, The Dallas Group of America Inc.), and 3.6 g of ZSM-5 (Alfa Aesar) were added without a stir bar. To remove the water, the mixture was dried overnight under high vacuum at 100 °C. After cooling the flask to room temperature, a PTFE coated magnetic stir bar was added and the flask was sealed with a Suba-Seal rubber septum, evacuated, and filled with argon. To the sealed flask, as-received redistilled-grade COD (26.5 g, 0.24 mol, Sigma Aldrich purity >99%) was syringe transferred and stirred at room temperature overnight. The COD was then vacuum distilled at 36 °C from the mixture to a 100 mL Schlenk flask in a plastic tub filled with dry ice. After distillation, the flask was sealed with a Suba-Seal rubber septum under a continuous flow of argon and stored at -30 °C. Yield 96%

Synthesis of macro chain transfer agents (mCTA)

Macro chain transfer agents were synthesized using either DA-CTA, DB-CTA or cis-2-hexene (Sigma Aldrich, 95%) as CTAs. CTA (1 mmol) and 2,6-di-tert-butyl-4-methylphenol (BHT, 0.1 g, 0.45 mmol) were dissolved in THF (10 mL) in a 100 ml Schlenk flask. The dissolved solution was degassed by three freeze-pump-thaw cycles and the flask was filled with argon. To the degassed mixture of CTA, 1 mL of degassed THF solution of 2nd generation Grubbs Catalyst (**G2**, 8.4 mg, 9.89 μmol) was syringe transferred, immediately followed by the addition of degassed, freshly vacuum distilled purified COD (5.0 g, 45.8 mmol). The mixture was stirred at 40 °C overnight. The reaction was stopped by exposing to air, and diluted with THF (40 mL), and the polymers were precipitated into a large excess of methanol (500 mL) dropwise. Methanol was decanted, and the polymers were collected in a 20 mL vial with a silicone/PTFE septum cap, and dried under high vacuum. The vial was degassed by three cycles of pulling vacuum/filling argon and stored at -30 ºC.

Synthesis of Telechelic Polycyclooctadiene (PCOD)

Telechelic PCOD was synthesized following the same procedure used for the synthesis of mCTA, using mCTA instead of CTA. All telechelic polymers used in this paper were synthesized using 5 g of purified COD, 0.16 mL of **G2** (from 1 mg/mL degassed THF solution), 0.1 g of BHT, and 10 mL of THF. In the ROMP of COD, in addition to the growth of linear chains, there is also a competing intramolecular secondary metathesis that generates small cyclic oligomers (backbiting)[10]. To compensate for the formation of small cyclic species, the amount of mCTA was adjusted using the following empirical formula:

$$mCTA\_M_w \times \frac{(M_{mCTA} + M_{COD})}{M_{mCTA}} \times 0.85 = Target\_M_w$$

Synthesis of non-associative polycyclooctene (NA-PCOE)

Non-associative polycyclooctene (PCOE) was synthesized following the same procedure used for the synthesis of mCTA using cis-2-hexene as CTA, and cis-cyclooctene (used as received, 95% purity, TCI America) instead of cyclooctadiene.

Synthesis of Poly 1,5 Dimethyl-1,5-cyclooctadiene (PDMCOD)

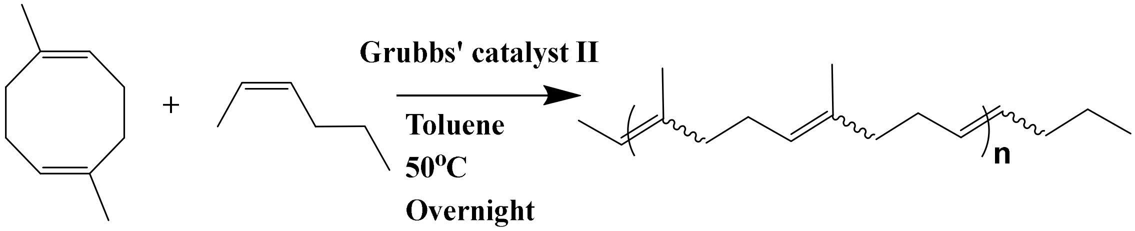

Scheme 3.10 Synthesis of polydimethylcyclooctadiene (PDMCOD)

Procedure modified from[11]

Cis-2-hexene (28 mg, 333 µmol) and 2,6-di-tert-butyl-4-methylphenol (BHT, 0.1 g, 0.45 mmol) were dissolved in toluene (10 mL) in a 100 mL Schlenk flask. The dissolved solution was degassed by three freeze-pump-thaw cycles and filled with argon. To the degassed mixture, 1 mL of a degassed toluene solution of 2nd generation Grubbs Catalyst (**G**2, 31 mg, 36.7μmol) was syringe transferred, immediately followed by the addition of degassed, 1,5 dimethyl-1,5-cyclooctadiene (TCI, 75% purity, remaining 25% = 1,6 dimethyl-1,5-cyclooctadiene) (5 g, 36.7 mmol). The mixture was stirred at 50℃ overnight. The reaction was stopped by exposing to air, and diluted with THF (40 mL), and the polymers were precipitated into a large excess of methanol (400 mL) dropwise. Methanol was decanted, and the polymers were collected in a 20 mL vial with a silicone/PTFE septum cap and dried under high vacuum. The vial was degassed by three cycles of pulling vacuum/filling argon and stored at -30 °C. The resulting polymer had M_w 19 kg/mol and a polydispersity of 1.6. This PDMCOD was used as an mCTA for chain extension reactions to synthesize higher molecular weight PDMCOD following the same procedure described above.

3.2.4 Polymer dissolution and methods to influence solubility

Polymer dissolution

DA-PCOD, DB-PCOD, NA-PCOD, and NA-PCOD-co-COE were dissolved in PAO by stirring at 60 °C for 8 hours. Associative polymers (DA, DB, or DA and DB mixture) were dissolved with co-solutes as described below. Polyisobutylene (PIB) and NA-PDMCOD were dissolved in PAO by stirring at room temperature overnight.

Cosolvents and Co-solutes

Benzene, xylene, DCM, THF, decalin, tetralin, and cyclohexane were used as co-solvents, and BHT was used as a co-solute. The co-solvents were added to 1 mL of the polymer solution slowly in small (10 μL) increments until the solution became clear. BHT co-solute was added in small (10 mg) increments, and the vial was shaken to dissolve BHT fully. BHT was added until the solution became fully clear. The amount of BHT needed to get a clear solution varied based on the concentration and molecular weight of the associative polymers. For example, to make a 0.5 wt% solutions in PAO with roughly 670 kg/mol DA or DB PCODs, the required BHT was approximately three times the weight of the polymers.

Partial hydrogenation of PCOD backbone via diimide reduction (polyCOD-co-COE)

Non-associative PCOD (NA-PCOD) (0.5 g, 9.26 mmol of double bonds) was dissolved in DCM (38 mL, 1wt %) in a 250 mL round bottom flask, and potassium azodicarboxylate (3.6 g, 18.5 mmol) was added to the mixture. Glacial acetic acid (1.05 mL) was diluted in DCM (5 mL) and added dropwise to the mixture, and evolution of CO_2 bubbles was observed. After complete addition of the glacial acetic acid, the reaction flask was sealed with a rubber septum with a 25G needle as a vent to prevent over pressurization of the flask due to the generation of N_2 gas during the reaction. The mixture was stirred at room temperature overnight. The next day, the mixture was filtered to removed salts (potassium acetate), and the polymers were precipitated in methanol (400 mL), dissolved in THF (20 mL), and precipitated in methanol (100 mL) again for three times, and dried to completeness under reduced pressure. ^{1}H-NMR analysis showed that roughly 14% of the double bonds were hydrogenated.

3.3 Results and discussion

Table 3.1 List of polymers synthesized: GPC characterization

Polymer	Mw (kg/mol)	Mn(kg/mol)	Polydispersity Index
NA-PCOD 13k	13.3	9.9	1.35
NA-PCOD 550k	550	385	1.43
NA-PCOD 670	670	433	1.55
NA-PCOD 852k	852	544	1.56
DA-PCOD 350k	350	274	1.28
DA-PCOD 663k	663	444	1.49
DB-PCOD 365k	365	270	1.35
DB-PCOD 673k	673	466	1.44
NA-PCOE 14k[#]	14.2	10.0	1.30
NA-PCOD-co-COE 850k	874	586	1.49
NA-PDMCOD 19k	19.2	11.9	1.60
NA-PDMCOD 65k	65	45	1.45
PIB 1.2M	1264	704	1.80
PIB-co-isoprene 392k	392	186	2.10

PCOD = polycyclooctadiene. PCOE = polycyclooctene.
PDMCOD = polydimethylcycloctadiene. NA= non-associative DA = di-acid DB = di-base.
#The molecular weight of PCOE was determined using dn/dc=0.11 mL/g[12]
PIB = polyisobutylene (purchased from Sigma Aldrich) PIB-co-isoprene = random isobutylene-isoprene copolymer (purchased from Sigma Aldrich)

3.3.1 Solubility of PCOD with alkyl, di-acid or di-base end groups

Solubility of PCOD backbone

Table 3.2 Turbidity of polycycloctadiene solutions in PAO (without co-solutes)

Polymer	**Mw (kg/mol)**	**60°C**	**20°C**	**4°C**	**-20°C**	**# Monomers/ #End groups**
NA-PCOD	13.3	Clear	Clear	Clear	Clear	N/A
NA-PCOD	550	Clear	Clear	Clear	Cloudy	N/A
NA-PCOD	852	Clear	Clear	Clear	Cloudy	N/A
DA-PCOD	350	Clear	Cloudy	Cloudy	Cloudy	~1620
DA-PCOD	663	Clear	Cloudy	Cloudy	Cloudy	~3064
DB-PCOD	365	Clear	Cloudy	Cloudy	Cloudy	~1690
DB-PCOD	673	Clear	Cloudy	Cloudy	Cloudy	~3100
DA-PCOD & DB-PCOD (1:1)	350 365	Clear	Cloudy	Cloudy	Cloudy	~1655
DA-PCOD & DB-PCOD (1:1)	663 673	Clear	Cloudy	Cloudy	Cloudy	~3082

PCOD = polycyclooctadiene. NA= non-associative DA = di-acid DB = di-base.

Non-associative PCODs were synthesized to study the solubility of the PCOD backbone without any polar end groups. The PCOD backbone was soluble in PAO, as the non-associative PCODs with linear alkane end groups were dissolved in PAO at 60 °C and stayed in solution down to 4°C. However, DA or DB PCODs were soluble in PAO at 60 °C but came out of the solution upon cooling to ambient temperature (20 °C). Despite the long polymer backbone being soluble in PAO, the end groups, which account for less than 0.05% of the total molecular weight of the polymers, were causing the entire molecule to come out of the solution. This observation was unexpected, because associative PCODs were soluble in other fully saturated hydrocarbon solvents like decalin or cyclohexane.[3]

We hypothesized that fully saturated hydrocarbons like decalin or cyclohexane must interact somehow with the DA or DB groups and allow the dissolution of the end groups in solution.

The fact that both acid and base end groups behave similarly suggests that the interaction is with a moiety that is present in both DA and DB. This is further supported by the behavior of DA-PCOD:DB-PCOD 1:1, which shows that pairing the acid and base fails to improve solubility. To identify the mode of interaction between the solvent molecule and DA and DB ends, we looked at the list of solvent molecules that our group previously used to dissolve the associative PCOD (Schematic 3.11). Looking at the structures of the solvent molecules, we hypothesized that the aromatic components of the associative end groups might be responsible for the lack of solubility in PAO. The previously used solvent molecules had the ability to interact with the aromatic component of the end groups via π-π stacking (tetralin, toluene) or aliphatic-aromatic (decalin, cyclohexane, THF, and chlorinated solvents) interactions.

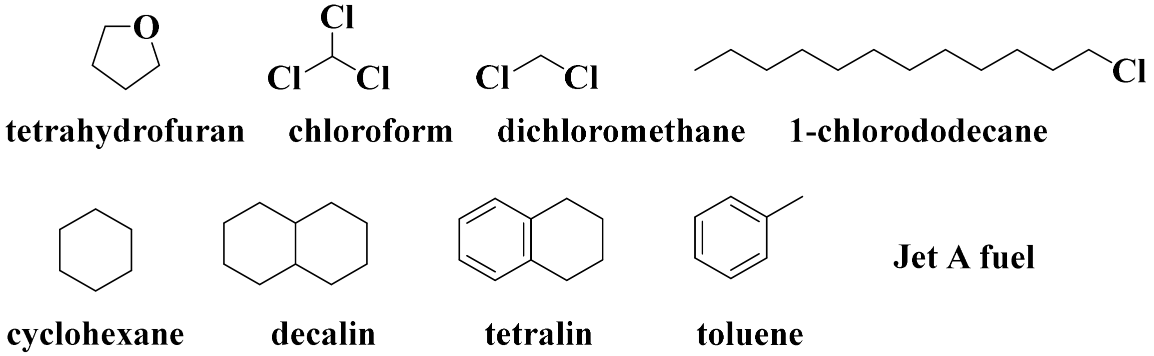

Schematic 3.11 Structure of solvent molecules that can dissolve DA and DB PCOD

Solubilizing DA and DB end groups using co-solvents or co-solutes

To test our hypothesis, we tried adding co-solvents or co-solutes that could participate in π-π stacking (toluene, benzene, and xylene) or aliphatic-aromatic interactions (DCM, cyclohexane) to cloudy solutions of DA/DB mixtures and the solutions became clear immediately. The 1 wt% DA/DB PCOD (M_w ~ 670kg/mol) solutions contained roughly 28 μM end group concentration; approximately a 1.3-molar excess (ca 40 μM) of co-solvent molecules was sufficient to achieve homogenous solutions. This result suggested that rather than changing the solvent quality of the solution, the added species selected to disrupt π-π interactions between end groups appeared to localize near the polymer end groups, acting as co-solutes.

Although adding minimal amounts of the above-mentioned solvent molecules (such as toluene) allowed solubilization of the associative PCOD, the solvent molecules were too volatile to be useful in practice, and slow evaporation of these solvents caused the polymer solutions to be cloudy again. Looking for a non-volatile co-solute that could participate in π-π stacking or aromatic-aliphatic interactions, we noticed that the antioxidant butylated hydroxytoluene (BHT) could be a potentially useful molecule. BHT is already approved to be used in PAO as an antioxidant and is nontoxic (commonly used as a food additive) and nonvolatile (boiling point 265 °C). BHT was effective in solubilizing the end groups, but a relatively large excess was required (3-5 times the weight of the dissolved polymer) to yield a completely clear solution. This is most likely due to the presence of bulky t-butyl groups which makes π-π interactions with the end groups less efficient. We checked for possible interference of BHT with the hydrogen bond between DA and DB molecules. We measured the shear viscosity of DA:DB=1:1 solution with and without BHT in decalin, and the resulting specific viscosity (η_{specific}) was almost the same, suggesting that the association between DA and DB was not affected by the presence of excess BHT in the solution. (Figure 3.1)

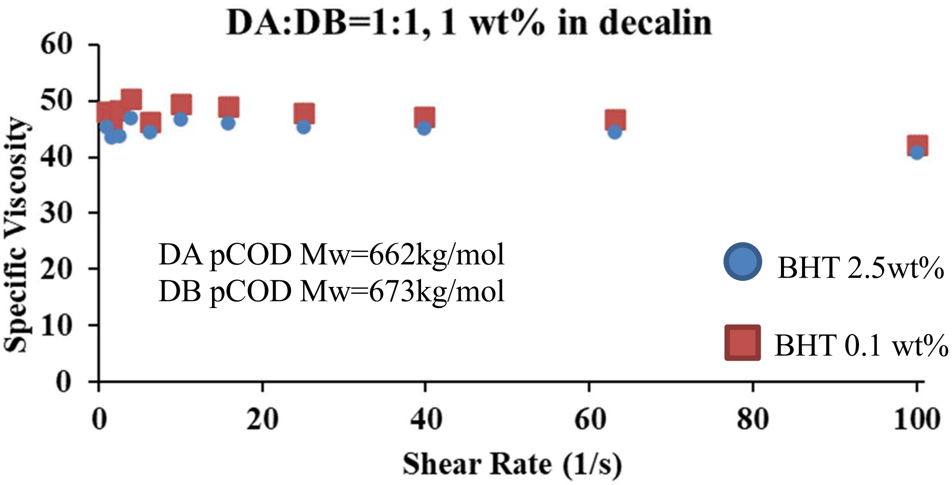

Figure 3.1 Specific viscosity ($\eta_{specific}$) of DA:DB=1:1 solution with DA PCOD (M_w 662 kg/mol) and DB PCOD (M_w 673 kg/mol) with and without BHT in solution.

Using BHT, we were able to prepare associative PCOD solutions in PAO at room temperature, and the DA-DB association was achieved even at concentration as low as 0.25 wt% as shown in Figure 3.2.

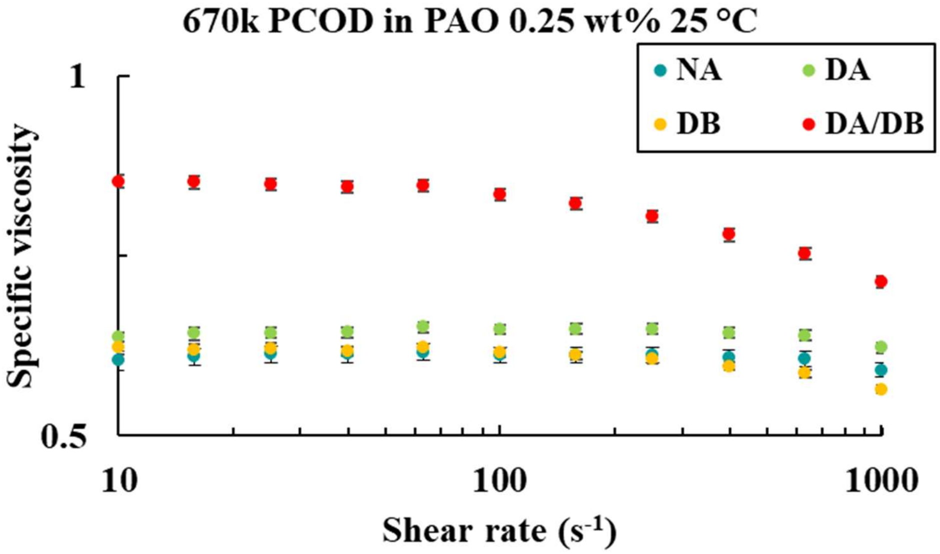

Figure 3.2 Specific viscosities of PCOD solutions in PAO at 0.25 wt% at 25 °C. NA=non-associative PCOD (M_w 670 kg/mol), DA PCOD (M_w 662 kg/mol), DB PCOD (M_w 673 kg/mol), DA:DB=1:1 (v/v).

3.3.2 Backbone structures for improving solubility in PAO at sub-ambient temperatures

The PCOD backbone without end groups was soluble only down to 4 °C (Table 3.2), suggesting the need for backbone structure modification for achieving solubility at lower temperatures to allow the use of the polymers in places with cold weather. The first strategy was to decrease the extent of unsaturation of the backbone, and we decreased the extent of the unsaturation by two different synthetic strategies. The first approach was via partial hydrogenation of the PCOD backbone to decrease double bond content by 10-15%.

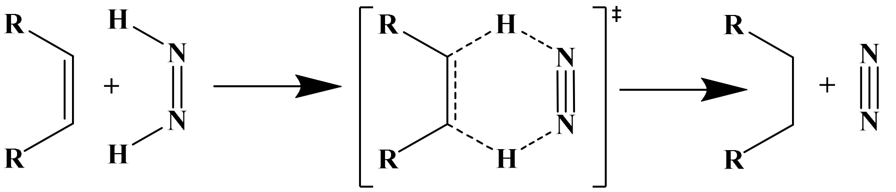

Scheme 3.12 Diimide reduction of alkene to alkane.

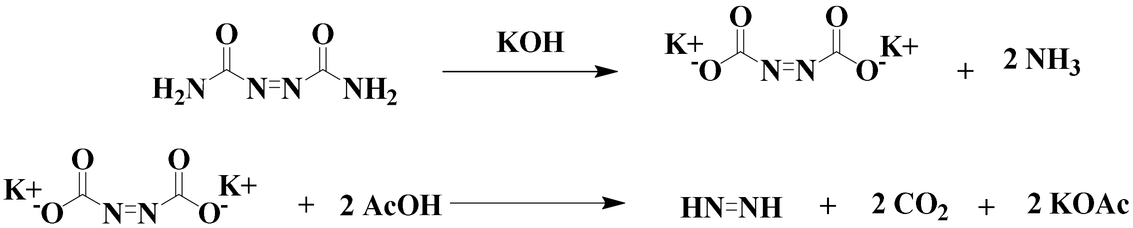

Scheme 3.13 In situ generation of diimide via reaction of potassium azodicarboxylate and acetic acid.

There are several methods reported in the literature for the hydrogenation of polyalkenamers. While catalytic hydrogenation is the most common method, it requires an expensive metal catalyst (palladium or platinum), high temperature and high pressure H_2, and a special high pressure reactor.[13] Therefore, we performed noncatalytic hydrogenation using diimide (Scheme 3.12). Diimide is an unstable compound that needs to be generated in situ. While there are several methods for diimide generation, for hydrogenation of polymers, the most common method is using the thermolysis of p-toluenesulfonyl hydrazide (TSH).[13–15] However, this method requires high temperatures and a nitrogen atmosphere, and can covalently add undesired residual TSH to the polymer.[13,16] We chose diimide generation via decarboxylation of potassium azodicarboxylate (Scheme 3.13). Decarboxylation of potassium azodicarboxylate can be carried out at room temperature, and the byproducts are easy to remove. The potassium acetate salts can be simply filtered from the solution, and CO_2 evaporates as well as the N_2 generated during diimide reduction. Using this method, we were able to decrease the extent of unsaturation by 14%. However, this partially hydrogenated PCOD was not soluble at 4°C, while plain PCOD was soluble at 4 °C. We hypothesized that the hydrogenation of PCOD would have two effects on the solubility. First, the polymer becomes more non-polar since alkenes are generally more polar than alkanes due to the presence of more polarizable π-bond electrons that can contribute to instantaneous dipole moments.[17] Secondly, the sections of backbones that are fully hydrogenated would be chemically equivalent to linear polyethylene, and therefore have higher crystallinity and lower solubility in solvents.[18]

To confirm our observation that the decrease in the number of double bonds along the backbone results in a decrease in solubility of the polymer in PAO, we synthesized polycyclooctene (PCOE), which would have exactly 50% double bond content in comparison to PCOD. We synthesized PCOE via ROMP of COE, but due to lower ring strain in COE (COE (31 kcal/mol) relative to COD (56 kcal/mol) relatively small molecular weight PCOE (M_n = 13 kg/mol) was synthesized. This short PCOE was insoluble in PAO at 4°C, while 13 kg/mol PCOD was soluble even at -20 °C. Thus, we concluded that decreasing the extent of unsaturation along the PCOD backbone caused a decrease in solubility in PAO in comparison to that of unaltered PCOD in PAO.

We hypothesized that runs of sequential –(CH$_2$)– along the backbone allowed greater packing efficiency with one another while unsaturation causes kinks along the backbone, making it difficult for the chains to pack closely. For example, unsaturated compounds such as vegetable oil stay as liquids at room temperature, while more saturated compounds, such as butter, exist as solids at room temperature. In fact, even for comparing cis-1,4 polybutadiene and 1,4-polybutadiene, cis isomers have very low crystallinity and low melting point while trans isomers have higher crystallinity and higher melting point.[19]

We hypothesized that the solubility of polymers in PAO could be improved by adding nonpolar, hydrocarbon side groups that disrupt the packing between the polymer chains. To test this hypothesis, we tested the solubility of a commercially available polymer with alkyl branching in the backbone. We tried dissolving ultrahigh molecular weight polyisobutylene (Mw=1.26Mg/mol) in PAO, and the solution remained clear down to -20°C in the freezer. Another commercial polymer poly isobutylene-co-isoprene was also soluble in PAO down to -20 °C in the freezer.

Motivated by the solubility of PIB and PIB-co-isoprene in PAO, even at -20 °C, we tried to synthesize end-associative polymers with alkyl side chains along the backbone. For designing long telechelic polymers for mist-control applications, the backbone solubility is not the only parameter that should be considered. Depending on the backbone structure, the polymers could be more susceptible to chain scission. PIB is known to be susceptible to chain scission due to having backbone carbons that are quaternary.[20,21] In general, the activation energy (E_a) for C-C bond scission decreases with increasing degree of substitution (2°, E^a = 181 kJ/mol > 3°, E^a = 99 kJ/mol > 4°, E_a = 42 kJ/mol).[22] Wei and coworkers designed the end-associative polymers with a polycyclooctadiene backbone for mist-control in jet-A-fuel for two reasons. PCOD is soluble in jet-A-fuel and remains in solution at -30 °C indefinitely without any need for additives like surfactants or stabilizers. The PCOD backbone does not have tertiary/quaternary carbons along the backbone, and 33% of the backbone is made of C=C double bonds which are stronger than any C-C single bonds.[23,24] Therefore, a polyisoprene backbone would be more shear degradation resistant than polyisobutylene. We synthesized polydimethylcyclooctadiene (PDMCOD) by ROMP of dimethylcyclooctadiene (DMCOD) and the resulting polymer had a chain structure that is analogous to polyisoprene. DMCOD is trisubstituted cyclic olefin, so it is a less reactive monomer than COD.[11] Due to the highly unreactive nature of the DMCOD, the polymerization was carried out in toluene following the protocol reported by Thomas and Grubbs.[11] The longest PDMCOD that we could produce had a molecular weight of 65 kg/mol by ROMP of DMCOD. The resulting polymer dissolved in PAO without heating the solution, unlike PCOD chains that required initial heating of the solution to 60 °C for dissolution, and stayed soluble even at -20 °C. However, it was not possible to make associative PDMCOD because both DA and DB-CTA and as well as the corresponding macroCTAs (short DA-PCOD and DB-COD chains with M_w ~ 20 kg/mol) were not soluble in toluene. Future work could include synthesis of telechelic PDMCODs via ROMP of DMCOD using modified forms of CTAs. For example, to overcome the solubility issue of di-tetra-acid ended cis-2-butene in DCM, Dr. Ming Hsin (Jeremy) Wei synthesized polymers using di-tert-butyl ester ended CTAs to make long telechelic PCOD, and the end groups of the polymer were hydrolyzed using tetrafluoro acetic acid post-polymerization.[24] The solubility of non-associative polymer backbones (different from PCOD) is summarized in Table 3.3.

Table 3.3 Turbidity of (non-PCOD) polymer solutions in PAO

	60°C	20°C	4°C	-20°C
NA-PCOE 14k	Clear	Clear	Cloudy	Cloudy
NA-PCOD-co-COE 850k	Clear	Clear	Clear	Cloudy
NA-PDMCOD 19k	Clear	Clear	Clear	Clear
NA-PDMCOD 65k	Clear	Clear	Clear	Clear
Commercial PIB 1.2M	Clear	Clear	Clear	Clear
Commercial PIB-co-isoprene 392k	Clear	Clear	Clear	Clear

COD = cyclooctadiene, COE = cyclooctene, DMCOD = dimethyl cyclooctadiene, PIB=polyisobutylene, NA = non-associative

3.3.3 Effect of PCOD on spray behavior of PAO

The non-associative PCOD (M_w ~ 1 Mg/mol) and 1:1 mixture of DA-PCOD and DB-PCOD (M_w ~ 670 kg/mol) solutions PAO at various concentrations were prepared and used by our collaborators at ARL (Dr. Jacob Temme and coworkers) for spray experiments. Comparing the spray of PAO with and without the added PCODs, both non associative PCOD and the DA:DB mixture were able to modify the spray behavior significantly (pressurized fluid at 120 psi was released through a 5 mm orifice). For DA:DB mixtures, even at a concentration as low as 0.03 wt%, the use of the polymers decreased spray angle, increased ligament diameter and inhibited ligament breakup into droplets in comparison to those of untreated PAO.

3.4 Conclusion

Long end-associative polymers can be used as mist-control agents in polyalphaolefin oil, mitigating the fire vulnerability of PAO which is used widely in a variety of applications as a lubricant, hydraulic fluid, and coolant. Unfortunately, the previously designed long end-associative polymers with polycyclooctadiene backbones (DA-PCOD and DB-PCOD) were not soluble in PAO. Dissolution of the associative PCODs at room temperature (20 °C) was possible upon the addition of the co-solute BHT, which can interact with the aromatic component of the end groups via π-π stacking to solubilize the end groups, without affecting the hydrogen bonding between DA and DB groups. The dissolution of associative PCODs in PAO at room temperature allowed our collaborators at ARL to study the spray behavior of PAO, demonstrating the efficacy of the associative polymers as mist-control agents. However, at sub-ambient temperatures (below 4 °C), even the PCOD backbone without the end groups was not soluble in PAO, so we tried to modify the polymer backbone. Reducing the extent of unsaturation along the backbone resulted in decrease in solubility in PAO, while polymers with alkyl branches along the backbone (PIB, polyisoprene, or copolymers of the two) were soluble in PAO even at -20 °C. For improving low temperature solubility of long end-associative polymers in PAO, both end group and backbone structure should be modified. To increase the solubility of the associative PCODs in PAO, the end groups should not contain aromatic structures or heteroatoms (O, or N) except for parts of the end groups that are directly responsible for hydrogen bonding (e.g carboxylic acids).

3.5 Supplementary data

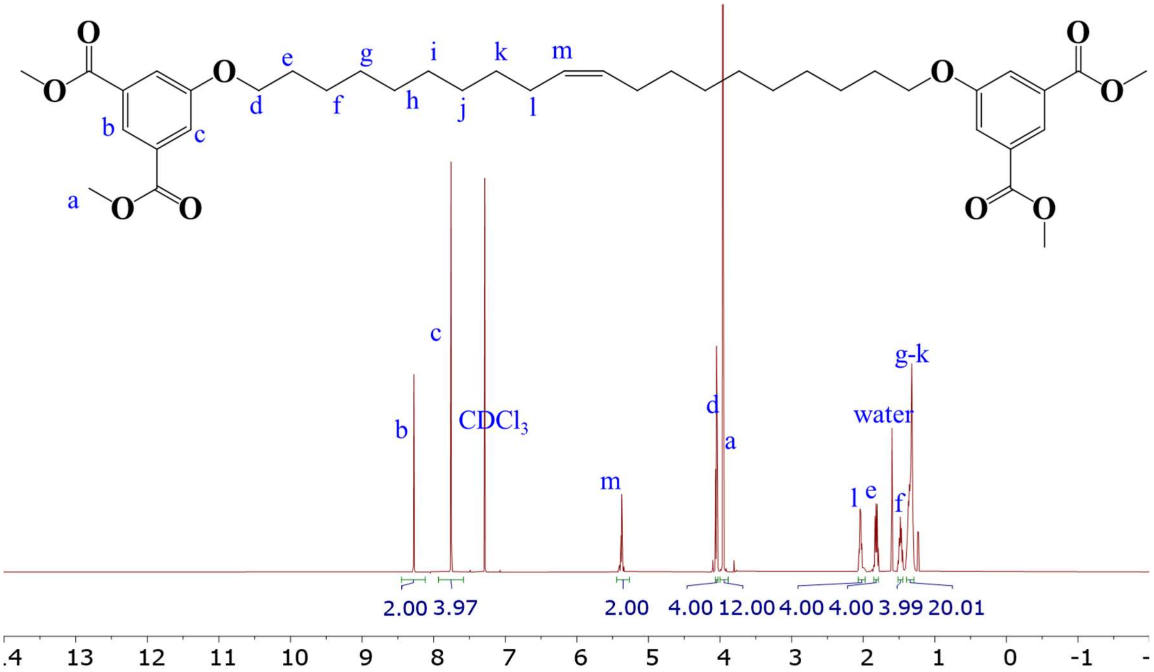

Figure 3.3 ^{1}H-NMR of diester CTA (DE-CTA) in CDCl$_3$.

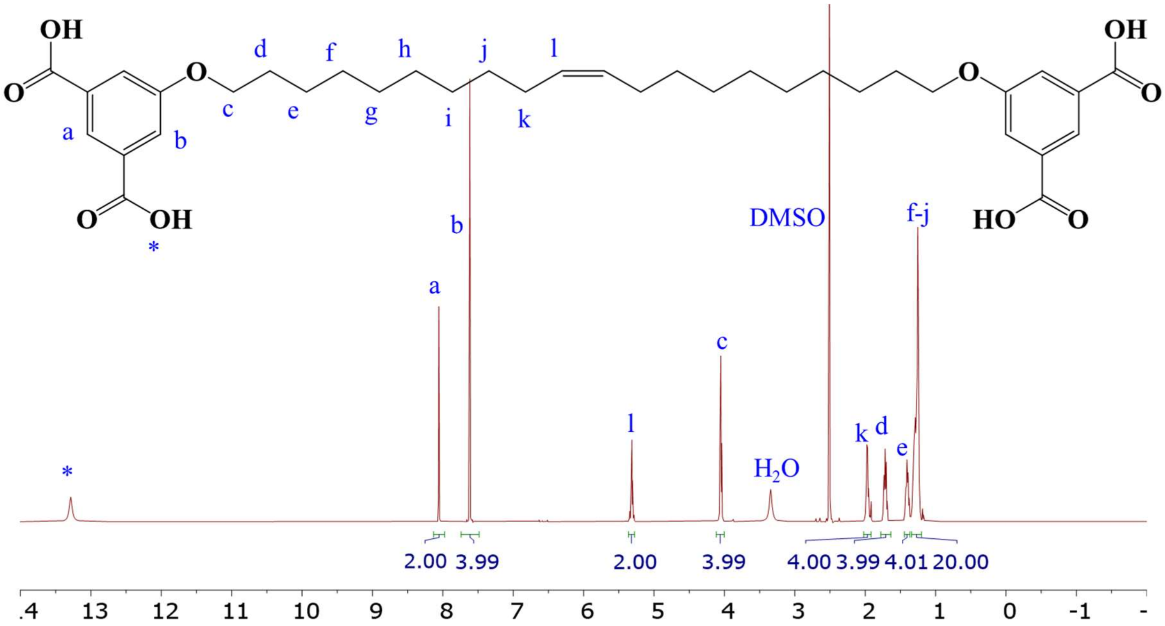

Figure 3.4 ^{1}H-NMR of diacid CTA (DA-CTA) in d-DMSO.

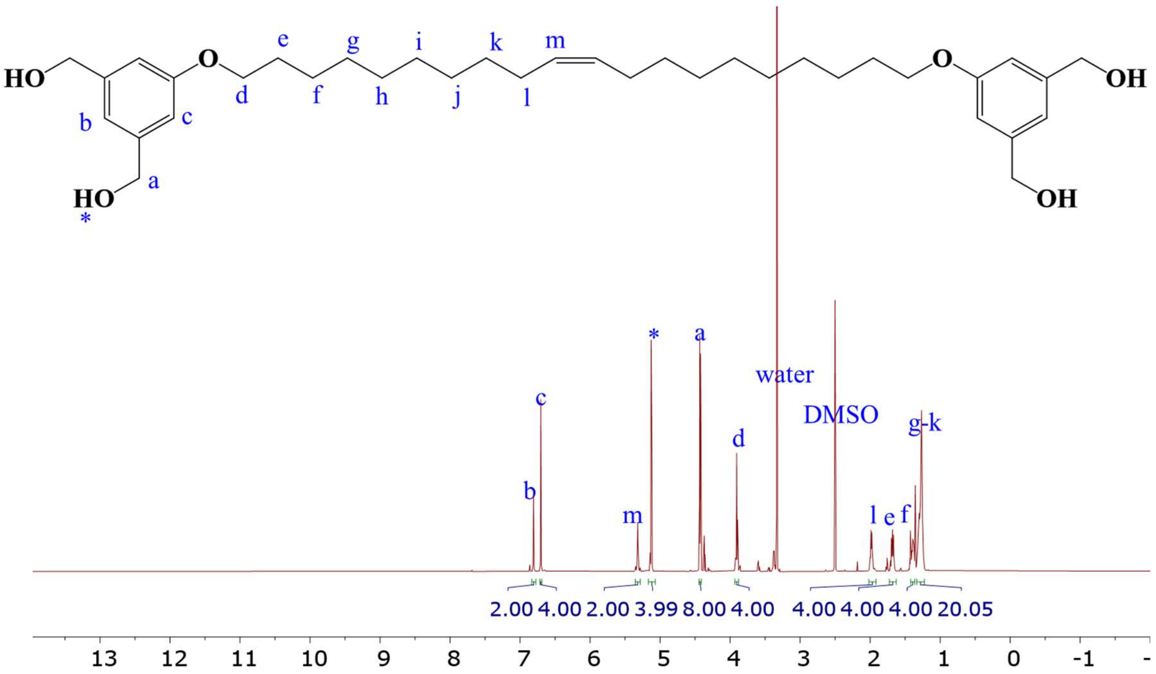

Figure 3.5 ^{1}H-NMR of dihydroxy CTA in d-DMSO.

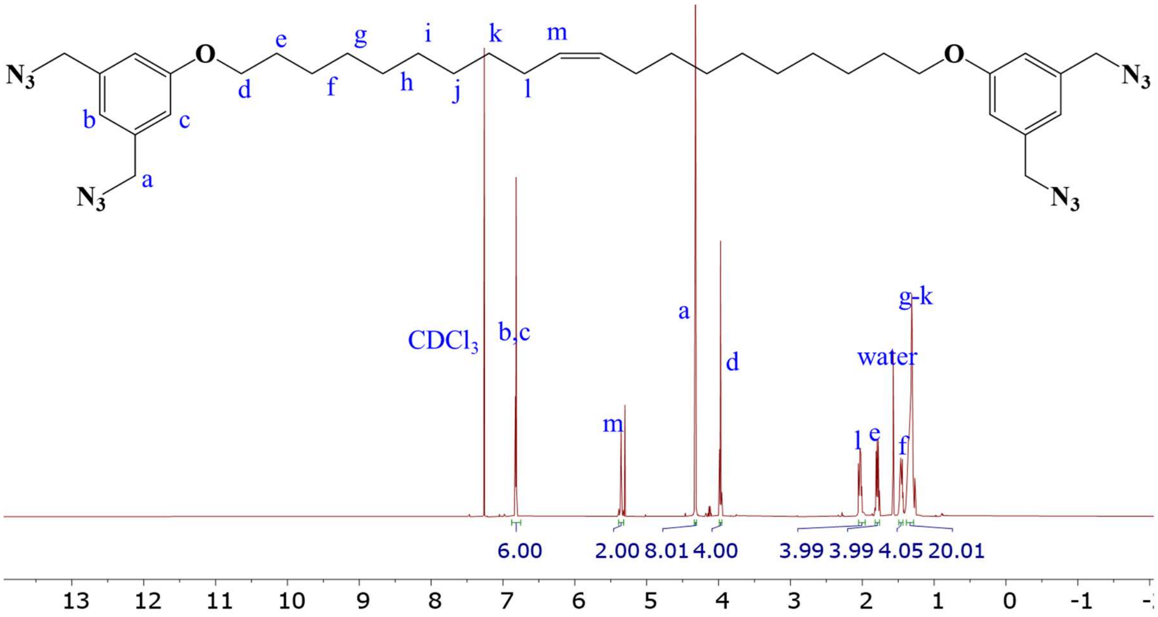

Figure 3.6 ^{1}H-NMR of di-azido CTA in $CDCl_3$.

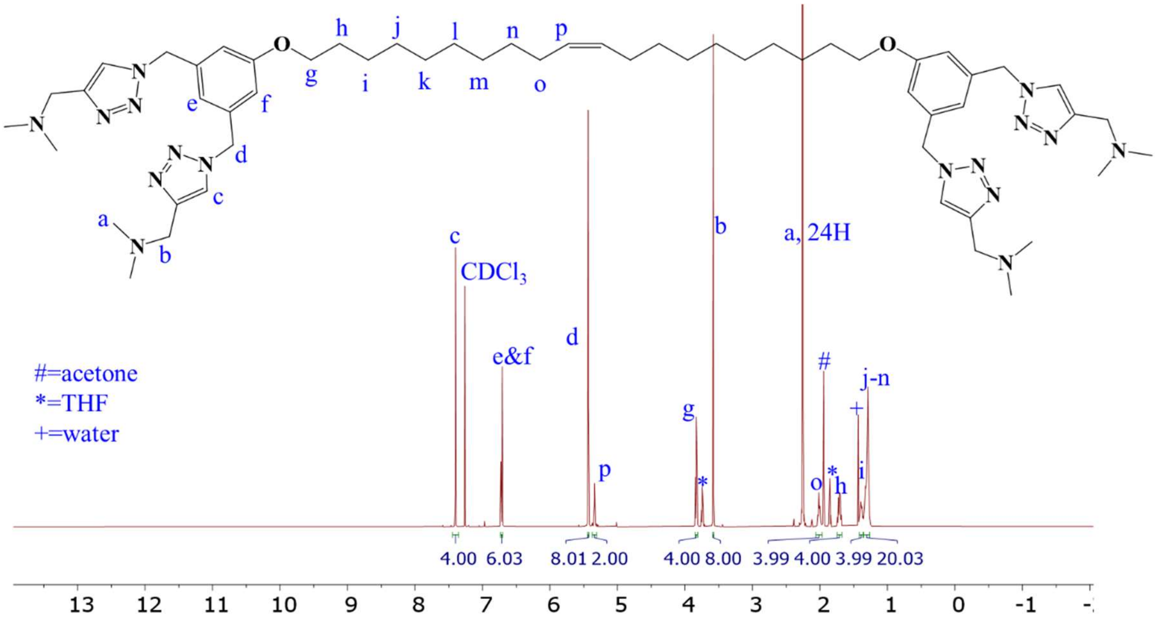

Figure 3.7 ^{1}H-NMR of di base CTA (DB-CTA) in CDCl$_3$.

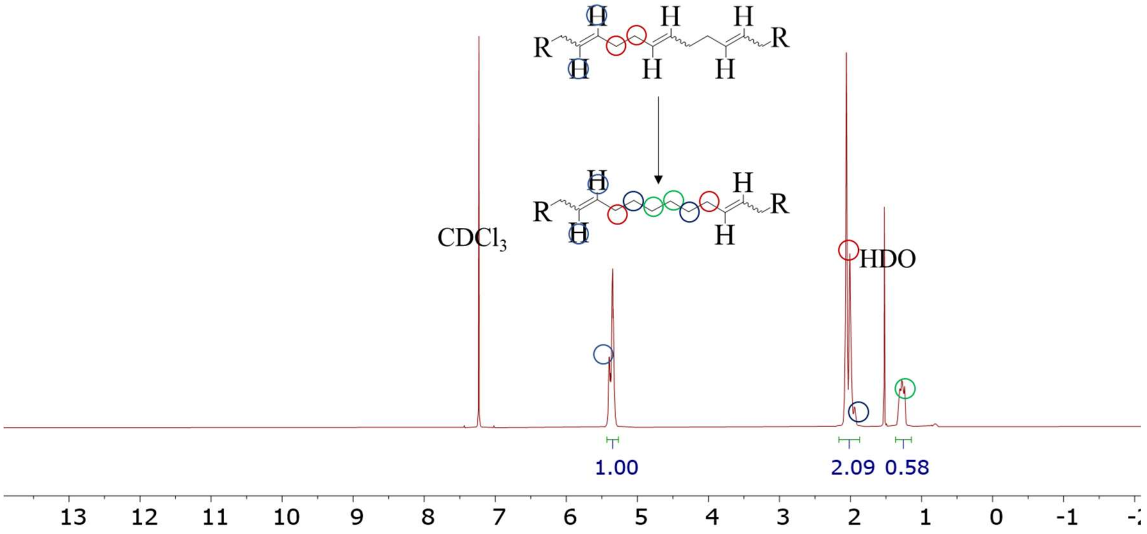

Figure 3.8 ^{1}H-NMR of partially hydrogenated polycyclooctadiene (M_w 852 kg/mol). The extent of hydrogenation was calculated as below. Before hydrogenation (# of protons from saturated carbons/ # of protons from unsaturated carbons) = 2. After hydrogenation (# of protons from saturated carbons/# of protons from unsaturated carbons) =2.68. Solve (1-x):(2+2x)=1:2.68, x=0.14, 14% of the double bonds.

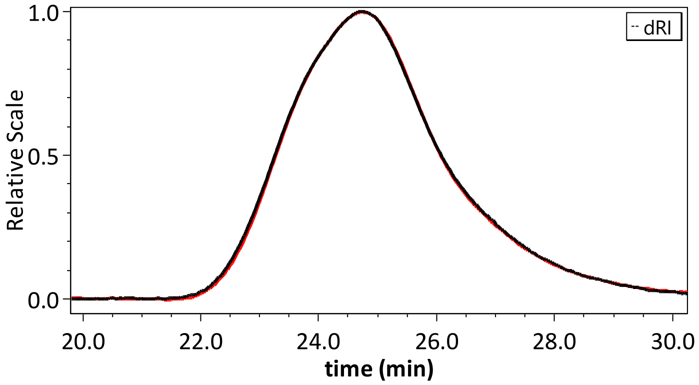

Figure 3.9 GPC chromatogram of polycyclooctadiene (M_w 852 kg/mol) (black) and partially hydrogenated poylcycloctadiene (red). The GPC chromatogram shows no significant changes in molecular weight before and after hydrogenation.

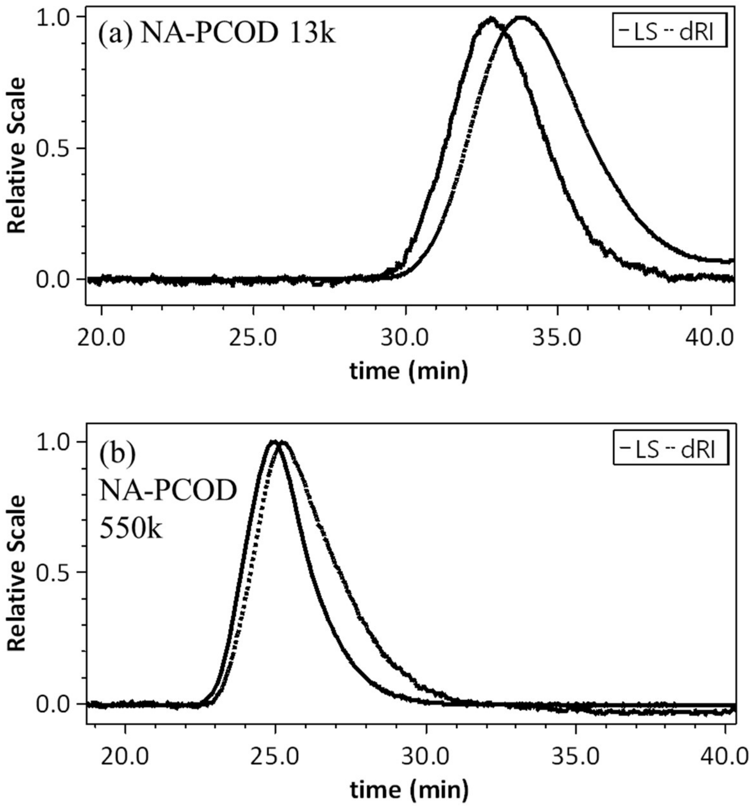

Figure 3.10 GPC chromatograms of telechelic PCODs (a) NA-PCOD M_w 13 kg/mol, (b) NA-PCOD M_w 550 kg/mol

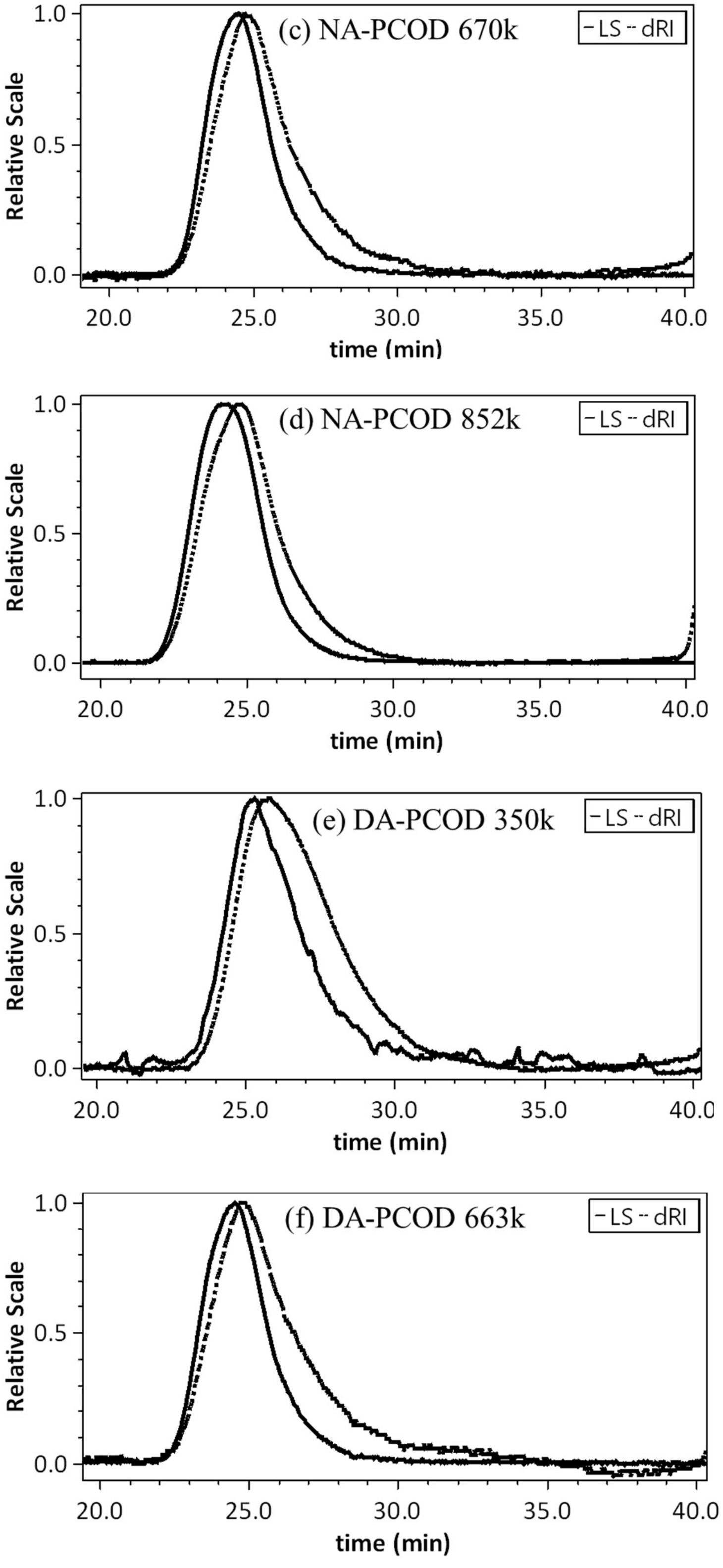

Figure 3.10 Continued (c) NA-PCOD M_w 670 kg/mol, (d) NA-PCOD M_w 852 kg/mol (e) DA-PCOD M_w 350 kg/mol, (f) DA-PCOD M_w 663 kg/mol

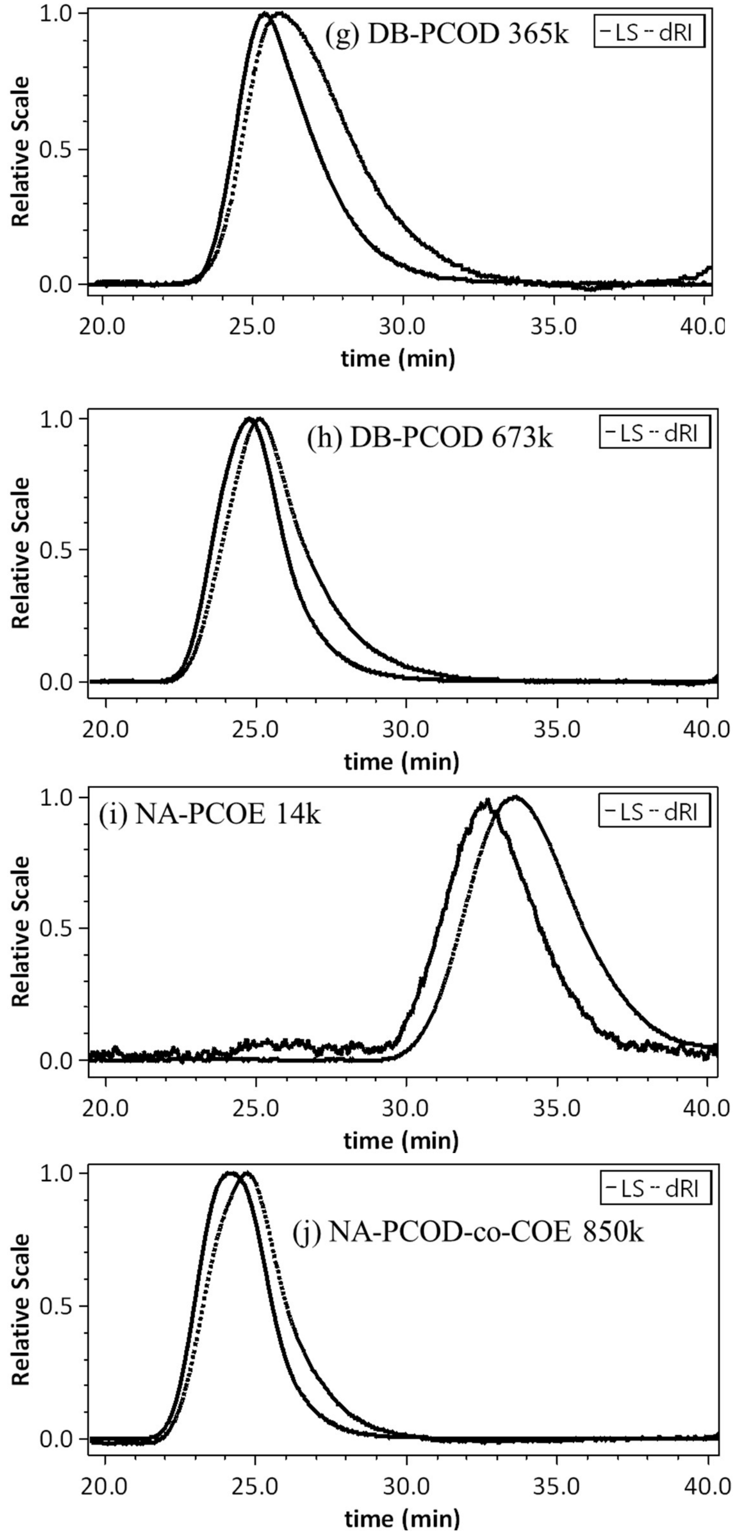

Figure 3.10 Continued (g) DB-PCOD M_w 365 kg/mol, (h) DB-PCOD M_w 673 kg/mol (i) NA-PCOE M_w 14 kg/mol, (j) NA-PCOD-co-COE M_w 850 kg/mol

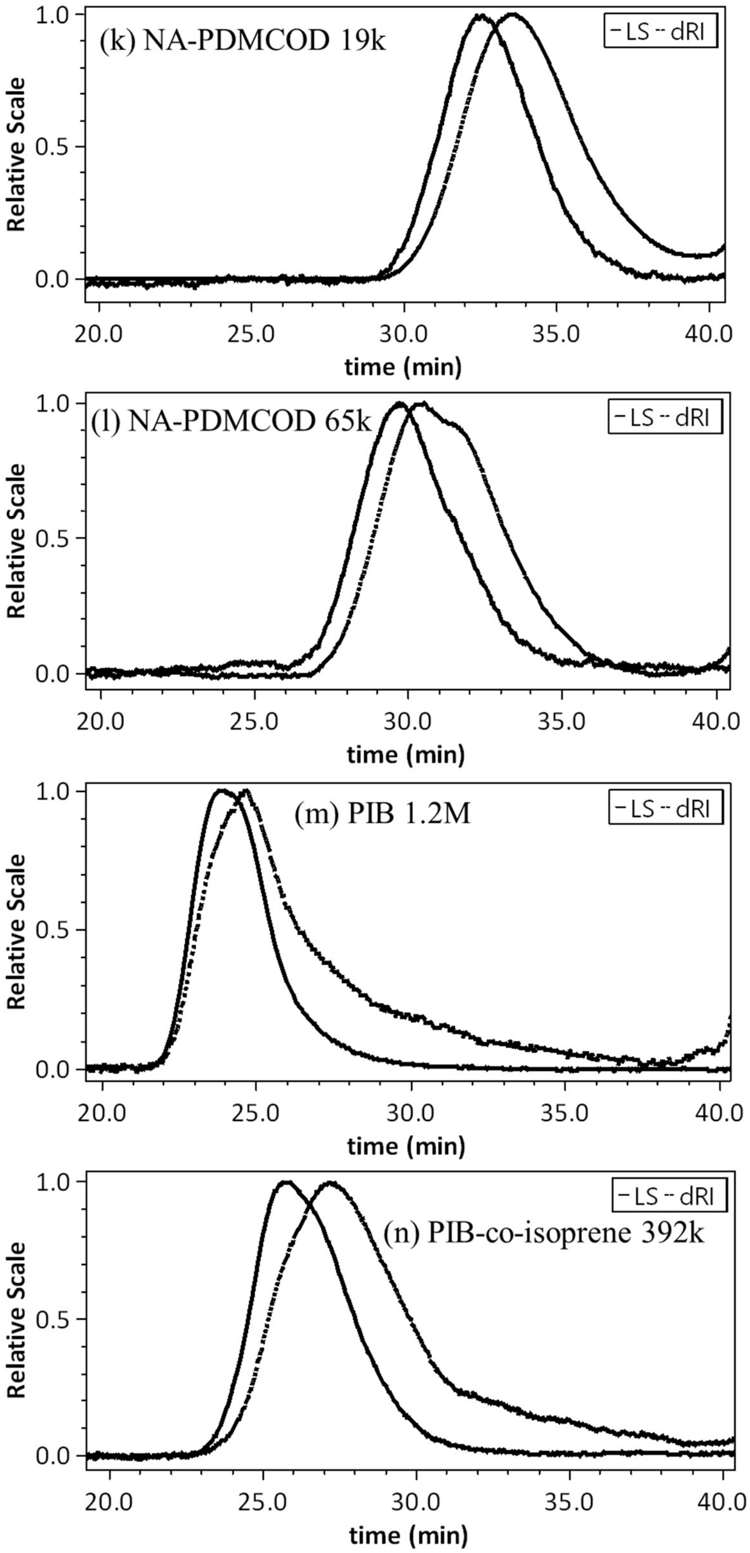

Figure 3.10 Continued (k) NA-PDMCOD M_w 19 kg/mol, (l) NA-PDMCOD M_w 65 kg/mol (m) PIB M_w 1.2 Mg/mol, (n) PIB-co-isoprene M_w 392 kg/mol

References

1. Atiqullah, Al-Sarkhi, Al-Thenayan, Al-Malki & Alasiri. Energy-Saving UHMW Polymeric Flow Aids: Catalyst and Polymerization Process Development. *Catalysts* **9**, 1002 (2019).
2. Chao, K. K., Child, C. A., Grens, E. A. & Williams, M. C. Antimisting action of polymeric additives in jet fuels. *AIChE J.* **30**, 111–120 (1984).
3. Wei, M.-H.; Li, B.; David, R. L. A.; Jones, S. C.; Sarohia, V.; Schmitigal, J. A.; Kornfield, J. A. Megasupramolecules for Safer, Cleaner Fuel by End Association of Long Telechelic Polymers. *Science (80-.).* **2015**, *350* (6256), 72–75.
4. Santon, R. C. Mist fires and explosions - An incident survey. *Inst. Chem. Eng. Symp. Ser.* 370–374 (2009).
5. Mortier, R. *Chemistry and Tech of Lubricants*. (2010).
6. Mattie, D. R. *et al.* Acute and two-week inhalation toxicity studies in rats for Polyalphaolefin (PAO) fluid. *J. Toxicol. Environ. Heal. Part A* **84**, 1–19 (2021).
7. Gant, S. (Health and safety laboratory). *Generation of flammable mists from high flashpoint fluids: Literature review*. (2013).
8. Ji, S., Hoye, T. R. & Macosko, C. W. Controlled Synthesis of High Molecular Weight Telechelic Polybutadienes by Ring-Opening Metathesis Polymerization. *Macromolecules* **37**, 5485–5489 (2004).
9. Kornfield, J. A., Davis, M. E., Wei, M.-H. & Jones, S. C. Molecular sieves mediated unsaturated hydrocarbon separation and related compositions, materials, methods and systems. (2017).
10. Martinez, H., Ren, N., Matta, M. E. & Hillmyer, M. A. Ring-opening metathesis polymerization of 8-membered cyclic olefins. *Polym. Chem.* **5**, 3507–3532 (2014).
11. Thomas, R. M. & Grubbs, R. H. Synthesis of Telechelic Polyisoprene via Ring-Opening Metathesis Polymerization in the Presence of Chain Transfer Agent. *Macromolecules* **43**, 3705–3709 (2010).
12. Pitet, L. M., Chamberlain, B. M., Hauser, A. W. & Hillmyer, M. A. Synthesis of linear, H-shaped, and arachnearm block copolymers by tandem ring-opening polymerizations. *Macromolecules* **43**, 8018–8025 (2010).
13. Rachapudy, H., Smith, G. G., Raju, V. R. & Graessley, W. W. Properties of amorphous and crystallizable hydrocarbon polymers. III. Studies of the hydrogenation of polybutadiene. *J. Polym. Sci. Polym. Phys. Ed.* **17**, 1211–1222 (1979).
14. Hahn, S. F. An improved method for the diimide hydrogenation of butadiene and isoprene containing polymers. *J. Polym. Sci. Part A Polym. Chem.* **30**, 397–408 (1992).
15. Phinyocheep, P., Pasiri, S. & Tavichai, O. Diimide hydrogenation of isoprene-styrene diblock copolymers. *J. Appl. Polym. Sci.* **87**, 76–82 (2003).
16. Yan, X. Syntheses of Polymers with Diverse Architectures via Metathesis Polymerization and Investigation of Their Structure-Property Relationships. (California Institute of Technology, 2010).
17. Vollhardt, P. & Schore, N. *Organic Chemistry: Structure and Function*. (Macmillan, 2018).

18. Richards, R. B. Polyethylene-structure, crystallinity and properties. *J. Appl. Chem.* **1**, 370–376 (2007).

19. Short, J. N., Thornton, V. & Kraus, G. Effect of Cis-Trans Ratio on the Physical Properties of 1,4 Polybutadienes. *Rubber Chem. Technol.* **30**, 1118–1141 (1957).

20. Odell, J. A., Muller, A. J., Narh, K. A. & Keller, A. Degradation of polymer solutions in extensional flows. *Macromolecules* **23**, 3092–3103 (1990).

21. Lee, K. *et al.* Mechanical degradation of polyisobutylene under turbulent flow. *Colloid Polym. Sci.* **280**, 779–782 (2002).

22. Nyden, M. R., Stoliarov, S. I., Westmoreland, P. R., Guo, Z. . & Jee, C. Applications of reactive molecular dynamics to the study of the thermal decomposition of polymers and nanoscale structures. *Mater. Sci. Eng. A* **365**, 114–121 (2004).

23. Smith, M.; March, J. *March's advanced organic chemistry : reactions, mechanisms, and structure*. (John Wiley, 2001).

24. Wei, M.-H. Synthesis and Potency of Long End-Associative Polymers for Mist Control. (California Institute of Technology, 2014).

C h a p t e r 4

Synthesis of tri-acid ended long polycyclooctadiene for formation of ultralong supramolecules in hydrocarbon solvents

4.1 Introduction

In Chapter 3, we observed how the end group with an aromatic component in the structure could make the entire associative polycyclooctadiene (PCOD) insoluble in polyalphaolefin oil, a fully saturated hydrocarbon solvent. In this chapter, we describe the synthesis of long end-associative polymers with a new end group, which has three carboxylic acids without any additional heteroatoms or aromatic components. Previously, Wei and coworkers[1] synthesized many variations of end groups with different numbers of carboxylic acids (N = 1, 2, 4, 8) by growing dendrimers of 5-hydroxyisophthalic acid. As the number of carboxylic acids increased in the end group, the corresponding PCOD became less soluble in solvents. When N = 8, polymers were too polar to be soluble in most non-polar organic solvents. When N = 4, the resulting polymer tetra-acid PCOD (TA PCOD) was soluble in jet-A-fuel, but not readily soluble in other solvents. For example, TA PCOD (M_w 24 kg/mol) was not soluble in chloroform, and TA PCOD (M_w 570 kg/mol) was not soluble in dodecane or PAO. We hypothesized that the lack of additional heteroatoms or aromatic component in the end group would make the polymer more soluble in highly non-polar solvents.

In this chapter we examine a small organic tri-carboxylic acid (TriA) end group for three reasons. First, we chose a structure that satisfies the criteria that it should have no aromatic ring and no non-essential heteroatoms. Second, the potential to form three carboxylic acid hydrogen-bonds with an association energy of roughly 22.8 kT at 25 °C, providing an association strength that has never been explored previously in our group's work with associative polymers. If three optimal carboxylic acid pairs form, it would provide an association energy that is slightly higher than the theoretically predicted optimal association energy of 16-18 kT.[2] DA self-association has an association energy of roughly 15.2 kT, (4 hydrogen bonds total between two carboxylic acids), and TA could potentially self-associate with roughly 30.4 kT.[1] DA-DB associate via charge assisted hydrogen bonding (CAHB) between carboxylic acid and tertiary amine and has roughly 16-18 kT association energy.[1,3] Having different associative end groups allows us to choose the end group that is most practical for each application. For example, a stronger association between end groups would be required in order to use the polymers in solvents that may contain additives that could interfere with the hydrogen bonding of the end groups.

Third, TriA PCOD is amenable to dissemination and scale-up as the synthesis protocol is relatively simple and minimizes the use of hazardous reagents. Herein, we describe the synthesis of the TriA chain transfer agent and TriA PCODs, and we compare the shear viscosity of the TriA-PCOD to that of non-associative (NA), DA, DB, DA:DB, and TriA:DB, PCODs in 5 different solvents (decalin, tetralin, dodecane, PAO, and jet-A-fuel).

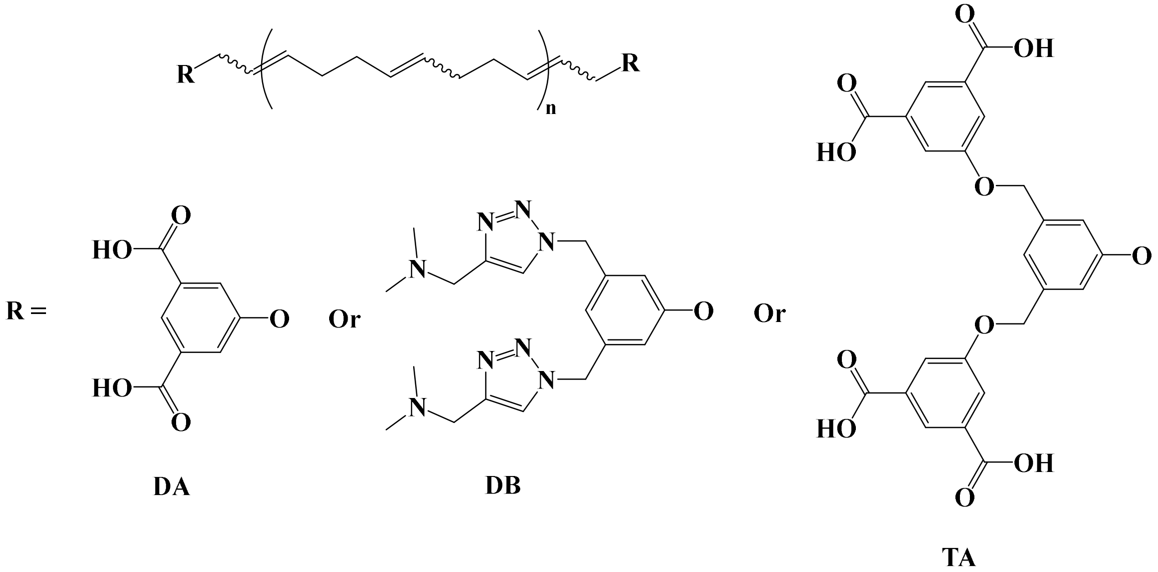

Scheme 4.1 Structure of associative end groups previously synthesized in Kornfield group. DA = Di-acid, DB = Di-base, TA = Tetra-acid.

4.2 Experimental

4.2.1 Materials and instrumentation

All chemical reagents were obtained from Sigma Aldrich at 98% purity or higher unless otherwise stated. Polyalphaolefin (Brayco micronic 889) was obtained from QC lubricants. Jet-A fuel was purchased from El Monte Airport (El Monte, California, USA) and used as received. All solvents were obtained from Sigma Aldrich, at ACS reagent grade or higher (> 99.5% purity) and used as received without further purification.

NMR spectroscopy

^{1}H-NMR spectra were obtained using a Varian Inova 500 spectrometer (500 MHz); all spectra were recorded in $CDCl_3$ and d-DMSO (purchased from Cambridge Isotope Laboratories). Chemical shifts were reported in parts per million (ppm) and were referenced to residual solvent resonances.

Gel permeation chromatography (GPC)

The molecular weights and dispersity index of the polymers were determined on a GPC system with a Wyatt DAWN EOS multi-angle laser light scattering detector (λ=690nm), a Waters 410 differential refractometer (RI) (λ=930nm), and four Agilent PLgel columns (pore size 103, 104, 105, and 106 Å) connected in series. THF was used as the eluent at the flow rate of 0.9 mL/min with a temperature of 35 ºC. The data were analyzed using Wyatt Astra (version 5.3.4) using the Zimm fitting formula with *dn/dc* = 0.125 for each polymer reported.

Viscosity measurement

The shear viscosity of the polymer solutions was measured using a strain-controlled rheometer TA ARES-RFS, equipped with a cone-plate geometry (angle 2°, diameter 50mm). Specific viscosity ($\eta_{specific}$) is defined as $\eta_{specific} = (\eta_{solution}/\eta_{solvent} - 1)$. Three replicates were measured to obtain the error bars (standard error).

4.2.2 Synthesis of chain transfer agents

Synthesis of (E)-1,20-dibromoicos-10-ene, di-acid CTA (DA-CTA), di-base (CTA) (DB-CTA) and relevant intermediates was described in Chapter 3.

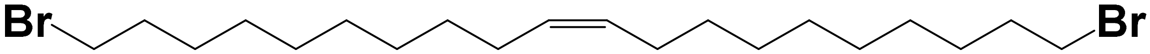

Scheme 4.2 (E)-1,20-dibromoicos-10-ene (Di-bromoicosene)

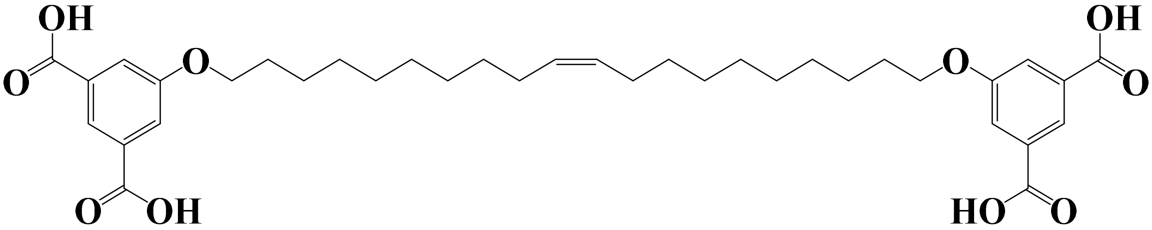

Scheme 4.3 Di-acid CTA (DA-CTA)

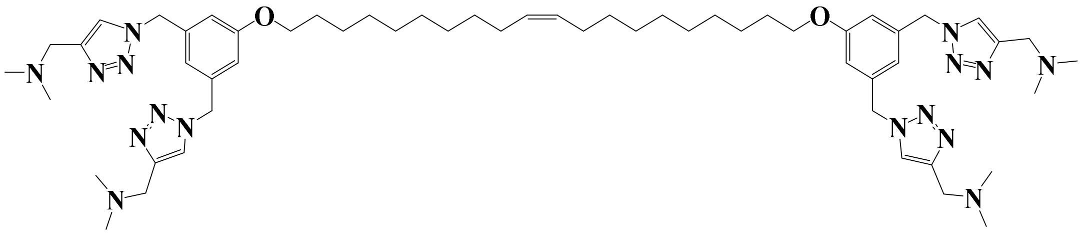

Scheme 4.4 Di-base CTA (DB-CTA)

Synthesis of hexamethyl ester CTA intermediate

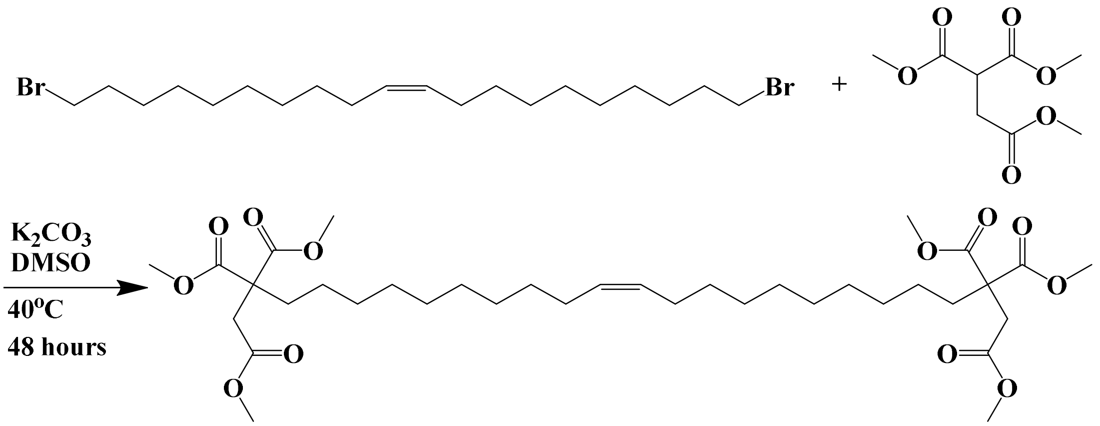

Scheme 4.5 Synthesis of hexamethyl ester CTA intermediate

Trimethyl ethane-1,1,2-tricarboxylate (4.97g, 24.34 mmol) (Sigma Aldrich, 95%), di-bromoicosene (4.85g, 11.06 mmol) and K_2CO_3 (3.05 g, 22.2 mmol) were dissolved in DMSO (40 mL). The mixture was stirred at 40 °C for 48 hours. After 48 hours, the mixture was diluted with ethyl acetate (180 mL) and washed with 1M $HCl_{(aq)}$ (100mL, 3 times), DI water (100mL), and saturated brine (100mL). The organic phase was dried over $MgSO_4$, filtered and the solvent was removed by rotary evaporation. The crude product was purified by silica gel column chromatography using a mixture of ethyl acetate and DCM, 1:20 (v/v) as eluent. The collected fractions were evaporated using a rotary evaporator, and the product was collected as a yellow viscous oil. 75% yield.

^{1}H-NMR ($CDCl_3$, 500MHz) 1.20-1.4 (Br, 28H), 1.98 (m, 8H), 2.95 (s, 4H), 3.64 (s, 6H), 3.72 (s, 12H), 5.35 (td, 2H)

Synthesis of tri-acid CTA (TriA-CTA)

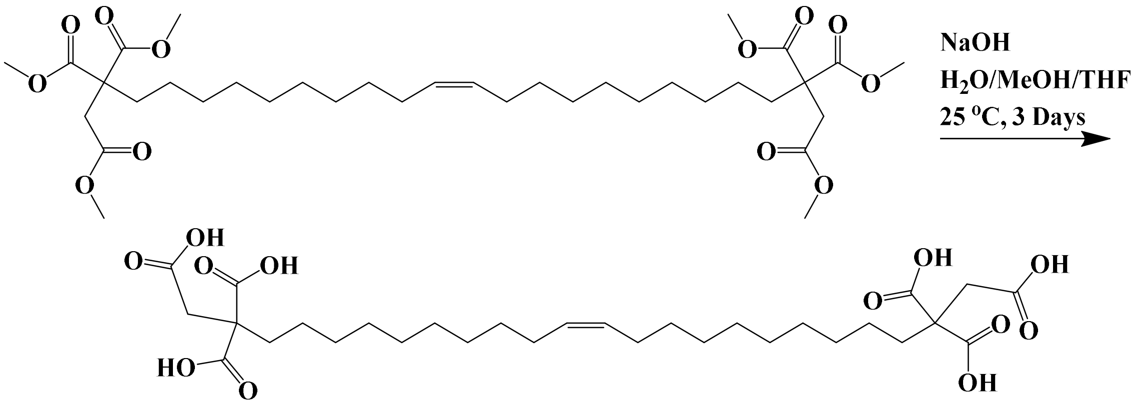

Scheme 4.6 Synthesis of tri-acid CTA (TriA-CTA)

The hexamethyl ester intermediate (4g, 5.15mmol) was dissolved in THF (36 mL). In a 250 mL round bottom flask, NaOH (6.18g, 0.154mol) was dissolved in water (12 mL), and methanol (24 mL) was added. The THF solution was added to NaOH solution, and the mixture was stirred at room temperature for 3 days. After 3 days, the mixture was slowly neutralized to pH = 6 using 3M $HCl_{(aq)}$. The product was extracted with ethyl acetate (150 mL), and the organic phase was washed with DI water (100 mL) and saturated brine (100 mL), dried over $MgSO_4$ and filtered, and the solvent was removed under reduced pressure using a rotary evaporator. The final product was a brown viscous solid. 95% yield.

^{1}H-NMR (d-DMSO, 500MHz) 1.20-1.4 (Br, 28H), 1.87 (m, 4H), 2.00 (m, 4H), 2.76 (s, 4H), 5.35 (td, 2H) 12.6 (br, 6H)

4.2.3 Polymer Synthesis

Synthesis of macro chain transfer agents (mCTA)

Macro chain transfer agents were synthesized using either TriA-CTA, DA-CTA, DB-CTA or cis-2-hexene (Sigma Aldrich, 95%) as CTAs. CTA (1 mmol) and 2,6-di-tert-butyl-4-methylphenol (BHT, 0.1 g, 0.45 mmol) were dissolved in THF (10 ml) in a 100 ml Schlenk flask. The dissolved solution was degassed by 3 freeze-pump-thaw cycles and the flask was filled with argon. To the degassed mixture of CTA, 1 ml of degassed THF solution of 2nd generation Grubbs Catalyst (**G2**, 8.4 mg, 9.89 μmol) was syringe transferred, immediately followed by the addition of degassed, freshly vacuum distilled purified COD (5.0 g, 45.8 mmol). The mixture was stirred at 40 °C overnight. The reaction was stopped by exposing to air, and diluted with THF, (40 ml) and the polymers were precipitated into a large excess of methanol (500 mL) dropwise. Methanol was decanted, and the polymers were collected in a 20 ml vial with silicone/PTFE septum cap, and dried under high vacuum. The vial was degassed by 3 cycles of pulling vacuum/filling argon and stored at -30 °C.

Synthesis of Telechelic Polycyclooctadiene (PCOD)

Telechelic PCOD was synthesized following the same procedure used for the synthesis of mCTA, using mCTA instead of CTA. All telechelic polymers used in this paper were synthesized using 5 g of purified COD, 0.16 ml of **G2** (from 1 mg/ml degassed THF solution), 0.1 g of BHT, and 10 ml of THF. In ROMP of COD, in addition to growth of linear chains there is also competing intramolecular secondary metathesis that generates small cyclic oligomers (backbiting)[4]. To compensate for the formation of small cyclic species, the amount of mCTA was adjusted using the following empirical formula:

$$mCTA\_M_w \times \frac{(M_{mCTA}+M_{COD})}{M_{mCTA}} \times 0.85 = Target\_M_w.$$

Polymer solution preparation

Non-associative PCOD, DA-PCOD, DB-PCOD, and TriA-PCOD were weighed and loaded into 20 mL glass scintillation vials with a magnetic stir bar. To the vials, a necessary amount of solvent (jet-A fuel, n-dodecane, decahydronaphthalene (mixture of cis and trans), 1,2,3,4-tetrahydronaphthalene (tetralin), PAO) was added to make 0.25 wt% concentration. (Approximately 10 mL of each of the solutions). BHT was added in small quantity (0.01 wt%) to prevent crosslinking of the PCOD backbones. For DA-PCOD and DB-PCOD in PAO, BHT was added such that the total weight of BHT was up to 5 times the weight of the polymers. The vials were sealed with PTFE lined plastic screw caps, and the solutions were stirred at 70 °C for up to 24 hours to allow complete dissolution of the polymers.

4.3 Results and discussion

Synthesis of TriA CTA and TriA PCOD

We synthesized TriA CTA by reacting alkyl bromide with commercially available trimethyl ethane-1,1,2-tricarboxylate. The hydrogen atom bonded to a carbon atom in the α position relative to a carbonyl group shows unusual acidity because the resulting carbanion after deprotonation can be resonance stabilized as shown in Scheme 4.7.

Trimethyl ethane-1,1,2-tricarboxylate has one α proton, which can be deprotonated by a base. In prior literature, a variety of bases was used to deprotonate the α proton to react the resulting carbanion with alkyl halides. NaH[5–7] (or potassium hydride), sodium ethoxide[8,9] and potassium carbonate[10,11] were used; we chose potassium carbonate because it is non-toxic, non-flammable, and inexpensive. The reaction between trimethyl ethane-1,1,2-tricarboxylate with dibromoeicosene yielded hexamethyl ester CTA intermediate, and subsequent hydrolysis of methyl esters yielded TriA-CTA.

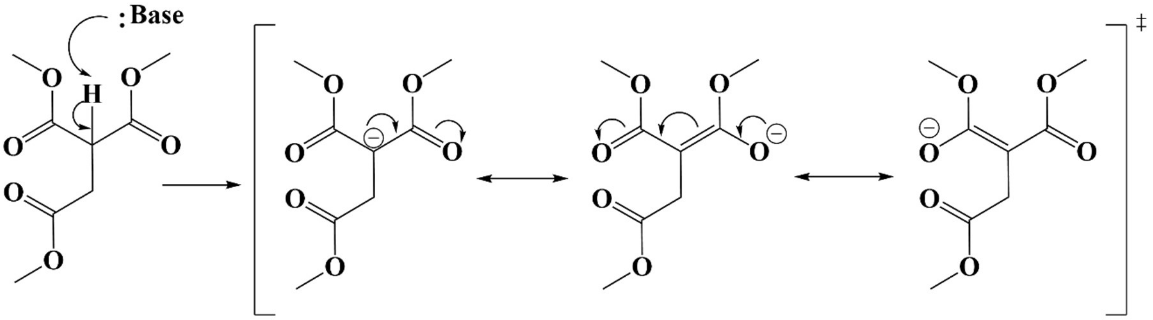

Scheme 4.7 Transition state of deprotonated trimethyl ethane-1,1,2-tricarboxylate. The transition state is resonance stabilized.

TriA-CTA required 3 steps for synthesis, like DA-CTA which also required three steps (Scheme 4.8). Synthesis of TA-CTA requires 5 steps, and the purification of the tetra methyl ester CTA (Scheme 4.10) can be difficult. Tetra hydroxy CTA is reacted with excess dimethyl 5-hydroxyisophthalate via the Mitsunobu reaction between the hydroxyl group and the phenol. This reaction creates byproducts when two hydroxy groups of the tetra hydroxy CTA react to form oligomeric species. Chromatographic separation of these oligomeric species from the desired product could be very time consuming and challenging. Synthesis of DB-CTA requires 6 steps (Scheme 4.9), so if TriA PCOD can be used in place of a DA:DB mixture in the application, the amount of effort and resources required for the polymer synthesis can be significantly reduced.

While we used chromatographic separation to purify the hexamethyl ester CTA intermediate, we believe the protocol could be further optimized if scale-up of the reaction is necessary. Excess trimethyl ethane-1,1,2-tricarboxylate could be used relative to the amount of di-bromoicosene to ensure the complete reaction of di-bromoicosene. The crude product can be hydrolyzed, and the excess trimethyl ethane-1,1,2-tricaboxylate would become water-soluble tricarboxylic acids that could be removed by liquid extraction since TriA-PCOD is not water-soluble.

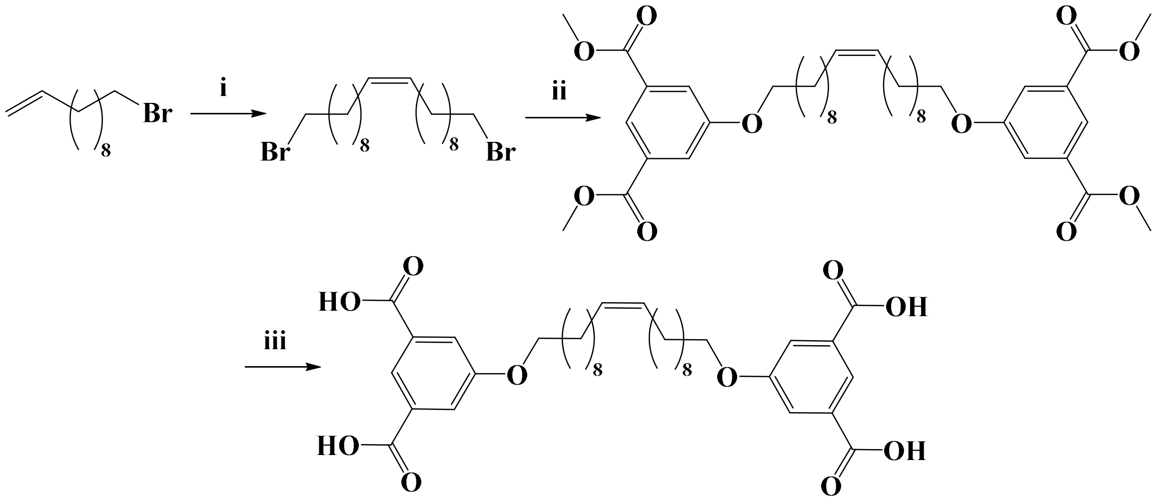

Scheme 4.8 Overview of DA-CTA synthesis. i) Cis-selective Grubbs' catalyst, 35 °C overnight, ii) dimethyl 5-hydroxyisophthalate, K_2CO_3, DMF, 60 °C overnight, iii) NaOH, THF/MeOH/Water mixture, room temperature, overnight.

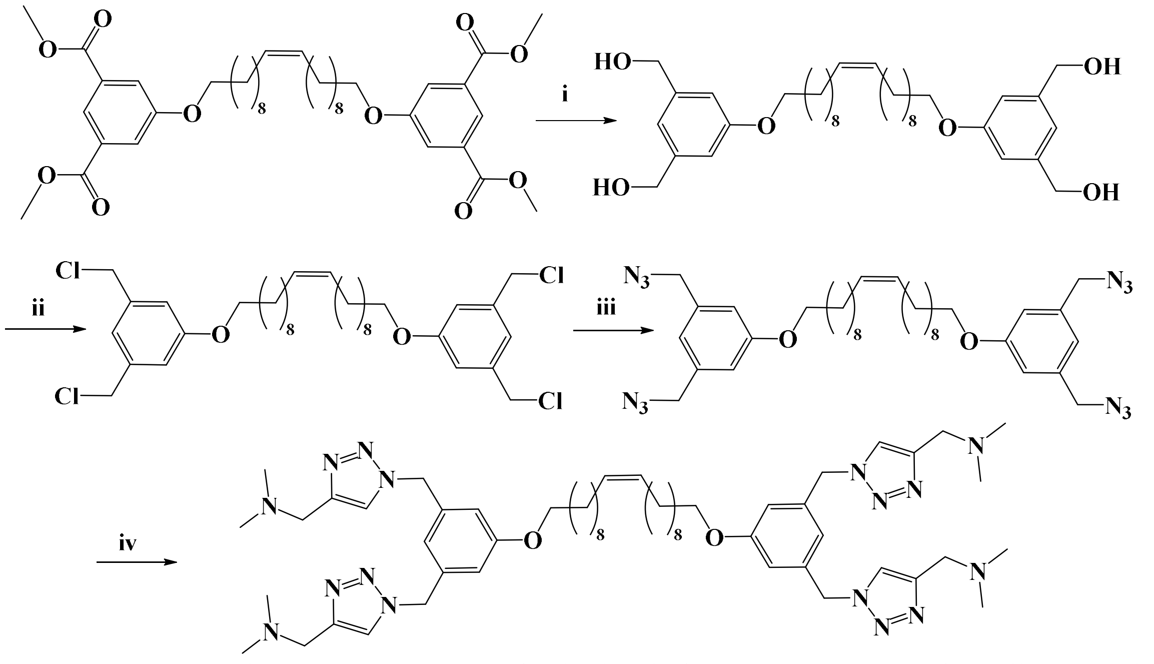

Scheme 4.9 Overview of DB-CTA synthesis. i) $LiAlH_4$, THF, 40 °C 2 days, ii) cyanuric chloride, DMF/THF, room temperature overnight, iii) NaN_3, DMF, 40 °C overnight iv) 3-dimethylamino-1-propyne, CuBr, PMDETA, 40 °C overnight.

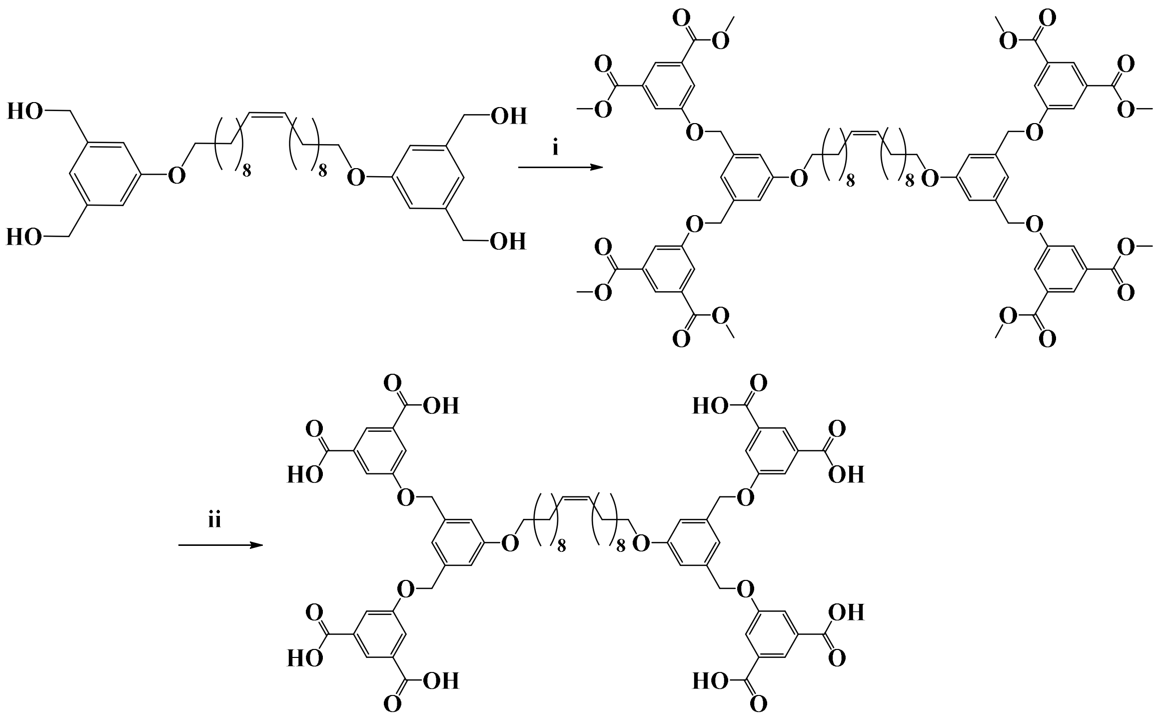

Scheme 4.10 Overview of tetra-acid-CTA (TA-CTA) synthesis
i) dimethyl 5-hydroxyisophthalate, PPh_3, DIAD, room temperature overnight,
ii) NaOH, THF/MeOH/Water, room temperature, overnight.

Using the TriA-CTA, we were able to synthesize TriA-PCODs. (Table 4.1)

Table 4.1 GPC molecular weight characterization of telechelic polycyclooctadiene

Polymer	Mw (kg/mol)	Mn (kg/mol)	PDI
NA mCTA	12.7	9.4	1.35
DA mCTA	14.1	9.5	1.49
DB mCTA	16.9	12.5	1.35
TriA mCTA	19.2	14.4	1.33
NA-PCOD 60k	64.3	43.3	1.48
DA-PCOD 60k	60.5	42.8	1.41
DB-PCOD 60k	54.8	39.1	1.40
TriA-PCOD 60k	58.6	40.6	1.44
NA-PCOD 300k	303.0	217.3	1.39
DA-PCOD 300k	313.1	244.3	1.28
DB-PCOD 300k	362.1	268.1	1.35
TriA-PCOD 300k	293.1	233.0	1.26
NA-PCOD 670k	670.5	433.0	1.55
DA-PCOD 670k	652.8	451.1	1.45
DB-PCOD 670k	657.3	457.0	1.44
TriA-PCOD 670k	641.0	454.3	1.41

Viscosity measurements

We chose 5 solvents for preparing polymer solutions. Three are fully saturated: decalin was bicyclic, dodecane was a C_{12} linear, and polyalphaolefin oil (PAO) was a ~C_{30} branched hydrocarbon. Two are unsaturated hydrocarbons: tetralin, a C_{10} bicyclic, and Jet-A-fuel, a C_8-C_{16} mixture of aliphatic and aromatic hydrocarbons and additives.

In a fully saturated solvent (decalin) at 25°C, the TriA end groups confer effects similar to pairwise complementary association (DA/DB), much stronger than the effect of DA end groups for all three PCOD lengths examined at 0.25 wt% (Figure 4.1). For the previously studied end groups (NA, DA, DB, DA/DB) on a similar set of three PCOD backbone lengths, the results accord with prior experiments and theory[1,2]. The DA groups are able to self-associate; however their geometry precludes pairwise association and favors six-fold association. The TriA end group affords greater conformational freedom than DA which might permit stronger association (three carboxylic acids), perhaps with a smaller aggregation number. However, we did not expect TriA self-association to be so similar to complementary (DA/DB) association.

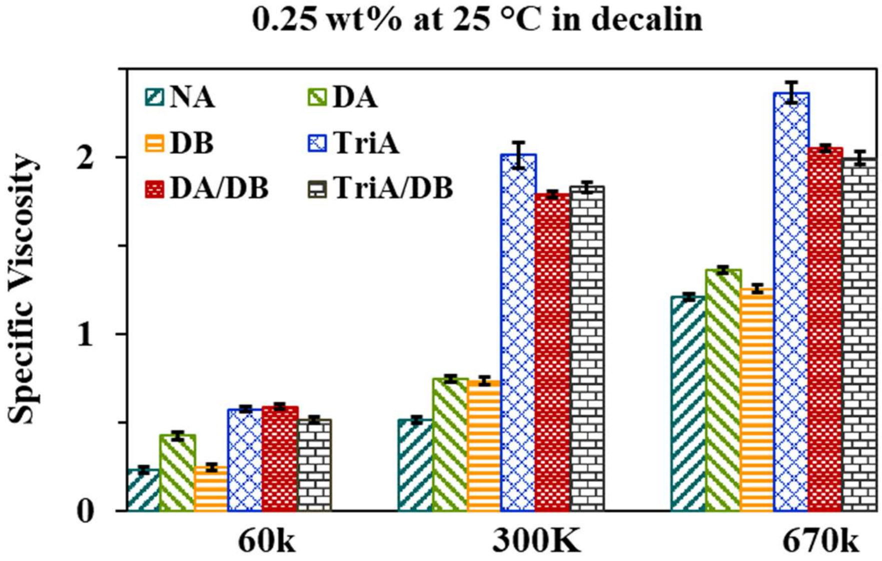

Figure 4.1 Effect of size of telechelics (k=kg/mol) on specific viscosity ($\eta_{specific}$) of supramolecular solutions and nonassociative (NA) controls in decalin at 0.25 wt%, at 25°C. For DA/DB and TriA/DB the ratio between two polymers was 1:1. The reported values were averaged over shear rates 10-250 s^{-1}. Overlap concentration (C^*) of 50k PCOD in decalin at 25°C is ~0.8 wt%. C^* of 670k PCOD in decalin at 25°C is ~0.25 wt%.

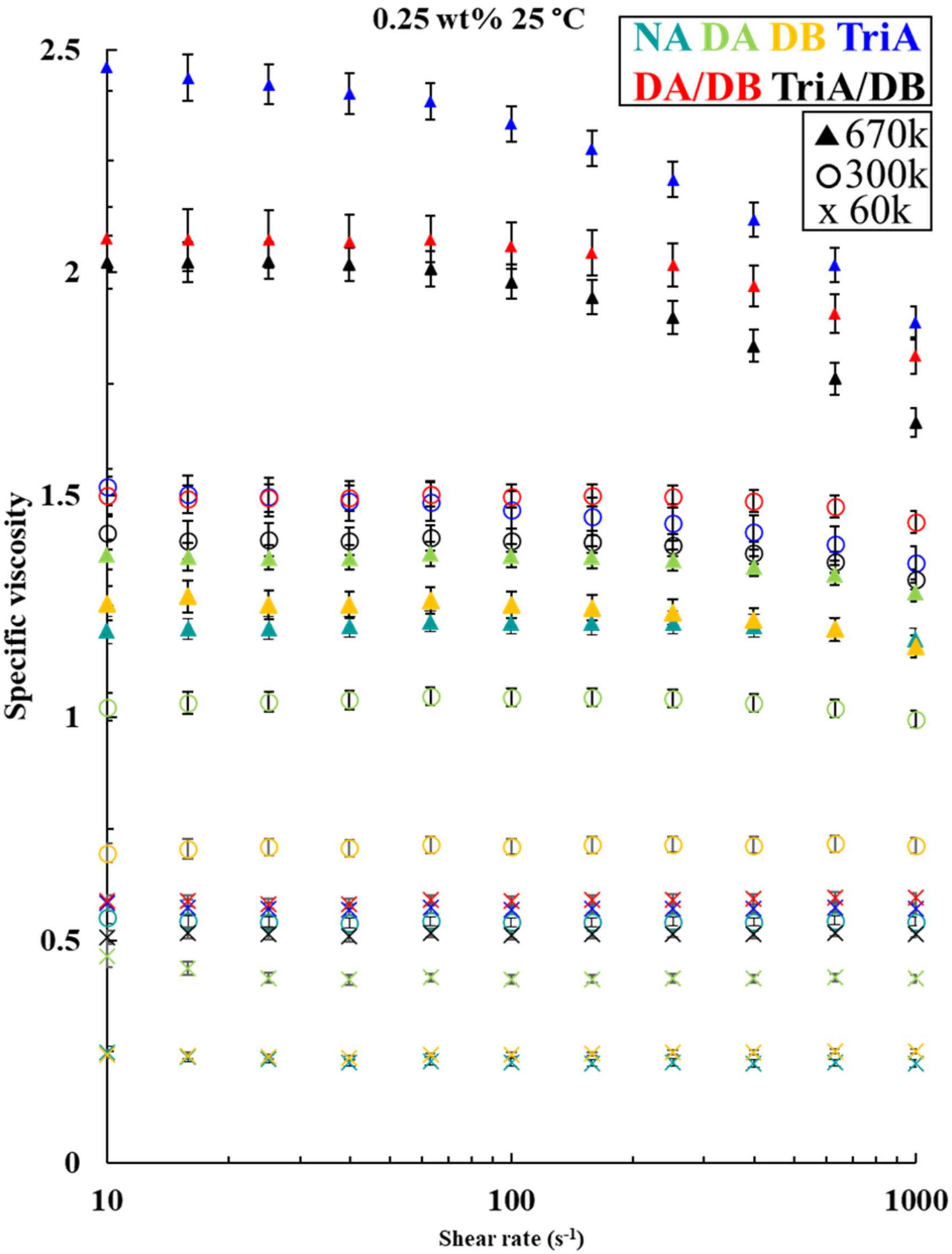

Figure 4.2 Specific viscosity ($\eta_{specific}$) of supramolecular solutions and nonassociative (NA) controls in decalin at 0.25 wt%, 25°C. For DA/DB and TriA/DB the ratio between two polymers was 1:1.

DA solutions had only slightly higher viscosities than those of non-associative polymers (NA and DB).

The self-association of the carboxylic-acid-ended polymers was examined previously in our group. The self-association can lead to loop formation of individual chains. Depending on the concentration of the polymers in the solution, the looped chains can also form flower-like micelles, and at high polymer concentration ($C > C^*$), the flower-like micelles could be linked by bridging chains, forming transient networks.[12–14] (Scheme 4.11)

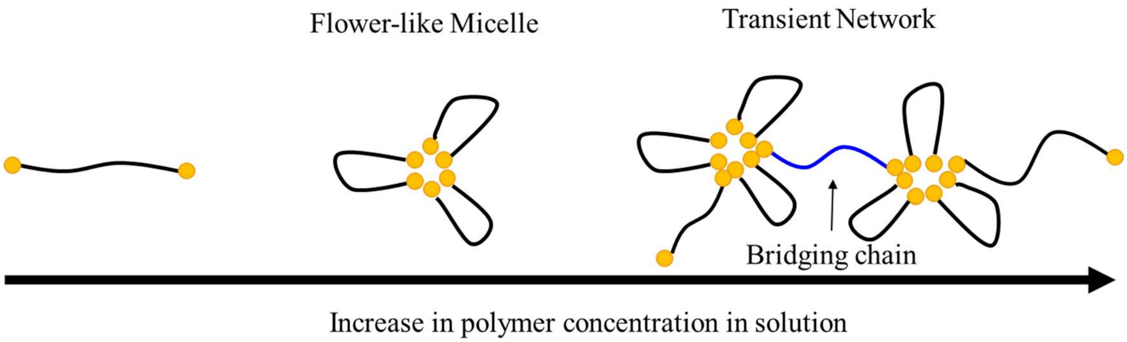

Scheme 4.11 Concentration-dependent self-association of end-associative polymers. The scheme was adapted from[1,12]

At low concentrations ($C < C^*$), flower-like micelles have a weak effect on viscosity[12,15,16], but as the concentration increases (must exceed C^*), more flower-like micelles could be interconnected by bridging chains, significantly increasing solution viscosity. For 60k PCOD solutions, 0.25 wt% would be far below the overlap concentration in decalin (C^* of 50k PCOD in decalin at 25 °C is ~ 0.8 wt%[17]), and therefore very few interconnected flower-like micelles would be present in the solution.

There are two advantages for increasing the backbone length of associative PCODs. The entropy cost of loop formation increases with increase in the chain length, leading to more formation of higher ordered supramolecular chains rather than formation of small cyclic species. The increase in chain length decreases the overlap concentration and increases the probability of bridging between flower-like micelles, that could lead to a further increase in the viscosity of the solution. Nevertheless, there is little viscosity increase associated with DA-PCOD – even for 670k.

Viscosity of TriA vs. TriA/DB

While the TriA solution had a higher viscosity than that of the DA/DB solution, the viscosity of the TriA/DB solution was close to that of the DA/DB solution, suggesting that the DA/DB and TriA/DB pairs might form supramolecular aggregates in a similar manner. The charge-assisted hydrogen bonds between tertiary amine and carboxylic acid have a higher association constant ($\Delta G \sim 20 \pm 3$ kg/mol)[18–20] than the resonance-assisted hydrogen bonds (RAHB) between carboxylic acids ($\Delta G \sim 8 \pm 1$ kg/mol)[21–24] (Scheme 4.12). In our group's previous work on DA/DB, the ^{1}H-NMR studies showed that mixing DA and DB results in complete consumption of available tertiary amines and the elimination of acid-acid hydrogen bonds.[3] The viscosity of TriA/DB suggests that TriA/DB association utilizing 2 of the 3 carboxylic acid groups is preferred over TriA/TriA self-association.

Resonance assisted hydrogen bond (RAHB)

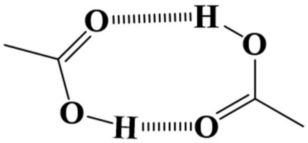

Charge assisted hydrogen bonds (CAHB)

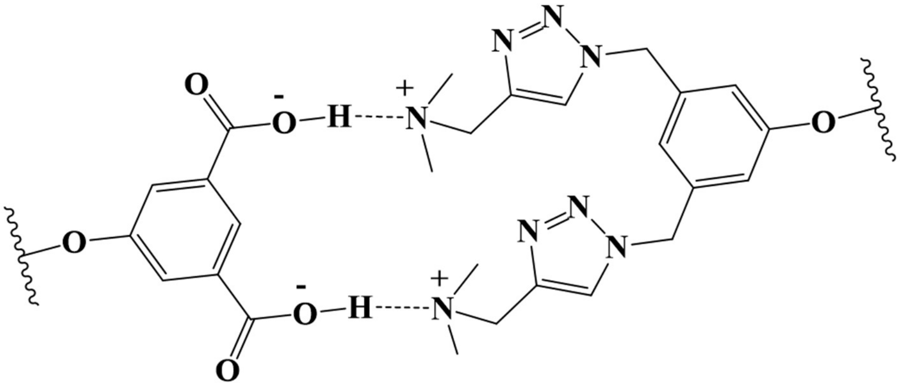

Scheme 4.12 Resonance assisted hydrogen bond (RAHB) between two carboxylic acids and charge assisted hydrogen bond between carboxylic acid and tertiary amine (DA/DB)

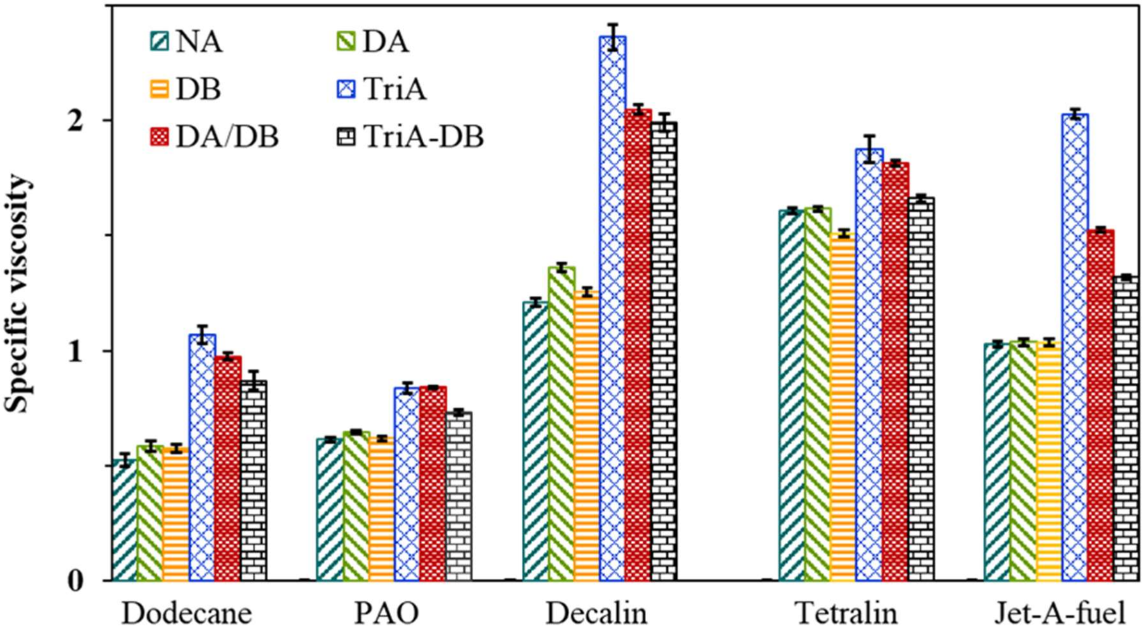

Figure 4.3 Effect of solvent on specific viscosity ($\eta_{specific}$) for 0.25 wt% solutions at 25°C of telechelics with $M_w \sim 670$ kg/mol. The reported values were averaged over 10-300 s^{-1}.

A similar trend was observed for viscosities in other solvents we used for the viscosity measurements (Figure 4.3). TriA 670k had the highest specific viscosity ($\eta_{specific}$) in all solvents used, followed by the viscosity of DA/DB and TriA/DB. Both decalin and tetralin are known as good solvents for the PCOD backbone. The specific viscosity ($\eta_{specific}$) of NA was higher in tetralin than in decalin, suggesting that the PCOD chains adopt a more extended conformation in tetralin. The greater solvent quality acts on end associative PCODs to; nevertheless, the associative polymers had lower viscosities in tetralin than in decalin. Wei and coworkers mentioned that increasing solvent polarity decreases the degree of end-association between the polymers.[3] Tetralin is a more polar solvent (dielectric constant of 2.77 at 25 °C) than decalin (dielectric constant of 2.23 at 25 °C), so the lower specific viscosity ($\eta_{specific}$) of associated polymer solutions in tetralin than in decalin was expected based on weaker hydrogen bonds.

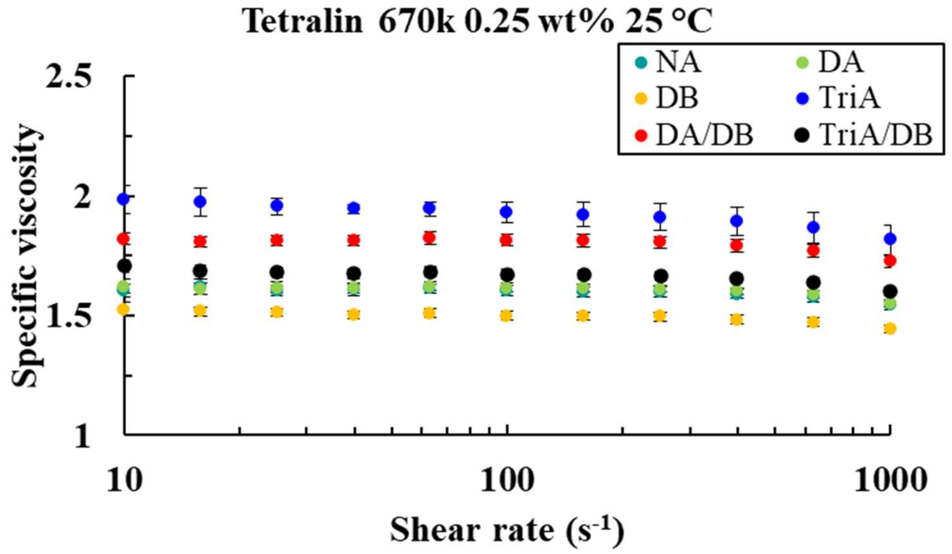

Figure 4.4 Specific viscosity ($\eta_{specific}$) of supramolecular solutions and non-associative (NA) controls in tetralin at 0.25 wt%, 25°C.

Specific viscosities of telechelic polymer solutions in jet-A-fuel

Comparing the viscosities of telechelic polymer solutions in decalin and in jet-A-fuel, the specific viscosity ($\eta_{specific}$) in jet-A-fuel was generally lower than that in tetralin or decalin with the exception of TriA (Figure 4.4).

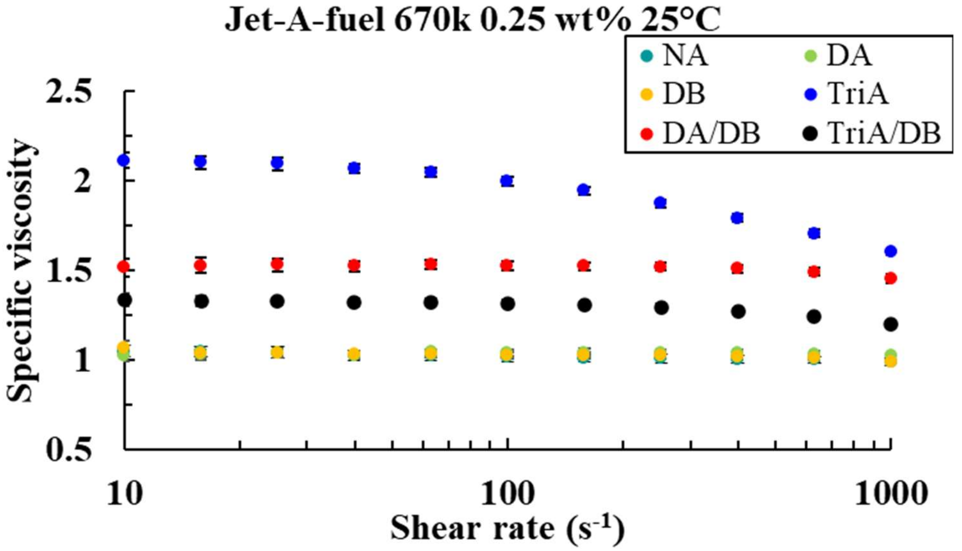

Figure 4.5 Specific viscosity ($\eta_{specific}$) of supramolecular solutions and non-associative (NA) controls in jet-A-fuel at 0.25 wt%, 25°C.

The observation that $\eta_{specific}$ of TriA-PCOD is higher in jet-A-fuel than in tetralin was surprising because jet-A-fuel contains additives that can potentially interfere with the hydrogen bonds between the telechelics (Scheme 4.14) and the $\eta_{specific}$ of DA/DB was lower in jet-A-fuel than in tetralin. Even a low concentration of a potential interferant (~6 μM) could potentially "cap" all of the chain ends in a 0.25 wt% solution of 670k PCOD.

The high $\eta_{specific}$ of TriA-PCOD in jet-A-fuel suggests that TriA-PCOD could be effective as a mist-control agent in jet-A-fuel. In our group's previous work, TA-PCOD with M_w 430k at 0.3 wt% concentration was effective at preventing mist-fire in jet-A-fuel. The measured $\eta_{specific}$ of 430k TA-PCOD at roughly 0.3 wt% (~ 2.4 mg/mL) was roughly 1 over

10-1000 s^{-1}. An interesting future experiment could compare the efficacy of TriA-PCOD as a mist-control agent.

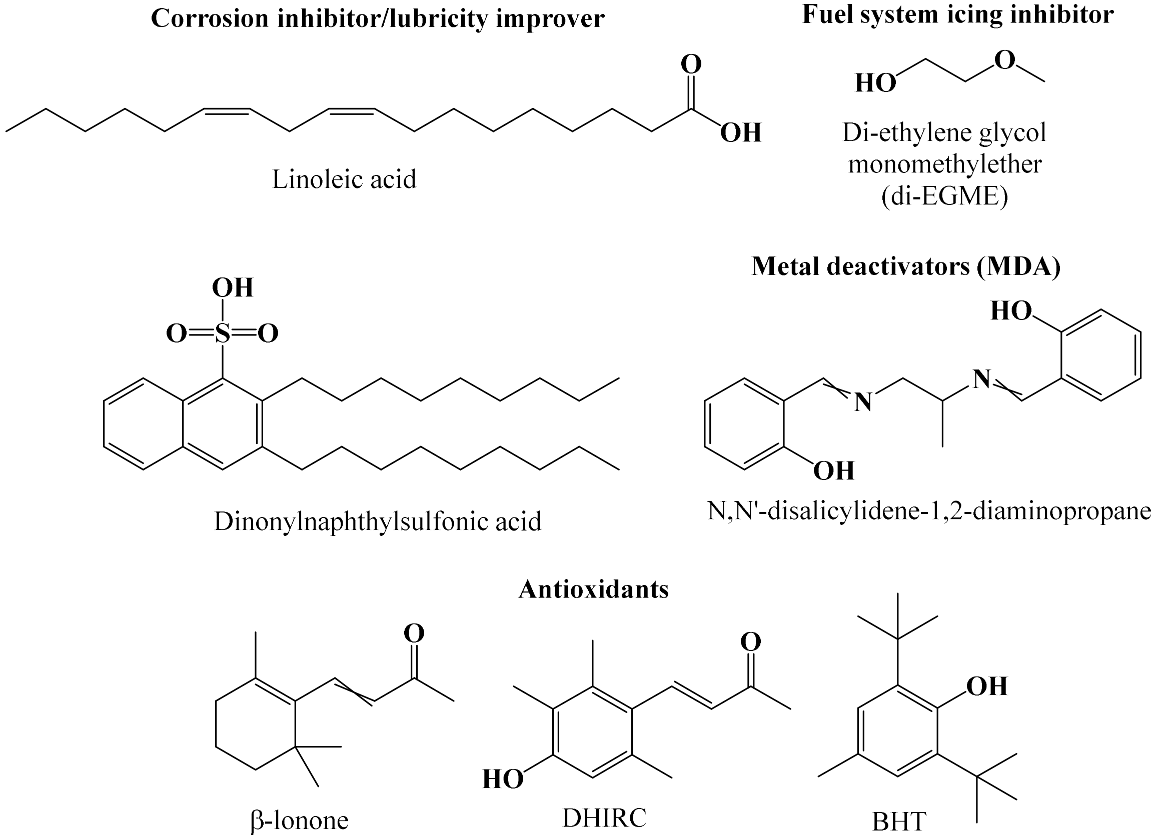

Scheme 4.13 Common additives found in jet-A-fuel.[25] DHIRC = dihydroxy isorenieratene cleavage product, BHT = butylated hydroxytoluene.

Specific viscosities of telechelic polymer solutions in dodecane and PAO

In dodecane and PAO, the specific viscosities of the telechelic polymers were generally lower than in decalin (Figure 4.3). Both dodecane and PAO are fully saturated non-polar solvents with dielectric constants close to 2 at 20 °C. The $\eta_{specific}$ of NA PCOD 670k was around 0.5, suggesting that the PCOD backbone adopts a more compact conformation in these solvents than in more polar solvents like decalin, and the tested concentration of 0.25 wt% would be far below the critical overlap concentration. At a concentration far below c*, we hypothesized that the viscosity of DA/DB (directional, complementary end-association) would be higher than that of TriA (self-association) since many of the TriA chains would be forming loops. However, even in dodecane and PAO, TriA-PCOD solutions had higher (or similar) $\eta_{specific}$ compared to DA/DB.

In PAO, DA and DB PCODs were insoluble even at room temperature, and obtaining homogenized solutions required the use of co-solutes (Chapter 3). However, TriA-PCOD dissolved in PAO without the need for co-solutes and stayed soluble at room temperature. To see if the TriA-PCOD solution would stay clear at lower temperatures, TriA-PCOD solution in PAO was stored in the refrigerator (4 °C), and the solution turned cloudy. It would be interesting to study if a more soluble backbone such as PIB or polyisoprene with carboxylic acid end groups would be soluble in PAO if telechelic polymers could be synthesized. Nevertheless, for mist-control in PAO, using TriA-PCOD is better than using DA/DB PCOD since it can be solubilized without the addition of co-solutes and TriA-PCOD can be prepared more easily in comparison to DA/DB.

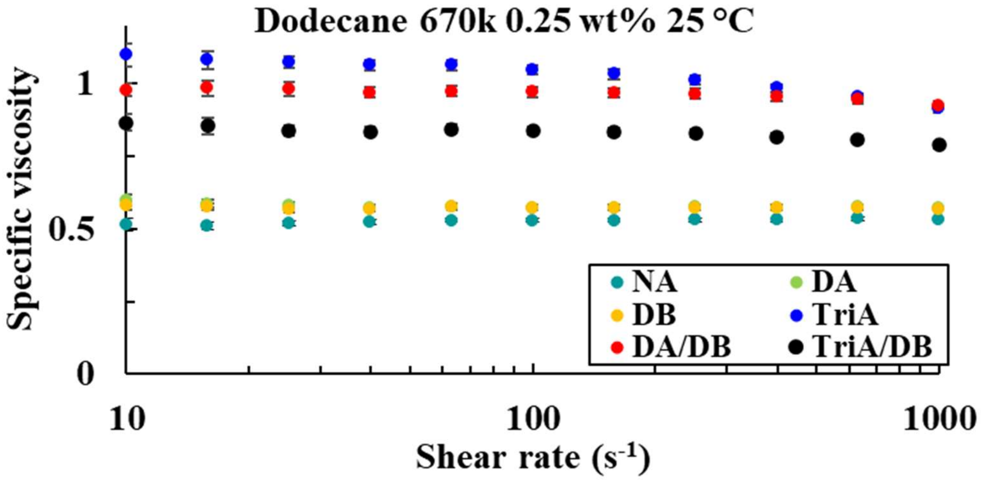

Figure 4.6 Specific viscosity ($\eta_{specific}$) of telechelic polymer solutions in dodecane (0.25 wt%) at 25°C, M_w ~ 670 kg/mol.

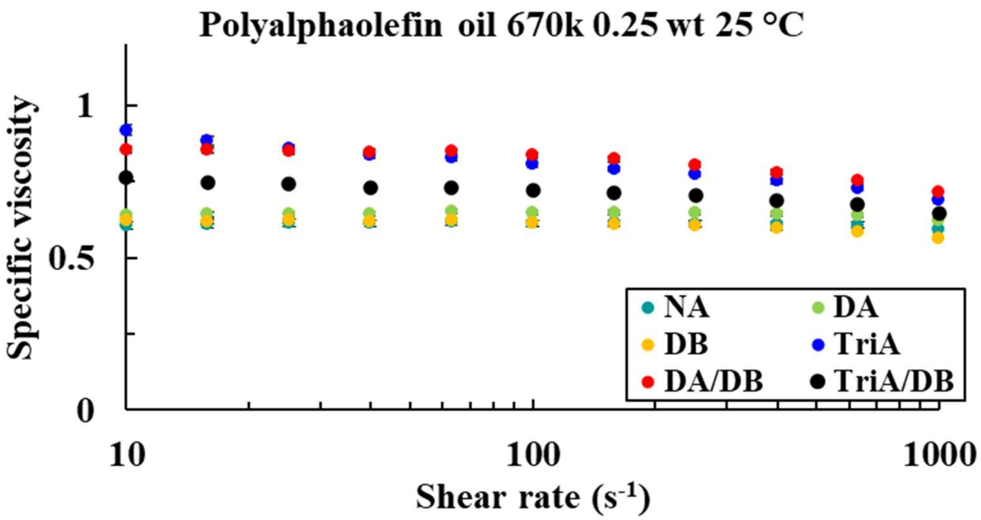

Figure 4.7 Specific viscosity ($\eta_{specific}$) of telechelic polymer solutions in polyalphaolefin (0.25 wt%) at 25°C, M_w ~ 670 kg/mol.

4.4 Conclusion

Seeking hydrogen-bond associative end groups that are free of aromatic moieties and excess heteroatoms, we discovered that PCOD with 1,1,2-tricarboxylic acid end groups – a self-associating system – is at least as effective as the complementary end-associative DA/DB system in the variety of hydrocarbon liquids tested, including jet fuel and a polyalphaolefin. This surprised us, as supramolecular assembly into long, unbranched supramolecules usually requires pairwise end-to-end association. 1) TriA is self-associative, so unimer rings can form while dimers would be the smallest ring possible in a complementary pairwise associative system. 2) TriA could join a cluster of hydrogen bonded chain ends that link with carboxylic acid end groups from multiple chains to optimize carboxylic acid-carboxylic acid pairings; binding multiple chain ends to a single aggregate reduces the number of unimers in long linear assemblies. 3) TriA has the possibility of association energy that is greater than the optimum according to the model of ring-chain equilibrium, which would cause supramolecules to close into rings that are more compact than and harder to stretch than a linear supramolecule of the same size. The surprising potency of these end groups presents interesting questions and opportunities.

4.5 Additional figures and information

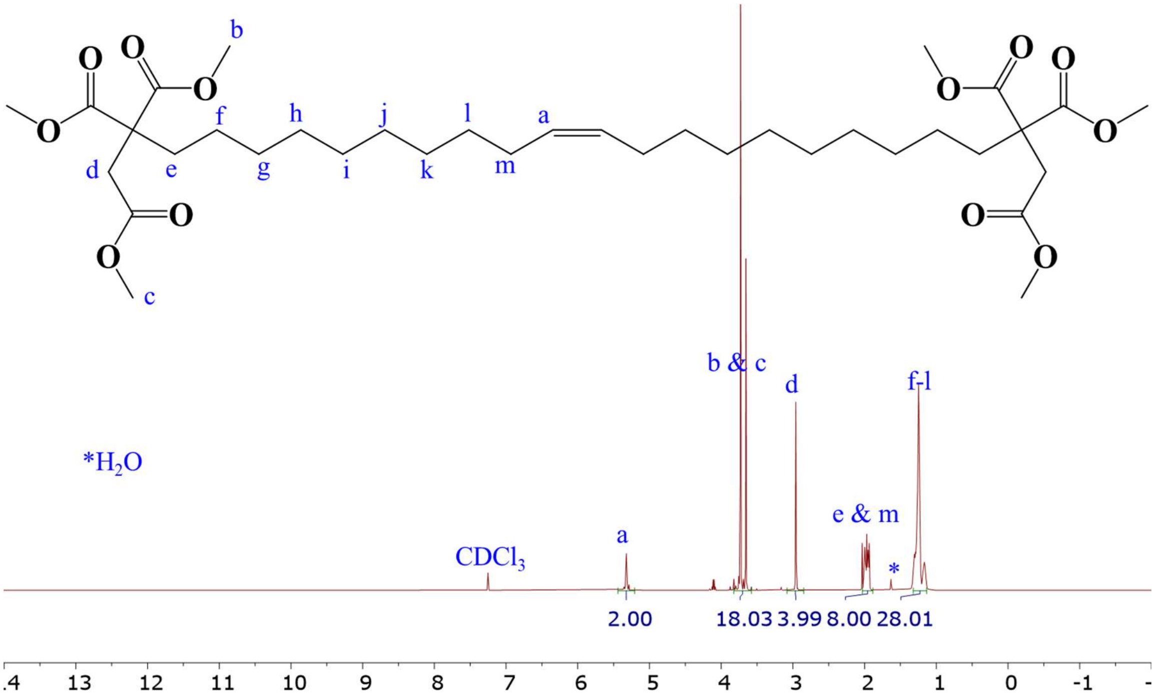

Figure 4.8 ^{1}H-NMR of hexamethyl ester CTA intermediate in $CDCl_3$.

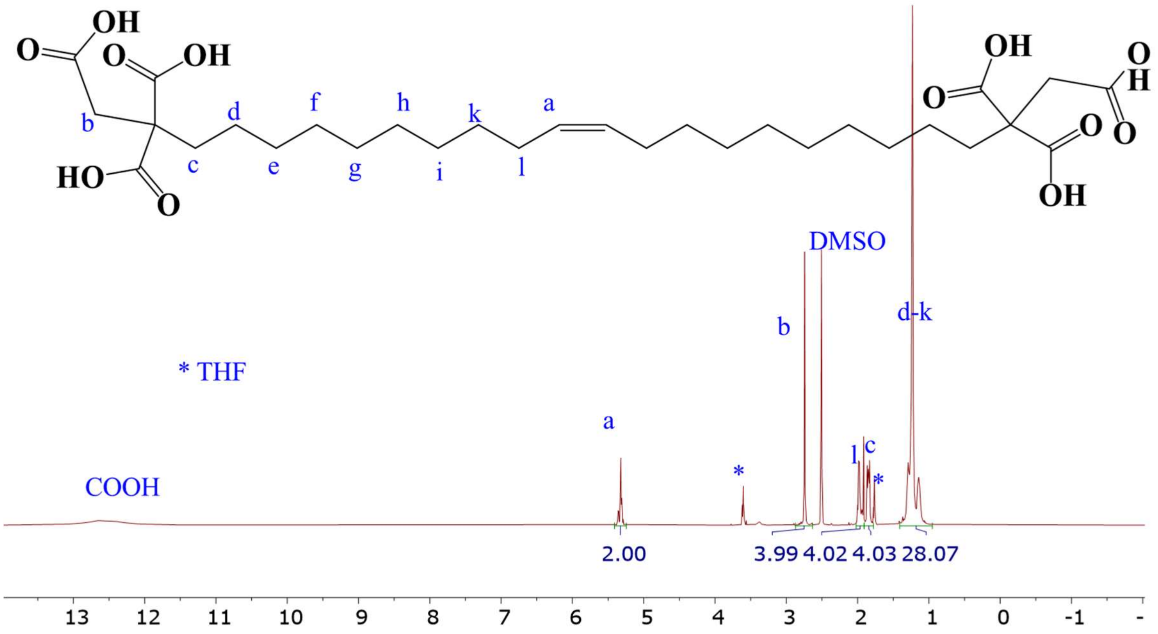

Figure 4.9 ^{1}H-NMR of tria-cid CTA (TriA-CTA) in d-DMSO.

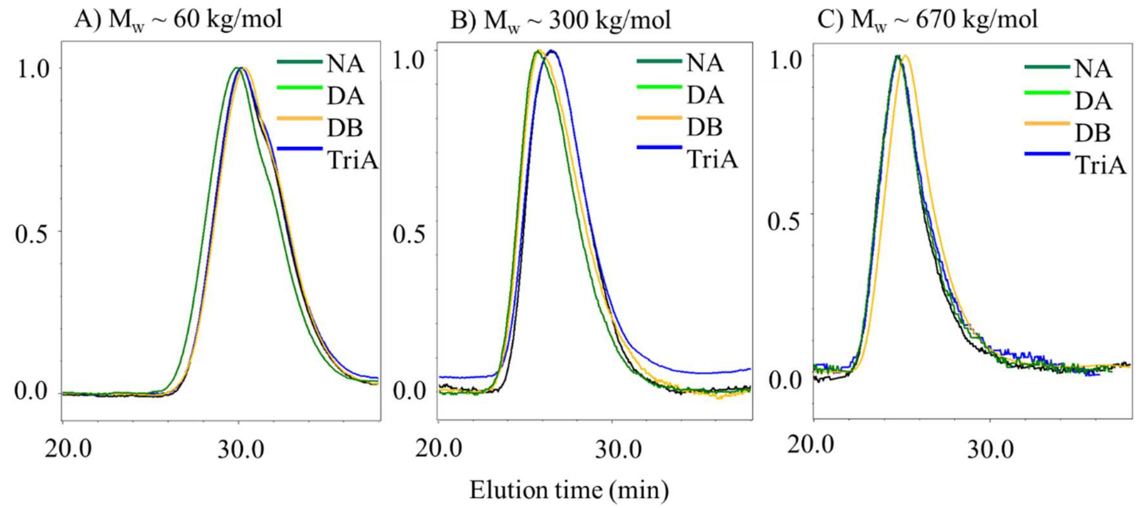

Figure 4.10 GPC chromatogram (RI detector) of the telechelic polymers shown in Table 4.1 A) M_w ~ 60 kg/mol, B) M_w ~ 300 kg/mol, C) M_w ~ 670 kg/mol. Note that end association is disrupted in THF eluent.

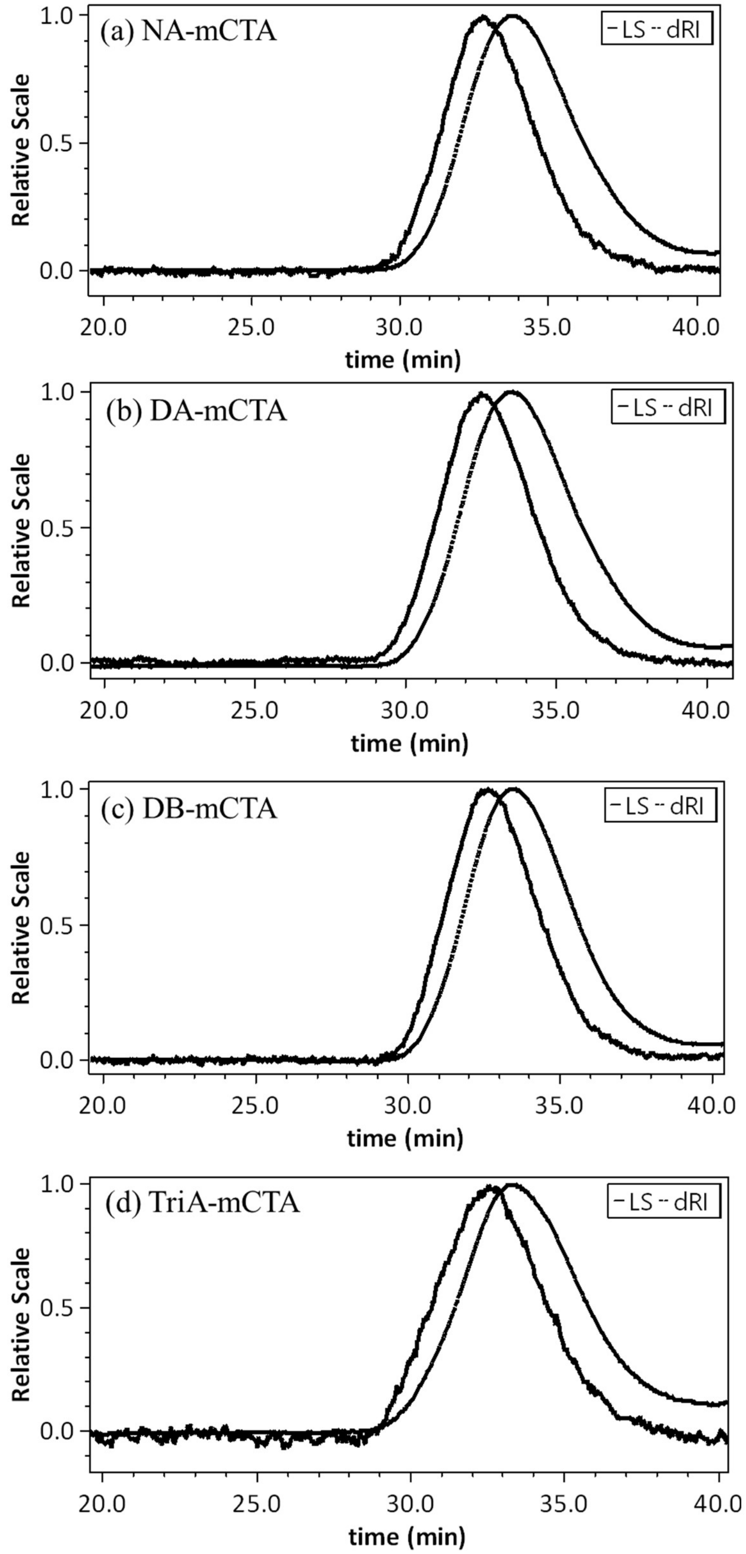

Figure 4.11 GPC chromatogram of telechelic polycyclooctadiene (a) NA-mCTA (b) DA-mCTA (c) DB-mCTA (d) TriA-mCTA.

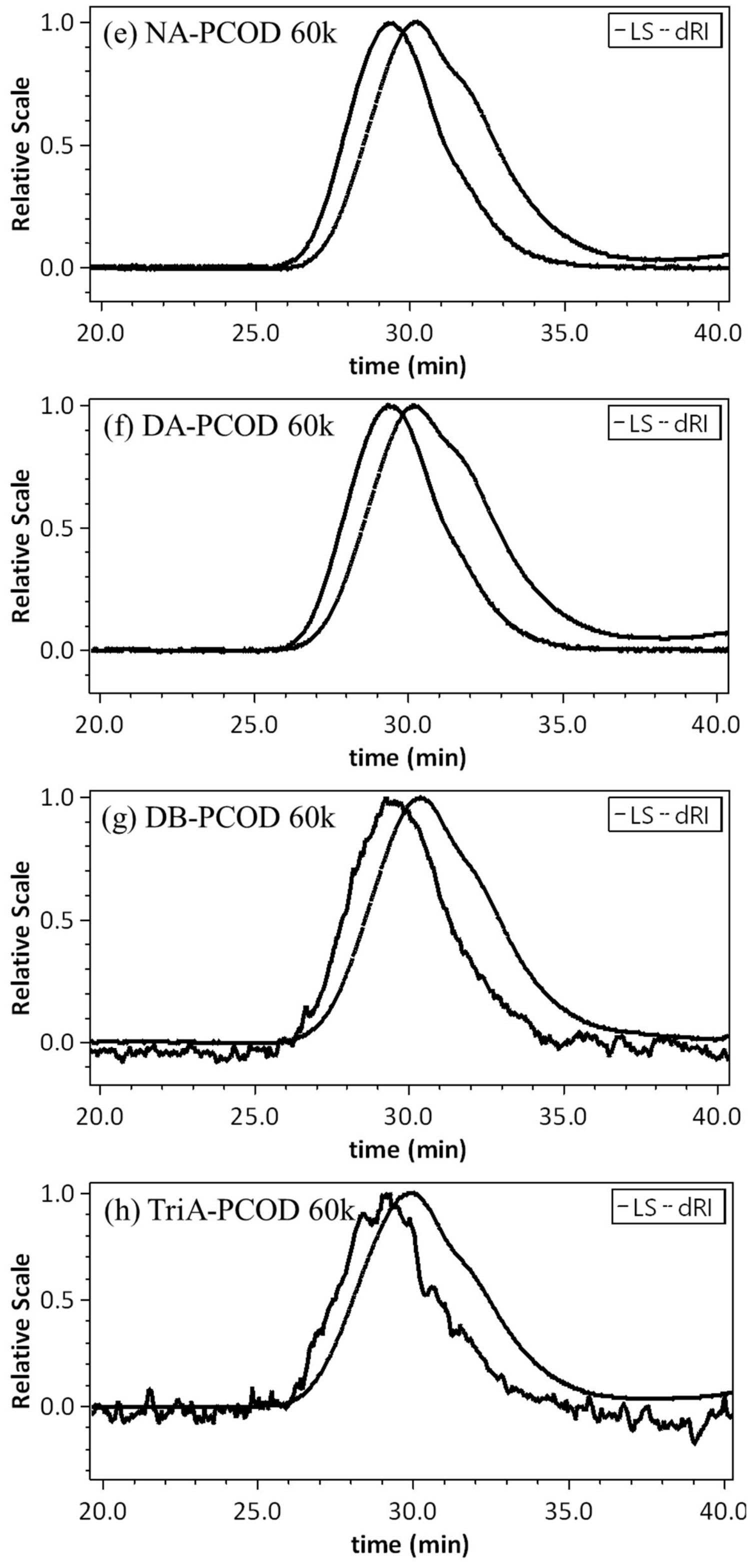

Figure 4.11 continued (e) NA-PCOD 60kg/mol (f) DA-PCOD 60kg/mol (g) DB-PCOD 60 kg/mol (h) TriA-PCOD 60 kg/mol.

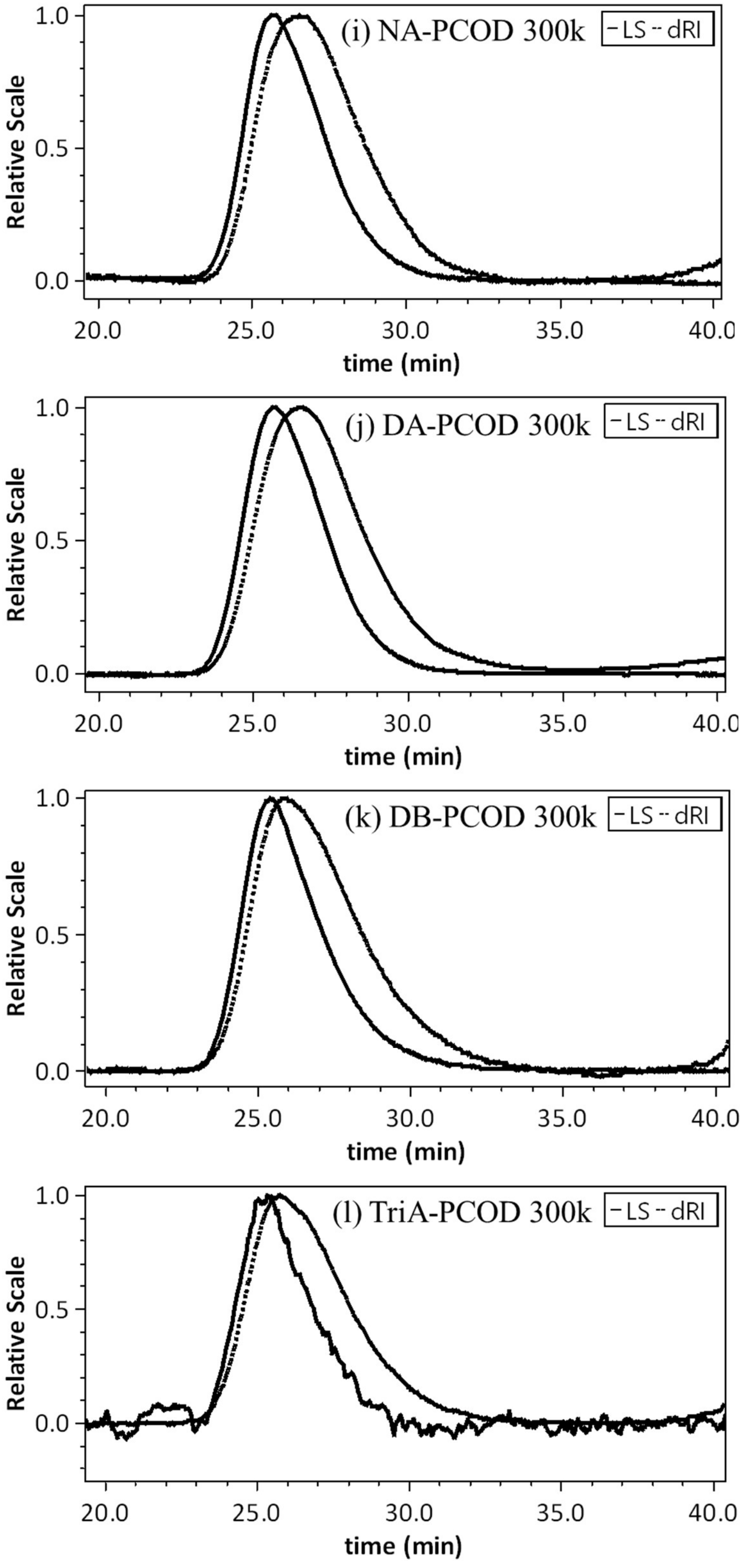

Figure 4.11 continued (i) NA-PCOD 300 kg/mol (j) DA-PCOD 300 kg/mol (k) DB-PCOD 300 kg/mol (l) TriA-PCOD 300 kg/mol.

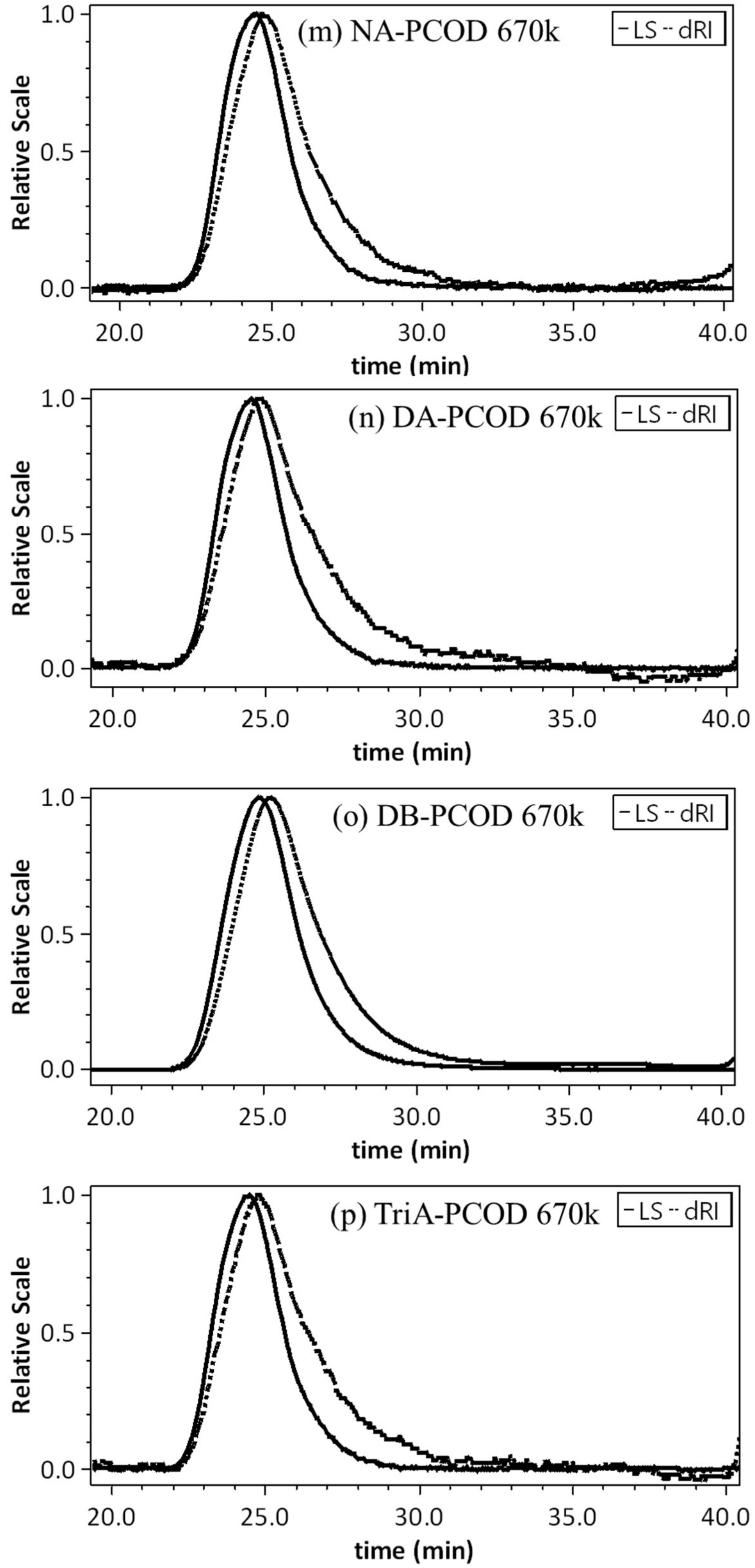

Figure 4.11 continued (m) NA-PCOD 670 kg/mol (n) DA-PCOD 670 kg/mol (o) DB-PCOD 670 kg/mol (p) TriA-PCOD 670 kg/mol.

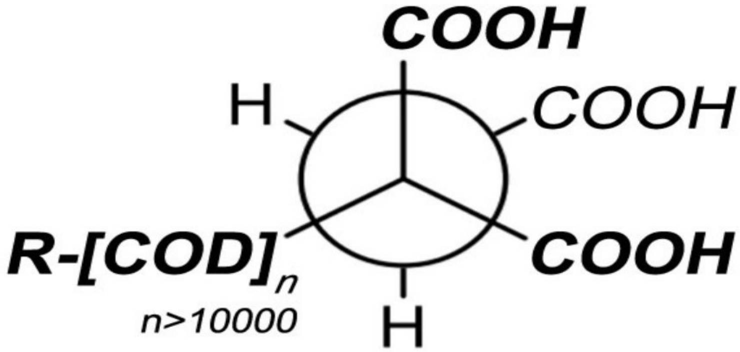

Figure 4.12 Possible conformation of TriA-PCODs

Comment for Figure 4.12

Based on our prior experience with DA self-association, we expected the carboxylic acids to find H-bond partners from different chain ends. The observed potency of the Tri-A self-associative system relative to the DA/DB complementary association system suggests that the Tri-A groups associate pairwise (association of multiple chain ends in multimeric aggregates results in loop formation, which reduces the viscosity relative to a fully pairwise system). To form pairwise associations, all three carboxylic acids would need to be oriented in a direction that is accessible to all three carboxylic acids on a binding partner. Examining the rotational isomeric states about the C1-C2 bond, we noticed that the polymer chain (the bulkiest group on C1) will preferentially be trans to the COOH on C2 (its bulkiest substituent). This places all three carboxylic acids on the same "face" of the end-group. The observed potency of the TriA system also suggests that the strength of association is in the optimal range (not exceeding it). The favored rotational state makes the three carboxylic acids accessible on one face; however, they are not optimally oriented to form full strength hydrogen bond pairs. This may explain an association energy in the range of 16-18kT instead of the maximum possible 22kT.

References

1. Wei, M.-H. Synthesis and Potency of Long End-Associative Polymers for Mist Control. (California Institute of Technology, 2014).
2. Leonard, R. & David, A. Associative Polymers as Antimisting Agents and Other Functional Materials via Thiol-Ene Coupling. (California Institute of Technology, 2008).
3. Wei, M.-H.; Li, B.; David, R. L. A.; Jones, S. C.; Sarohia, V.; Schmitigal, J. A.; Kornfield, J. A. Megasupramolecules for Safer, Cleaner Fuel by End Association of Long Telechelic Polymers. *Science (80-.).* **2015**, *350* (6256), 72–75.
4. Martinez, H., Ren, N., Matta, M. E. & Hillmyer, M. A. Ring-Opening Metathesis Polymerization of 8-Membered Cyclic Olefins. *Polym. Chem.* **5**, 3507–3532 (2014).
5. Brillon, D. New Synthesis of 1,1,1-Tricarboalkoxy Derivatives: Masked 1,1-Diesters. *Synth. Commun.* **16**, 291–298 (1986).
6. Melot, R. *et al.* Palladium(0)-Catalyzed Enantioselective Intramolecular Arylation of Enantiotopic Secondary C−H Bonds. *Angew. Chemie Int. Ed.* **60**, 7245–7250 (2021).
7. Chiu, A. A., Gorby, R. R., Hancock, J. E. H. & Hustedt, E. J. Malonic Ester Derivatives. 2. *J. Org. Chem.* **49**, 4313–4315 (1984).
8. Bian, X.-Y. *et al.* Synthesis of 2-[2H]-2-(1-methylalkyl)succinic Acids. *Chinese Chem. Lett.* **26**, 619–622 (2015).
9. Bian, X.-Y. *et al.* Synthesis of Anaerobic Degradation Biomarkers Alkyl-, Aryl- and Cycloalkylsuccinic Acids and Their Mass Spectral Characteristics. *Eur. J. Mass Spectrom.* **20**, 287–297 (2014).
10. Janza, B. & Studer, A. Isonitrile Trapping Reactions under Thermolysis of Alkoxyamines for the Synthesis of Quinolines. *Org. Lett.* **8**, 1875–1878 (2006).
11. Rajput, B. S. *et al.* Renewing polyethylene: Insertion Copolymerization of Sugar Derived Hydrophilic Monomers with Ethylene. *Eur. Polym. J.* **134**, 109775 (2020).
12. Lo Verso, F. & Likos, C. N. End-Functionalized Polymers: Versatile Building Blocks for Soft Materials. *Polymer (Guildf).* **49**, 1425–1434 (2008).
13. Cass, M. J., Heyes, D. M., Blanchard, R.-L. & English, R. J. Simulations and Experiments of Self-Associating Telechelic Polymer Solutions. *J. Phys. Condens. Matter* **20**, 335103 (2008).
14. Annable, T., Buscall, R., Ettelaie, R. & Whittlestone, D. The rheology of solutions of associating polymers: Comparison of experimental behavior with transient network theory. *J. Rheol. (N. Y. N. Y).* **37**, 695–726 (1993).
15. Sprakel, J. *et al.* Shear Banding and Rheochaos in Associative Polymer Networks. *Soft Matter* **4**, 1696 (2008).
16. Michel, E., Appell, J., Molino, F., Kieffer, J. & Porte, G. Unstable Flow and Nonmonotonic Flow Curves of Transient Networks. *J. Rheol. (N. Y. N. Y).* **45**, 1465–1477 (2001).
17. Li, B. Ring / Chain versus Network : Architecture Induced by Self- versus Pairwise-Association of Telechelic Polymers. (California Institute of Technology, 2016).
18. Gur'yanova, E. N., Gol'dshtein, I. P. & Perepelkova, T. I. The Polarity and Strength of the Intermolecular Hydrogen Bond. *Russ. Chem. Rev.* **45**, 792–806 (1976).
19. Davis, M. M. & Paabo, M. Acid-Base Equilibria in Benzene at Three Temperatures.

The Comparative Reactivities of a Phenolic Acid and a Carboxylic Acid with Triethylamine and with 1,3-Diphenylguanidine 1. *J. Am. Chem. Soc.* **82**, 5081–5084 (1960).

20. Nakanishi, H., Morita, H. & Nagakura, S. Charge-Transfer Bands Observed with the Intermolecular Hydrogen-Bonded Systems between Acetic Acid and Some Aliphatic Amines. *J. Mol. Spectrosc.* **65**, 295–305 (1977).
21. Johnson, E. W. & Nash, L. K. The Vapor-Phase Association of Acetic and Trimethylacetic Acids. *J. Am. Chem. Soc.* **72**, 547–556 (1950).
22. Allen, G., Watkinson, J. G. & Webb, K. H. An Infra-Red Study of the Association of Benzoic Acid in the Vapour Phase, and in Dilute Solution in Non-Polar Solvents. *Spectrochim. Acta* **22**, 807–814 (1966).
23. Clague, A. D. H. & Bernstein, H. J. The Heat of Dimerization of Some Carboxylic Acids in the Vapour Phase Determined by a Spectroscopic Method. *Spectrochim. Acta Part A Mol. Spectrosc.* **25**, 593–596 (1969).
24. Gilli, P. G. *The Nature of the Hydrogen Bond: Outline of a comprehensive hydrogen bond theory*. (Oxford Univ. Press, 2009).
25. Woortman, D. V. *et al.* Greener Aromatic Antioxidants for Aviation and Beyond. *Sustain. Energy Fuels* **4**, 2153–2163 (2020).

Chapter 5

New methods for the synthesis and characterization of PolyDODT, a highly cyclic polydisulfide

5.1 Introduction

Polydisulfide(s)

Polydisulfides(s) are polymers with disulfide repeats along the polymer backbone.[1] The disulfide bond can be cleaved and reformed in response to physical or chemical stimulation (redox pulses, thiols, mechanical force, nucleophiles, radicals, heat or light), which accounts for properties of polydisulfides such as adaptability and self-repair.[2] Polydisulfides are used in a variety of applications such as preparation of self-healing materials,[3] gene-delivery,[4] drug-delivery[5–7], and catalysis[8]. A more comprehensive review of the synthesis methods and applications of polydisulfides can be found in recently published review articles.[2,5]

PolyDODT: A macrocyclic elastomer

Among many different types of polydisulfides, polyDODT is synthesized by oxidation of 2-[2-(2-sulfanylethoxy)ethoxy]ethanethiol (DODT, also known as 3,6-dioxa-1,8-octanedithiol) using a system comprised of air, 3% H_2O_2 and triethylamine (TEA) as a catalyst. The polymerization method is named reversible radical recombination polymerization (R3P) and was developed by Puskas and coworkers in 2012.[9–11] The R3P method offers a few advantages over other polymerization methods: polymerization is extremely fast, and high molecular weight polymers can be synthesized (up to M_w 600,000 g/mol) at scale (10-100g). The resulting polymer is a transparent elastomer and can be depolymerized completely back to monomers using reducing agents like dithiothreitol (DTT) in 33 hours. The polymerization method is also environmentally benign since the reaction occurs at room temperature in aqueous solutions with a mild oxidation system without any heavy metal catalysts (TEA could be recycled). Furthermore, the R3P method tends to produce cyclic polymers. The R3P method offers a convenient way to synthesize high molecular weight cyclic polymers at a 10-100g scale, allowing rheological studies of cyclic polymers.[12]

An existing challenge in the field, however, is that depending on the reaction conditions, polyDODT can be either cyclic or a mixture of cyclic and linear polymers. The presence of linear contaminants in cyclic polymers can affect the rheological properties of the polymer melts and solutions. The prior literature on putative rings is replete with inconclusive studies and conflicting results from different research groups due to variations in linear contaminants in putative rings.[13–17]

To resolve controversies in the rheological studies of cyclic polymers, Professor Gregory B. McKenna and his team studied the rheological behavior of highly pure cyclic polyDODT in collaboration with Professor Judit E. Puskas' team at The Ohio State University, who provided purified cyclic polyDODT. We participated in this collaboration by testing the stability of polyDODT under various conditions, developing a new method to detect linear polyDODT in the polymer mixture, and proposing an alternate route for the synthesis of polyDODT via a different mechanism.

Detecting (and removing) linear polymers from the mixture of cyclic and linear polymers is not an easy task. While liquid chromatography at critical condition (LCCC) was considered to be one of the best methods for this purpose,[13,15,19–22] recently published work showed that the LCCC method was not capable of measuring < 6 wt% of linear contents in the ring/linear mixture of polyDODT.[23] Even using an 800 MHz NMR, the detection limit was ~1.3 wt% for a sample with M_n 35,800 g/mol.[11]

5.2 Experimental

5.2.1 Materials and instrumentation

All chemical reagents were obtained from Sigma Aldrich at 98% purity or higher unless otherwise stated. 3,6-dioxa-1,8-octanedithiol (DODT) was purchased from Sigma Aldrich at 95% purity. All solvents were obtained from Sigma Aldrich, at ACS reagent grade or higher (> 99.5% purity) and used as received without further purification. For stability testing, poly(3,6-dioxa-1,8-octanedithiol) (polyDODT) was supplied by Prof. Judit Puskas' research group at The Ohio State University.

NMR spectroscopy

^{1}H-NMR spectra were obtained using a Varian Inova 500 spectrometer (500 MHz); all spectra were recorded in $CDCl_3$ and d-DMSO (purchased from Cambridge Isotope Laboratories). Chemical shifts were reported in parts per million (ppm) and were referenced to residual solvent resonances.

Gel permeation chromatography (GPC)

The molecular weights and dispersity indices of the polymers were determined on a GPC system with a Wyatt DAWN EOS multi-angle laser light scattering detector (λ=690nm), a Waters 410 differential refractometer (RI) (λ=930nm), and four Agilent PLgel columns (pore size 103, 104, 105, and 106 Å) connected in series. THF was used as the eluent at the flow rate of 0.9 mL/min with a temperature of 35 °C. The data were analyzed using Wyatt Astra (version 5.3.4) using the Zimm fitting formula with *dn/dc* = 0.132 for each polymer reported.

Synthesis of polyDODT using DMSO and trimethylsilyl chloride (TMSCl)

In a 100 mL round bottom flask with a magnetic stir bar, 2 mL of DODT (2.24 g, 12.28 mmol) was added. While stirring at 500 rpm, DMSO (5.76 g, 73.68 mmol) was added followed by trimethylsilyl chloride (1.23 - 7.37 mmol). After a few minutes of stirring (5-10 minutes), polymers were observed as white solids. The mixture was left to stir overnight. The next day, stirring was stopped, and the mixture was left to settle for 15 minutes. Polymers sank to the bottom of the flask, leaving a clear liquid on top. The clear liquid was decanted, and the polymer was dissolved in 10 mL of THF and precipitated in 200 mL of methanol. After precipitation, and drying under vacuum to remove residual methanol, the polymers had a faint cabbage-like smell that indicated residual dimethyl sulfide (Me_2S), the byproduct of the polymerization, which was still mixed with the polymer. To remove dimethyl sulfide and residual DMSO, the precipitated polymer was re-dissolved in 10 mL of THF, and precipitated in 200 mL of methanol again, and dried under vacuum.

Catalytic stability testing of polyDODT using TEA

PolyDODT was measured in a 40 mL glass vial with a plastic screw cap. THF was added to prepare approximately 35 mL of 1.25 wt% solution. The solutions were split into 7 glass scintillation vials (5 mL each) and appropriate amounts of DODT, TEA, or DODT+TEA were added to each vial (see Table 5.1). The number of polyDODT chains in the polymer system was estimated by dividing the total weight of the polymer in solution by M_n (obtained from GPC). The solutions were covered in aluminum foil, stored at 25°C, stirred at 120 rpm for 3 days, and submitted for GPC analysis after filtering through a syringe filter (pore size 0.45μm, PTFE).

Table 5.1 Amounts of DODT and TEA added to 5 mL 1.25 wt% PolyDODT solutions in THF

Entry	M_n of polyDODT (kg/mol)	polyDODT (nmol)	DODT (nmol)	TEA (nmol)
1	54.26	1059.14	-	-
2			10.59	-
3			-	21.18
4			10.59	21.18
5			1.06	-
6			-	2.12
7			1.06	2.12
8	187.5	29.63	-	-
9			0.30	-
10			-	0.60
11			0.30	0.60
12			0.03	
13			-	0.06
14			0.03	0.06
15	190.7	29.14	-	-
16			0.29	-
17			-	0.58
18			0.29	0.58
19			0.03	-
20			-	0.06
21			0.03	0.06

DODT and TEA were added from 1 μM stock solution in THF (Prepared by serial dilution).

5.3 Results and discussion

5.3.1 Catalytic stability testing using TEA

When the polyDODT samples were shipped between collaborating laboratories, we observed that some samples had changes in their molecular weights. To understand possible causes of the changes in molecular weights, we tested the stability of polyDODT in THF solution under various conditions such as the presence of oxygen, light exposure, and temperature. We observed that the storage temperature (4 °C vs. 20 °C vs. 60 °C) did not induce significant changes in the molecular weight (monitored by GPC) of the polyDODT. We also observed that the presence of oxygen (air vs. argon atmosphere) did not explain the significant changes in molecular weights. It is well known that disulfide bonds are most susceptible to cleavage when exposed to UV radiation.[18] As expected, irradiation using a UV lamp (UVP® 95-0017-09, 4W) degraded polyDODT (M_n = 99 kg/mol) to short oligomers (M_n = 3,200 g/mol) by placing the lamp approximately 2 cm away from the vials. However, UV light exposure did not explain the changes in the molecular weights of polyDODT during the shipping since the polymers were stored in a box and kept in the dark.

Looking for other explanations for molecular weight changes, we hypothesized that if small amounts of TEA base (the polymerization catalyst) remained in the sample after purification, the TEA would turn thiols into thiolate ions and lead to thiolate-disulfide exchange. If a sample were pure cyclic polymer, no -SH would be present. To test this hypothesis, we set up experiments using 1 wt% polyDODT solution in THF. We divided the solutions into 4 glass vials, added DODT (0.1 wt%), TEA, or TEA+DODT to each and monitoring the changes in molecular weights after 3 days using GPC (Table 5.2).

Table 5.2 Molecular weights of polyDODT 3 days(a) after addition of DODT, TEA, or DODT+TEA.

Time (day)	DODT(b)	TEA(c)	M_w (kg/mol)	M_n (kg/mol)	PDI
0	-	-	160	135.4	1.19
3	-	-	154	131.2	1.17
3	-	+	145.8	122	1.2
3	+	-	117.7	97.4	1.21
3	+	+	49.7	39.4	1.261
0	-	-	200	118	1.7
3	-	-	203	119	1.7
3	-	+	169	104	1.64
3	+	-	165	98	1.7
3	+	+	14.2	11.4	1.79

(a) All vials contain 5 ml of 1 wt% solution of polyDODT in THF

(b) Vials to which DODT was added (indicated by + in DODT column) contain 0.1 wt% DODT (24 μmol DODT, 48 μmol -SH)

(c) Vials to which TEA was added (indicated by + in TEA column) contain 48 μmol TEA

We observed that the addition of TEA or DODT caused a decrease in molecular weights while the addition of both TEA and DODT caused the most dramatic changes in the molecular weights (160 kg/mol to 49.7 kg/mol, and 200 kg/mol to 14.2 kg/mol). Based on these results, we concluded that the TEA should be carefully removed during the purification of the polyDODT to avoid changes in molecular weights due to thiolate-disulfide exchange. After observing the effect of thiolate-disulfide exchange on the molecular weights of polyDODT, we were curious about the possibility of using thiolate-disulfide exchange as a tool for monitoring the presence of linear polyDODT in a putative cyclic polyDODT by adding TEA, which had negligible effect in the absence of thiol. If reaction occurs, it would signal the presence of free thiol present at each end of a linear polyDODT.

To test whether we could design a method with an improved detection limit, (relative to the 6% threshold for LCCC or 1.3% for 800 MHz NMR) we set up a new stability test in which the amount of DODT to add was based on the molar concentration of polymer: one molecule of DODT was added per 100 polymer molecules or less (Table 5.1). We added TEA, DODT, or TEA+DODT to polyDODT solutions in THF such that (moles of DODT)/(moles of polyDODT) = 0.01 (e.g. entries 2 and 4 of Table 5.1) or 0.001 (e.g. entries 5 and 7 of Table 5.1), and corresponding TEA to make (moles of DODT)/(moles of TEA) = 2 (e.g. entries 3, 4, 6 and 7 of Table 5.1), to account for each DODT molecule having two -SH groups.

All three starting materials, M_n = 54.26, 187.5, and 190.7 kg/mol, showed obvious shifts of their GPC traces to later times (lower molecular weight) when both DODT and TEA were present in the "mock 1% linear impurity test" (green traces in Figures 5.1-3; entries 4, 11 and 18 of Table 5.1). The 54.26k polyDODT showed the same shift when only DODT was added (navy blue trace overlaps green in Figure 5.1), which may indicate significant TEA was present in that specific polymer, as DODT had a much weaker effect than DODT+TEA on the 187.5 and 190.7 kg/mol polyDODT. When only TEA was added (entries 3, 10, and 17 of Table 5.1), the GPC traces were very close to those of the "Original" and "3 Day" specimens. This suggests that the amount of linear contaminant is less than 1% in all three of these polyDODT. Future work could investigate the addition of DODT as a means to detect residual TEA.

When (moles of DODT)/(moles of polyDODT) = 0.001, the GPC traces for all three treatments (DODT, TEA, and DODT+TEA) are nearly indistinguishable from "Original" and "Day 3" (Figure 5.4-6). Thus, the present method cannot reliably detect the presence of linear contaminant at a level of 1 in 1000.

The obtained GPC results suggest that the three samples we tested were at least 99% pure cyclics. One additional advantage of this method is that it could be used for even high molecular weight samples (> 100 kg/mol), unlike other methods such as LCCC or NMR. The catalytic stability testing of polyDODT using TEA is also easy to set up, since it only requires adding reagents to polymer solutions and monitoring the changes in molecular weights using GPC. We believe this method can be used to lower the detection limit for linear polyDODT in the mixture. It seems that the detection limit would be somewhere between 0.1 and 1 mol%. Future studies with DODT and TEA added below 1 mol% and above 0.1 mol% of moles of polyDODT would be useful in establishing a new detection limit. Future work could also examine longer reaction times or using a constant TEA/polymer molar ratio (e.g., 1/50) to further improve the threshold for detection of linear impurities in polyDODT.

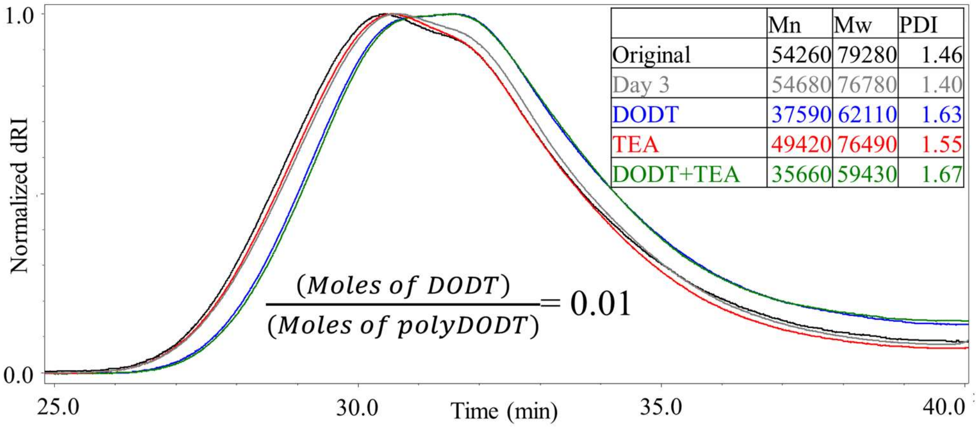

	Mn	Mw	PDI
Original	54260	79280	1.46
Day 3	54680	76780	1.40
DODT	37590	62110	1.63
TEA	49420	76490	1.55
DODT+TEA	35660	59430	1.67

$$\frac{(Moles\ of\ DODT)}{(Moles\ of\ polyDODT)} = 0.01$$

Figure 5.1 GPC chromatogram (refractive index detector signal) of polyDODT (M_n = 54,260 g/mol) samples 3 days after addition of DODT, TEA, or DODT+TEA. Samples correspond to entries 1, 2, 3, 4 in Table 5.1.

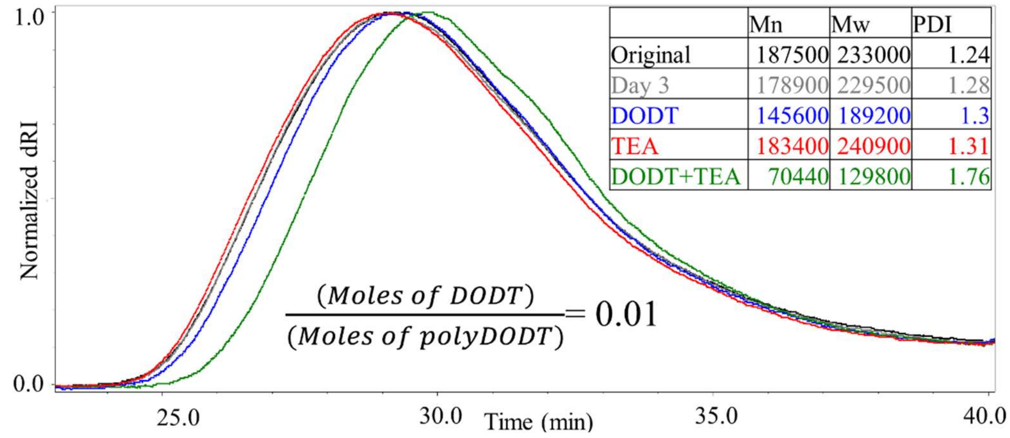

Figure 5.2 GPC chromatogram (refractive index detector signal) of polyDODT (M_n = 187,500 g/mol) samples 3 days after addition of DODT, TEA, or DODT+TEA. Samples correspond to entries 8, 9, 10, 11 in Table 5.1.

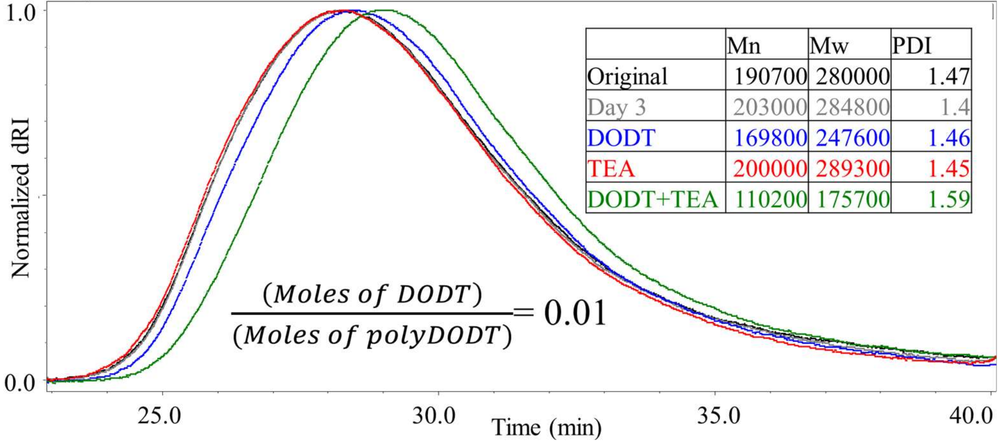

Figure 5.3 GPC chromatogram (refractive index detector signal) of polyDODT (M_n = 190,700 g/mol) samples 3 days after addition of DODT, TEA, or DODT+TEA. Samples correspond to entries 15, 16, 17, 18 in Table 5.1.

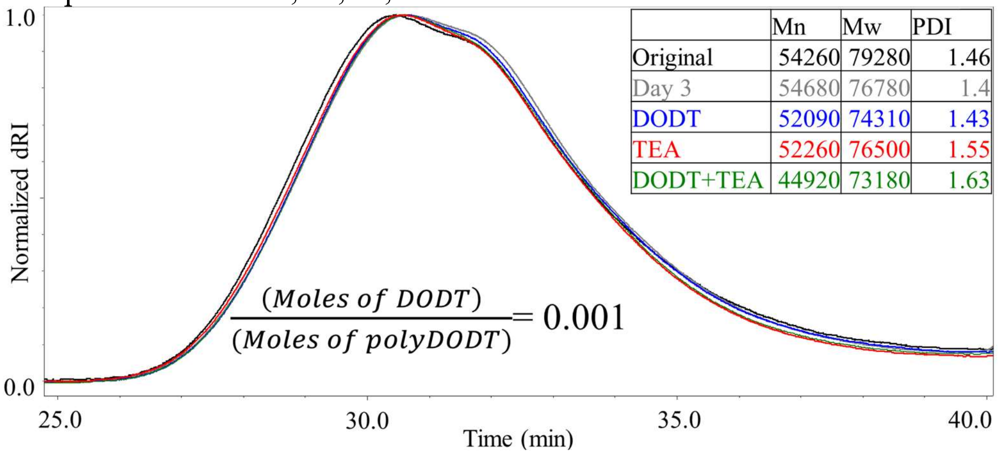

Figure 5.4 GPC chromatogram (refractive index detector signal) of polyDODT (M_n = 54,260 g/mol) samples 3 days after addition of DODT, TEA, or DODT+TEA. Samples correspond to entries 1, 5, 6, 7 in Table 5.1.

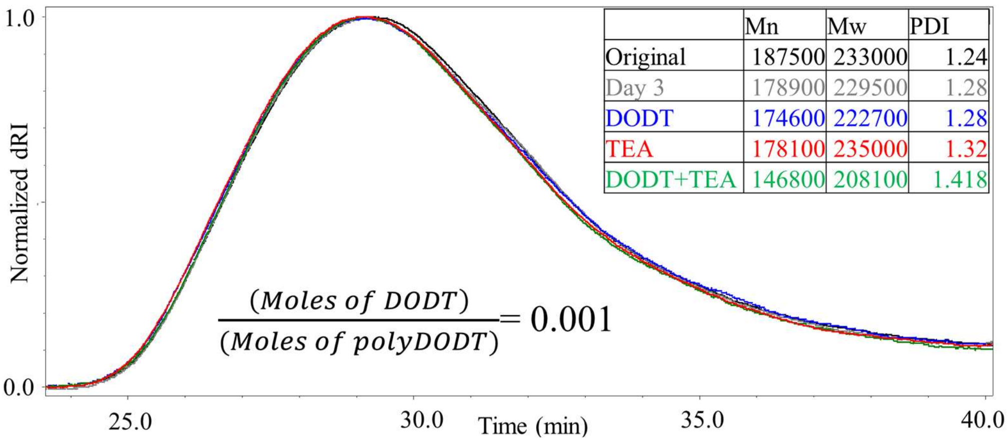

	Mn	Mw	PDI
Original	187500	233000	1.24
Day 3	178900	229500	1.28
DODT	174600	222700	1.28
TEA	178100	235000	1.32
DODT+TEA	146800	208100	1.418

$$\frac{(Moles\ of\ DODT)}{(Moles\ of\ polyDODT)} = 0.001$$

Figure 5.5 GPC chromatogram (refractive index detector signal) of polyDODT (M_n = 187,500 g/mol) samples 3 days after addition of DODT, TEA, or DODT+TEA. Samples correspond to entries 8, 12, 13, 14 in Table 5.1.

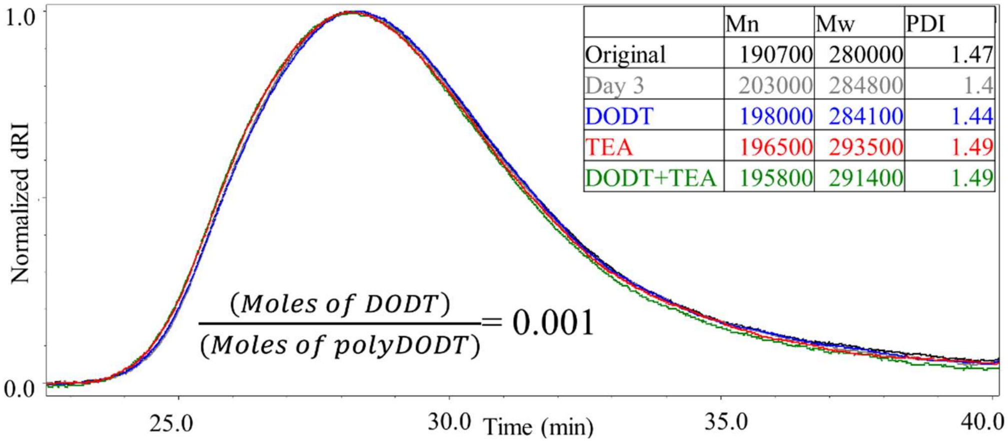

	Mn	Mw	PDI
Original	190700	280000	1.47
Day 3	203000	284800	1.4
DODT	198000	284100	1.44
TEA	196500	293500	1.49
DODT+TEA	195800	291400	1.49

$$\frac{(Moles\ of\ DODT)}{(Moles\ of\ polyDODT)} = 0.001$$

Figure 5.6 GPC chromatogram (refractive index detector signal) of polyDODT (M_n = 190,700 g/mol) samples 3 days after addition of DODT, TEA, or DODT+TEA. Samples correspond to entries 15, 19, 20, 21 in Table 5.1.

Possible effect of solvent on thiolate-disulfide exchange

We chose THF as our reaction medium for the catalytic stability testing because our GPC system uses THF as the eluent. Future work could examine a less polar solvent to increase the rate of thiolate-disulfide exchange, and hence increase the sensitivity of catalytic stability testing. The thiolate-disulfide exchange reaction proceeds via an S_N2 mechanism and involves a trisulfide transition state where the negative charge is delocalized[24–27] (Scheme 5.1). The delocalization of negative charge makes the transition state less influenced by solvation than the ground state thiolate anion. Therefore, in polar solvents, the stabilization of the ground state is greater than the effect on the transition state, so the activation energy would be higher and the reaction would be slower. Conversely, in non-polar solvents, the activation energy would be lower, and the reaction would be faster.[24–26]

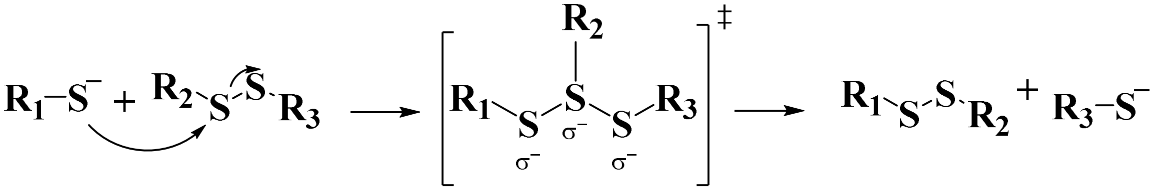

Scheme 5.1 Thiolate-disulfide exchange: a thiolate anion (R-S$^-$) attacks a disulfide bond, displacing one S atom and forms a new bond with the other S atom. The reaction proceeds via an S_N2 mechanism, involving a trisulfide transition state with a delocalized negative charge.

For example, Singh and Whitesides[24] reported that the rates of thiolate-disulfide interchange in DMSO and DMF were 1000 times higher than the rate in water or methanol. The authors explained that in a more polar solvent, the solvent molecule stabilizes the reactants preferentially over the transition state. Among many different solvents that could be used to dissolve polyDODT, toluene is one of the most non-polar solvents, and therefore using toluene rather than THF might increase the sensitivity of the catalytic stability testing for detecting the presence of free thiols in the polyDODT mixture.

5.3.2 Polymer synthesis with molecular weight control

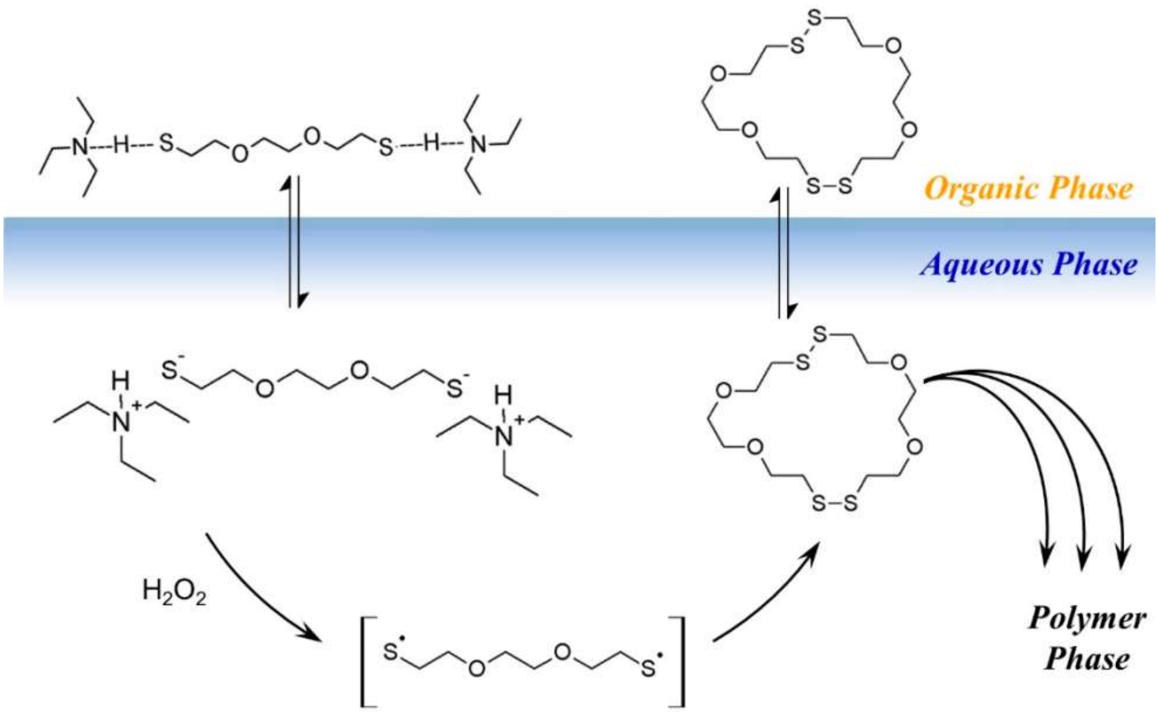

Figure 5.7 Proposed mechanism of reversible radical recombination polymerization (R3P). Figure from Rosenthal-Kim and Puskas[10] (open access)

The proposed mechanism for the synthesis of polyDODT using the R3P method is shown in Figure 5.7. In a typical polymerization reaction via the R3P method, DODT is mixed with the base TEA, and hydrogen peroxide is added slowly while air is optionally bubbled into the reaction flask depending on the target molecular weight of the reaction. The molecular weight of the resulting polymer could be controlled by changing the reaction time, temperature, rate of reagent addition (hydrogen peroxide 3-30% concentration in water, using a syringe pump), and air bubbling.

The synthesized polymers had M_w between ~2000 and 556,000 g/mol, with PDI between 1.15 and 2.74. Looking at the proposed polymerization mechanism, we identified that there are two factors that may affect the molecular weights. Despite resembling the structure of polyethylene oxide, which is a highly water-soluble polymer, polyDODT is not water-soluble, so the polymer precipitates out of the reaction medium upon the addition of aqueous hydrogen peroxide. Furthermore, in addition to the thiyl radicals shown in the proposed reaction mechanism (Figure 5.7), the thiolate anion can also directly react with existing disulfide bonds via thiolate-disulfide exchange (Scheme 5.1).

We hypothesized that perhaps the molecular weight of the polyDODT could be more easily controlled using a different polymerization method that does not involve a non-solvent and the formation of thiolate anions. After reviewing various methods of disulfide bond formation, we found an interesting method for disulfide bond formation: oxidative coupling of thiols. Zareyee and coworkers demonstrated oxidative coupling of thiols with DMSO in the presence of trimethylchlorosilane (TMSCl) or cyanuric chloride[28]. A variety of thiols were converted to disulfides in good to excellent yield at room temperature upon the addition of DMSO and TMSCl or cyanuric chloride. While the exact mechanism is not known, the authors proposed a possible mechanism as shown in Scheme 5.2.

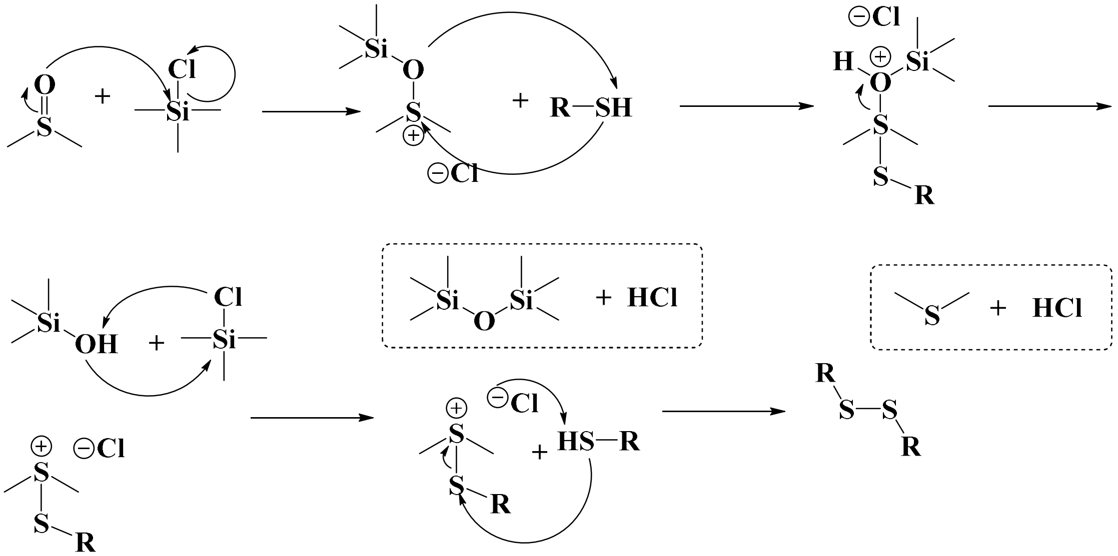

Scheme 5.2 Proposed mechanism for oxidative coupling of thiols with DMSO in presence of trimethylchlorosilane. Mechanism proposed by Zareyee and coworkers[28].

According to the proposed mechanism, DMSO first reacts with oxophilic reagent (TMSCl or cyanuric chloride) and activates the DMSO. The activated form of DMSO then reacts with thiol and releases hexamethyldisiloxane and HCl, while forming the intermediate product that reacts with a second thiol to form disulfide while releasing dimethylsulfide and HCl. The authors also investigated whether the atmospheric oxygen was responsible for the oxidation of thiols by repeating the reaction under a nitrogen atmosphere, and concluded that the thiol oxidation was not due to atmospheric oxygen. However, when the same reaction was conducted in the presence of two molar equivalents of pyridine (with respect to the moles of thiol), the reaction did not go to completion even after longer reaction times.

We tested whether thiol oxidation in the presence of DMSO and TMSCl could be adopted for the synthesis of polyDODT. PolyDODT is soluble in DMSO, so we would not have a solubility issue for the polyDODT upon the addition of DMSO. Furthermore, the reaction does not require any addition of base and generates HCl as a byproduct, so thiolate ion formation seemed unlikely.

While Zareyee and coworkers[28] carried out the thiol oxidation in DCM, we chose to carry out the reaction in DMSO since polyDODT is soluble in DMSO. We initially set up polymerization reactions using the same thiol:DMSO=1:3 ratio used by Zareyee and coworkers, while varying the TMSCl:thiol ratio to see if we could achieve molecular weight control (Table 5.3). As shown in Table 5.3, as the TMSCl/SH ratio increases, the molecular weight of the polyDODT also increases up to TMSCl/SH=0.25 and M_w seemed to reach a plateau around 160 kg/mol.

Table 5.3 Molecular weights of polyDODT synthesized via thiol oxidation with DMSO and TMSCl

TMSCl/SH	Thiols (mmol)	DMSO (mmol)	TMSCl (mmol)	Mn (g/mol)	Mw (g/mol)	PDI
0.05	24.56	73.68	1.228	1,524	2,070	1.36
0.075	24.56	73.68	1.842	1,878	2,320	1.20
0.1	24.56	73.68	2.456	4,198	5,512	1.31
0.125	24.56	73.68	3.07	4,073	5,117	1.26
0.15	24.56	73.68	3.684	6,892	8,945	1.30
0.175	24.56	73.68	4.298	30,120	38,900	1.29
0.2	24.56	73.68	4.912	35,820	58,800	1.64
0.225	24.56	73.68	5.526	68,160	119,000	1.75
0.25	24.56	73.68	6.14	92,460	167,400	1.81
0.275	24.56	73.68	6.754	107,800	154,300	1.43
0.3	24.56	73.68	7.368	110,500	167,800	1.52

In contrast to the R3P method, for which the low molecular weight polyDODT tended to be mostly cyclics when $M_w < 2000$ g/mol, the current method seemed to yield low molecular weight mixtures with predominantly linear chains. ^{1}H-NMR of the low molecular weight samples (TMSCl/SH = 0.05 or 0.075) showed a clear triplet at 1.58 ppm (-S**H**), and the methylene protons adjacent to the thiol 2.71 ppm (-C**H₂**SH). Thiol peaks were observed until TMSCl/SH ratio increased up to 0.15 and disappeared when TMSCl/SH ratio was higher than 0.175, suggesting the possibility of polymer chains being mostly cyclic when TMSCl/SH $\geq$ 0.175.

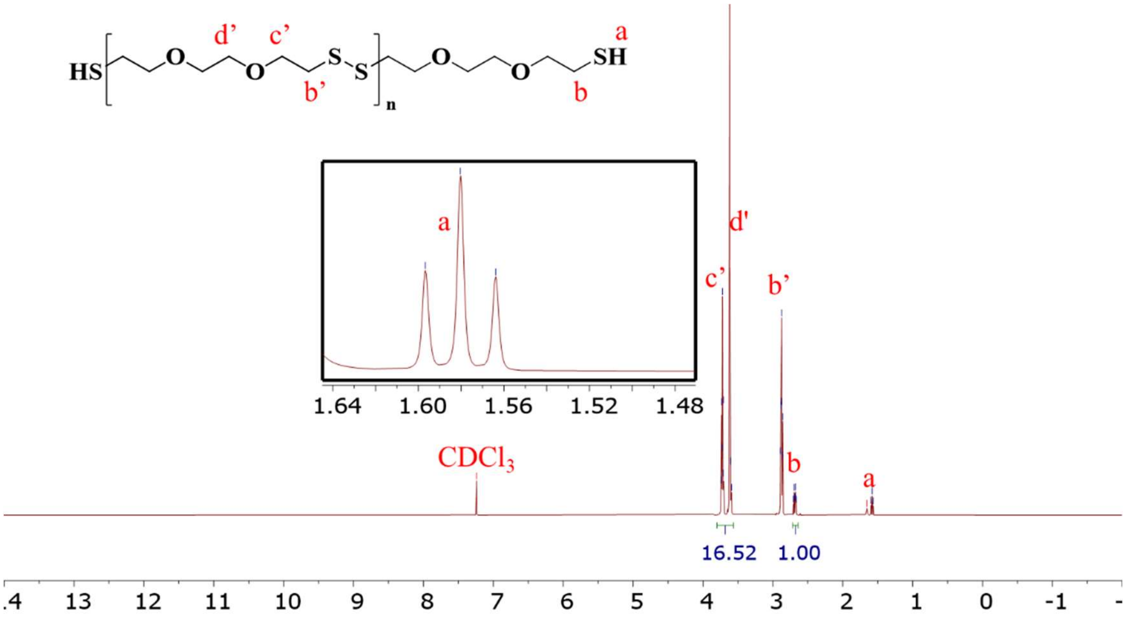

Figure 5.8 ^{1}H-NMR of polyDODT synthesized via thiol oxidation with DMSO and TMSCl. [TMSCl]/[-SH] = 0.05. Inset shows the indicated region magnified 20 times. Thiol peak (1.58 ppm) was observed.

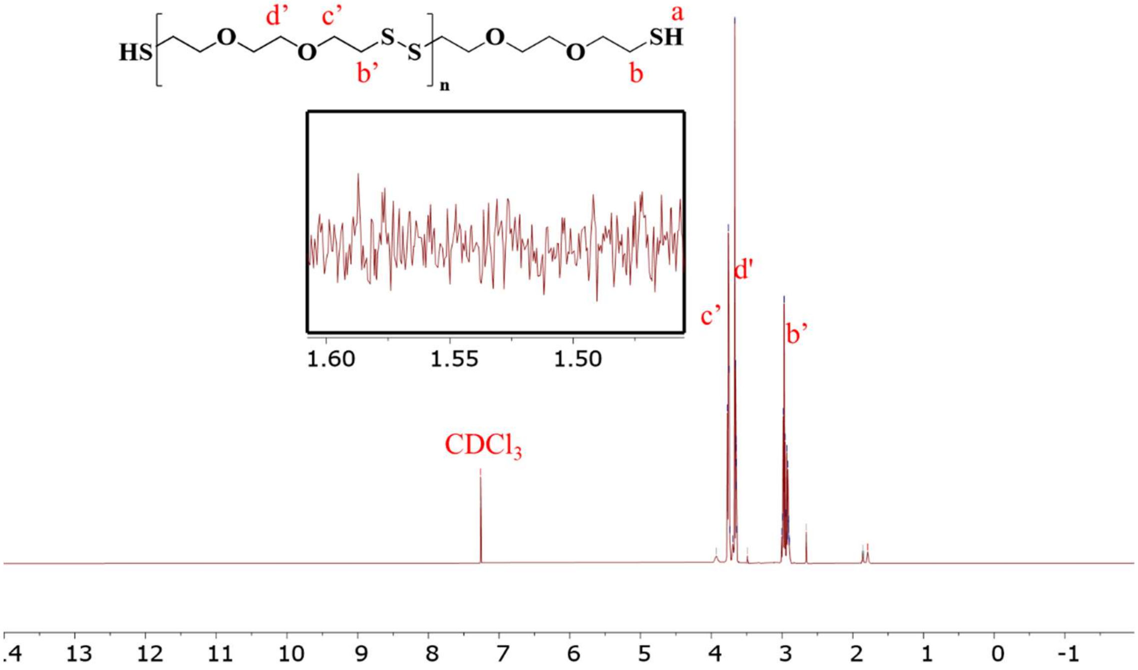

Figure 5.9 ^{1}H-NMR of polyDODT synthesized via thiol oxidation with DMSO and TMSCl. [TMSCl]/[-SH] = 0.175. Thiol peak (1.58 ppm) was not observed. Inset shows the indicated region magnified 100 times

We also repeated a few reactions with twice the volume of DMSO, and for TMSCl/SH up to 0.2, the resulting polymers had higher molecular weights in comparison to those of polymers from more concentrated DMSO solutions (Table 5.4). One possible explanation is that disulfide bond formation due to oxidation of thiols is an exothermic process, so increasing the volume of the reaction helps with dissipating the heat, lowering the reaction temperature. Zareyee and coworkers also reported a faster reaction time (10 minutes) for oxidation of thiophenols using a 5 molar excess of DMSO with respect to thiols compared to that using a 3 molar excess of DMSO, which required 30 minutes for complete consumption of thiols.[28]

Table 5.4 Molecular weights of polyDODT synthesized via thiol oxidation with DMSO and TMSCl with varying volumes of DMSO

TMSCl/SH	**Thiols (mmol)**	**DMSO (mmol)**	**TMSCl (mmol)**	**Mn (g/mol)**	**Mw (g/mol)**	**PDI**
0.1	24.56	73.68	2.456	4,198	5,512	1.31
0.15	24.56	73.68	3.684	6,892	8,945	1.30
0.2	24.56	73.68	4.912	35,820	58,800	1.64
0.25	24.56	73.68	6.14	92,460	167,400	1.81
0.3	24.56	73.68	7.368	110,500	167,800	1.52
0.1	24.56	147.36	1.228	8,435	11,670	1.38
0.15	24.56	147.36	1.842	27,830	37,480	1.35
0.2	24.56	147.36	2.456	79,210	137,800	1.74
0.25	24.56	147.36	3.07	109,900	179,600	1.63
0.30	24.56	147.36	3.684	97,170	170,900	1.76

While the R3P method was capable of synthesizing high molecular weight polymers ($M_w >$ 560 kg/mol), the highest M_w of the polyDODT using DMSO and TMSCl was roughly 170 kg/mol. Further optimization of the polymerization conditions (effect of solvent, the concentration of DODT, temperature, rate of reagent addition, and time) would be an interesting future direction. The R3P method and oxidation of thiols with DMSO and TMSCl have clearly different mechanisms, and therefore we expect the two methods would generate polymers with different topologies (ring vs. linear, or existence of polycatenane).

5.4 Conclusion

In this chapter, we described how the presence of TEA in mixtures of linear and cyclic polyDODT could lead to thiolate-disulfide exchange that can cause the molecular weight of the polyDODT to fluctuate. To prevent polyDODT molecular weight from changing over time, it is important to make sure that the sample does not contain any bases that could deprotonate the free thiol ends of linear polyDODT. We also used TEA to intentionally promote thiolate-disulfide exchange to detect the presence of linear polyDODT (free thiols) in a ring/linear mixture. The method can be used to complement existing techniques for linear polyDODT detection such as LCCC or NMR and can be used for qualitatively checking linear contaminants even when the molecular weight is high (> 100 kg/mol). The method showed that our polyDODT samples had less than 1 mol% of linear contaminants. Suggestions for future work to improve the detection limit include adding DODT or TEA below 1 mol% and performing the catalytic stability test in solvents that are less polar than THF. We also described a new method for synthesizing polyDODT samples with molecular weight control up to M_w ~170 kg/mol. The new method used DMSO and TMSCl for oxidation of thiols and seemed to proceed without formation of thiyl radicals and thiolate anions as in the R3P method.

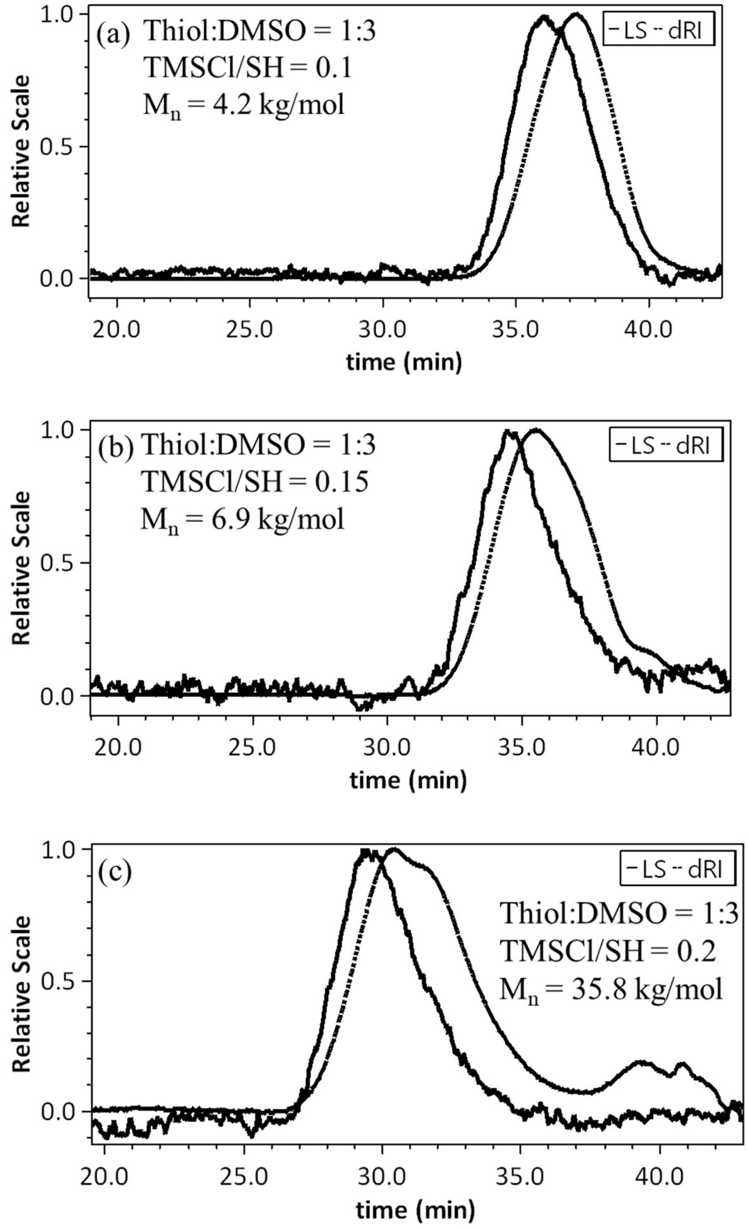

Figure 5.10 GPC chromatograms of polyDODT synthesized using DMSO and TMSCl. Thiol:DMSO = 1:3. (a) TMSCl/SH = 0.1, M_n = 4.2 kg/mol (b) TMSCl/SH = 0.15, M_n = 6.9 kg/mol, (c) TMSCl/SH = 0.2, M_n = 35.8 kg/mol

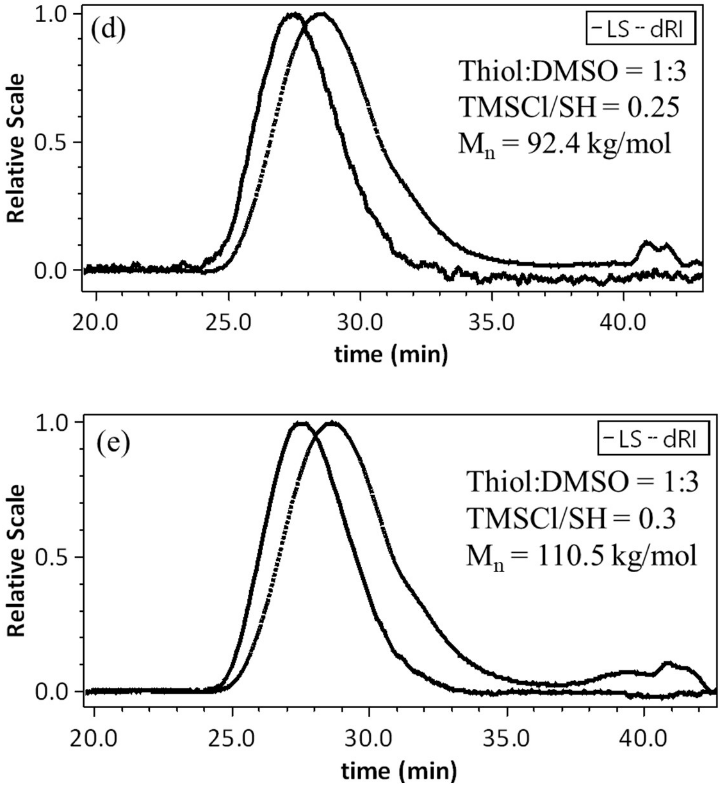

Figure 5.10 continued (d) TMSCl/SH = 0.25, M_n = 92.4 kg/mol (e) TMSCl/SH = 0.3, M_n = 110.5 kg/mol

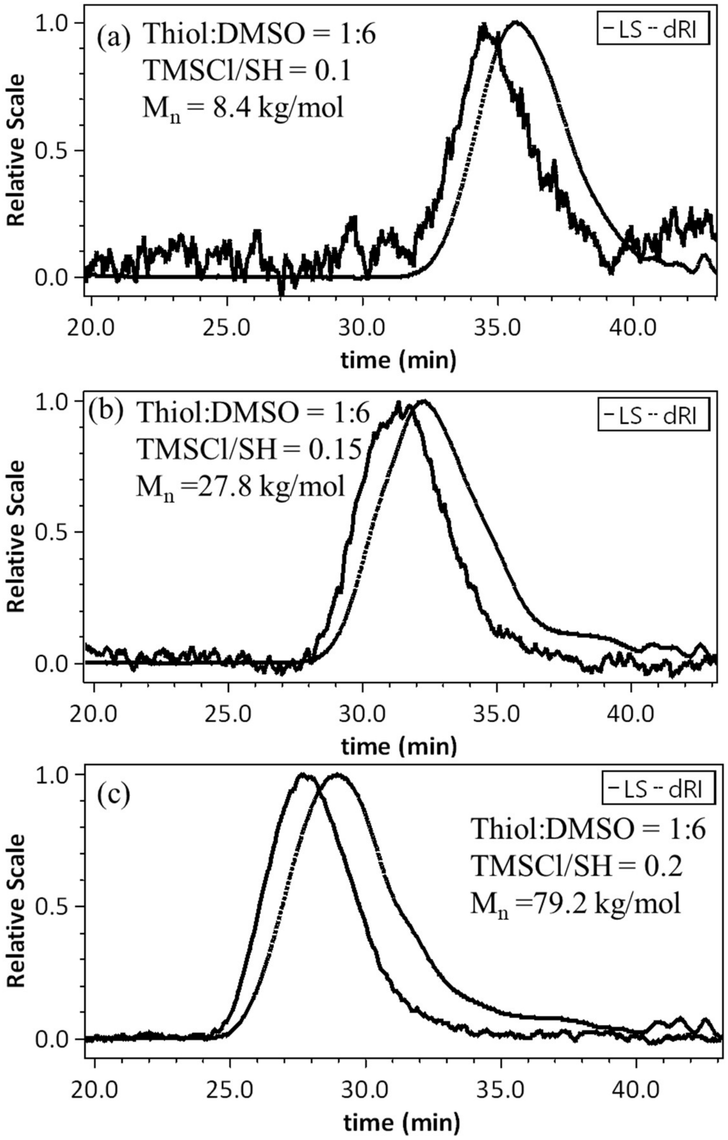

Figure 5.11 GPC chromatograms of polyDODT synthesized using DMSO and TMSCl. Thiol:DMSO = 1:6. (a) TMSCl/SH = 0.1, M_n = 8.4 kg/mol (b) TMSCl/SH = 0.15, M_n = 27.8 kg/mol, (c) TMSCl/SH = 0.2, M_n = 79.2 kg/mol

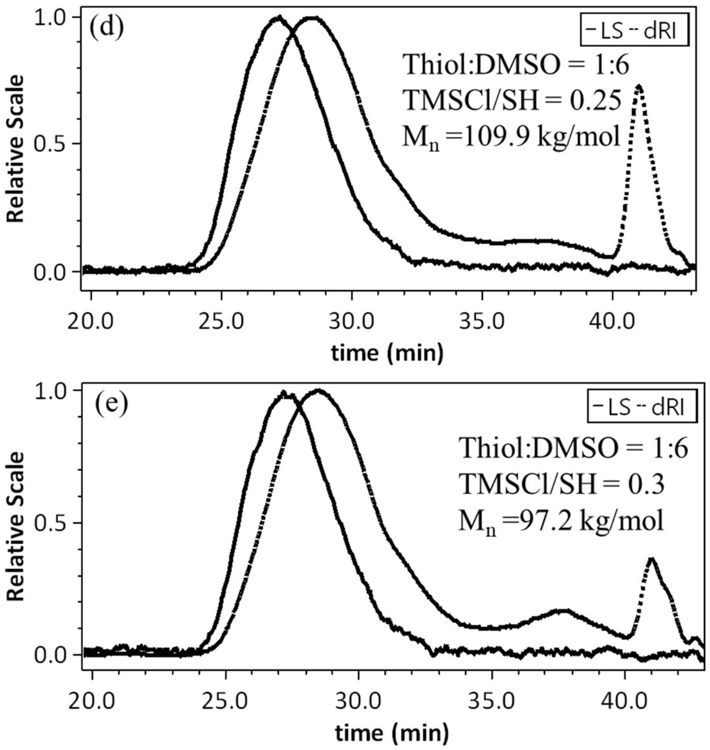

Figure 5.11 continued (d) TMSCl/SH = 0.25, M_n = 109.9 kg/mol (e) TMSCl/SH = 0.3, M_n = 97.2 kg/mol

References

1. Kishore, K. & Ganesh, K. Polymers Containing Disulfide, Tetrasulfide, Diselenide and Ditelluride Linkages in the Main Chain. in *Polymer Synthesis/Polymer Engineering* 81–121 (Springer-Verlag). doi:10.1007/BFb0018579.
2. Bang, E.-K., Lista, M., Sforazzini, G., Sakai, N. & Matile, S. Poly(disulfide)s. *Chem. Sci.* **3**, 1752 (2012).
3. Nevejans, S., Ballard, N., Miranda, J. I., Reck, B. & Asua, J. M. The Underlying Mechanisms for Self-Healing of Poly(disulfide)s. *Phys. Chem. Chem. Phys.* **18**, 27577–27583 (2016).
4. Ou, M. *et al.* Novel Biodegradable Poly(disulfide amine)s for Gene Delivery with High Efficiency and Low Cytotoxicity. *Bioconjug. Chem.* **19**, 626–633 (2008).
5. Zhang, R., Nie, T., Fang, Y., Huang, H. & Wu, J. Poly(disulfide)s: From Synthesis to Drug Delivery. *Biomacromolecules* **23**, 1–19 (2022).
6. Wang, X.-L., Jensen, R. & Lu, Z.-R. A Novel Environment-Sensitive Biodegradable Polydisulfide with Protonatable Pendants for Nucleic Acid Delivery. *J. Control. Release* **120**, 250–258 (2007).
7. Bej, R., Achazi, K., Haag, R. & Ghosh, S. Polymersome Formation by Amphiphilic Polyglycerol- b -polydisulfide- b -polyglycerol and Glutathione-Triggered Intracellular Drug Delivery. *Biomacromolecules* **21**, 3353–3363 (2020).
8. Xiang, Y.-Z. *et al.* Linear Disulfide-Containing Low Polymer as Efficient DNA Cleavage Reagent. *Bioorg. Med. Chem. Lett.* **19**, 3458–3460 (2009).
9. Rosenthal, E. Q. & Wesdemiotis, C. Green Polymer Chemistry: Living Dithiol Polymerization via Cyclic Intermediates. (2012) doi:10.1021/bm201395t.
10. Rosenthal-kim, E. Q. & Puskas, J. E. Green Polymer Chemistry: Investigating the Mechanism of Radical Ring-Opening Redox Polymerization (R3P) of 3,6-Dioxa-1,8-octanedithiol (DODT). 6504–6519 (2015) doi:10.3390/molecules20046504.
11. Molnar, K. *et al.* PolyDODT: A Macrocyclic Elastomer with Unusual Properties. 668–676 (2022) doi:10.1039/d1py01426a.
12. Cheung, H., Puskas, J., McKenna, G. & Kornfield, J. *Collaborative Research: Polymer Macrocycles: A Novel Topology to Control Dynamics of Rubbery Materials*. https://www.osti.gov/servlets/purl/1654432/ (2020) doi:10.2172/1654432.
13. Pasquino, R. *et al.* Viscosity of Ring Polymer Melts. *ACS Macro Lett.* **2**, 874–878 (2013).
14. Doi, Y. *et al.* Re-Examination of Terminal Relaxation Behavior of High-Molecular-Weight Ring Polystyrene Melts. *Rheol. Acta* **56**, 567–581 (2017).
15. Kapnistos, M. *et al.* Unexpected Power-Law Stress Relaxation of Entangled Ring Polymers. *Nat. Mater.* **7**, 997–1002 (2008).
16. Cho, D. *et al.* Preparation and Characterization of Cyclic Polystyrenes. *Polym. J.* **37**, 506–511 (2005).
17. Kawaguchi, D. *et al.* Comparison of Interdiffusion Behavior between Cyclic and Linear Polystyrenes with High Molecular Weights. *Macromolecules* **39**, 5180–5182 (2006).

18. Ochmann, M. *et al.* UV-Photochemistry of the Disulfide Bond: Evolution of Early Photoproducts from Picosecond X-ray Absorption Spectroscopy at the Sulfur K-Edge. *J. Am. Chem. Soc.* **140**, 6554–6561 (2018).
19. Doi, Y. *et al.* Melt Rheology of Ring Polystyrenes with Ultrahigh Purity. *Macromolecules* **48**, 3140–3147 (2015).
20. Belenky, B. G., Gankina, E. S., Tennikov, M. B. & Vilenchik, L. Z. Fundamental Aspects of Adsorption Chromatography of Polymers and Their Experimental Verification by Thin-layer Chromatography. *J. Chromatogr. A* **147**, 99–110 (1978).
21. Macko, T. & Hunkeler, D. Liquid Chromatography Under Critical and Limiting Conditions: A Survey of Experimental Systems for Synthetic Polymers. in 62–136 (2003). doi:10.1007/b11053.
22. Takano, A., Kushida, Y., Ohta, Y., Masuoka, K. & Matsushita, Y. The Second Virial Coefficients of Highly-Purified Ring Polystyrenes in Cyclohexane. *Polymer (Guildf).* **50**, 1300–1303 (2009).
23. Molnar, K. *et al.* Liquid Chromatography at Critical Conditions (LCCC): Capabilities and Limitations for Polymer Analysis. *J. Mol. Liq.* **322**, 114956 (2021).
24. Singh, R. & Whitesides, G. M. *Thiol-Disulfide Interchange in Sulphur-Containing Functional Groups (1993)* 633–658 (John Wiley & Sons, Inc., 2010). doi:10.1002/9780470034408.ch13.
25. Fernandes, P. A. & Ramos, M. J. Theoretical Insights into the Mechanism for Thiol/Disulfide Exchange. *Chem. - A Eur. J.* **10**, 257–266 (2004).
26. Netto, L. E. S., de Oliveira, M. A., Tairum, C. A. & da Silva Neto, J. F. Conferring Specificity in Redox Pathways by Enzymatic Thiol/Disulfide Exchange Reactions. *Free Radic. Res.* **50**, 206–245 (2016).
27. Rosenfield, R. E., Parthasarathy, R. & Dunitz, J. D. Directional Preferences of Nonbonded Atomic Contacts with Divalent Sulfur. 1. Electrophiles and Nucleophiles. *J. Am. Chem. Soc.* **99**, 4860–4862 (1977).
28. Karimi, B., Hazarkhani, H. & Zareyee, D. Trimethylchlorosilane (TMSCl) and Cyanuric Chloride (CC) Catalyzed Efficient- Oxidative Coupling of Thiols with Dimethylsulfoxide. *Synthesis (Stuttg).* 2513–2516 (2002) doi:10.1055/s-2002-35634.

Appendix A

Terpyridine end functionalized polyethylene oxides

A.1. Introduction

The main goal of our research was to create end-associative telechelic polymers for the formation of water-soluble ultralong supramolecules (effective Mw > 2000 kg/mol) at low overall polymer concentration (< 0.3 wt%). In agricultural spray drift control applications, polyethylene oxide (PEO) and polyacrylamide (PAM) are the most commonly used synthetic polymeric additives.[1] Based on our group's previous work on long end-associative polymers in jet fuel, we recognized that the length of the individual polymers is one of the key factors determining the ratio of ultralong linear supramolecules to small cyclic species. We chose to work with PAM as the backbone for water-soluble long end-associative polymers because it could be synthesized by RAFT polymerization with precise control over molecular weight.[2,3] (Chapter 1-2)

PEO is typically synthesized by ring-opening polymerization of ethylene oxide using a metallic catalyst[4] and due to the highly exothermic nature of the polymerization it is difficult to control the reaction. Commercially available high molecular weight PEOs usually have high polydispersity (e.g., PEO with an average molecular weight of 100 kg/mol from Sigma Aldrich has a PDI of 3.27). Furthermore, PEO is more susceptible to mechanical[5,6] and thermal[6] degradation than PAM. Therefore, most of the work related to end group functionalization of PEO used relatively short PEO chains, modifying the terminal hydroxyl groups of commercially available PEO. As for making water-soluble building blocks for supramolecular polymers, Schubert and coworkers[7,8] successfully synthesized low molecular weight PEOs (Mn > 16,500 g/mol) functionalized with terpyridine. While Schubert and coworkers demonstrated the successful formation of metal coordinated terpy-PEOs that resulted in an apparent molecular weight up to 80,000 g/mol, a relatively high polymer concentration of terpy-PEOs (25 mg/mL in methanol, ~3 wt%) was used. We hypothesized that if longer terpy-PEO could be synthesized, the formation of longer coordinated polymers would be possible. Herein, we describe the synthesis of higher molecular weight terpy-PEO than previously reported.

A.2 Experimental methods

Materials

All chemical reagents were obtained from Sigma Aldrich at 98% purity or higher unless otherwise stated. All solvents were obtained from Sigma Aldrich, at ACS reagent grade or higher (> 99.5% purity) and used as received without further purification. PEOs were obtained from Fluka (M_w 20,000 g/mol and 35,000 g/mol), and from Sigma Aldrich (M_v 100,000 g/mol).

NMR spectroscopy

^{1}H-NMR spectra were obtained using a Varian Inova 500 spectrometer (500 MHz); spectra were recorded in $CDCl_3$, d-DMSO, and D_2O (purchased from Cambridge Isotope Laboratories). Chemical shifts were reported in parts per million (ppm) and were referenced to residual solvent resonances.

Gel permeation chromatography

The molecular weights and dispersity index of the polymers were determined on a GPC system with an Agilent pump (G7110B), equipped with an autosampler (G7129A), a Wyatt DAWN 8 multi-angle laser light scattering detector (λ=658.9nm), a Wyatt Optilab refractive index detector (RI) (λ=658nm), and an Agilent PL Aquagel-OH MIXED-H column. Aqueous buffer was prepared containing 0.2M $NaNO_3$, with 200 ppm NaN_3. Filtered aqueous buffer was used as the eluent at the flow rate of 0.3mL/min at 25°C. The data were analyzed using Wyatt Astra 7 using the Zimm fitting formula with *dn/dc* = 0.1360 mL/g to obtain molecular weight (M_w, and M_n) for each polyethylene oxide reported.

Synthesis of bis terpyridine functionalized PEO (terpy-PEO) via Williamson ether synthesis reaction.

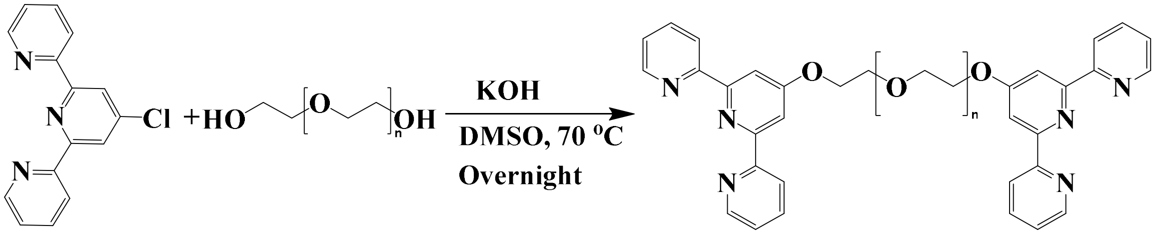

Scheme A.1 Synthesis of bis-terpyridine functionalized polyethylene oxide
Procedure was modified from[8]

Representative procedure for PEO with M_n 12,200 g/mol

Finely crushed KOH (0.055 g, 0.98 mmol) was suspended in 25 mL of dry DMSO in a 50 mL round bottom flask. Polyethylene oxide (1.20 g, 0.0983 mmol) was added to the flask. The head space of the flask was constantly purged with N_2. The mixture was stirred for 30 minutes at 50 °C and 4'-chloro-2,2':6',2''-terpyridine (262.4 mg, 0.98 mmol) was added at once and the flask was sealed with a rubber septum. The mixture was stirred at 70 °C for 24 hours. After 24 hours, the reaction mixture was cooled to room temperature and neutralized with 3M HCl_{aq} to neutral pH and vacuum filtered. The filtrate was transferred to dialysis tubing with MWCO 3500 Da (Spectra/Por 6) and dialyzed against water for 1 day, and the water was evaporated. The polymers were redissolved in THF (10 mL) and precipitated in diethyl ether. The precipitated polymers were dried under vacuum. The polymers were obtained as white powders. Yield 30%.

Coordinated terpy-PEO solution preparation

1 wt% terpy-PEO solutions were prepared by dissolving the polymer in molecular biology grade water in a 20 mL glass scintillation vial. The coordination polymers were formed by adding precise amounts of nickel ion stock solution (20 mM), which was prepared from dissolving $NiCl_2$ in molecular biology grade water. After the addition of the metal solutions, the scintillation vials were placed on a wrist-action shaker (Burrell Scientific) for 1 hour and used for shear viscosity measurements.

Rheology

The shear viscosity of the polymer solutions was measured using a strain-controlled rheometer TA ARES-RFS, equipped with a cone-plate geometry (angle 2^o, diameter 50mm) with shear rates ranging from 1 s^{-1} to 1000 s^{-1}. Three replicates were measured to obtain the error bars (standard error).

A.3 Result and discussion

In the work of Schubert and coworkers[7,8], the highest molecular weight PEO functionalized with terpyridine was M_n = 16,500g/mol, and our goal was functionalizing higher molecular weight PEOs. We tried using PEOs with three different molecular weights (See Table A.1).

Table A.1 Molecular weights of commercial PEO and terpy-PEO (GPC)

Label on the product	Mn (g/mol)	Mw (g/mol)	PDI
PEO 20,000 (Fluka)	12,220	14,930	1.222
PEO 35,000 (Fluka)	23,980	27,350	1.140
PEO 100,000 (Sigma Aldrich)	59,300	193,900	3.27
Terpy-PEO 100,000	115,200	167,800	1.46

Table A.2 $M_{n,nmr}$ after terpyridine functionalization

	Terpy-PEO 20,000	Terpy-PEO 35,000	Terpy-PEO 100,000
M_n (g/mol)	12,426	21,238	31,764

For relatively low molecular weight PEO samples (PEO 20k and 30k), $M_{n,NMR}$ after the functionalization agreed reasonably well with $M_{n,GPC}$. These results suggest that the terpyridine functionalization occurred without significant degradation of PEO chains. However, the molecular weight of the PEO 100k sample changed significantly after the reaction. The decrease in $M_{w,GPC}$ from ~ 200 kg/mol to 167 kg/mol and increase in $M_{n,GPC}$ from ~60 kg/mol to 115 kg/mol suggest that chain scission of high molecular weight PEOs occurred. The polydispersity index also decreased from 3.27 to 1.46 due to chain scission of high molecular weight PEOs. In addition to the changes in molecular weights before and after the reaction observed by GPC, the $M_{n,GPC}$ for Terpy-PEO 100k differed significantly from the $M_{n,NMR}$ (115.2 kg/mol vs. 31.7 kg/mol). The relative viscosity (relative to the viscosity of water) of the terpy-PEO 100k was 2.95, slightly lower than the relative viscosity of PEO 100k, which was 3.05. The relative viscosity of unfunctionalized PEO 35k was 1.58, so based on viscosity measurements, the molecular weight of terpy-PEO 100k is closer to $M_{n,GPC}$ of 100 kg/mol, rather than $M_{n,NMR}$ of 31.7 kg/mol. The lower M_n of the Terpy-PEO 100k from NMR analysis indicate that the PEO chains are functionalized with more terpyridine groups than expected. High molecular weight PEO suffers from mechanical, oxidative, and thermal degradation (or combination of the three). The reaction occurs with continuous stirring of the mixture in DMSO (a mild oxidant)[13], and elevated temperature of 70°C for 24 hours. Whatever the cause of the mechanism may have been, the fragmented polymers can contain more hydroxyl groups and other functional groups such as aldehyde, formate, and dihydroxy groups[14]. The newly formed hydroxyl (and dihydroxy) groups would be functionalized by terpyridine groups since an excess of chloro-terpyridine was used in the reaction, leading to over functionalization of PEO chains.

Shear viscosity measurement

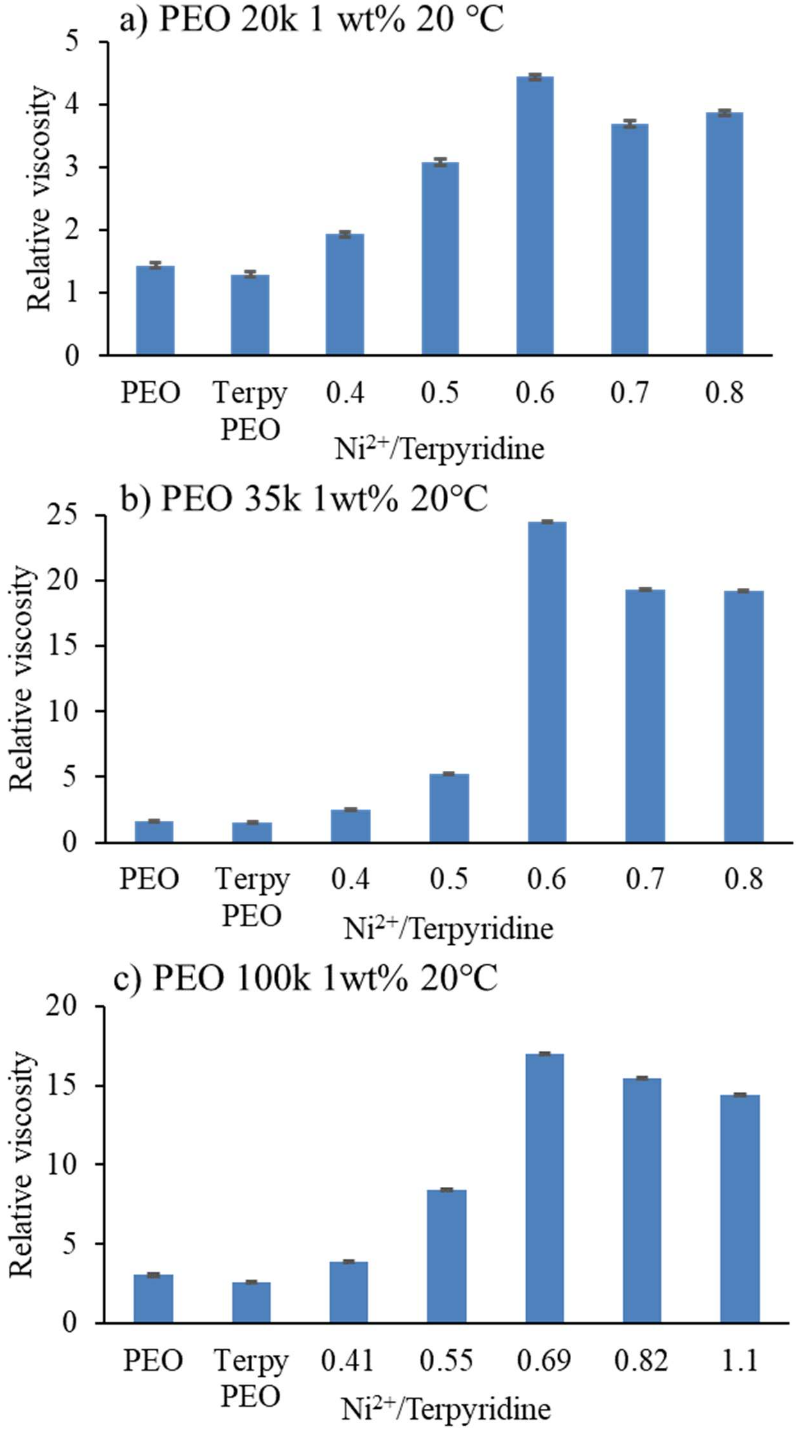

Figure A.1 Relative viscosity of Ni^{2+} coordinated terpy-PEO solutions. The number of terpyridine groups in solution was estimated using $M_{n,NMR}$. (a) terpy-PEO 20k, (b) terpy-PEO 35k, (c) terpy-PEO 100k.

After the functionalization, all three terpy-PEO samples (uncoordinated with Ni^{2+}) showed a slight decrease in viscosity in comparison to unreacted PEO, suggesting that the chain degradation could have occurred during the reaction even for relatively small molecular weight samples. Nevertheless, all three terpy-PEO samples showed significant increases in viscosity upon coordination with Ni^{2+}.

The terpy-PEO 30k had the highest relative viscosity among the three terpy-PEO samples. We expected the viscosity of the coordinated polymers to increase with an increase in molecular weight of the individual chains since longer chains tend to form fewer cyclic supramolecules. Terpy-PEO 30k sample had higher viscosity than the terpy-PEO 100k. As described above, the terpy-PEO 100k sample suffered more from chain scission during the functionalization reaction, and the lower viscosity of terpy-PEO 100k with Ni^{2+} is most likely the result of having polymer chain scission products. For example, mono-terpyridine functionalized polymers can act as chain cappers for the formation of ultralong linear coordinated polymers.

A.4 Conclusion

We concluded that it would be challenging to obtain terpy-PEOs with high molecular weight (> 100 kg/mol) without the polymers experiencing degradation. Therefore, polyacrylamide was a more useful backbone for the synthesis of long end-associative polymers for aqueous solutions.

A.5 Supplementary information

Determination of M_n of the terpy-PEOs using ^{1}H-NMR

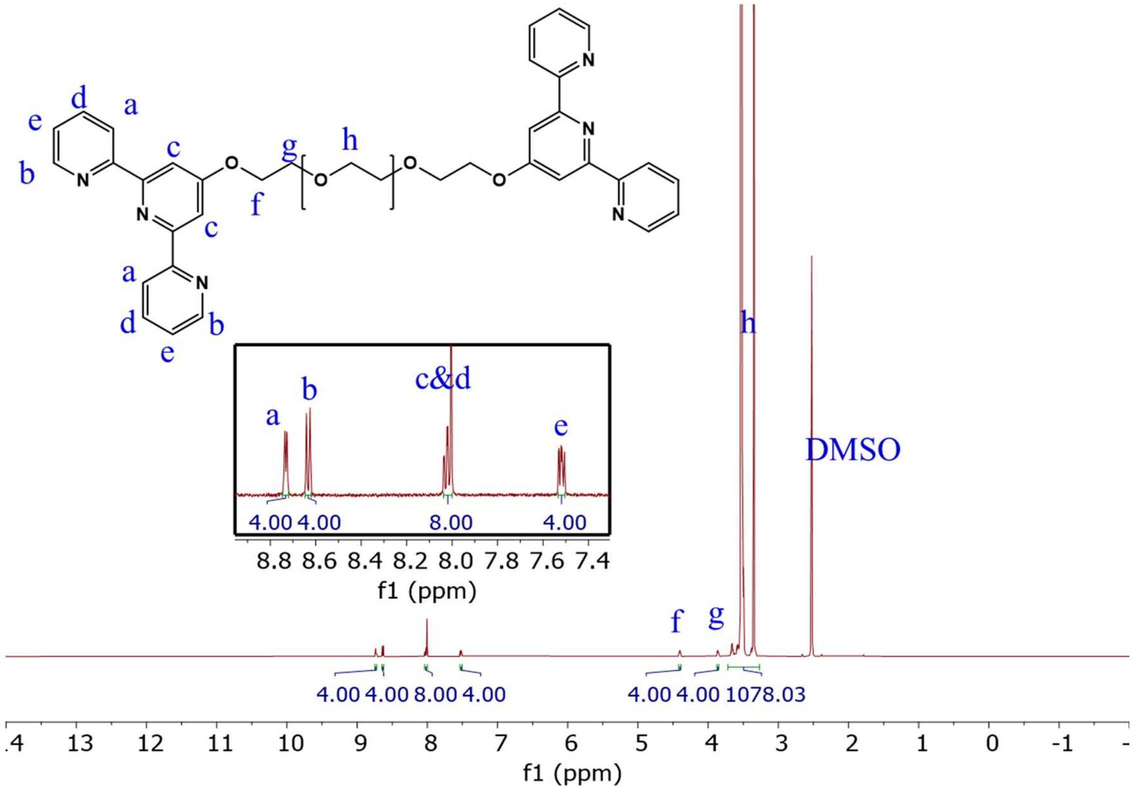

Figure A.2 ^{1}H-NMR spectra of terpy-PEO 20k.

Number of protons in repeat unit = 4. Number of protons corresponding to peak “a” from terpyridines on both ends = 4. Molecular weight of the repeat unit = 44.05 g/mol. The molecular weight of the end groups = 554.66g/mol.
Therefore, M_n=1078.03/4*44.05+554.66 = 12426.47g/mol.

References

1. Lewis, R. W., Evans, R. A., Malic, N., Saito, K. & Cameron, N. R. Polymeric Drift Control Adjuvants for Agricultural Spraying. *Macromol. Chem. Phys.* **217**, 2223–2242 (2016).
2. Carmean, R. N., Becker, T. E., Sims, M. B. & Sumerlin, B. S. Ultra-High Molecular Weights via Aqueous Reversible-Deactivation Radical Polymerization. *Chem* **2**, 93–101 (2017).
3. Lewis, R. W., Evans, R. A., Malic, N., Saito, K. & Cameron, N. R. Ultra-Fast Aqueous Polymerisation of Acrylamides by High Power Visible Light Direct Photoactivation RAFT Polymerisation. *Polym. Chem.* **9**, 60–68 (2018).
4. Gelardi, G. *et al.* Chemistry of Chemical Admixtures. in *Science and Technology of Concrete Admixtures* 149–218 (Elsevier, 2016).
5. Fisher, D. H. & Rodriguez, F. Degradation of Drag-Reducing Polymers. *J. Appl. Polym. Sci.* **15**, 2975–2985 (1971).
6. Sung, J. H. *et al.* Turbulent Drag Reduction Efficiency and Mechanical Degradation of Poly(Acrylamide). *J. Macromol. Sci. Part B* **43**, 507–518 (2004).
7. Schmatloch, S., van den Berg, A. M. J., Alexeev, A. S., Hofmeier, H. & Schubert, U. S. Soluble High-Molecular-Mass Poly(ethylene oxide)s via Self-Organization. *Macromolecules* **36**, 9943–9949 (2003).
8. Lohmeijer, B. G. G. & Schubert, U. S. Water-Soluble Building Blocks for Terpyridine-Containing Supramolecular Polymers: Synthesis, Complexation, and pH Stability Studies of Poly(ethylene oxide) Moieties. *Macromol. Chem. Phys.* **204**, 1072–1078 (2003).
9. Rabasco, J. & Bobsein, B. R. Rheology Modifier. (2013).
10. Shaira, A. & Jaganyi, D. Understanding the Role of Flexible 4’-Functionalized Polyethylene Glycoxy Chains on the Behavior of Platinum(II)(4’-(ethylene glycoxy)-2,2’:6’,2’’-terpyridine: A Kinetic and a Mechanistic Study. *J. Coord. Chem.* (2014)
11. Abd-El-Aziz, A. S., Dalgakiran, S., Vandel, M., Owen, E. M. & Wagner, B. D. Synthesis and Electrochemical Characterization of Thiophenes with Pendant Fluorescent Terpyridine. *J. Electrochem. Soc.* (2013)
12. Schubert, U. S., Eschbaumer, C., Hien, O. & Andres, P. R. 4′-Functionalized 2,2′:6′,2″-terpyridines as Building Blocks for Supramolecular Chemistry and Nanoscience. *Tetrahedron Lett.* **42**, 4705–4707 (2001).
13. Tidwell, T. T. Oxidation of Alcohols by Activated Dimethyl Sulfoxide and Related Reactions: An Update. *Synthesis (Stuttg).* **1990**, 857–870 (1990).
14. Payne, M. E., Kareem, O. O., Williams-Pavlantos, K., Wesdemiotis, C. & Grayson, S. M. Mass Spectrometry Investigation into the Oxidative Degradation of Poly(ethylene glycol). *Polym. Degrad. Stab.* **183**, 109388 (2021).